# The Cellular and Molecular Mechanisms by which the Insert Negative Isoform of the Human Calcitonin Receptor Regulates Cell Growth

This thesis is submitted to the University of Adelaide as a requirement for the degree of Doctor of Philosophy

By

**Liza-Jane Raggatt B.Sc. (Hons)**

Department of Orthopaedics and Trauma, University of Adelaide

August 2000

*Happy is the person that findeth wisdom,*
*And the person that getteth understanding.*

*For the gaining of it is better than the gaining of silver,*
*and the profit thereof finer than gold.*

*Proverbs 3:13-14*

# Table of Contents

## Abstract

Calcitonin (CT) is a 32 amino acid peptide hormone, known to inhibit osteoclastic bone resorption by direct interaction with cell surface calcitonin receptors (CTR). Several CTR isoforms have been identified in human tissues other than bone, including primary breast cancers, and these isoforms are known to induce different intracellular signalling responses. This evidence, in conjunction with the finding that CT can modulate the growth of breast cancer cell lines *in vitro*, has prompted this comparison of two human CTR (hCTR) isoforms, and their ability to influence cellular proliferation. The aim of the study was to define the intracellular mechanisms by which CT treatment results in decreased cellular proliferation.

Stable HEK-293 transfectants expressing the insert-negative human CTR (insert –ve hCTR) or the insert-positive human CTR (insert +ve hCTR) were established. The transfected cells were characterised for their ability to bind CT, elevate intracellular calcium and activate adenylate cyclase and ERK1/2 intracellular signalling cascades. CT treatment of clonal cell lines expressing the insert –ve hCTR, but neither vector transfected HEK-293 cells nor cells expressing the insert +ve hCTR, induced a concentration dependent decrease in cell growth, compared with untreated cells. The CT-induced reduction in cell proliferation could not be attributed to necrosis or apoptosis. However, analysis by fluorescent activated cell scanning showed that CT-treatment of cells expressing the insert –ve hCTR receptor was associated with an accumulation of cells at the G2/M transition. Subsequent analysis of the chromosomal alignment showed that CT induced a specific block in G2, preventing cells from progressing into mitotic division. This G2 phase arrest was dependent on an up-regulation of nuclear p21 mRNA and protein. The p21-mediated G2 arrest was shown to be due to a maintenance of tyrosine 15 phosphorylation on

cdc2 and thus inactivation of cyclin B1/cdc2 kinase activity, however it was not possible to detect p21 protein bound to the cyclin B1/cdc2 complex.

To determine whether p21 induction was due to increased transcription of the p21 gene, and further explore the specific CT responsive elements within the p21 promoter, luciferase reporter constructs were used. CT was able to stimulate transcription from a p21 promoter attached to a luciferase reporter gene. Using deletion and mutation analysis of the p21 promoter, we identified that transcriptional activation of p21 by CT was p53 independent and is mediated through specific activation of Sp1 binding sites in a region of the promoter between –82 and –69, relative to the transcription start site. This CTR-mediated transcriptional activation of p21 was specific for the insert –ve isoform of the hCTR. In addition treatment of cells expressing the insert –ve hCTR with butyrate, which has been previously shown to activate the same Sp1 sites, synergised with CT to increase further p21 promoter activity.

The possible intracellular signalling pathways through which CT is mediating these nuclear events were also investigated. Treatment of cells expressing the insert –ve hCTR, but not the insert +ve hCTR, with CT induced a delayed and sustained up to (72h) phosphorylation of p44/p42 MAP kinases (Erk1/Erk2). Treatment of cells expressing the insert -ve hCTR with the MAP kinase kinase (MEK) inhibitor, PD98059, inhibited the phosphorylation of Erk1/2 and abrogated the growth inhibitory effects of sCT, the accumulation of cells in G2, and the associated induction of $p21^{WAF1/CIP1}$.

These results show for the first time that the growth regulating actions of CT are receptor isoform specific. In addition, CT inhibition of cellular proliferation occurs by arresting cells in the G2 phase of the cell cycle *via* a p21 mediated mechanism, which is at least partially activated through the Erk1/2 Map Kinase pathway.

## DECLARATION

This thesis contains no material which has been accepted for the award of any other degree or diploma in a University or other tertiary institution and, to the best of my knowledge and belief, contains no material previously published or written by another person, except where due reference has been made in the text.

I give consent for this copy of my thesis, when deposited in the University Library, to be available for loan and photocopying.

Liza-Jane Raggatt

August 2000

# ACKNOWLEDGMENTS

I would like to thank my supervisors, Dr David Findlay and Dr Stephen Graves.
I especially thank David for the opportunity to undertake this PhD, the subsequent support he has given me, his enthusiasm, encouragement, and the opportunity to present this work both locally and internationally. I particularly thank him for his patience and persistence during the writing of this thesis, the completion of which would have been impossible without him.

I would like to sincerely thank Dr Andreas Evdokiou, who has worked together with me on this project. Andreas' friendship, guidance, advice and supervision in the laboratory have been greatly appreciated. Andreas' personal contribution to this project has been significant and his critical reading of this thesis has been most important.

I owe a special thank you to each of my work colleagues Gerald Atkins, Shelley Hay, Steve Bouralexis and Jodie Stanley. Their assistance has been invaluable and their friendship a privilege to have shared, it will remain with me always.
I would also like to thank Lisa Edwards for her enduring friendship and her statistical input into this project.

I extend my thanks to Professor Don Howie and the Department of Orthopaedics and Trauma for their support. In addition, I am grateful for the assistance of many individuals within the Institute of Medical and Veterinary Science and the Hanson Center for Cancer Research. I would also like to thank Dr Henry Betts, of the Department of Rheumatology at the Queen Elizabeth Hospital, for his assistance with the intracellular calcium measurements.
I extend my appreciation to the Australian Research Council Small Grants scheme for supporting this work.

Lastly, a very special thank you to my family and friends.
Thank you to my Mum and Dad for their support and unshakable belief in my ability.
To my friends, I thank you for your support over the last three years, particularly during the writing of this thesis.

Finally to Duncan, thank-you for your love and patience.

## PUBLICATIONS ARISING

Evdiokiou A, **Raggatt L-J**, Atkins GJ and Findlay DM 1999 Calcitonin receptor-mediated growth suppression of HEK-293 cells is accompanied by induction of p21 $^{WAF1/CIP1}$ and $G_2$/M arrest. *Molecular Endocrinology* 10 1738-1750.

Evdokiou A, **Raggatt L-J**, Sakai T and Findlay MD 2000 Identification of a novel calcitonin receptor element in the promoter of the human p21$^{WAF1/CIP1}$ gene. *Journal of Molecular Endocrinology* (accepted for publication 31$^{st}$ May 2000).

**Raggatt L-J**, Evdokiou A and Findlay DM 2000 Sustained activation of Erk1/2 MAPK and cell growth suppression by the insert-negative, but not insert-positive isoform of the human calcitonin receptor. *Journal of Endocrinology* (accepted for publication 5$^{th}$ June 2000).

## CONFERENCE PRESENTATIONS

**L-J. Raggatt**, A. Evdokiou, DM. Findlay 1999 Calcitonin inhibits cell growth and causes sustained phosphorylation of MAPK kinase. ASMR National Scientific Conference, Leura, Australia.

A. Evdokiou, GJ. Atkins, S. Bouralexis, S. Hay, **L-J, Raggatt**, SE. Graves, DM. Findlay 1999 Differential expression of MDM2 splice variants in bone tumors. Americal Society of Cell Biology (ASCB), Washington D.C., USA.

**L-J. Raggatt**, A. Evdokiou, DM. Findlay 1999 Activation of the insert-negative human calcitonin receptor, Phosphorylation of MAP kinase and inhibition of cellular proliferation. American Society for Bone and Mineral Research (ASBMR), St. Louis Missouri, USA.

**L-J. Raggatt**, A. Evdokiou, DM. Findlay 1999 Activation of the insert-negative human calcitonin receptor, Phosphorylation of MAP kinase and inhibition of cellular proliferation. Australian Orthopaedic Association (AOA) South Australian Branch Meeting, Adelaide Australia.

**L-J. Raggatt**, A. Evdokiou, DM. Findlay 1999 Activation of the insert-negative human calcitonin receptor, Phosphorylation of MAP kinase and inhibition of cellular proliferation. Australian and New Zealand Bone and Mineral Society (ANZBMR), Cairns, Australia.

**L-J. Raggatt**, A. Evdokiou, DM. Findlay 1999 Activation of the insert-negative human calcitonin receptor, Phosphorylation of MAP kinase and inhibition of cellular proliferation. ASMR SA Local Scientific Meeting, Adelaide Australia.

A. Evdokiou, **L-J. Raggatt**, GJ. Atkins, DM. Findlay 1998 Growth inhibition by calcitonin of HEK-293 cells is accompanied by induction of $p21^{CIP1/WAF1}$ and $G_2$/M arrest. The American Society of Cell Biology, San Francisco, USA.

A. Evdokiou, **L-J. Raggatt**, GJ. Atkins, DM. Findlay 1998 Calcitonin receptor-mediated growth suppression of HEK-293 cells is associated with an accompanied by induction of $p21^{CIP1/WAF1}$ and $G_2$/M arrest. ASBMR Scientific Meeting, San Francisco, USA.

**L-J. Raggatt**, A. Evdokiou, GJ. Atkins, DM. Findlay 1998 Calcitonin growth suppression of HEK-293 cells is accompanied by induction of $p21^{CIP1/WAF1}$ and $G_2$/M arrest. ASMR National Scientific Conference, Hobart, Australia.

**L-J. Raggatt**, A. Evdokiou, GJ. Atkins, DM. Findlay 1998 Growth inhibition by calcitonin of HEK-293 cells is accompanied by induction of $p21^{CIP1/WAF1}$ and $G_2$/M arrest. 1998 Hanson Symposium – From Genes to Therapeutics, Adelaide, Australia.

**L-J. Raggatt**, A. Evdokiou, GJ. Atkins, DM. Findlay 1998 Calcitonin receptor-mediated growth suppression of HEK-293 cells is accompanied by induction of $p21^{CIP1/WAF1}$ and $G_2$/M arrest. ANZBMS National Scientific Conference, Perth, Australia.

**L-J. Raggatt**, A. Evdokiou, GJ. Atkins, DM. Findlay 1998 Calcitonin receptor mediated growth suppression of HEK-293 cells is accompanied by induction of $p21^{CIP1/WAF1}$ and $G_2$/M arrest. ASMR Local Scientific Meeting, Adelaide, Australia.

**L-J. Raggatt**, A. Evdokiou, GJ. Atkins, DM. Findlay 1998 Calcitonin receptor mediated growth suppression of HEK-293 cells is accompanied by induction of $p21^{CIP1/WAF1}$ and $G_2$/M arrest. Australia Orthopaedic Association South Australian Branch Meeting, Adelaide, Australia.

**L-J. Raggatt**, A. Evdokiou, GJ. Atkins, DM. Findlay 1998 Calcitonin receptor-mediated growth inhibition is associated with the induction of p21 (wAF1/CIP1) gene expression. Lorne Cancer Conference, Lorne, Australia.

**L-J. Raggatt**, A. Evdokiou, GJ. Atkins, DM. Findlay 1997 Growth inhibitory effects of calcitonin on HEK-293 cells transfected with rat or human calcitonin receptors. ASMR National Scientific Meeting, Adelaide, Australia.

## AWARDS

**The Roger Melick Young Investigator Award** at the Australian and New Zealand Bone and Mineral Society (ANZBMS) Annual Scientific Conference, 1999.

**Ansett Australia Prize for Best Oral Presentation** at the Australian Society for Medical Research (ASMR) South Australian Local Scientific Meeting, 1999.

**Ansett Australia Prize for Best Oral Presentation** at the ASMR South Australian Local Scientific Meeting, 1998.

## ABBREVIATIONS

| | |
|---|---|
| 7TMD receptor | seven transmembrane domain receptor |
| AR | adrenergic receptor |
| BHK cells | baby hamster kidney cells |
| bp | base pairs |
| BSA | bovine serum albumin |
| $Ca^{++}$ | free calcium |
| cDNA | complementary deoxyribonucleic acid |
| CGRP | calcitonin gene-related peptide |
| CMV | cytomegalovirus |
| CT | calcitonin |
| CTR | calcitonin receptor |
| CNS | central nervous system |
| cAMP | cyclic adenosine monophosphate |
| CRLR | calcitonin receptor-like receptor |
| CDK | cyclin dependent kinase |
| CKI | cyclin dependent kinase inhibitor |
| CC | chelerythrine chloride |
| Cyto D | cytochalasin D |
| DAG | diacylglycerol |
| Erk | extracellular signal-regulating kinase |
| EGF | epidermal growth factor |
| EGFR | epidermal growth factor receptor |
| FCS | fetal calf serum |
| FAK | focal adhesion kinase |
| FRET | fluorescence resonance energy transfer technique |
| GCT | giant cell tumor |
| GDP | guanidine diphosphate |
| GTP | guanidine triphosphate |
| GPCR | G-protein coupled receptor |
| GRK2 | G-protein coupled receptor kinase 2 |
| GAPDH | glyceraldehyde-3-phoshate dehydrogenase |
| GHrH | growth hormone releasing hormone |
| hCTR | human calcitonin receptor |

| | |
|---|---|
| HCT | human calcitonin |
| hSSTR2 | human somatistatin receptor 2 |
| [$^{125}$I]amylin | radio-iodinated amylin |
| [$^{125}$I]sCT | radio-iodinated salmon calcitonin |
| insert –ve hCT | insert negative human calcitonin receptor |
| insert +ve hCTR | insert positive human calcitonin receptor |
| IP | inositol phosphate |
| $IP_3$ | 1,4,5-Inositol triphosphate |
| JNK | c-Jun N-terminal kinase |
| MAPK | mitogen activated protein kinase |
| MAPKK (MEK) | mitogen activated protein kinase kinase |
| mRNA | messenger ribonucleic acid |
| MTC | medullary thyroid carcinoma |
| $Na^+/H^+$ exchanger | sodium hydrogen exchanger |
| NHERF | sodium hydrogen exchanger regulatory factor |
| NHE3 | sodium hydrogen exchanger 3 |
| NGF | nerve growth factor |
| NF-κB | nuclear factor kappa beta |
| ORF | open reading frame |
| PKA I | cAMP dependent protein kinase type I isoenzyme |
| PKA II | cAMP dependent protein kinase type II isoenzyme |
| PCNA | proliferating cell nuclear antigen |
| PCR | polymerase chain reaction |
| PTX | pertusiss toxin |
| PKC | protein kinase C |
| PTH | parathyroid hormone |
| PBS | phosphate buffered saline |
| PTHrP | parathyroid hormone related peptide |
| PACAP | pituitary adenylate cyclase activating peptide |
| PKA | protein kinase A |
| PLC | phospholipase C |
| PLD | phospholipase D |
| PI | propidium iodide |
| PI-3 kinase | phosphatidylinositol 3-kinase |
| Rb | retinoblastoma protein |

| | |
|---|---|
| rCTR | rat calcitonin receptor |
| RAMPS | receptor activity modifying proteins |
| RT-PCR | reverse transcription-polymerase chain reaction |
| sCT | salmon calcitonin |
| TSH | thyroid stimulating hormone |
| TGFβ | transforming growth factor β |
| TYR 15 | tyrosine 15 |
| THR 14 | threonine 14 |
| VIP | vasoactive intestinal polypeptide |

# Chapter 1

# Literature Review

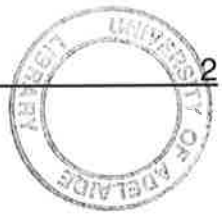

## 1.1 Calcitonin

### 1.1.1 Discovery of calcitonin

Calcitonin (CT) was first described by Copp *et al.*, as the factor secreted in response to perfusion of the thyroid-parathyroid glands of dogs with hypercalcaemic blood *(Copp et al., 1962)*. This initial report suggested that the hypercalcaemic factor was produced by the parathyroid gland, as perfusion of the thyroid gland failed to induce production of CT *(Copp et al., 1962)*. A similar rapidly acting factor was coincidentally reported by Hirsch *et al.* in acid extracts of rat thyroid glands and was shown to induce hypocalcaemia when injected into rats *(Hirsch et al., 1963)*. This second factor was named "thyrocalcitonin" and was extractable from the thyroid glands of several species. It soon became clear that calcitonin and thyrocalcitonin were the same molecule. Confirmation of the thyroid gland as the origin of CT secretion came from perfusion studies performed in dogs *(Kumar et al., 1963)* and goats *(Foster et al., 1964)*. These studies allowed complete perfusion of the parathyroid gland alone, or together with the thyroid glands, and showed this hypocalcaemic factor to be thyroidal in origin. Further, when the thyroid extract was injected into the goats systemically, serum calcium decreased rapidly *(Foster et al., 1964)*. Electron microscopy studies suggested the specific site of production of CT to be the parafollicular or C cells of the thyroid *(Foster et al., 1965)*. This was subsequently confirmed with immunofluorescence *(Polak et al., 1974)*, immunohistochemistry *(Wolfe et al., 1973)* and finally with *in situ* hybridization *(Jacobs et al., 1983)*. C cells originate from the ultimobranchial bodies *(Pearse et al., 1967)*, which are neural crest in origin. In lower vertebrates, ultimobranchial bodies remain as distinct structures, while in mammals they fuse with the thyroid glands and give rise to calcitonin secreting cells. The detection of immunoreactive CT in the

serum and urine of thyroidectomised monkeys *(Becker et al., 1980)* and humans *(Silva et al., 1978)* suggested that the hormone may be produced in extrathyroidal sites. Subsequently it has been shown that the prostate gland contains the second highest levels of human CT- (hCT)- immunoreactivity *(Davis et al., 1989)*, while there are extractable quantities of CT in the gastrointestinal system, thymus, bladder, lung and central nervous system (CNS) *(Becker et al., 1979)*. Immunoreactivity to CT has subsequently been localized to the hypothalamus and pituitary glands of the CNS *(Flynn et al., 1981)*.

In addition to the identification of extrathyroidal CT, cross-species CT-like immunoreactive material has been identified in a range of animals spanning all animal classes *(Fischer et al., 1983; Henke et al., 1983)*. Specifically, in the human there are significant amounts of salmon CT- (sCT)- like immunoreactive material, primarily in the hypothalamus where high concentrations of calcitonin receptors (CTR) are also found *(Fischer et al., 1983)* (refer section 1.2.2.2). Similarly, in the rat brain a biologically active sCT-like peptide has been identified *(Sexton et al., 1992)*. The existence of hCT-immunoreactivity in the nervous system of pre-vertebrate animals, which do not have a bony skeleton *(Fritsch et al., 1979; Schot et al., 1981; Girgis et al., 1980)*, and the presence of sCT-immunoreactive compounds in vertebrate brains, indicates a potential role of these materials beyond calcium homeostasis and skeletal protection, for example as neurotransmitters and neuromodulators (discussed in section 1.2.4.3).

### 1.1.2 Calcitonin isolation and structure

Porcine CT was the first CT to be sequenced *(Kahn 1968; Potts et al., 1968)*, salmon CT followed *(Niall et al., 1969)* and human was isolated from a medullary thyroid carcinoma (MTC) *(Neher et al., 1968)*, which led to its sequencing. The CT

molecules which have been isolated from salmon *(Niall et al., 1969)*, eel *(Otani et al., 1976)*, goldfish *(Sasayama et al., 1993)*, chicken *(Homma et al., 1986)*, porcine *(Brewer et al., 1968)*, ovine *(Potts et al., 1968)*, human *(Neher et al., 1968)* and rat *(Raulais et al., 1976)* have been identified as 32 amino acid peptides with a carboxy terminal proline amide, that is important for activity, a disulfide bridge between cystine residues 1 and 7, and a predicted alpha helix between amino acids 8-22. Based on the amino acid sequences, the CTs from different species have been classified into 3 groups; artiodactyl, that includes porcine, bovine and ovine CT, which differ by 4 amino acids; primate /rodent group, that encompasses human and rat CT, which differ by 2 amino acids; teleost/avian group of salmon, eel, goldfish and chicken, which differ by 4 amino acids. The three-CT groups have different potencies in different systems. Generally teleost CT has greater potency than artiodactyl with respect to activating intracellular signalling pathways, with human being the least effective activator of CTR. However, the observed potency depends on the particular combination of CT and CTR, with respect to both species and isoform *(Sexton et al., 1991; Houssami et al., 1994)*.

### 1.1.3 Calcitonin gene organization and calcitonin synthesis

Following the cloning of hCT cDNA from MTC cells, a second mRNA transcript was discovered when serially transplanted rat MTC cells spontaneously changed from states of high to low CT production *(Roos et al., 1979)*. This switch was associated with the appearance of a new mRNA species from the CT gene *(Rosenfeld et al., 1982)*, termed calcitonin gene-related peptide (CGRP) *(Amara et al., 1982)*. CGRP is produced by alternative splicing of the primary RNA transcript through the use of alternative polyadenylation sites *(Amara et al., 1982)* and the

tissue mRNA expression of CT and CGRP have been found to indicate the protein produced in the tissue *(Zaidi et al., 1987)*.

The human CT gene (Calc-I) is located on the short arm of chromosome 11p14 qter *(Przepiorka et al., 1984; Hoovers et al., 1993)* and is one of 4 members of the gene family Calc-I-IV. Calc-I encodes both CT and calcitonin gene related peptide 1 (CGRP1) *(Jonas et al., 1985)*, Calc-II encodes calcitonin gene related peptide 2 (CGRP2) *(Wind et al., 1993)*, Calc-III is believed to be a pseudo-gene without known function and Calc-IV, located on chromosome 12 *(Mosselman et al., 1988)* encodes another calciotropic hormone, islet amyloid polypeptide or amylin *(Born et al., 1993)*. Amylin is a 37aa peptide hormone with a number of actions, including modulation of glycogen synthesis and glucose uptake in skeletal muscle cells *(Sheriff et al., 1992)*. Although CGRP and amylin have distinct biological effects from CT, at high concentrations they are able to mediate CT-like actions, for example inhibition of bone resorption *(Alam et al., 1993b)*. This is partly due to the cross reactivity of the receptors, and partly because of receptor modulation by accessory proteins (discussed in section 1.2.5.7).

## 1.2 Calcitonin receptors (CTR)

### 1.2.1 CTR structure

Cloning of the human CTR *(Gorn et al., 1992)* permitted homology comparisons to be performed and led to the classification of the receptor as a member of a sub family of the seven transmembrane domain (7TMD) G-protein coupled receptor (GPCR) class, which now includes receptors for parathyroid hormone (PTH), parathyroid hormone related peptide (PTHrP), secretin, growth hormone releasing hormone (GHrH), vasoactive intestinal polypeptide (VIP),

glucagon-like peptide-I, pituitary adenylate cyclase activating peptide (PACAP), gastric inhibitory polypeptide, and corticotrophin releasing factor. The CTR cDNA has an open reading frame of approximately 500 amino acids, depending on the species *(Lin et al., 1991a; Gorn et al., 1992)* and receptor isoform *(Lin et al., 1991a; Gorn et al., 1992; Kuestner et al., 1994)*. Hydrophobic plots of the CTR were consistent with 7 transmembrane domains and a signal peptide at the far N-terminus. Four potential N-linked glycosylation sites were identified in the human CTR (hCTR) and rat CTR (rCTR) cDNA, which agreed with previous reports of N-acetyl-D glucosamine residues associated with the receptor *(Moseley et al., 1983)*. Comparison of the predicted receptor size of 50kDa with the 80kDa product identified from western blot and ligand cross-linking, confirmed that the receptor was modified post-translationally *(Quiza et al., 1997)*.

Cloning of the CTR from different species led to the identification of CTR isoforms and confirmed the receptor heterogeneity proposed from cross-linking studies. The first evidence of structural heterogeneity within the CTR came with the isolation of the hCTR from a small cell ovarian carcinoma cell line *(Gorn et al., 1992)*. The hCTR amino acid sequence was 73% homologous with the porcine CTR clone, the major structural difference being the presence of a 16 amino acid insert in the first putative intracellular loop, which is not present in the porcine CTR. This receptor will be referred to hereafter as the insert positive hCTR (insert +ve hCTR). Following cloning of the insert +ve hCTR, a second hCTR clone was isolated from cells of the T47D human breast cancer cell line *(Kuestner et al., 1994)*, which lacked the 16 amino acid insert. This isoform will be referred to as the insert negative hCTR (insert –ve hCTR). The insert -ve and +ve hCTR are the dominant isoforms expressed in human tissues. The relative abundance of the insert +ve and –ve isoforms is highly

tissue specific (see section 1.2.3). Subsequently a number of receptor isoforms have been identified, which arise from alternative splicing of the primary mRNA transcript. Two human isoforms have been cloned from giant cell tumors of the bone (GCT) *(Gorn et al., 1995)* GC10 (+ve) and GC2 (-ve). These are identical to the insert +ve hCTR and insert –ve hCTR, respectively, except that they both lack 18 amino acids in the extracellular $NH_2$-terminal sequence due to the absence of a 5' in-frame initiation codon (ATG/AUG). Another isoform has been cloned from human breast carcinoma MCF7 cells, which lacks both the 16 amino acid insert in the first intracellular domain, as well as the first 47 amino acids of the amino terminus extracellular domain *(Albrandt et al., 1995)*.

CTR isoforms have also been identified in other species *(Sexton et al., 1993; Albrandt et al., 1993; Yamin et al., 1994)*. Two rat CTR's have been identified from a hypothalamic library *(Sexton et al., 1993)* and subsequently from a rat nucleus accumbens library *(Albrandt et al., 1993)*. The isoform termed C1a has 67% homology with the amino acid sequence of the porcine CTR *(Lin et al., 1991b)* and is 78% homologous to the amino acid sequence of the insert –ve human CTR. It lacks the 16 amino acid insert in the first putative intracellular loop of the insert –ve hCTR. A second rat receptor, designated C1b, has been described, and is identical to C1a except that it contains a 37 amino acid insert in the first putative extracellular loop between the second and third transmembrane domains. Two CTR isoforms have been identified from screening of a rabbit osteoclastic cDNA library *(Shyu et al., 1996)*. The first is a C1a isoform homologous to the rat receptor and the second is a novel variant known as CTRDeltae13 (CTRΔ13). This second receptor isoform lacks exon 13 that encodes the 14 amino acids of the seventh transmembrane domain

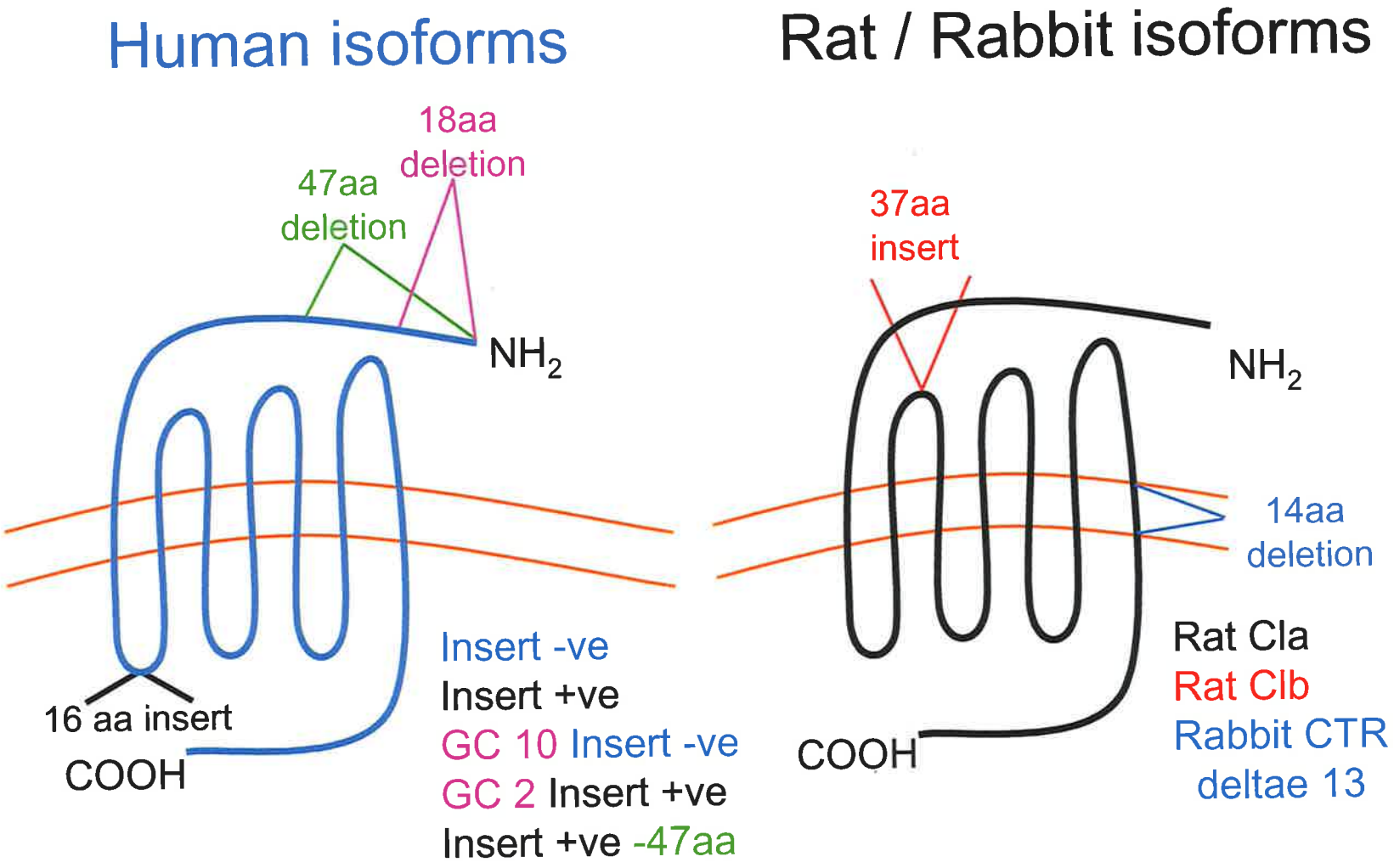


**Figure 1.1 Schematic representation of human, rat and rabbit CTR isoforms.** (discussed in section 1.2.1)

*(Shyu et al., 1996).* Figure 1.1 shows a schematic representation of the human, rat and rabbit CTR isoforms described above.

### 1.2.2 Tissue Distribution of CTR

CT binding sites have been identified using radioactively labeled calcitonin, usually iodinated salmon calcitonin ([$^{125}$I]sCT). sCT has been the CT of choice, as it has greater potency than the mammalian CTs in *in vitro* binding assays and in cell culture receptor binding and activation studies *(Findlay et al., 1983).* In addition hCT, unlike sCT, has a methionine at position 8, which becomes oxidized during iodination, resulting in the peptide's biological activity being lost. Using direct binding studies, CTR's have been identified in bone, kidney and the central nervous system, where their location and physiological significance has been characterised (discussed in section 1.2.4). In addition CT binding has been shown in other body tissues where its function has yet to be delineated (discussed in section 1.2.5.7). Described below, are specific tissues and cell lines where CTR's have been identified.

#### *1.2.2.1 Bone*

Three bone cell populations are found in mineralized bone, osteoblasts, osteocytes and osteoclasts. Multinuclear bone resorbing osteoclasts were identified to be the primary CTR expressing cells in rat bone, using direct binding assays *(Warshawsky et al., 1980).* Binding of [$^{125}$I]sCT was also observed on mononuclear bone cells, which were believed to be developing mononuclear osteoclasts and not bone forming osteoblasts *(Warshawsky et al., 1980).* These conclusions have been subsequently confirmed using immunohistochemistry in rat bone *(Rao et al., 1981).* Definitive proof that the osteoclast is the CTR expressing cell in bone came with the ability to isolate viable rat osteoclasts. Autoradiography was used to identify CTR on

multinuclear osteoclasts and mononuclear cells (presumed to be osteoclast precursors) in isolated rat osteoclast-containing cell populations *(Nicholson et al., 1986b)*.

To date the osteoclasts are the only human bone cell confirmed to express CTR. However CTR have been identified on osteoblastic and osteocytic rodent cell lines. The CTR was identified on late stage passages of a rat osteogenic sarcoma, which has subsequently been sub cloned and is known as UMR106-06 *(Forrest et al., 1985)*. The relevance of these osteoblastic cells acquiring CTR expression is not known and may simply reflect phenotypic drift due to long-term culture. Alternatively these cells may represent a phenotype along the osteoblast differentiation pathway, as [$^{125}$I]sCT binding assays on the mouse osteocyte cell line, MLO-Y4, also indicate the presence of CTR *(Plotkin et al., 1999)*. Controversy remains over the presence of CTR on bone cells other than osteoclasts. Evidence exists for the presence of CTR on osteocytic and osteoblastic cell lines, together with proposed actions (as discussed in section 1.2.4), however the expression and functional significance of CTR in osteoblasts and osteocytes *in vivo* has yet to be confirmed.

#### *1.2.2.2 Kidney*

CTR have been identified in the rat kidney using [$^{125}$I]sCT binding *(Marx et al., 1972; Sexton et al., 1987)*. Binding was most intense in the medulla over the thick ascending limb of the loop of Henle, in the cortex and in the proximity of the distal convoluted tubule *(Sexton et al., 1987)*. These findings have subsequently been confirmed by polymerase chain reaction (PCR) performed on mRNA extracted from different regions of the rat nephron *(Firsov et al., 1995)*. More recently, studies have addressed the CTR distribution in the primate kidney using radioligand [$^{125}$I]sCT *(Chai et al., 1998)*. The CTR distribution is preserved across the rodent and primate

species, with high density binding of [$^{125}$I]sCT in the primate cortex over the distal tubule, and low density binding in the medulla in the region of the thick ascending limb of the loop of Henle and at the juxtaglomerula apparatus *(Chai et al., 1998)*.

#### *1.2.2.3 Central nervous system*

[$^{125}$I]sCT binding studies performed on human *(Fischer et al., 1981b)*, monkey *(Christopoulos et al., 1995)*, rat *(Koida et al., 1980; Rizzo et al., 1981; Fischer et al., 1981a; Nakamuta et al., 1981; Henke et al., 1983; Henke et al., 1985)*, sheep *(Sexton et al., 1991)* and cat *(Guidobono et al., 1987)* brain preparations indicated the existence of CT-binding sites in the brain. Comparison of binding distribution between different species revealed a great deal of similarity, with the highest CT binding being located in the hypothalamus. More recently, the localization of CTR mRNA in the mouse brain has been confirmed using *in situ* hybridization *(Nakamoto et al., 2000)*.

#### *1.2.2.4 Primary cancers and cancer cell lines*

Binding studies have identified CTRs in numerous transformed cells and cell lines, including cell lines derived from human breast *(Findlay et al., 1980b; Martin et al., 1980)*, lung *(Findlay et al., 1980a; Hunt et al., 1977)*, prostate *(Shah et al., 1994)* and bone *(Nicholson et al., 1987)* cancers. In addition CTR expression has been shown by reverse transcription polymerase chain reaction (RT-PCR) in primary breast cancers *(Gillespie et al., 1997)* and *via* [$^{125}$I]sCT binding in prostate tumors *(Shah et al., 1994)*.

#### *1.2.2.5 CTR expression in other tissues*

CTR have been identified using receptor binding assays in a number of other sites including the human lymphoid system *(Marx et al., 1974)*, placenta *(Nicholson et al., 1988)* and testicular Leydig cells *(Chausmer et al., 1982)*. In addition receptor

expression has been investigated using RT-PCR and CTR mRNA reported in a range of human tissues *(Kuestner et al., 1994)*. The physiological significance of the CTR/CT system in these tissues is currently unknown. However the recent evidence showing that receptor activity modifying proteins (RAMPS) are able to modify the CTR, such that it has increased affinity for amylin, indicates that the CTR may respond physiologically to a peptide hormone other than CT (discussed in section 1.2.5.7).

### 1.2.3 Differential expression of CTR isoforms

Heterogeneous CT binding sites, were initially identified when two apparent receptor populations were identified in the rat brain from binding studies using helical and non-helical sCT and hCT analogues *(Nakamuta et al., 1990)*. Cloning of the rat C1a and C1b isoforms (discussed in section 1.2.1), followed by RT-PCR analysis *(Sexton et al., 1993)*, confirmed the presence of both of these CTR isoforms in rat brain. Binding studies using sCT had failed to distinguish these two receptor populations, as both receptor isoforms demonstrate high affinity for this ligand, but were found to vary significantly in their affinity for hCT *(Houssami et al., 1994)*. The use of alternative ligands in binding studies made it possible to identify two receptor populations with respect to their binding specificity and kinetics. The C1a receptor isoform has reduced affinity for hCT compared with sCT, while the C1b isoform fails to bind hCT *(Houssami et al., 1994)*. In addition to the C1a and C1b CTR receptors, sCT has high affinity for the C3 amylin receptor in the rat brain *(Beaumont et al., 1993)*. The C3 amylin receptor has until recently been an unidentified receptor known to couple to cAMP *(Sheriff et al., 1992)*. The identification of RAMPS and their ability to change the affinity of the CTR for calciotropic peptides, suggests the amylin receptor is a modified CTR (discussed in section 1.2.5.7). Binding studies

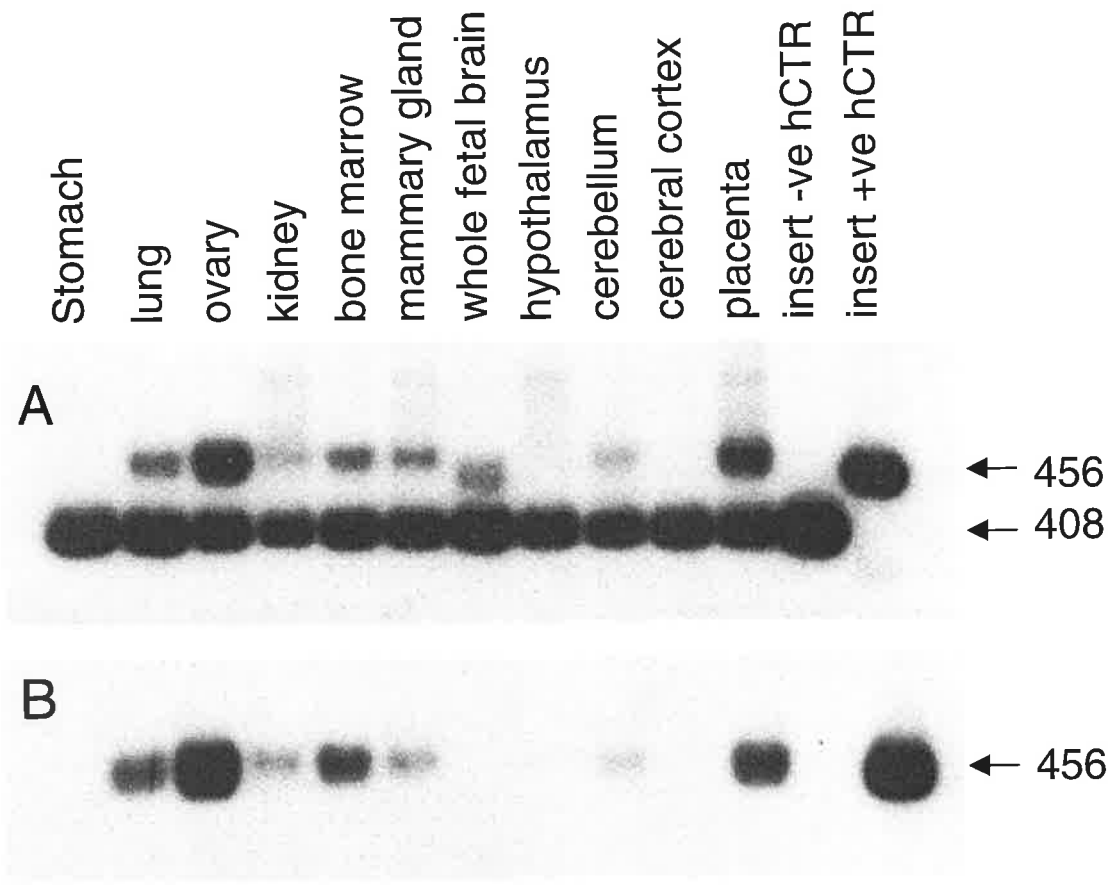


**Figure 1.2 Tissue specific distribution of hCTR receptor isoforms**

This figure is reproduced from Kuestner *et al.*, 1994. cDNAs prepared from the indicated human tissues were PCR amplified using primers that flank the cDNA region containing the hCTR insert. Panel A and B are Southern blots; panel A was hybridized with a probe that recognizes both forms of the hCTR receptor, and panel B was hybridized with a probe that is specific for the insert +ve hCTR. The size of the product amplified from the insert -ve hCTR was 408 base pairs and the product from the insert +ve hCTR was 456 base pairs.

show the C3 amylin receptor is co-expressed in the rat brain with the C1a CTR, supporting the proposal that the C3 amylin receptor is a modified CTR. However the C3 amylin receptor is also expressed uniquely in regions of the accumbens nucleus and fundus striati of the rat brain *(Hilton et al., 1995)*, suggesting that the identity of the amylin receptor remains to be fully elucidated.

In the human there is tissue specific expression of CTR isoforms, although they are different molecular species from those in the rat. As mentioned previously, two isoforms of the CTR predominate in the human, the insert -ve isoform *(Kuestner et al., 1994)* and the insert +ve isoform *(Gorn et al., 1992)* (discussed in section 1.2.1). RT-PCR analysis of human tissues identified CTR expression in a wide range of tissues and organs (figure 1.2) *(Kuestner et al., 1994)*. Interestingly, the ratio of CTR isoform expression varied significantly across the different tissues investigated. The insert –ve hCTR was more abundantly expressed in most tissues compared with the insert +ve isoform *(Kuestner et al., 1994)*. The two notable exceptions to this were in the reproductive organs, the placenta and ovaries, which show comparable levels of expression of both the insert –ve and +ve isoforms *(Kuestner et al., 1994)*. The physiological significance of this differential receptor isoform expression has yet to be determined, but the ability of RAMPS to alter the binding characteristics of the CTR (discussed in section 1.2.5.7) and receptor cross modulation (discussed in chapter 9) are possibilities that remain to be investigated.

### 1.2.4 Actions of calcitonin

The best known action of CT is its ability to lower serum calcium by inhibiting bone resorption. This hypocalcaemic effect of CT was originally tested in rats and was reported to decrease with increasing animal age *(Cooper et al., 1967)*. In adult humans the hypocalcaemic effect of CT appears to be limited to individuals

experiencing high bone turnover for example Paget's disease *(Martin et al., 1969)*. Thus CT may not be a vital calciotropic hormone in adult physiology, however may be essential to calcium homeostasis during times of rapid bone metabolism i.e. growth, pregnancy and lactation.

The CT/CTR system has been identified in a number of other cell types and tissue sites, both in developing *(Jagger et al., 1999)* and mature animals *(Kuestner et al., 1994)*, which are not involved in calcium homeostasis. Thus it appears possible that CT has physiological roles outside those of calcium metabolism. Specific examples are discussed below that illustrate the diversity of the known and potential actions of the CT/CTR system.

#### *1.2.4.1 Bone*

The initial experiments performed in rats, showed that CT treatment reduced hydroxyproline excretion (a by-product of collagen degradation), indicating that CT reduced bone resorption *(Martin et al., 1966)*. Subsequent *in vitro* and *in vivo* studies, reviewed by Martin *et al.* (1997), have identified that CT inhibits bone resorption by acting directly on bone resorbing osteoclasts. For example, CT induces loss of the osteoclastic ruffled border *(Kallio et al., 1972; Singer et al., 1976)* and cytoplasmic retraction *(Chambers 1982)*.

The actions of CT on osteoclasts are accepted. However controversy remains over the effects of the hormone on osteoblasts. An early *in vivo* experiment in adult rats, involving pre-loading of the animals with $^{45}Ca$ and then treatment with CT, showed that CT treatment lowered plasma calcium, but failed to alter the plasma levels of $^{45}Ca$ *(Robinson et al., 1967)*. This finding suggested that the physiological calcium-regulating action of CT in bone is specific for inhibition of bone resorption, with no effect on osteoblastic bone formation. This theory was subsequently

supported by the finding that CT did not increases bone formation in the adult rat skeleton *(Kalu et al., 1971)*. However, *in vitro* experiments have shown that CT can increase the alkaline phosphatase activity and stimulate proliferation of both chicken and murine osteoblastic cell lines *(Farley et al., 1988)*, in addition to human osteoblast cell lines *(Farley et al., 1991)*. The current lack of evidence confirming the presence of CTR on osteoblast cells *in vivo* (discussed section 1.2.2.1), makes it difficult to understand how CT influences these cells.

The influence of CT on osteocytes also remains controversial. There is an historic report that CT is able to act on osteocytes *(Matthews et al., 1972)*, differentiated osteoblastic cells that are embedded in the mineralized matrix at regularly spaced intervals. As mentioned above, a recent report shows the expression of the CTR by an osteocyte cell line *(Plotkin et al., 1999)*, in which the authors claimed that CT has an anti-apoptotic effect on osteocytic cells. The implication of these findings is that CT protects the osteocyctic network and thus its ability to detect and instigate repair of microdamage. The end result of this would be maintenance of bone integrity and strength that is independent of bone mineral density. This mechanism may explain how CT treatment decreases fracture risk without increasing bone mineral density.

#### *1.2.4.2 Kidney*

A number of actions of CT in the kidney have been reported and are reviewed in *(Martin et al., 1998)*. These *in vivo* studies suggest that CT has many effects on the kidney, however the CT concentrations and the experimental conditions used in these studies were often pharmacological, and thus the specific physiological significance of these findings is not clear. However, CT was found to increase renal clearance of calcium by inhibiting reabsorption of calcium in the ascending limb of the

loop of Henle and the distal collecting duct *(Cochran et al., 1970)*, a mechanism agreed to be important in the CT reversal of hypercalcaemia of malignancy *(Hosking et al., 1984)*. These findings suggest that this renal action of calcitonin is biologically relevant.

CT has been reported to stimulate expression of the 25-hydroxyvitamin $D_3$ 1α-hydroxylase in the rat and mouse kidney *(Kawashima et al., 1981; Murayama et al., 1999; Shinki et al., 1999)*, suggesting that CT is involved in the regulation of vitamin D production in these animals. Shinki *et al.* (1999) showed that this effect was occurring in the proximal tubule of the kidney, however CTRs have not been detected in this region of the kidney by either autoradiography *(Sexton et al., 1987)* or RT-PCR *(Firsov et al., 1995)* so that the mechanism of this CT-mediated action is not clear.

#### *1.2.4.3 Central nervous system*

The CT/CTR system has a number of different components in the CNS. For example in humans, there are several hCTR isoforms (section 1.2.2), sCT-like immunoreactive material (section 1.1.1) and various molecular species of circulating hCT. The presence of these components indicates the potential for diverse interactions between the CTR and their potential ligands, and thus varied biological actions of this hormone in the CNS.

Central administration of sCT induces significant analgesic *(Morimoto et al., 1985)* and anorexic *(Yamamoto et al., 1982)* effects in rats, indicating a potentially important role for this hormone centrally. However, to date, these functional studies of CT in the rat CNS have principally used sCT, which binds with high affinity to C1a, C1b and the C3 amylin binding sites *(Beaumont et al., 1993; Sexton et al., 1994)*, thus blurring whether CT or amylin mediate the reported effects *in vivo* (refer section 1.2.5.7).

With respect to the analgesic actions of CT, these appear to be specifically CT-mediated, as amylin is unable to mimic the effect of sCT *(Sexton et al., 1994)*. In addition to this ligand specific functional response, the central localization of CTR in the periaqueductal grey, an important region in the central regulation of pain, indicates that these analgesic actions are CT-mediated *(Guidobono et al., 1986; Fabbri et al., 1985)*. The recent identification of mouse CTR mRNA in serotonergic neurons, which are known to project into the spinal cord, forming a decending inhibitory system against pain transmission, also strongly supports a central analgesic role of CT *(Nakamoto et al., 2000)*.

Anorexia is not exclusively induced by sCT, but is also an action of amylin *(Chance et al., 1992)*. In the rat brain, amylin binding sites have an almost 100% overlap with C1a CTR binding sites *(Sexton et al 1994; Hilton et al., 1995)*. These findings, together with the now recognized role of RAMPs in altering the CTR's phenotype, such that it can preferentially bind amylin (refer section 1.2.5.7), strongly suggest that the anorectic effect observed with sCT administration may be pharmacological and that amylin is the physiological ligand at these receptor sites in the mammalian brain.

#### *1.2.4.4 Proliferation*

There are several reports of regulation by CT of cell proliferation, in a variety of cell types, including porcine kidney cell line LLC-PK *(Dayer et al., 1981; Jans et al., 1987)*, human osteoblastic cells *(Farley et al., 1991)* and human gastric carcinoma KATO III *(Nakamura et al., 1992)*, breast *(Ng et al., 1983)*, and prostate *(Shah et al., 1994; Ritchie et al., 1997)* cancer cell lines. The direction of regulation appears to be cell type-specific. The influence of CT on prostate cancer cells may be dependent on androgen receptor status, with CT decreasing proliferation of androgen

receptor-negative PNCaP cells *(Shah et al., 1994)* but inducing proliferation in androgen receptor-positive Du145 and Pc3 cell lines. Treatment of porcine LLC-PK *(Dayer et al., 1981; Jans et al., 1987)* and human breast cancer *(Ng et al., 1983)* cell lines with CT inhibits cell proliferation, but the same treatment is mitogenic in osteoblast-like osteosarcoma cells *(Farley et al., 1991)*. The specific physiological significance of these findings are unknown, but in the instances where CT treatment is anti-proliferative, a greater understanding of the mechanisms involved, may pave the way to use the hormone in cancer therapy.

#### *1.2.4.5 Calcitonin involvement in blastocyst implantation*

Extrathyroidal production of CT has been reported in the rat uterus *(Zhu et al., 1998a)*. Blocking CT function in the uterus with CT antisense oligonucleotides significantly decreased the number of blastocysts that successfully implanted into the mouse uterus, suggesting a direct role for CT in regulating blastocyst implantation *(Zhu et al., 1998a)*. In addition, CT treatment of isolated blastocysts induced an elevation in intracellular calcium that is involved in blastocyst differentiation *(Wang et al., 1998)*. Taken together, these data provide evidence that CT is able to regulate cell decisions associated with growth and differentiation *in vivo*.

### 1.2.5 Regulation of the CTR "phenotype" by receptor activity modifying proteins (RAMPS)

As discussed previously, identification of the gene encoding the receptor for the calciotropic hormone amylin, has been elusive. The identification of human receptor activity modifying proteins (RAMPs), which are single transmembrane proteins involved in the transport of the calcitonin receptor-like receptor (CRLR) to the cell surface, revealed a class of proteins able to interact with this receptor and change the CRLR "phenotype" to that of an adrenomedullin receptor *(McLatchie et*

*al., 1998).* The use of chimeric RAMPs showed that the receptor glycosylation status of CRLR was altered with RAMP association and that this correlated with the receptor phenotype, as assessed by radioligand binding *(Fraser et al., 1999).*

The involvement of RAMPs in altering the CTR phenotype has been addressed. Specifically, co-transfection of rabbit aortic endothelial cells with the insert –ve hCTR and RAMP 1 or 3 decreased the binding of [$^{125}$I] hCT to the cells, while increasing the binding of [$^{125}$I]amylin *(Muff et al., 1999).* These results implied a potential action of RAMPs in changing the insert –ve hCTR from a CTR phenotype to that of an amylin receptor. Subsequently, these findings have been confirmed in COS-7 cells *(Christopoulos et al., 1999).* In addition, Christopoulos *et al.* (1999) performed cross-linking experiments with [$^{125}$I]amylin, which suggested a cell surface association of RAMP 1 and the insert –ve hCTR *(Christopoulos et al., 1999).* Chimeric proteins of the amino and carboxy terminals of RAMP proteins have been used to identify the specific RAMP domains, which determine the receptor phenotype *(Zumpe, et al., 2000).*

Currently, the published data on RAMP-induced phenotypic changes relate to the insert –ve hCTR. However co-transfection of RAMP 1 or 2 with the insert +ve hCTR dramatically improves binding of [$^{125}$I]amylin (Dr Patrick Sexton, personal communication). Similarly, the Cla rCTR, when co-expressed with RAMP 1, produces an amylin receptor phenotype (Dr Patrick Sexton, personal communication). The ability of RAMPs to change the CTR phenotype has implications for identifying functions of the CTR receptors, as the possibility exists that these receptors have a modified phenotype and respond to ligands in addition to, or other than, CT.

### 1.2.6 Regulation of CTR

Regulation of the CTR has been studied in cell lines endogenously expressing the CTR *(Findlay et al., 1981)*, transfected cell lines *(Houssami et al., 1994; Houssami et al., 1995; Findlay et al., 1996; Moore et al., 1995)* and cultured mouse *(Wada et al., 1994; Wada et al., 1996a; Wada et al., 1996b)* and human (Wada ASBMR 1999) osteoclasts. In addition to regulation by ligand-independent agents, for example glucocorticoids *(Wada et al., 1994; Wada et al., 1997)*, the CTR is also regulated by CT itself. Ligand activation of the CTR induces a reduction in the specific binding of [$^{125}$I]sCT on the surface of osteoclastic, non-osteoclastic and transfected cells expressing the CTR. The specific mechanism of receptor internalization by CT is still unknown, but is likely to involve clathrin-coated pit endocytosis, as described for other GPCRs, reviewed in Bünemann *et al.*, (1999). The initial event in GPCR desensitization involves phosphorylation of the agonist occupied receptor by a G-protein coupled receptor kinase (GRK). Receptor phosphorylation promotes the binding of β-arrestin proteins to the receptor, which results in the uncoupling of the receptor from G-protein complexes, thus terminating the receptor signalling. In addition, β-arrestins initiate receptor internalisation, targeting the receptor to clathrin coated pits *(Bünemann et al., 1999)*. The process of clathrin-coated pit endocytosis has not been confirmed for the CTR, however the C-terminal tail of the CTR is important for receptor internalisation. Specifically, C-terminal truncation of the porcine CTR inhibited receptor internalisation *(Findlay et al., 1994)*, and ligand activation of the hCTR induced phosphorylation at the receptor C-terminus *(Nygaard et al., 1997)*. The specific kinases responsible for phosphorylation of the hCTR are unknown, but the PKA and PKC kinases activated by ligand binding are apparently not directly involved *(Nygaard et al., 1997)*. The

GRK2 protein influences cell surface expression of the CTR and regulates the receptors signalling ability in chinese hamster ovary cells *(Horie and Insel 2000)*. This recent finding provides strong evidence to suggest that the ligand regulation of the CTR may involve clathrin-coated pit endocytosis.

CT activates PKA- and PKC-mediated signalling pathways, which are involved in receptor regulation. In the mature mouse osteoclast, the loss of CTR expression on the cell surface was PKA-mediated and the process was associated with a decrease in CTR mRNA levels *(Wada et al., 1996a)*. Recent studies by Inoue *et al.*, suggested that the reduction in CTR mRNA, was not due to reduced mRNA stability, but rather suppression of receptor transcription *(Inoue et al., 1999)*. This mechanism of CTR regulation is not universal, since in non-osteoclastic cells, ligand induced loss of CTR expression on the cell surface was shown to be independent of PKA and of changes in steady state levels of CTR mRNA *(Findlay et al., 1996)*. The signalling pathway involved in the regulation of hCTR in human osteoclasts has recently been reported, and unlike the mouse system, CTR mRNA levels are regulated through the PKC pathway *(Samura et al., 1999)*. These findings indicate that the mechanism of ligand induced CTR regulation is dependent on the species from which the receptor originates and the cellular context in which the receptor is expressed. In addition, the specific CTR isoforms influence the ability of CT to regulate receptor internalization (as discussed in chapter 3).

### 1.2.7 Signal transduction

#### *1.2.7.1 G-Proteins*

Figure 1.3 depicts schematically the events involved in extracellular ligand activation of G-protein signalling pathways, reviewed in Bünemann *et al.*, (1999). G proteins are heterotrimeric molecules that bind to guanine nucleotides on the inner

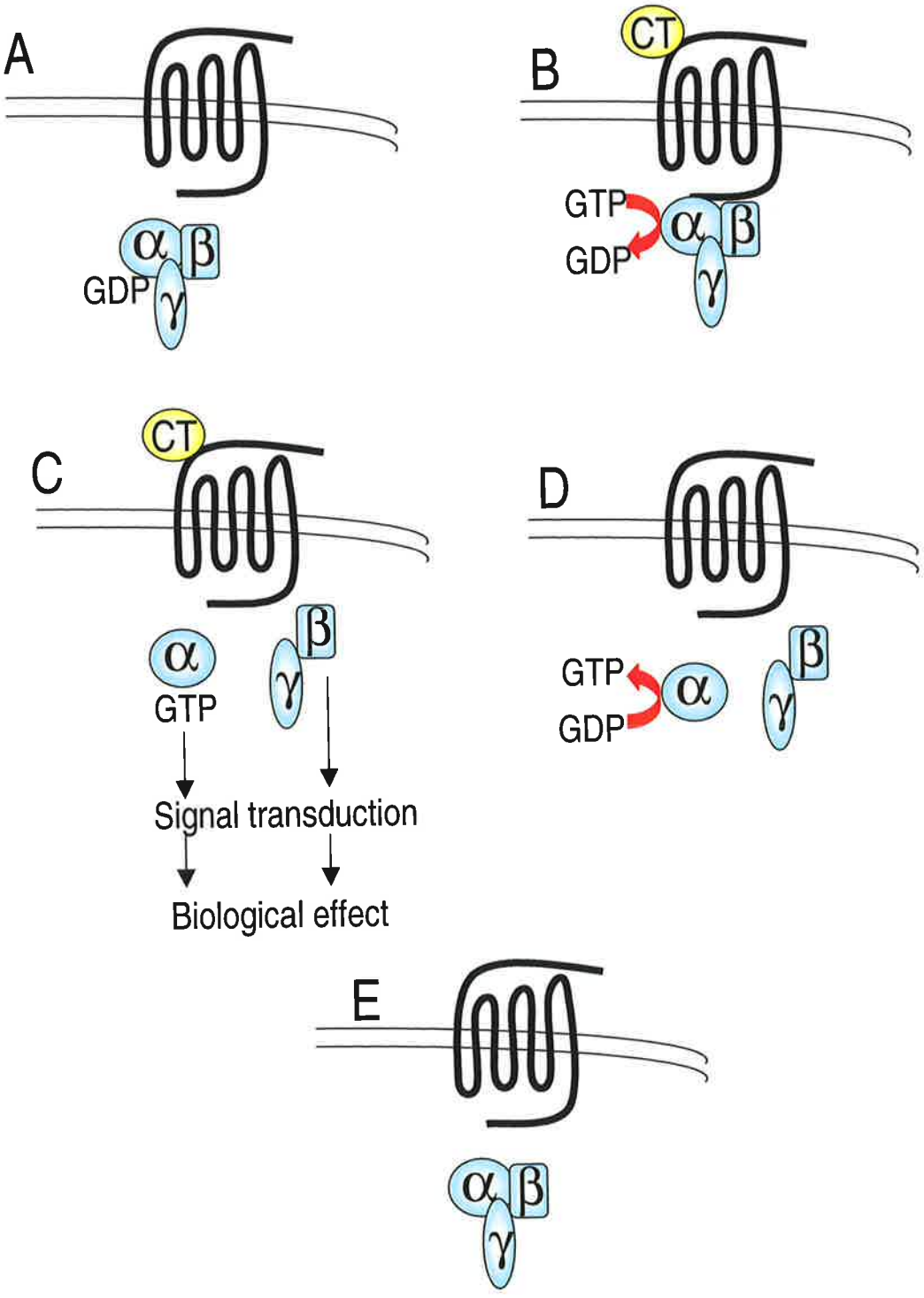


**Figure 1.3 Diagramatic representation of G-protein activation.**

(discussed in section 1.2.7.1)

side of the plasma membrane and consequently transfer signals from the cell surface receptors to various intracellular effector molecules. G proteins consist of α, β and γ subunits, as shown schematically in figure 1.3A. Binding of the receptor ligand changes the conformation of the transmembrane helices, in turn altering the conformation of the intracellular loops and exposing the G-protein binding sites. Binding of the trimeric G-protein to the receptor-binding site induces exchange of GDP for GTP on the α subunit and thus dissociates the α subunit from the βγ dimer, simultaneously activating it (figure 1.3B). The α and βγ subunits are free to activate intracellular effectors within the cell (figure 1.3C), for example adenylate cyclases, phospholipases, phosphodiesterases, ion channels and ion transporters. Termination of this activation state occurs following hydrolysis of GTP by the intrinsic GTPase activity of the α sub-unit (figure 1.3D) and hence re-association of the α-GDP to the βγ dimer (figure 1.3E) *(Bünemann et al., 1999)*.

Currently, over 16 distinct α sub-units have been identified and they are divided into 4 classes, Gαs, Gαi/o, Gαq, Gα12, each of which contain multiple isoforms. Similarly, there are multiple different β and γ sub-units described *(Gutkind 1998)*. The initial proposed action of the βγ dimer was to increase the affinity of the α sub-unit for GDP and induce de-activation of the stimulated α-GTP. However there is now abundant evidence that indicates that the βγ dimer has signalling ability and independently activates cellular effector proteins *(Sternweis 1994)*, for example $K^+$ channels *(Logothetis et al., 1987)*, adenylate cyclase *(Taussig et al., 1993)*, phospholipase C *(Camps et al., 1992)* GPCR kinases *(Boekhoff et al., 1994)* and the MAPK pathway. It is the multiplicity of these α, β and γ sub-units, which allows for much diversity and specificity of signal transduction within eukaryotic cells.

#### 1.2.7.2 CTR activation of G-proteins

#### *1.2.7.2.1 CTR activation of the adenylate cyclase / cAMP pathway*

Two classes of G-proteins regulate adenylate cyclase activity, $G\alpha_s$ and $G\alpha_i$ subunits. $G\alpha_s$ subunits elevate intracellular cAMP *via* activation of adenylate cyclase (figure 1.4 & 1.5) and $G\alpha_i$ subunits negatively regulate adenylate cyclase, and inhibit cAMP accumulation (figure 1.4 &1.5).

##### *1.2.7.2.1.1 Involvement of Gαs subunits*

In bone, CT binds to the CTR on the surface of osteoclasts causing an elevation in intracellular cAMP *(Nicholson et al., 1986a)*. Simultaneously there is a decrease in cell motility and bone resorbing activity *(Chambers 1982; Su et al., 1992)*. The cAMP analogue dibutyryl cAMP and the adenylate cyclase activator forskolin, had previously been shown to mimic the CT inhibition of bone resorption *(Chambers et al., 1983)*. These findings confirm the involvement of the cAMP pathway in transducing the anti-resorptive CT effect.

CT-mediated cAMP production has also been reported in a number of kidney cell preparations *(Murad et al., 1970; Marx et al., 1975)* and in renal epithelial cells *(Chao et al., 1983)*. CT-induced adenylate cyclase activity has been reported in the medullary and cortical areas of the thick descending limb of the Loop of Henle, and in the proximal end of the collecting duct, of the human nephron *(Chabardes et al., 1980)*. Experiments performed in preparations of isolated distal tubules from rabbit kidneys suggest that the CT-mediated elevation of cAMP in kidney cells is required for CT-mediated calcium re-absorbtion in the kidney *(Zuo et al., 1997)*.

In the central nervous system there have been reports of CT-induced cAMP activation, which are species specific. In rat, but not mouse membrane preparations of brain cells, high concentrations of hCT stimulated cAMP (Loffler *et al.,* 1982). sCT was unable to activate cAMP in these rat brain preparations, and inhibited cAMP

production when used at high concentrations *(Rizzo et al., 1981; Nicosia et al., 1986)*. In contrast, experiments performed on fetal rat hypothalamic cells have convincingly reported an increase in cellular cAMP in response to sCT treatment within the same concentration range. The authors suggested that these divergent results may be due to the different experimental preparations used, and that intact cells may be required for functional activation of adenylate cyclase. Alternatively the recent reports on the ability of RAMPS to change the CTR phenotype to that of an amylin receptor (as discussed previously in section 1.2.5), provide a possible explanation for the lack of cAMP accumulation in response to physiological concentrations of sCT.

CT-induction of cAMP has also been reported in a number of cell lines including human cancer cell lines of the lung *(Findlay et al., 1980a)*, breast *(Michelangeli et al., 1983; Ng et al., 1983)* and prostate *(Shah et al., 1994)* and UMR106-06 rat osteosarcoma cells *(Forrest et al., 1985)*. There is evidence that the cAMP-dependent protein kinase type I isoenzyme (PKA I), is involved in the regulation of cell growth, while differential activation of PKA II promotes cell differentiation *(Cho Chung 1990)*. CT treatment of BEN and UMR106-06 cells activated both cAMP isoenzymes *(Zajac et al., 1984; Forrest et al., 1985)*. However in T47D breast cancer cell lines, CT was found to activate only the type 2 isoenzyme of PKA, which correlated with a reduction in cell proliferation *(Ng et al., 1983)*. cAMP accumulation was also reported to initiate the transduction pathway, by which sCT inhibits cell growth in LLC-PK1 epithelial renal cells *(Jans et al., 1987)*. The growth inhibitory effect observed in LLC-PK1 cells was not seen in a cell clone which lacked cAMP dependent protein kinase activity or another clone that lacked CTR, indicating

that the growth response was receptor mediated and dependent on cAMP-dependent protein kinase in these cells *(Jans et al., 1987)*.

Generation of hybrid insulin-like growth factor II and CT receptors, in which the insulin-like growth factor II receptors Gi-interacting domain was substituted with either the C-tail residues 404-418 or third intracellular domain of the porcine CTR, identified that these regions of the CTR are involved in activation of the cAMP pathway *(Orcel et al., 2000)*. This technique provides an alternative approach to the conventional deletion analysis of CTR's. The use of an alternative ligand and ligand-dependent binding sequence in the receptor, eliminates the issues of altering CT binding kinetics and allows the sequences signalling potential to be assessed independently.

#### *1.2.7.2.1.2 Involvement of Gαi subunits*

Intracellular cAMP accumulation is negatively regulated by $G\alpha_i$ protein, as indicated in figures 1.4 & 1.5. Several CT-induced effects have been reported to be insensitive to PTX, for example the CT-mediated elevation in cAMP in human breast cancer cells *(Michelangeli et al., 1984)* and the anti-nocioceptive activity of CT in the CNS *(Guidobono et al., 1991)*. Interestingly in LLC-PK1 renal epithelial cells $G\alpha_i$ proteins have been shown to be selectively activated by CT during the S phase of the cell cycle *(Chakraborty et al., 1991)*. Thus, in the LLC-PK1 cell system, the specific activation of G-protein signalling pathways by CT was dependent on the phase of the cell cycle. When cells were synchronised in the G2 phase of the cell cycle, CT-treatment elevated intracellular cAMP, an effect that could be replicated using artificial activators of adenylate cyclase and cAMP analogues. When the LLC-PK1 cells were synchronised in S phase of the cell cycle, the CT-induced elevation in cAMP was dramatically reduced. Co-treatment with CT and PTX during S phase restored the cAMP response, indicating that CT was able to activate Gi proteins

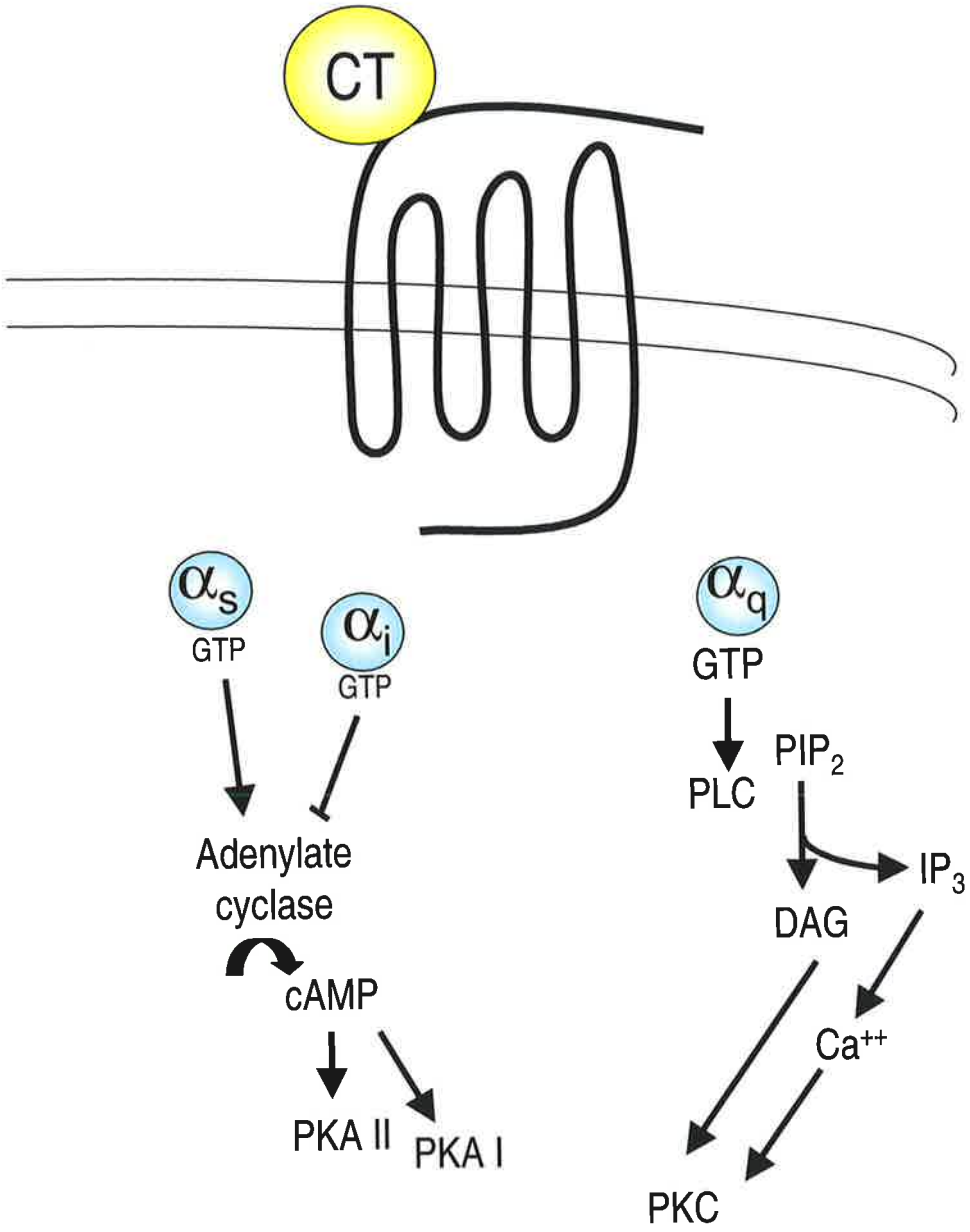


**Figure 1.4 G-protein subunit and second messenger systems that the CTR was known to couple to or activate, prior to 1997.**

during S phase *(Chakraborty et al., 1991)*. Taken together, these studies indicated that the hCTR can couple to the Gi signalling pathway (as shown in figure 1.4). This was the extent of evidence describing CT activation of Gi G-proteins prior to commencement of the present study in 1997.

Understanding of the activation of Gi G-proteins by CT has developed in the last few years and the current understanding is summarised in figure 1.5. CT dependent activation of Erk1/2 has now been reported in HEK-293 cells stably transfected with C1a rabbit CTR. This effect was partially sensitive to PTX *(Chen et al., 1998)*. In this system, activation of adenylate cyclase was not involved in the phosphorylation of Erk1/2. However, the authors used a dominant negative approach to inhibit activity of the $\beta\gamma$ subunits of the $G_i$ protein complex, and showed convincingly the involvement of this subunit in the activation of the Erk1/2 signalling pathway *(Chen et al., 1998)*. Further investigation into the CT activation of $G\alpha_i$ subunits, using myc-tagged rabbit CTRs, has confirmed the ability of CTR to directly interact with the $G\alpha_i$ subunit *(Shyu et al., 1999)*. Interestingly, the simultaneous activation of PKC by CT in HEK-293 cells, was found to inhibit the $G\alpha_i$ subunit ability to negatively regulate adenylate cyclase *(Shyu et al., 1999)*. This negative regulation of the $G\alpha_i$ subunit *via* PKC is likely to explain why some cAMP-mediated actions of CT are insensitive to PTX.

#### *1.2.7.2.2 CTR activation of PKC*

Receptor mediated activation of the $G\alpha_q$ family of G-protein subunits activates PLC *(Lee et al., 1992)*, which in turn mediates the hydrolysis of inositol phospholipids to diacylglycerol (DAG) and inositol triphosphate ($IP_3$) *(Dunlay et al., 1990)*, as shown in figure 1.4 and 1.5. DAG increases the affinity of the PKC enzyme for calcium and

phospholipids, leading to activation of the multifunctional serine/threonine kinase PKC.

The ability of CT to elevate inositol phosphate (IP) production was initially demonstrated in mouse MC-3T3 cells *(Force et al., 1992)* and human HEK-293 cells *(Chabre et al., 1992)* transfected with the porcine CTR. These reports implied that CT was a potential activator of PKC. Functional evidence showing that CT activation of PKC induced biological actions, came from a study on isolated rat osteoclasts, where the use of specific synthetic inhibitors and activators of PKC were found to respectively block and mimic, the CT-induced inhibition of bone resorption *(Su et al., 1992)*. The specific G-protein mechanism by which CT activates the PLC-PKC pathway was only confirmed recently *(Offermanns et al., 1996)*. Co- transfection of $G\alpha_q$ and CTR cDNA constructs into COS-7 cells dramatically increased the ligand dependent inositol phosphate production, suggesting that the CTR was able to directly interact with the $G\alpha_q$ subunit to induce activation of the PLC signalling pathway *(Offermanns et al., 1996)*. The specific PKC isoenzymes responsible for the CT-mediated effects are currently unknown, however some of the PKC isoenzymes activated by CT have been identified. Specifically CT is known to induce significant membrane translocation of PKC$\alpha$, and to a lesser extent PKC$\zeta$ isoenzmes, but not the PKC$\delta$ isoenzyme *(Naro et al., 1998)*. Additionally, it now appears that CT-mediated activation of phospholipids is not restricted to PLC, but also includes PLD *(Naro et al., 1998)* (as shown schematically in figure 1.5).

#### *1.2.7.2.3 CTR mobilisation of Intracellular calcium*

Mobilization of intracellular calcium in response to ligand binding involves a rapid transient increase in intracellular calcium due to 1,4,5-inositol triphosphate ($IP_3$) induced release of calcium from intracellular stores *(Berridge et al., 1989)*.

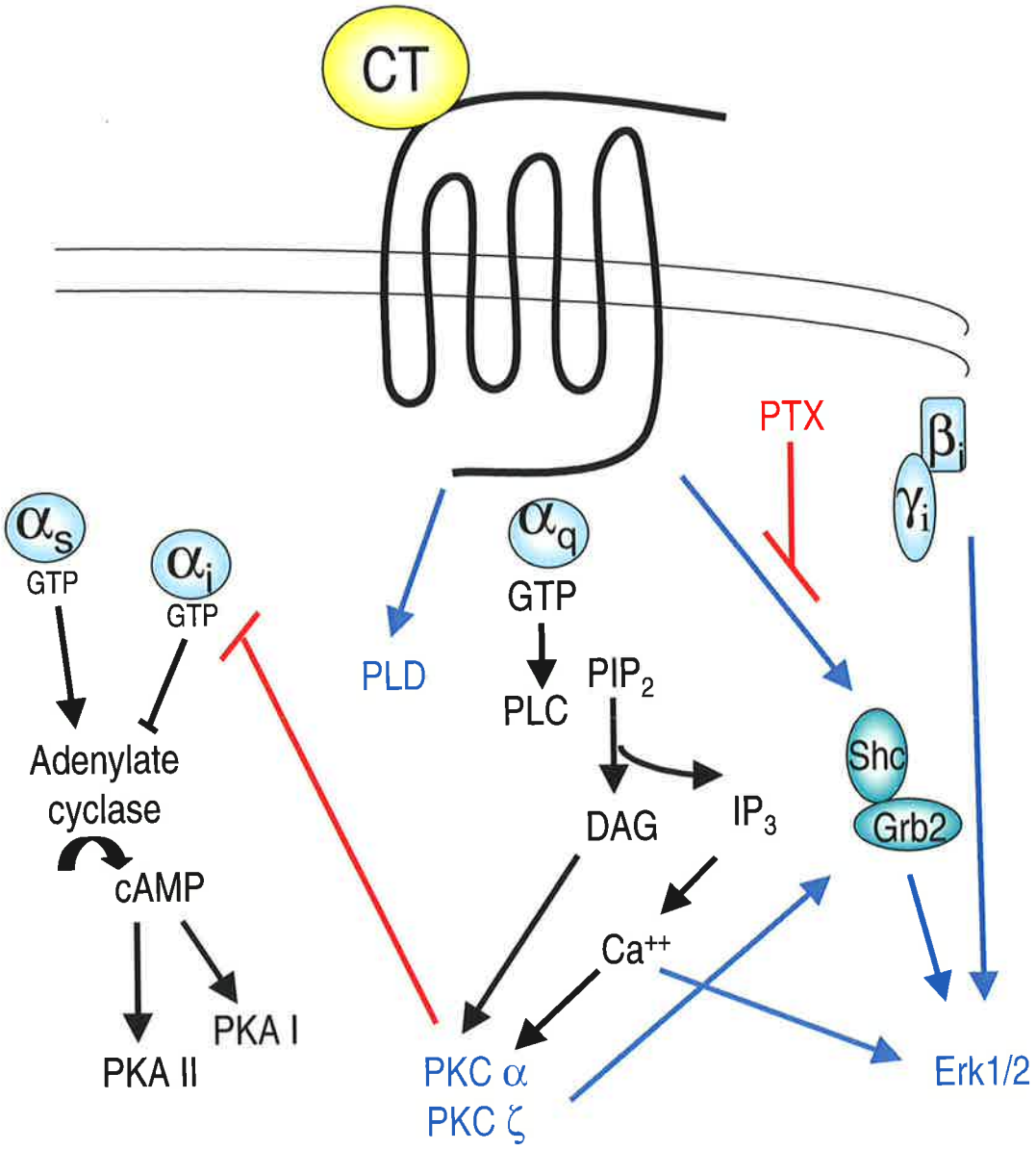


**Figure 1.5 G-protein-mediated second messenger systems that the CTR is currently known to couple to or activate, as of July 2000.**

Treatment of osteoclasts with CT, induces a biphasic elevation of intracellular calcium *(Moonga et al., 1992)*. This initial CT-induced elevation in intracellular calcium occurs independently of extracellular calcium *(Malgaroli et al., 1989)*. However, the second phase of the CT-mediated calcium flux is a longer sustained increase in intracellular calcium due to the influx of calcium from the extracellular fluid *(Moonga et al., 1992)*. The use of transfected cell systems has subsequently shown that the CTR participates in receptor- activated calcium inflow, in which depletion of intracellular calcium pools leads secondarily to influx of extracellular calcium *(Findlay et al., 1995; Stroop et al., 1995)*. Initially, the involvement of extracellular calcium in the CT-induced elevation of intracellular calcium led to the hypothesis that the CTR may be a calcium sensing receptor *(Stroop et al., 1993)*. However this theory has subsequently been disproven *(Teti et al., 1995)*, and the observations are likely to reflect the receptor-activated calcium channel operation described for other receptor systems *(Findlay et al., 1995; Lu et al., 1996)*.

In bone, the anti-resorptive properties of CT are partially due to the intracellular calcium fluxes *(Zaidi et al., 1990; Alam et al., 1993a)*. CT-induced calcium fluxes have also been reported in the thick ascending limb of the rabbit renal tubule *(Murphy et al., 1986)*. However in mouse brain synaptosome preparations CT treatment has been reported to paradoxically increase and decrease intracellular calcium under different experimental conditions *(Welch et al., 1991)*. These studies show a functional role for calcium signalling in bone and suggest a potential role for CT in regulating biological actions *via* intracellular calcium signals in both the kidney and the CNS.

### 1.2.7.3 hCTR isoform activation of G-Proteins

As discussed in section 1.2.3, most human tissues and cells express both isoforms of the hCTR *(Kuestner et al., 1994)*. In order to understand the biology of the individual receptors, it is therefore necessary to use model systems, in which cloned receptor isoforms are transfected into cells. These experimental systems have shown that the hCTR isoforms have different signalling potential. The insert –ve hCTR is able to activate the adenylate cyclase/cAMP pathway, when it is expressed in COS *(Nussenzveig et al., 1994)*, BHK *(Moore et al., 1995)*, and HEK cells (chapter 3). Activation of this signalling pathway by the insert +ve hCTR is, however, dependent on the particular transfected cell model used. CT was unable to induce a cAMP signal when the insert +ve hCTR was expressed in HEK-293 cells (chapter 3). However, when expressed in COS *(Nussenzveig et al., 1994)* and BHK *(Moore et al., 1995)* cells, the insert +ve hCTR produced a CT-dependent elevation in cAMP, albeit with an $EC_{50}$ for CT stimulation of adenylate cyclase much greater when compared to the same cells expressing the inset –ve hCTR. The cell type also influences the maximal activation of adenylate cyclase induced by the CTR isoforms. Expression of the insert +ve hCTR in COS cells resulted in a greatly reduced maximal CT-stimulated adenylate cyclase activation compared to COS cells expressing the insert –ve hCTR *(Nussenzveig et al., 1994)*. In comparison, the maximal activation of adenylate cyclase by CT was the same in BHK cells transfected with either the insert +ve or -ve hCTR *(Moore et al., 1995)*.

The ability of the hCTR isoforms to elevate intracellular calcium is not dependent on cell type. The insert –ve hCTR is able to mediate an elevation of intracellular calcium when expressed in HEK (chapter 3) and BHK *(Moore et al., 1995)* cells and increase production of IP in the context of COS cells *(Nussenzveig et*

*al., 1994)*. However, the insert +ve hCTR is unable to mediate increased intracellular calcium or activation of IP in any transfected cell model examined to date.

## 1.3 Cell growth

There is extensive literature pertaining to cell growth, and the following account is a brief summary highlighting the information relevant to the studies undertaken here.

### 1.3.1 The cell cycle

In the process of replicating itself, a mammalian cell progresses through a "cell cycle", as shown schematically in figure 1.7. Prior to replication, a cell contains a single copy of its nuclear DNA in GAP phase 1 (G1). Extracellular signals induce cell cycle progression and DNA synthesis, such that replication ensues in synthesis (S) phase. Chromatid separation follows and division of the cell into two daughter cells takes place in Mitosis (M) phase. The S and M phases are separated by intervals of cytoplasmic growth and re-organization GAP phases (G1 and G2). Having completed mitosis, cells may exit cell cycling and enter a quiescent state called Go, reviewed in Pestell *et al.,* (1999).

### 1.3.2 Regulation of the cell cycle

Progression through the cell cycle is regulated by at least two independent mechanisms (figure 1.6). The cell is propelled forward through the cell division cycle by a cascade of protein phosphorylations, which regulate the timing of progression *(Collins et al., 1997)*. Cyclins are regulatory molecules expressed periodically during the cell cycle, that bind to and activate cyclin dependent kinases (CDKs). The active CDK/cyclin complexes then alter gene transcription to allow the cell to progress through the cell cycle *(Sherr 1994)*. For example, in G1 phase of the cell cycle, cyclin

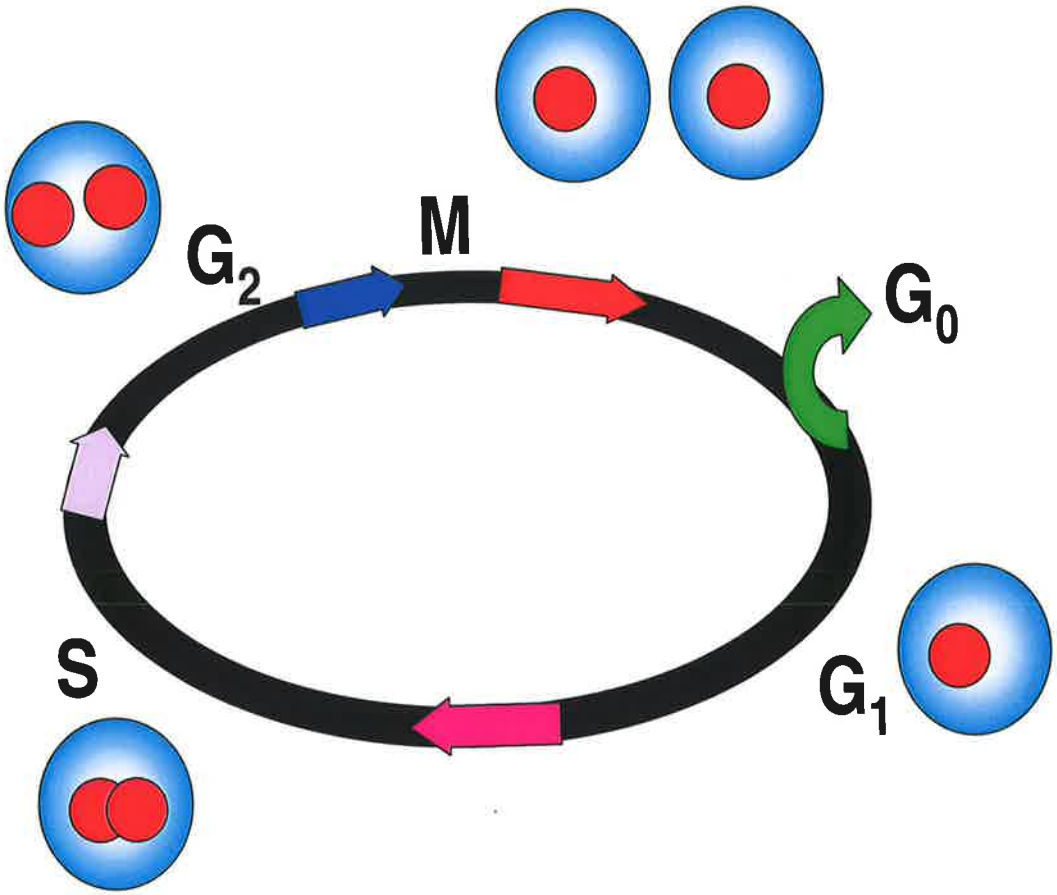


**Figure 1.6 Schematic representation of the eukaryotic cell cycle.**

(discussed in section 1.3.1)

D1 binds to and activates CDK4 and CDK6, and phosphorylation of the retinoblastoma protein Rb follows. Subsequent to this initial phosphorylation of Rb, the cyclin E/CDK2 complex further phosphorylates Rb, allowing release of the E2F transcription factors, which promote transcription of genes required for the cells to progress into S phase (shown schematically in figure 1.7) *(Pestell et al., 1999)*.

The cell cycle is also negatively regulated by cellular checkpoints that delay progression through the cell cycle. The G1/S and G2/M checkpoints are shown schematically in figure 1.7. Delay of cell cycle progression can be instigated in response to DNA damage *(Weinert 1998)*. However cessation of DNA replication and cell proliferation are also required for cellular differentiation to occur *(Coffman et al., 1999)*. Thus physiological regulatory molecules, such as cyclin dependent kinase inhibitors (CKI's) (discussed in section 1.3.2.1 and chapter 6) and non-physiological stimuli, for example DNA damaging agents *(Weinert 1998)* can block cell proliferation at the G1/S and G2/M boundaries.

### *1.3.2.1. The G1/S check-point*

Arrest at the G1/S cell cycle interface is perhaps the best understood cell check-point. The CKI p21, can induce G1/S cell cycle arrest *via* several different mechanisms. Firstly, binding of p21 to the CDK2/cyclinD1 and CDK4/cyclinD1 complexes inactivates them *(Harper et al., 1995)* and prevents the phosphorylation of retinoblastoma (Rb) protein *(Weinberg 1995)*. Hypophosphorylated Rb binds to and represses the activity of transcriptional factors, for example E2F, thus blocking expression of genes required for progression into S phase *(Almasan et al., 1995)*. Alternatively the CKI p21 can associate with the proliferating cell nuclear antigen (PCNA), which is required for DNA polymerase δ activity, and inhibit DNA replication *(Chen et al., 1995)* or block nucleotide excision repair of DNA *(Pan et al., 1995)*.

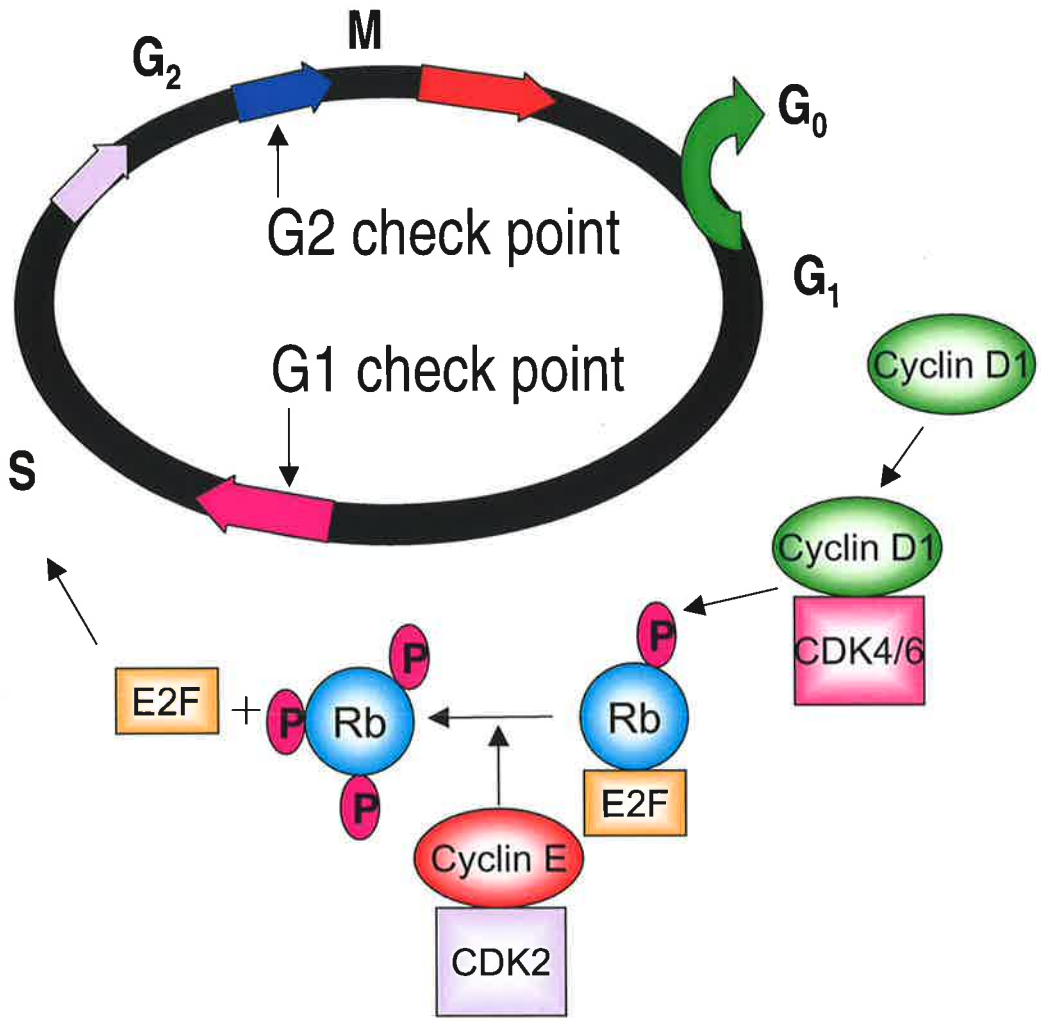


**Figure 1.7 Schematic representation of the G1/S and G2/M cell cycle check points.** Diagramatic depiction of the cyclin and CDK molecules involved in the progression form G1 to S phase of the cell cycle, (described in section 1.3.2).

#### *1.3.2.2 The G2/M check-point*

The G2/M checkpoint is poorly understood in comparison to the G1 checkpoint and is important in halting cell cycle progression following DNA damage during replication *(Aguda 1999)*. For a cell to progress from G2 into mitosis (M phase) the cyclin dependent kinase (CDK) cdc2 must be activated, an event that has several pre-requisites. The priming of cdc2 requires it to bind to cyclin B1, which is expressed during late G2, and to become phosphorylated on threonine 161 *(Desai et al., 1992)* (figure 1.8A). Cdc2 activation then requires the de-phosphorylation of both threonine 14 and tyrosine 15 *(Krek et al., 1991)*. The phosphorylation and de-phosphorylation of threonine 14 and tyrosine 15 is performed respectively by the kinase wee1 and the phosphatase cdc25 *(Sebastian et al., 1993)*, as shown in figure 1.8B. As a critical amount of cdc25 becomes active the cdc2/cyclin B1 complex is activated, which inhibits the activity of wee1. The current theory suggests that these events are self-perpetuating, continuing until there is sufficient active cdc2/cyclin B1 present, when the cell proceeds from G2 into mitosis (M phase) *(Aguda 1999)* (figure 1.8B).

The specific mechanisms involved in a G2/M arrest are currently under investigation, however the G1/S CKI, p21, has been implicated in G2 cell cycle arrest *(Bunz et al., 1998)*, as discussed in chapter 6.

### 1.3.3 Cell surface receptor-mediated regulation of cell growth

Regulation of cellular growth has historically been understood to be a function of tyrosine kinase (TK) "growth factor" receptors, such as EGF and PDGF receptors *(Johnson et al., 1994)*. Activation of these receptors in turn activates mitogen-activated protein kinase (MAPK) pathways. MAPK's are serine threonine kinases that transduce environmental signals from cell surface to the nucleus.

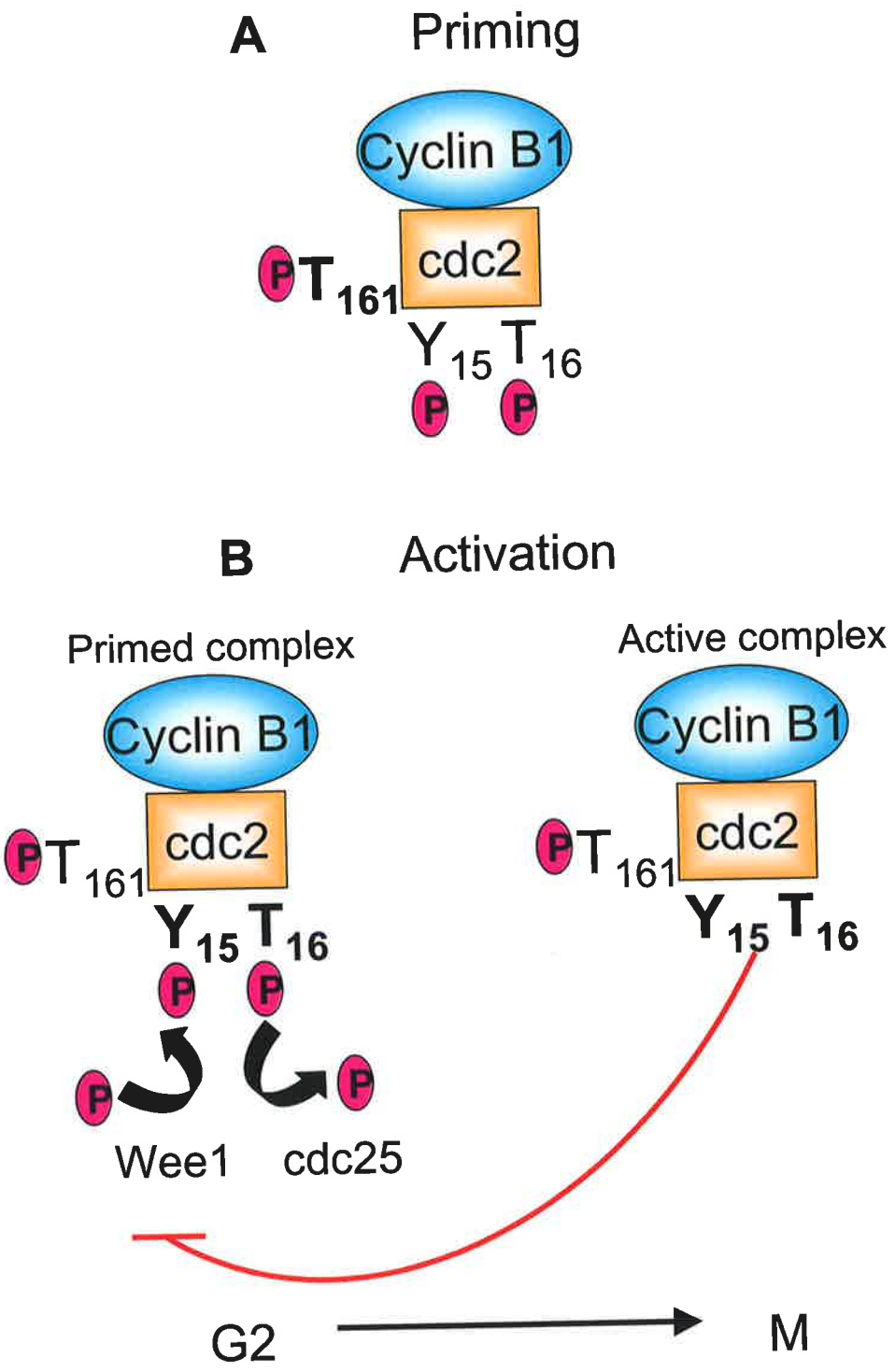


**Figure 1.8 Schematic representation of the G2/M transition in Eukaryotic cells.** (discussed in section 1.3.2.2)

Several MAPK subfamilies have been identified, including Erk, p38 and c-Jun N-terminal kinase (JNK). Perhaps the most well characterised of these MAPK pathways is the extracellular signal regulating kinase (Erk1/2 p44/p42), which influences a wide variety of cellular functions, including normal cell proliferation *(Powers et al., 1999)*, tumorigenesis *(Mansour et al., 1994)*, cell differentiation *(Herrera et al., 1998)* and development *(Alessandrini et al., 1997)*. Seven transmembrane G-protein coupled receptors, the largest known family of cell surface receptors, have also been shown more recently to regulate cellular growth *via* activation of the Erk1/2 pathway *(van Biesen et al., 1996)*.

#### 1.3.3.1 Tyrosine kinase receptor activation of Erk1/2

Classical TK receptors are single membrane spanning subunits with intrinsic TK activity and their ability to activate the Erk1/2 signalling pathway is well characterised. The specific events involved in Erk1/2 activation outlined below are reviewed by van Biesen *et al.*, (1996). Ligand binding and dimerisation of receptors leads to autophosphorylation on specific tyrosine (Y) residues. Figure 1.9 shows the MAPK pathway involved in the activation of the Erk1/2. Phosphorylation of specific tyrosine residues converts them into high affinity binding sites for Src homology 2 (SH2) domain sequences, which are encoded in different proteins. The binding of the SH2 domain protein Shc to TK receptors leads to recruitment of Sos, a Ras guanine nucleotide exchange factor that complexes with Grb2 *via* an SH3 domain. The Grb2/Sos complex is then translocated to the plasma membrane where Sos is able to interact with the membrane bound Ras-GDP and activate it by catalyzing the exchange of GDP for GTP. Active Ras-GTP interacts with and activates the serine-threonine protein kinase Raf-1, the first of three protein kinases in the MAPK cascade. Raf-1 activates the mitogen activated protein kinase kinases (MAPKK)

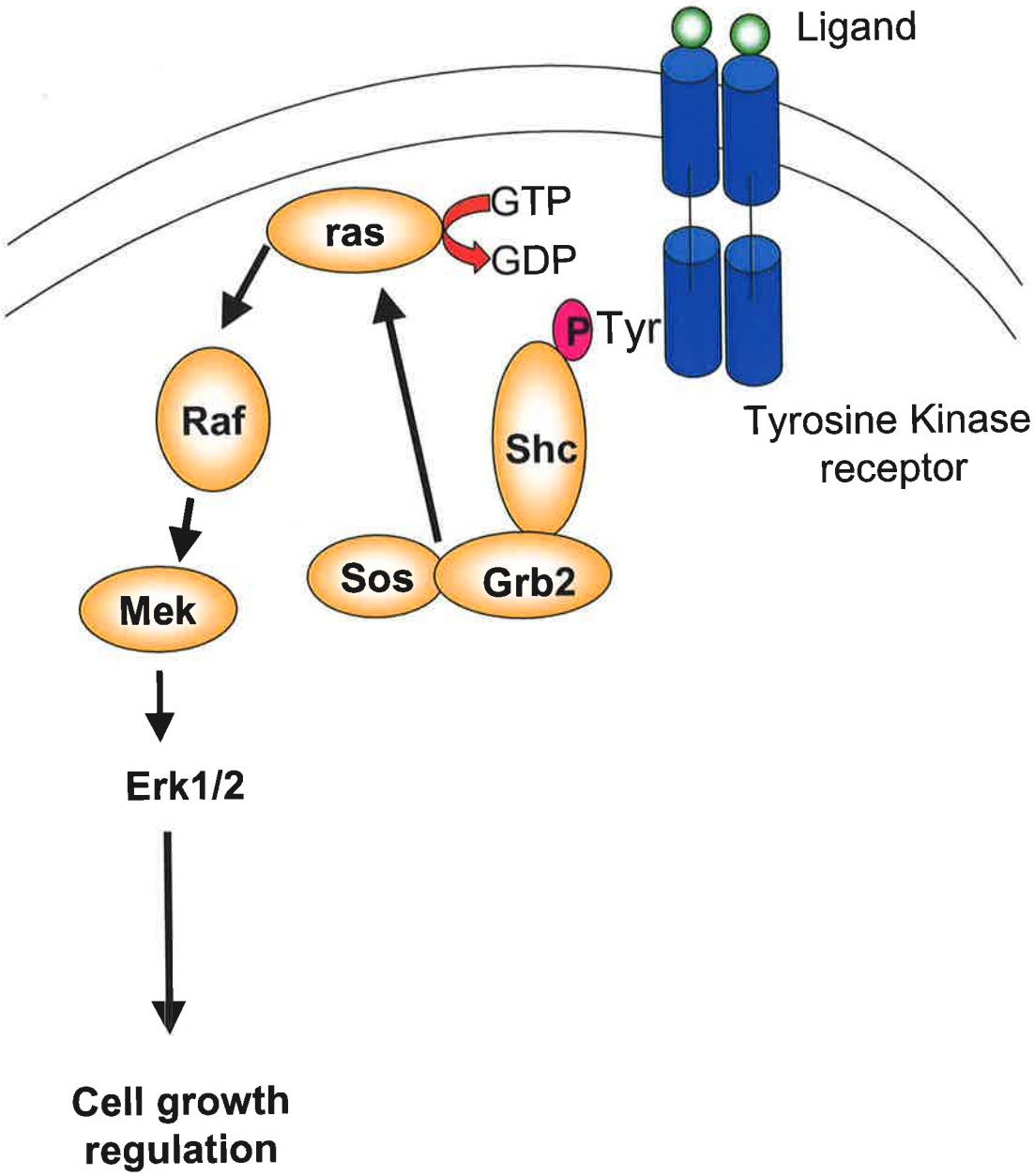


**Figure 1.9 Schematic representation of tyrosine kinase receptor activation of the Erk1/2 MAPK pathway.**

(discussed in section 1.3.3.1)

MEK1/2, which in turn phosphorylate the MAPK Erk1/2. Once activated, Erk1/2 are translocated to the nucleus where they interact with transcription factors to alter gene expression and thus regulate cell proliferation. The signal is ultimately terminated by de-phosphorylation of Erk1/2 by specific phosphatases *(van Biesen et al., 1996)*.

#### 1.3.3.2 G-protein coupled receptors

In the late 1980's the observation that the proliferative response of thrombin was sensitive to PTX *(Chambard et al., 1987)* suggested that G-protein coupled receptors, and specifically the Gi proteins, were involved in the regulation of cell growth. The identification of G-protein gain-of-function mutations in human endocrine tumors and in other human diseases, reviewed in Dhanasekaran *et al.,* (1995), further implicating a role for these GPCR in growth regulation.

Initial studies investigating the signal transduction pathways involved in GPCR growth regulation focused on the classical GPCR second messenger systems, for example adenylate cyclase *(Chabre et al., 1995)*. Evidence discussed extensively in reviews by van Biesen *et al.,* (1996) and Gutkind (1998) confirm that these GPCR signalling pathways are able to "cross-talk" with, and activate, MAPK pathways to regulate cell growth and differentiation.

##### 1.3.3.2.1 G-protein coupled receptor activation of MAPK

Several GPCR induced growth effects are sensitive to PTX, indicating the involvement of the Gi protein complex in this response. For example, the GPCR ligands, substance P and substance K *(Nilsson et al., 1985)*, thrombin *(Vouret Craviari et al., 1993)* and bombesin *(Letterio et al., 1986)* induce PTX-sensitive growth responses in cell culture systems. Subsequently, Gi-coupled GPCR have been shown to activate molecules within the Erk1/2 cascade *(van Biesen et al., 1995)*, in a similar manner to the tyrosine kinase receptors, by phosphorylating the

Shc adaptor protein (refer section 1.3.3.1). For example, the PTX-sensitive Gi coupled G beta gamma and alpha 2-C10 adrenergic receptors (AR) phosphorylate Shc in response to ligand activation *(Touhara et al., 1995)*.

Recently, interaction between Shc, Grb and Erk1/2 activation has been shown for the CT/CTR system. CT activation of the rabbit CTR was shown to induce phosphorylation of Shc, Shc/Grb association and Erk1/2 phosphorylation in HEK-293 cells *(Chen et al., 1998)*. These events were partially sensitive to PTX and use of the β-adrenergic receptor kinase 1 (βARK1ct) inhibitor, which prevents $G\beta\gamma_i$ signalling, prevented the CT-mediated Erk1/2 phosphorylation. However activation of Erk1/2 was not exclusively dependent on the $G\beta\gamma_i$ subunit, but also required the $G\alpha_q$ signalling pathways, PKC and calcium. Chemical activation of the PKC and intracellular calcium fluxes significantly dampened the CT-induced phosphorylation of Erk1/2, but was unable to completely abrogate the effect *(Chen et al., 1998)*. Thus the ability of the CTR to activate Erk1/2 in HEK-293 cells is dependent on multiple G-protein coupled pathways, which interact with the MAPK signalling cascade. Despite these investigations into the CT-induced activation of Erk1/2, there is no evidence as to the cellular consequences of this pathway with respect to growth.

## 1.4 Aims of this thesis

This chapter has outlined the current knowledge of the CT/CTR system with respect to its biological actions and the intracellular pathways activated by ligand binding. The concept of the cell cycle, and the mechanisms by which it is regulated have been introduced. GPCR regulation of growth has been discussed and evidence presented showing that GPCR, and in particular the CTR, activate the MAPK pathway. At the commencement of this project the CTR was known to regulate the

growth of several human cancer cell lines. Initial investigations of the signalling pathways involved in these specific cellular systems had been reported. However the specific receptor isoforms involved in this process were unknown. Thus there were three aims for this project.

**1. To develop and characterise transfected human cell models that express the insert +ve and insert -ve hCTR, independently.**

**2. To use this transfected system to investigate the ability of the insert +ve and insert -ve hCTR to regulate cell growth.**

**3. To assess the cellular and molecular mechanisms by which CT-mediated growth inhibition occurs.**

# Chapter 2

# Experimental materials and methods

## 2.1 Materials

### *2.1.1 General chemicals and reagents*

#### *2.1.1.1 The chemicals and reagents listed below were obtained from Sigma Chemical Co. Ltd., St Louis, MO, USA.*

Ampicillin
β-glycerophosphate
β-mercaptoethanol
Bovine serum albumin (BSA)
Bromophenol Blue
Chloramine T
Dextran Sulphate
Dithiothreitol (DTT)
Ethylene Glycol-bis (β-aminoethyl Ether) (EGTA)
Ethylenediaminetetraacetic acid (EDTA)
Ethidium Bromide
Formamide
Giemsa
Hepes
Herring sperm DNA
MOPS
Magnesium chloride
PolyoxyethyleneSorbitanMonolaerate (Tween 20)
Potassium chloride
Potassium Iodine
Phenol
Phenylmethylsulfaonyl Fluoride (PMSF)
Propidium iodide
Sephadex $G_{50}$
SDS
Sodium bicarbonate
Sodium chloride
Sodium Vanidate
Triton-X-100
Tris-HCl

#### *2.1.1.2 The general chemical and reagents listed below were obtained from BDH Laroratory Supplies*

Acetic acid
Ethanol
Chloroform
Dimethyl Sulphoxide (DMSO)
formaldehyde
Glycerol
Methanol
Sodium Bicarbonate
Sodium Hydroxide

### *2.1.1.3 Sources of other routinely used chemicals:*

| | |
|---|---|
| Agarose DNA grade<br>Low melt agarose | Progen Industries, QLD, Aust |
| ATP | Roche Diagnostic, Castle Hill, NSW, Aust |
| Fura-2AM | Calbiochem, La Jolla, CA, USA |
| Histone H1 | Roche Diagnostic, Castle Hill, NSW, Aust |
| Lipofectin | Gibco BRL, Glen Waverly, Vic, Australia |
| Protein A-sepharose | Amersham Pharmacia Biotech, Buckinghamshire, UK |
| Diploma Instant Skim Milk | Bonlac Foods Ltd, Vic, Australia |
| TRIZOL Reagent | Gibco BRL, Glen Waverly, Vic, Australia |
| QUSO | North American Silica Company, NJ, USA |

### *2.1.2 Intracellular signalling chemicals*

*The following chemicals used in the intracellular signalling experiments where purchased from Sapphire Bioscience Pty. Ltd. NSW, Australia. The manufacturer is listed below.*

*BIOMOL Research Laboratories Inc., PA, USA.*
8-Br cAMP
Chelerythrine chloride
Cytochalasin D
Forskolin

H-89 N-[2-(p-Bromocinnamylamino) ethyl] -5-isoquinolinesulfonamide-2HC

LY-294002 2-(4-Morpholinyl)-8-phenyl-4H-1-benzopyran-4-one

PD-98059

U7-3122 1- (6-((17β-3-methoxyestra-1,3,5(10)-trien-17-yl) amino) hexyl) –1H-pyrrole-2,5-dione

W7 N- (6-Aminohexyl) -5-chloro-1-naphthalene-Sulfonamide-HCl

*List Biological Laboratories Inc., CA, USA*

Pertussis toxin

*Tocris, MO, USA*

U1026

### *2.1.3 Synthetic peptides*

Human CT, salmon CT and 8-32 salmon CT were all purchased from Peninsula Laboratories Inc. CA, USA. The peptides were stored lypholised at 4°C on arrival. Prior to use, the peptides were dissolved in 0.01 M acetic acid and then stored in 10 ul aliquots at -20°C, until required.

### *2.1.4 Enzymes*

*The enzymes used in this study were obtained from the following companies*

| | |
|---|---|
| Calf intestinal phosphatase | New England Biolabs, MA, USA |
| Proteinase K | Roche Diagnostic, Castle Hill, NSW, Aust |
| RNAse | Roche Diagnostic, Castle Hill, NSW, Aust |
| T4 DNA ligase | Promega Biosciences Inc. Madison, WI, USA |

| | |
|---|---|
| Hind III | New England BioLabs, Beverly, MA, USA |
| Xba I | New England BioLabs, Beverly, MA, USA |

### *2.1.5 Antibodies*

| | |
|---|---|
| *Mouse monoclonal antibodies* | |
| Erk1/2 phosph (# 9105S)<br>Cdc2 phospho Tyr15 (#9111S) | New England BioLabs, Beverly, MA, USA |
| Erk1 (clone E16220)<br>P21 (clone C24420)<br>P27 (clone K25021) | Transduction Laboratories Inc., Lexington, KY, USA |
| P53 (clone PAB18001) | Zymed Laboratories Inc., San Fancisco, CA, USA |
| *Rabbit polyclonal antibodies* | |
| Cyclin B1 (H-433)<br>Cdc2 (C-19)<br>Rb (C-15)<br>P21 | Santa Cruz Bio-technology Inc., Santa Cruz, CA, USA |
| Anti-mouse and Anti-rabbit Alkaline phosphotase conjugate | Amersham Pharmacia Biotech, Buckinghamshire, UK |

### 2.1.6 Radionucleotides

[$\alpha$-$^{32}$P] dCTP, 3000Ci/mM, [$\gamma$-$^{32}$P] dATP, 3000Ci/mM, were all purchased from GeneWorks, SA, Australia.
[$^{125}$I], 100mCi/ml was purchased from Amersham Pharmacia Biotech, Buckinghamshire, UK

### 2.1.7 Kits

| | |
|---|---|
| β-Galactosidase Enzyme Assay System | Promega Biosciences Inc. Madison, WI, USA |
| Luciferase Assay System | Promega Biosciences Inc. Madison, WI, USA |
| Purification of PCR products (Wizard PCR preps DNA purification system) | Promega Biosciences Inc. Madison, WI, USA |
| Oligolabelling of DNA (Giga prime kit) | GeneWorks, SA, Australia |
| Plasmid Isolation Kit | GeneWorks, SA, Australia |
| Measurement of intracellular cAMP CAMP enzyme immunoassay kit | Amersham Pharmacia Biotech, Buckinghamshire, UK |
| Vistra ECF reagent kit | Amersham Pharmacia Biotech, Buckinghamshire, UK |

### *2.1.8 Solutions and buffers*

| | |
|---|---|
| HeBes (10x) | 5 g Hepes, 8 g NaCL, 0.125 g $Na_2HPO_4.2H_2O$, 1 g glucose, make to 100ml |
| DNA lysis solution | 10 mM Tris (pH8.0), 5 mM EDTA, 100 mM NaCl, % SDS, 10 mg/ml proteinase K, 200 µg/ml RNase A |
| DNA loading buffer (6X) | 0.25% bromophenol blue, 40% (w/v) sucrose in $H_20$ |
| Binding buffer | DMEM, 0.1% BSA |
| Elution buffer | 0.15 M NaCl, 0.05 M glycine (pH2.5) |
| RNA loading buffer (2X) | 50% formamide, 6.2% formaldehyde, 10% glycerol, 30 µg/ml ethidium bromide |
| MOPS buffer (10X) | 0.2 M MOPS, 50 mM Na acetate, 10mM EDTA |
| 0.3M $Na_2P0_4$ buffer | 8ml 0.6M $NaH_2P0_42H_20$ , 42ml $Na_2HP0_4.12H_20$ and 50ml $H_20$ |
| SSC | 3 M NaCl, 0.3 M Na citrate, (pH7.0) |
| Protein lysis solution<br>Greatful thanks are extended to Dr Mathew O'Connell for providing this protocol. | 25mM MOPS (pH 7.2), 60mM β-glycerolphosphate, 15mM $MgCl_2$, 5mM EGTA, 1mM DTT, 0.1mM Na Vanidate, 1% Triton X-100, 1mM PMSF |

| | |
|---|---|
| Western sample buffer | 12mM Tris-HCl (pH 6.8), 6% SDS, 10% β-mercaptoethanol, 20% glycerol, 0.03% bromophenol blue |
| Western running buffer (10X) | 29.0g Tris Base, 144g Glycine, 10.0g SDS in a 1l of $H_20$ |
| Western transfer buffer | 1.45g Tris Base, 7.21g Glycine, 200ml methanol in 1l of $H_20$ |
| Western blocking solution | PBS (1X), 0.1% Tween 20, 5% skim milk powder |
| Western washing solution | PBS (1X), 0.1% Tween 20 |
| Kinase assay buffer | 50 mM Tris-HCl (pH 7.4), 10 mM $MgCl_2$, 1 mM Dithiothreitol |

### *2.1.9 Bacterial media*

| | |
|---|---|
| L-broth | obtained from Media Production IMVS |
| L-agar plates | L-broth, 1.5% Bacto agar |
| L-amp | Poured into culture plates and allowed to set<br>L-broth, 1.5% Bacto agar, Ampicillin (50µg/ml)<br>Poured into culture plates and allowed to set |

### 2.1.10 *Antibiotics*

| | |
|---|---|
| G418 sulphate (Geneticine, Neomycine) | Bibco BRL, Glen Waverley, Vic, Australia |
| Penicillin and Streptomycin | Obtained from the IMVS media production area |

### *2.1.11 Bacterial strains*

| | |
|---|---|
| JM109 | Promega Biosciences Inc. Madison, WI, USA |

### *2.1.12 Plasmid vectors*

| | |
|---|---|
| pRc/CMV | Invitrogen, Carlsbad, CA, USA |
| Zem 228CC vector containing the insert-negative human calcitonin receptor | A kind gift from Zymogenetic Inc. WA, USA |
| pHz1 expression vector containing the insert positive human calcitonin receptor | A kind gift from Zymogenetics Inc. WA, USA |
| pGL2-Basic vector | Promega Biosciences Inc. Madison, WI, USA |

### *2.1.13 Plasmid reporter constructs*

Plasmid reporter constructs used in this study are listed below and the source from which they were obtained is indicated. Specific details on the constructs are discussed in chapter 7 section 7.2 and where applicable diagrams indicate the specific deletion and mutation sites.

| | |
|---|---|
| WWP-Luc | A kind gift from Dr B Vogelstein, John Hopkins Medical School. |
| PwwP<br>pWP124<br>pWP101<br>pWPdel-Sem1<br>pWP101-mt Sp1-3<br>pWP101-mt Sp1-4<br>pWP101-mt Sp1-5-6<br>pWP101-mt TATA<br>Sp1-mut | Kind gifts from Dr Sowa, Kyoto Prefectural University of Medicine, Kyoto. |
| Sp1-wild | A kind gift from Dr Peggy J Farnham McArdle Laboratory for Cancer Research, University of Wisconsin, Madison. |
| pRcCMV-βgalactosidase | A kind gift from J Woodcock, Hanson Centre for Cancer Research |

### *2.1.14 Cloned DNA sequences used as Northern blot probes*

| | |
|---|---|
| Human $p21^{WAF1/CIP1}$ cDNA | A kind gift from Dr Helena Richardson The University of Adelaide, SA, Australia |
| Human P53 cDNA | A kind gift from the Dr Rodger Reddel, Childrens Medical Research Institute, NSW, Aust. |

### *2.1.15 Synthetic oligonucleotides*

| | |
|---|---|
| HCTR 1 | 5'-TGCAATGCTTTCACTCCTGAGAAA-3' |
| 5pRcCMV | 5'-GAACCCACTGCTTAACTGGCTTAT-3' |
| 3pRcCMV | 5'-TGATCAGCGAGCTCTAGCATTTAG-3' |

***Phosphorothioate oligodeoxynucleotides*** purchased from Gibco BRL, Glen Waverley, Vic, Australia

| | |
|---|---|
| p21 antisense | 5'-TCCCCAGCCGGTTCTGACAT-3' |
| p21 sense | 5'-ATGTCAGAACCGGCTGGGGA-3' |

### *2.1.16 Tissue culture solutions*

| | |
|---|---|
| Dulbeccos minimum essential medium (DMEM) | ICN, OH, USA |
| Foetal calf serum (FCS) | Trace Bioscience PTY. LTD, Nobel Park, Vic, Aust |
| Glutamine and trypsin-EDTA | Obtained from the IMVS media production unit |

### *2.1.17 Cell lines*

| | |
|---|---|
| Parental HEK-293 (Human Embryonic Kidney cell line) | Department of Medicine, St Vincent's Hospital, Melbourne |
| D11 (HEK-293 transfected with C1a rat CTR) | Department of Medicine, St Vincent's Hospital, Melbourne |

| | |
|---|---|
| MCF7 and T47D (Human breast cancer cell line) | Renal Laboratory, Hanson Centre for Cancer Reseach |

### *2.1.18 Miscellaneous*

| | |
|---|---|
| 4-20% polyacrylamide gels | Novex, Ca, USA |
| PVDF membrane | Novex, Ca, USA |
| Hybond $H^+$ nylon membranes | Amersham Pharmacia Biotech, Buckinghamshire, UK |

## 2.2 Methods

### 2.2.1 Cell culture

Human embryonic kidney (HEK-293) cells, MCF7 and T47D breast cancer cell lines were maintained in Dulbecco's Modified Eagles medium (DMEM) supplemented with 10% heat inactivated fetal bovine serum (FCS), 2 mM glutamine, 100 U/ml penicillin, and 0.1 mg/ml streptomycin, 40 mM sodium bicarbonate and 20 mM hepes buffer. Stably transfected HEK-293 cells were maintained in 200 µg/ml G418, which was removed prior to commencement of experiments. Cells were grown at 37°C in a humidified atmosphere with 5% $CO_2$.

### 2.2.2 Generation of hCTR insert +ve expression vector

The hCTR insert +ve cDNA ligated into the pHz1 expression vector was transfected into HEK-293 cells, using the protocol described below. Three consecutive transfection attempts were unsucessful, failing to generate any neomycin resistant colonies three weeks following transfection. Consequently, a 1.9kB fragment corresponding to the open reading frame (ORF) of the insert +ve hCTR was excised from the pHz vector using the unique restriction sites Hind III and Xba I (refer chapter 3). Bands representing the restriction fragments, were visualised under UV light following staining of the gel with ethidium bromide, and the 1.9kb fragment corresponding to the insert +ve hCTR ORF was excised from the gel using a sterile scalpel blade. The insert +ve hCTR DNA insert was purified by placing the gel slice at 70°C until it melted and purified using the Wizard (PCR preps) DNA purification kit according to the instructions supplied by the manufacturer (Promega Bioscience Inc, Madison, WI, USA).

### *2.2.2.3 Preparation of the cloning vector*

The pRcCMV vector DNA was linearised using Hind III and Xba I restriction enzymes and the complete digestion of the DNA confirmed on an agarose gel. To prevent self-ligation of the vector, 5' terminal phosphate groups were removed by treatment with 10 units of calf intestinal phosphatase (CIP) in a total volume of 100 µl and in the buffer supplied by the manufacturer. The reaction was incubated at 37°C for 30 min, followed by a further addition of 10 units of CIP and an additional incubation for 45 min at 55°C. The vector was then purified using the Wizard (PCR preps) DNA purification kit according to the instructions supplied by the manufacturer (Promega Bioscience Inc, Madison, WI, USA). The amount of vector DNA recovered was estimated by agarose gel electrophoresis stained with ethidium bromide.

### *2.2.2.4 Ligation of insert +ve hCTR DNA fragment into pRc-CMV vector*

The 1.9kB insert +ve hCTR DNA and 100 ng of the pRc-CMV vector were combined in a 1:1 molar ratio, in a 20 ul reaction with 15 units of T4 DNA ligase and in the buffer supplied by the manufacturer. The reaction was incubated over night at 4°C.

### *2.2.2.5 Transformation of E.coli*

10-50 ng of the ligated plasmid was mixed with 200 ul of transformation competent JM109 bacteria and incubated on ice for 30 min. The cells were then heat shocked at 42° C for 2-5 min, placed in 1 ml of L-broth and incubated at 37° C with shaking for 30 min. Cells were pelleted and re-suspended in 100 ul of L-broth and plated using a sterile spreader onto L-agar plates containing 50 ug/ml of ampicillin. The agar plates were then incubated overnight at 37° C.

#### *2.2.2.6 Plasmid DNA mini-preparation*

Plasmid minipreps were prepared using a Plasmid Isolation Kit (section 2.1.7). Briefly, six single ampicillin resistant colonies were grown overnight in 5 ml of L-broth containing 50 ug/ml of ampicillin. Cells (2ml) were pelleted by centrifugation at 12,000 g for 1 min and the pellet was re-suspended in 100 ul of plasmid isolation kit BRP solution to re-suspend the pellet. Cell were then lysed using 200 ul of plasmid isolation kit BPL solution, mixed by inversion and incubated for 5 min before the addition of 150 ul of the neutralisation plasmid isolation kit BPN solution. The solution was then vortexed and the cellular debris and bacterial DNA pelleted by centrifugation at 12,000 g for 5 min. The supernatant was removed and the DNA extracted using an equal volume of phenol/chloroform, followed by precipitation in 2 volumes of ethanol. The DNA pellet was washed in 70% ethanol dried and re-suspended in 30 ul of sterile water. The plasmid preparations were digested with the restriction endonuclease Hind III as described above, to linearise the plasmids. The plasmids were then electrophorised on a 1% agarose gel to identify clones that contained the insert +ve hCTR DNA. Once identified, a clone was digested using both Hind III and Xba 1 restriction enzymes, as described above and the DNA fragments separated on a 1% agarose gel to confirm the presence of the 1.9 kb fragment corresponding to the insert +ve hCTR DNA.

### 2.2.3 Plasmid DNA preparation

For a large-scale plasmid preparation, the recombinant clone was grown overnight in 50 ml of L-broth supplemented with 50 ug/ml of ampicillin. The cells were pelleted by centrifugation at 4,000 rpm for 30 min at 4°C and the plasmids

isolated using the Midi protocol of the Plasmid Isoloation kit according to the instructions supplied by the manufacturer (Geneworks, SA, Australia).

### 2.2.4 Sequencing of the hCTR insert +ve expression vector

The newly generated insert +ve hCTR expression plasmid was sequenced using the QIAGEN Dye Terminator Protocol in the IMVS DNA Sequencing facility. DNA primers specific for the pRc-CMV vector (section 2.1.15) were used to confirm the presence and integrity of the initiation and termination region of then insert +ve hCTR gene. In addition, a primer specific for the insert +ve hCTR (section 2.1.15) was used to confirm the presence of the 48 bp insert of the insert +ve hCTR. The sequences obtained from the pRc-CMV insert +ve hCTR vector were aligned with the published insert +ve hCTR cDNA sequence *(Gorn et al., 1992)*, using the Genejockey DNA analysis software package (shown in chapter 3). The raw data obtained from the sequencing reactions is shown in appendix 1,2 and 3.

### 2.2.5 Stable transfection of HEK-293 cells

To enable comparison of the independent growth effects of the insert –ve and insert +ve hCTR, HEK-293 cell lines stably transfected with either the insert –ve or insert +ve hCTR isoform of the human CTR were established. The insert –ve hCTR cDNA ligated into the mammalian expression vector Zem228CC (a gift from Zymogenetics Inc, Seattle, WA) and the insert +ve cloned into the mammalian expression vector pRc-CMV (described above), were transfected into HEK-293 cells using a modified calcium phosphate transfection protocol *(Wigler et al., 1977)*. Cells at approximately 50% confluence were transfected with 10 μg plasmid DNA, together with 20 μg of herring sperm DNA, in 25-$cm^2$ culture flasks. Twenty-four hours after

transfection, G418 selection was commenced with the addition of 400 µg/ml of G418 and maintained for two weeks. Neomycin-resistant colonies were picked manually, propagated in the continual presence of G418 (200 µg/ml), and screened for binding of [$^{125}$I] sCT. A number of clones were obtained with different levels of receptor expression.

Parental HEK-293 cells were transfected with the mammalian expression vector Zem228CC alone, using the above protocol. In this case a pool of G418 resistant clones was used in the growth experiments described.

### 2.2.6 Receptor binding assays

#### *2.2.6.1 Iodination of salmon calcitonin*

Salmon CT was iodinated by Dr DM Findlay using the Chloramine T method, as previously described *(Findlay et al., 1980)*. 5 µg of chloramine T in 0.1M $Na_2PO_4$ was used to oxidize 1 mCi of $Na^{125}I$ for approximately 1 min. 2.5 µg sCT and 20 µl 0.1 M $K_2PO_4$ were added and allowed to react for 10 sec before the reaction was terminated by the addition of 1 ml 0.1 M $KPO_4$ containing 1 mg/ml KI and 5 mg /ml bovine serum albumin (BSA). To remove unincorporated [$^{125}$I], the reaction mixture was added to 10 mg QUSO silica and allowed to bind for 1 min. Following centrifugation for 2-3 min, the supernatant containing the free iodine was removed and the pellet was washed twice with distilled water. Labeled sCT was the eluted form the QUSO with 1ml elution buffer (20% v/v acetone, 0.1% v/v glacial acetic acid). The supernatant containing the labeled sCT was collected and the aliquots stored at -20°C.

### 2.2.6.2 Assessment of cell surface CTR expression following transfection

Cells were grown in 24-well plates until confluent, growth media was removed and binding buffer (DMEM containing 0.1% BSA refer section 2.1.8) was added. Cells were incubated with $^{125}$I-sCT ; ~80 pM alone or $^{125}$I-sCT and 100 nM unlabeled sCT for 1 h at 37°C in 5% $CO_2$. Following incubation, cells were washed twice in PBS (to remove unbound radioactivity) and solubilised with 0.5 ml 0.5 M NaOH. Samples were counted in a Packard γ counter to determine cell bound radioactivity.

### 2.2.6.3 Receptor binding dissociation curves

Cells were grown in 24-well plates until confluent, growth media was removed and binding buffer (DMEM containing 0.1% BSA refer section 2.1.8) added. Iodinated salmon calcitonin ($^{125}$I-sCT ; ~80pM) was added to all wells in the absence (total binding) and presence of increasing concentrations of unlabeled salmon calcitonin (sCT) ligand. Non-specific binding was defined as the binding in the presence of $10^{-7}$M, unlabelled sCT. Cells were incubated for 1h at 37°C in 5% $CO_2$, then washed twice with PBS to remove unbound radioactivity and solubilized in 0.5 M NaOH. Samples were counted in a Packard γ counter to determine cell bound radioactivity.

### 2.2.6.4 Receptor internalisation assay

Cells were grown in 24-well plates until confluent, growth media was removed and binding buffer added (DMEM containing 0.1% BSA refer section 2.1.8). Iodinated salmon calcitonin ($^{125}$I-sCT ; ~80pM) was added to all wells in the absence (total binding) and presence of $10^{-7}$ M sCT ligand (non-specific). After 30 min at 37°C in 5% $CO_2$, the medium was removed and replaced with fresh binding buffer containing no sCT. At the times indicated, the cells were washed with PBS to remove residual unbound $^{125}$I-sCT, followed by ligand elution buffer (0.5 ml ice cold 0.15 M NaCl -

0.05 M glycine [pH 2.5] refer section 2.1.8), added for 1 min, which was collected to measure the cell surface bound or acid elutable fraction of $^{125}$I-sCT. To determine the cell-associated radioactivity, the cells were solubilised as described above. The acid-eluted and cell associated fractions were then counted in a Packard γ counter. Internalisation was determined by calculating the acid-eluted counts as a percent of specifically bound cell associated radioactivity.

### 2.2.7 cAMP assay

To measure the ability of the two hCTR isoforms to activate adenylate cyclase, intracellular cAMP was measured using an enzyme immunoassay kit. $2x10^4$ cells were plated in 96 well plates for 3 days prior to performing the assay. Cells were exposed to the indicated concentrations of sCT for 15 min at 37°C in 5% $CO_2$. Media was then removed and cells were lysed, using the lysis buffer provided, to release intracellular cAMP. The assay was then performed as per the manufacturer's instructions (Amersham Pharmacia Biotech, Buckinghamshire, England).

### 2.2.8 Intracellular calcium assay

The quantification of CT induced changes in intracellular calcium was performed as described previously *(Halliday et al., 1993)*. Cells were grown in a 75 $cm^2$ culture flask until confluent, trypsinised and re-suspended in serum-deplete DMEM containing 1.0 μM Fura-2AM. Cells were incubated in Fura-2AM for 30 min at 37°C in 5% $CO_2$. Excess and non-hydrolysed Fura-2AM was removed by washing the cells twice in PBS. Cells were finally re-suspended at a concentration of $1x10^6$ cells/ml in Hanks solution containing 1.25 mM $Ca^{++}$, at 37°C. 2 ml of cells was pipetted into a glass cuvette, maintained in suspension with a magnetic stirrer and

placed in a Perkin-Elmer LS-50 fluorospectrophotometer. Using excitation and emission wavelengths of 340 and 510 nm, respectively, and slit widths of 5 mm, fluorescence was measured under basal and CT-stimulated conditions. Maximal and minimal fluorescence of each sample was established by addition of 0.1% Triton X-100 and then by simultaneous addition of 2 mM EGTA and 25 mM Tris-HCl, respectively. The free intracellular calcium concentration was calculated using the dissociation constant of 220 nM for Fura-2AM *(Grynkiewicz et al., 1985).*

### 2.2.9 Protein isolation and western blot analysis

Cells were lysed in lysis buffer containing 25 mM MOPS pH 7.2, 60 mM β-glycerophosphate, 15 mM $MgCl_2$, 5 mM EGTA, 1 mM DTT, 0.1 mM Sodium Vanadate, 1% Triton X-100, 1 mM PMSF. Lysates were centrifuged for 5 min at 12,000 rpm, the supernatant fraction of the lysate was then removed and stored at -70 $^0$C until ready to use. 25µl of cell extracts, containing approximately 50µg of protein, were mixed with an equal volume of sample buffer containing 12 mM Tris HCl pH 6.8, 6% SDS, 10% β-mercaptoethanol, 20% glycerol, and 0.03% bromophenol blue. Protein samples were boiled for 5 min and electrophoresed under reducing conditions in 4-20% polyacrylamide gels. Separated proteins were electrophoretically transferred to PVDF transfer membrane and blocked in PBS blocking solution containing 1x PBS, 0.1% Tween 20 and 5% skim milk powder for 1h at room temperature. Immunodetection was performed overnight at 4°C in PBS/blocking solution, using mouse monoclonal antibodies to phospho-ERK1/2 MAPK protein to the non-phosphorylated ERK1 MAPK protein, p21, p27, p53 (section 2.1.5) or rabbit polyclonal antibodies to cyclin B1 or cdc2 (section 2.1.5 Filters were rinsed several times with PBS containing 0.1% Tween 20 and incubated

with anti-mouse or anti-rabbit alkaline phosphatase-conjugate for 1h. Antibody labelled protein was detected using the Vistra ECF substrate reagent kit and quantified using a Fluorimager (Molecular Dynamics Inc., Sunnyvale, CA, USA).

### 2.2.10 Measurement of extracellular pH

Cells transfected with the insert –ve hCTR, insert +ve hCTR or vector alone, were plated at $1.5x10^6$ cells per well in 6 well plates and incubated in complete DME media, as described, which contained 40 mM sodium bicarbonate and 20 mM hepes buffer. 48 h after plating, cells were left untreated or were treated with 10 nM sCT. The extracellular pH in medium from triplicate wells was measured 12, 24, 36, 48 and 72 h after the commencement of treatment, using a pH electrode.

### 2.2.11 Cell growth analysis

#### *2.2.11.1 Effect of calcitonin concentration on cell proliferation*

To determine the effect of CT concentration on cell proliferation, cells were seeded at $5x10^4$ cells per well in 24 well plates and incubated for 72 h in the presence of increasing concentrations ($10^{-11}$ M – $10^{-6}$ M) of sCT, hCT or the 8-32 sCT analog, as indicated in the figures and tables. Cells were then harvested by trypsinisation and were counted manually in triplicate using a haemocytometer. To determine the effect of sCT treatment on cell number results were analysed by one-way analysis of variance and the level of significance was determined from a Duncan's Post Hoc test, using SPSS for windows version 10.0.5 on a PC compatible computer.

### *2.2.11.2 Time course of the calcitonin induced anti-proliferative effect*

To determine the effect of sCT on the rate of cell growth, cells were plated under the conditions described in the figure legends. 48 h after plating cells remained untreated or were treated with 10 nM sCT. At the indicated times after treatment, the cells were harvested by trypsinisation and counted manually in triplicate using a haemocytometer. To determine the effect of sCT treatment on cell number over time, results were analysed by two-way analysis of variance. Where a significant interaction was identified, the data was split on the basis of time and re-analysed using a Duncan's Post Hoc test to identify the significant differences. The analysis was performed using SPSS for windows version 10.0.5 on a PC compatible computer.

### *2.2.11.3 Growth recovery experiments*

To investigate the ability of CT-treated cells to recover from the growth retarding effect of the ligand, cells were plated at $3x10^5$ cells per flask in T25 $cm^2$ culture flasks. 48 h after seeding 3 flasks remained untreated (control) and 6 were treated once with 10 nM sCT (treated) for 3 days. On day three cells were washed once with 2 ml of elution buffer (0.15M NaCl – 0.05 M glycine (pH 2.5)), to remove all cell bound sCT and then 2 ml of 1x PBS to remove residual acid. Growth media was then replaced such that control cells again remained untreated for a further 3 days. However, the treated cells were divided into 2 groups of three and one was re-treated with 10 nM sCT (sCT), while the other remained untreated (sCT wash) for the final 3 days. At the end of this, 6 day period, cells were harvested by trypsinisation and counted manually using a haemocytometer. To determine the ability of cell growth to recover following sCT treatment, results were analysed by an analysis of variance (ANOVA). Where a significant interaction was identified, the data was split on the

basis of time and re-analysed using a Duncan's Post Hoc test to identify the significant differences. The analysis was performed using SPSS for windows version 10.0.5 on a PC compatible computer.

#### *2.2.11.4 Identification of important intracellular signalling pathways involved in the calcitonin growth effect*

To determine the intracellular signalling pathways involved in transducing the CT-mediated inhibition of cell growth, cells were plated at the indicated density and allowed to adhere to the plastic for the specified time. Following adherence, cells remained untreated or were treated in triplicate with the specified molecules which activated or inhibited the indicated intracellular signalling pathways, for 72 h. Following incubation cells were photographed using a Nikon Eclips TE300 microscope and a Nikon F70 camera under monochromatic light using Kodak Technical Pan film. Cells were then harvested by trypsinisation and counted manually using a haemocytometer. Data are expressed as mean cell number per well ± SEM. To determine the effect of treatment on cell number results were analysed by one-way analysis of variance and the level of significance was determined from a Duncan's Post Hoc test, using SPSS for windows version 10.0.5 on a PC compatible computer.

### 2.2.12 Cell viability assay

D11 cells expressing the C1a rat CTR and Hr12 cells expressing the insert –ve hCTR were plated into 12 well plates at $2x10^5$ cells per well and allowed to adhere. 48 h after plating the cells either remained untreated or were treated with 10 nM sCT. At the times indicated cells were harvested by trypsinisation and mixed in a 1:1 ratio with 0.4% trypan blue. Viable, cells able to extrude the trypane blue dye and non-viable cells, blue cells, were then counted using a haemocytometer.

### 2.2.13 Apoptosis assay

Cells were harvested by washing twice with PBS, after 72 h in the presence or absence of 10 nM sCT, and incubated overnight at 37°C in lysis buffer containing 10 mM Tris (pH 8.0), 5 mM EDTA, 100 mM NaCl, 1.0 % SDS and 200 µg/ml proteinase K. DNA was extracted twice with equal volumes of phenol-chloroform-isoamylalcohol (25:24:1) and then precipitated in ethanol. Samples were electrophoresed in a 1.2% agarose gel, stained with ethidium bromide and visualized under UV light.

### 2.2.14 Cell cycle analysis

Cells were trypsinisation and collected by centrifugation, re-suspended in ice-cold PBS and then fixed in absolute methanol for at least 30 minutes. Cells were then washed in PBS containing 0.5% Tween 20, followed by two washes in PBS containing 2% FCS and re-suspended in PBS/2% FCS containing 40 µg/ml RNase A and incubated for a further 20 min at 37°C. Cells were washed in PBS/2%FCS and were finally re-suspended in PBS containing propidium iodide (PI) at a final concentration of 20 µg/ml. The stained nuclei were analysed using a flow cytometer

(Epics Profile, Coulter, Hialeah, FL). Cell cycle distribution was based on 2N and 4N DNA content.

### 2.2.15 Mitotic index analysis

Cells treated or not with 10 nM sCT for 24 h were trypsinised, collected by centrifugation, washed in 1x PBS and treated with hypotonic solution of 0.075 M KCl at 37°C for 30 min. Following centrifugation, cells were fixed by the dropwise addition of freshly prepared fixative (methanol:acetic acid, 3:1), re-centrifuged, and re-suspended in fixative. Cells were dropped onto clean microscope slides and stained with a 1:25 dilution of Giemsa stain in 1x PBS for 30 min. Mitotic indices were calculated as the number of cells with condensed chromosomes with at least 3000 cells being examined from ten different fields of view.

### 2.2.16 RNA extraction and Northern blot analysis

For Northern blot analysis, cells were seeded at a density of $1x10^5$ cells/25 $cm^2$ flask, allowed to attach for 48 h and then incubated for various times in the absence or presence of 10 nM sCT. Total RNA was isolated using the TRIZOL Reagent, according to the manufacturer's instructions. Total RNA (10 µg per lane) was electrophoresed in formaldehyde/1% agarose gels, transferred to Hybond $N^+$ nylon membranes, and immobilised by UV cross-linking. Membranes were prehybridised for 3 h at 42°C in 1 M NaCl, 1% SDS, 10% Dextran sulphate, 50% formamide, 100 µg/ml of heat-denatured herring sperm DNA and hybridised with human $p21^{WAF1/CIP1}$ cDNA, or p53 cDNA radiolabeled with [$\alpha$-$^{32}$P]dCTP by random priming using the Giga prime kit. To allow quantitation of mRNA signals, the same filters were stripped. To remove the radioactive probe, filters were shaken vigorously

for 10 min in boiling stripping solution (0.1x SSC and 0.1% SDS) three times. Following the final wash the filters were rocked at room temperature in 2x SSC for 15 min. The filter was then re-probed with a 450 bp $^{32}$P-labelled PCR-generated DNA fragment of human glyceraldehyde-3-phosphate dehydrogenase (GAPDH). Signals were analysed using the PhosphorImager SF (Molecular Dynamics Inc., Sunnyvale, CA,USA).

### 2.2.17 Transfection of antisense oligonucleotides

Phosphorothioate oligodeoxynucleotides (2 µg/ml) and lipofectin (10 µg/ml) were incubated in serum free DMEM for 45 min at room temperature. The oligonucleotide-lipofectin mixture was diluted with serum-containing medium and added to the cells. Following 4 h of pre-incubation with the oligonucleotide mixture, cells were treated with 10 nM of sCT for up to 72 h. To confirm that the antisense oligonucleotide had the desired effect of blocking p21 up-regulation by sCT, p21 mRNA was monitored by Northern blotting at 24 and 48 h following treatment with sCT. At the indicated times cells were trypsinised from plates and counted. The antisense oligonucleotide (p21AS) was based on the p21 coding sequence, which is complementary to the region of the initiation codon (5'-TCC CCA GCC GGT TCT GAC AT-3') and the sense oligonucteotide (Sp21) was identical to the initiation sequence (5'-ATG TCA GAA CCG GCT GGG GA-3').

### 2.2.18 Immunoprecipitation and kinase activity

For immunoprecipitation and for kinase activity determination, 5µg/ml of rabbit polyclonal antibodies to $p34^{cdc2}$, p21, Rb or cyclin B1 (section 2.1.5) were attached to 25µl of protein A-sepharose slurry and 400µl of PBS by incubation at 4°C for 24 h. 500µl of cell lysate was simultaneously pre-cleared by incubation with 25µl of protein A-sepharose slurry at 4°C for 24 h. The pre-cleared cell lysate was then added to the antibody-attached sepharose and incubated for a further 24 h at 4°C on a rotating platform. Immune complexes were recovered and washed three times with lysis buffer. For immunoprecipitation, immune complexes were separated on 4-20% SDS-polyacrylamide gels as described above and a mouse monoclonal p21 antibody or rabbit polyclonal $p34^{cdc2}$ was used for immunoblot analysis. For $p34^{cdc2}$ kinase activity, immune complexes were washed three times with kinase assay buffer (50 mM Tris-HCl pH 7.4, 10 mM $MgCl_2$, 1 mM dithiothreitol). Phosphorylation of histone H1 was measured by incubating the beads with 40 µl of a reaction mixture containing 25 µM ATP, 2 µg histone H1 and 2.5 µCi [$^{32}$P]γ-ATP in kinase assay buffer for 30 min at 37°C. The reaction was stopped by boiling the sample in 2 X SDS sample buffer for 5 min and samples were resolved by SDS-PAGE. Gels were analyzed using the PhosphorImager SF (Molecular Dynamics Inc.).

### 2.2.19 Luciferase and β-galactosidase assays

#### *2.2.19.1 Reporter constructs*

The human wild type full-length p21 promoter luciferase fusion plasmid, WWP-Luc, was a kind gift from Dr B Vogelstein (Johns Hopkins Medical School). A series of p21 promoter deletion constructs (pWWP, pWP 124, pWP 101, pWPdel-Sma I), shown schematically in figure 7.3 and mutant constructs (pWP101-mt Sp1-3,

pWP101-mt Sp1-4, pWP101-mt Sp1-5-6 and pWP101-mt TATA) shown schematically in figure 7.4 were generated and provided by Dr Sowa (Kyoto Prefecturnal University of Medicine). Briefly, the 2.4-kilobase pair genomic fragment containing the transcription start site was subcloned into the luciferase reporter vector, PGL3-basic, to generate pWWP. The construct termed, pWWP-124 consists of sequences corresponding to the region of the promoter between –124 and the start of transcription and contains all six Sp1 consensus binding sites. PWWP-101 consists of a minimal promoter region between –101 relative to the transcriptional start site and contains four Sp1 binding sites termed Sp1-3, Sp1-4, Sp1-5-6. The construct termed pWP-del-SmaI was generated by digesting pWWP with SmaI and by religating. The wild type luciferase-reporter plasmid Sp1-luc, consisting of three consensus Sp1 binding sites was a kind gift from Dr Peggy J Farnham, whereas the mutant type-Sp1-luc construct was constructed by Dr Sowa (Kyoto Prefectural University of Medicine). A vacant vector pGL3-Basic was purchased from Promega and was used as a control reporter plasmid. The pRcCMV-βgalactosidase reporter construct was used to standardize for transfection efficiency.

### *2.2.19.2 Transient and stable transfections of reporter constructs*

Cells were seeded at a density of $1x10^5$ cells/25 $cm^2$ flask, and were allowed to attach for 2 days. Cells were transfected by a calcium phosphate co-precipitation technique using 10 µg of each of the reporter plasmid DNA together with 20 µg of sheared herring sperm DNA. Twenty-four h after transfection, cells were incubated for a further 24 h with various treatments, as indicated in the figure legends, and cell lysates were collected for luciferase assay. For stable transfections, 10 µg of each reporter plasmid DNA construct was co-transfected with 20 µg of herring sperm DNA. Twenty-four h after transfection, G418 was added to the medium at a final

concentration of 400 µg/ml. The medium was changed every three days and about three weeks later G418 resistant colonies were selected. For luciferase assay mass cultures of G418 resistant colonies were expanded and cells were seeded at a density of $2x10^5$ cells/flask. Cells were allowed to attach for two days, before treatment with sCT, butyrate or a combination of both and cell lysates were collected for measurement of luciferase activity, as indicated.

#### *2.2.19.3 Luciferase and β-galactosidase assays*

The luciferase and β-galactosidase activities of the cell lysates were measured 24 hr after the various treatments, as indicated in the figure legends. Luciferase and β-galactosidase were analyzed using the same cell extracts as per the manufacturer's instructions (Promega Bioscience Inc, Madison, WI USA). Luciferase activities were normalized for the amount of protein in cell lysates or β-galactosidase activity as indicated.

# Chapter 3

# Generation and characterisation of HEK-293 cells stably expressing either the insert –ve or insert +ve hCTR.

## 3.1 Introduction

CT is a 32 amino acid peptide, best known for its ability to inhibit osteoclastic bone resorption *(Chambers et al., 1982)*. CT acts through its seven transmembrane domain G-protein coupled cell surface receptor, the CTR, to inhibit osteoclast bone resportive function *(Chambers et al, 1982)*. The identification of CTR in many extra-skeletal cell types and tissue sites *(Martin et al., 1998)* indicates that the CT/CTR hormone receptor system also has effects other than those involved in calcium homeostasis. Accordingly, CT induces receptor-mediated effects as disparate as blastocyst differentiation *(Wang et al., 1998)* and implantation *(Zhu et al., 1998a)* and appetite regulation *(Yamamoto et al., 1982)* and analgesia *(Morimoto et al., 1984)* in the CNS. Expression of CTR has also been shown in human cancer cell lines *(Findlay et al., 1980a; Findlay et al., 1980b; Findlay et al., 1981; Shah et al., 1994)* and in primary cancer tissues *(Shah et al., 1994; Gillespie et al., 1997)*.

Multiple isoforms of the rat and human CTR have been reported (as discussed in section 1.2.1), which arise from alternative splicing of the primary mRNA species *(Moore et al., 1995; Nakamura et al., 1995; Nussenzveig et al., 1995)*. In the case of the rat CTR, two isoforms, C1a and C1b, have been identified (shown schematically in figure 1.1), which differ structurally by a 37 amino acid insert in the putative second extracellular domain, which is present in the C1b variant but not the C1a isoform *(Sexton et al., 1993)*. The presence of the 37 amino acid insert in the extracellular domain decreases the CT binding affinity of the receptor *(Sexton et al., 1993)*. The human CTR has two predominant isoforms, the insert -ve *(Kuestner et al., 1994)* and the insert +ve *(Gorn et al., 1992)* (as discussed in section 1.2.1). A 16 amino acid insert in the first putative intracellular loop is present in the insert +ve isoform but not the insert -ve hCTR isoform *(Kuestner et al., 1994; Gorn et al., 1992)* (shown

schematically in figure 1.1). When expressed in a number of cell types, the insert +ve isoform displays similar affinity for CT as the insert -ve receptor but has different G-protein coupling efficiency *(Moore et al., 1995; Nussenzveig et al., 1994)*. The 16 amino acid insert prevents CT stimulation of the insert +ve hCTR from mobilising intracellular calcium when it is expressed in BHK cells *(Moore et al., 1995)*. The ability of the insert +ve isoform to activate cAMP *via* Gs is cell type specific, CT having reduced potency in BHK *(Moore et al., 1995)* and COS *(Nussenzveig et al., 1994)* cells.

In addition to adenylate cyclase and PLC activation, CTR's activate other intracellular signalling pathways, involving phospholipase D *(Naro et al., 1998)* and tyrosine kinases *(Zhang et al., 1999; Chen et al., 1998)*. In particular, activation of the rabbit CTR transfected into HEK-293 cells caused a rapid, but transient activation of MAP kinase *via* Gi and PTX-insensitive PKC activation *(Chen et al., 1998)*. There are no published reports of the ability of the hCTR isoforms to activate the Erk1/2 MAP kinase pathway.

The insert +ve and -ve isoforms of the hCTR are co-expressed in variable ratios in a number of tissues and cell types *(Kuestner et al., 1994)*. Therefore, in order to study separately the biology of the isoforms it has been necessary to establish cell models, which specifically express either one of the hCTR isoforms. Previously, the C1a rCTR has been expressed in HEK–293 cells *(Houssami et al., 1994)*, while the insert -ve and +ve hCTR isoforms have been separately expressed in baby hamster kidney (BHK) cells *(Moore et al., 1995)*. When expressed in the HEK-293 cells, the Cla rCTR isoform responded to CT by inducing growth suppression (DM Findlay, personal communication). However no effect on growth was seen when BHK cells expressing the insert –ve hCTR were treated with CT (DM Findlay, personal

communication). In order to determine if the effect of CT on cell proliferation was a receptor- or cell-specific effect, and thus to develop an understanding of the growth regulating action of the hCTR isoforms, it was necessary to generate and characterise stably transfected HEK-293 cell lines expressing either the insert –ve or +ve hCTR. Cell lines expressing either the insert -ve or +ve hCTR isoform showed comparable CT binding kinetics. Single clones expressing either the insert positive or insert negative hCTR were chosen and characterised in terms of CT activated intracellular signalling. Cells expressing the insert –ve hCTR were able to elevate intracellular cAMP, elevate intracellular calcium and activate Erk1/2 MAP kinase. In contrast, cells expressing the insert +ve hCTR were unable to initiate intracellular signalling. However clones expressing either the insert –ve or +ve hCTR responded to CT by induction of a novel secretion of hydrogen ions. This latter result provided evidence that the insert +ve hCTR was capable of inducing intracellular effects and was not simply a decoy receptor.

## 3.2 Results

### 3.2.1 Generation of insert +ve hCTR expression plasmid

Removal of the insert +ve hCTR cDNA from the original pHZ1 plasmid and re-ligation into a pRc-CMV vector (described in section 2.2.2) was carried out by Dr Andreas Evdokiou, and is included here, as the construct was vital to achieving the objectives of this study.

#### *3.2.1.1 Excision of the insert +ve hCTR cDNA from the pHZ1 plasmid*

The unique restriction sites, Hind III and Xba I, were used to remove a 1.7kb fragment from the pHz1 plasmid, which contained the insert +ve hCTR DNA (figure

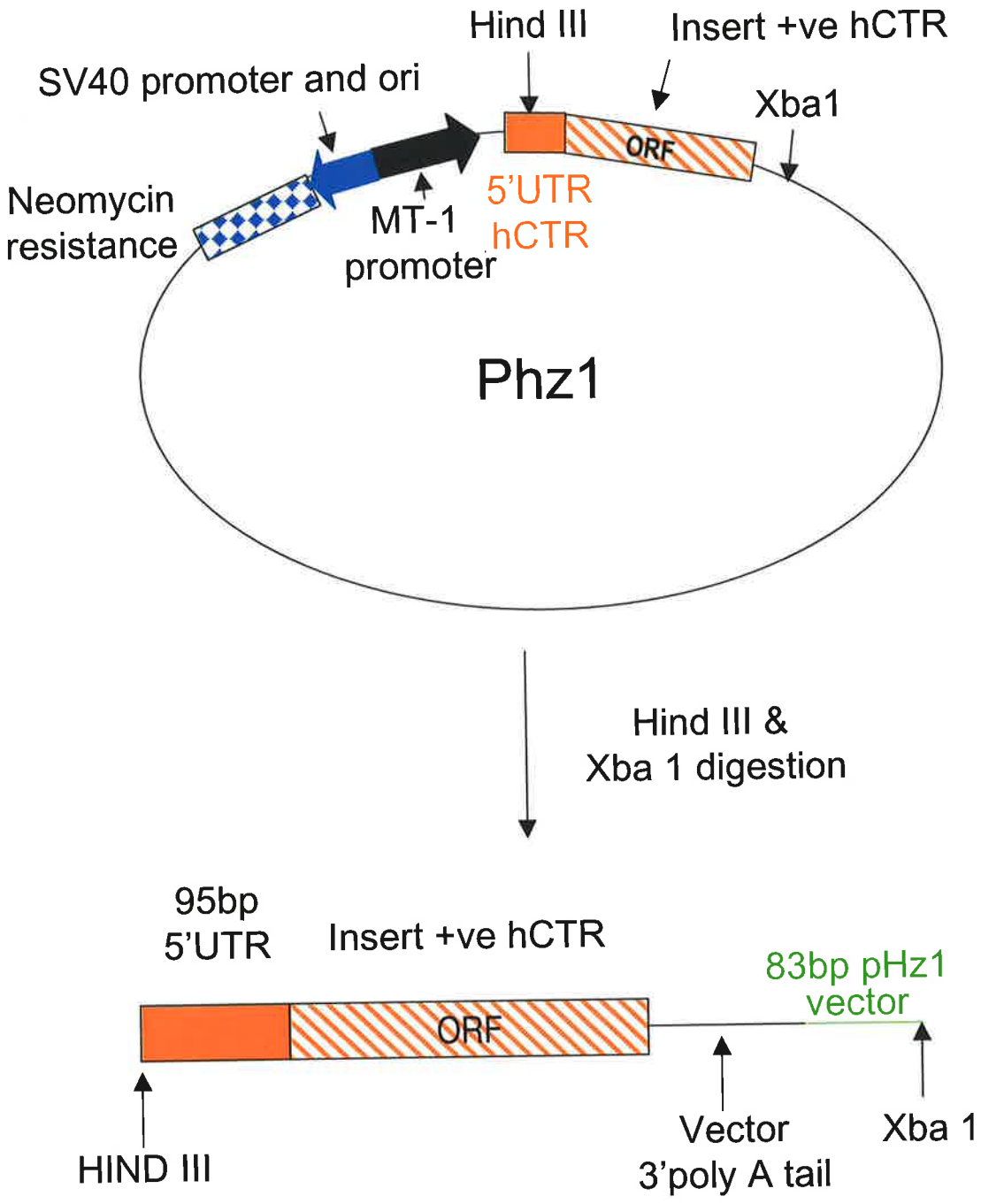


**Figure 3.1 Excision of the insert +ve hCTR cDNA from the pHZ1 vector.**

The insert +ve hCTR ORF was excised from the Phz1 plasmid using a Hind III and Xba I digest.

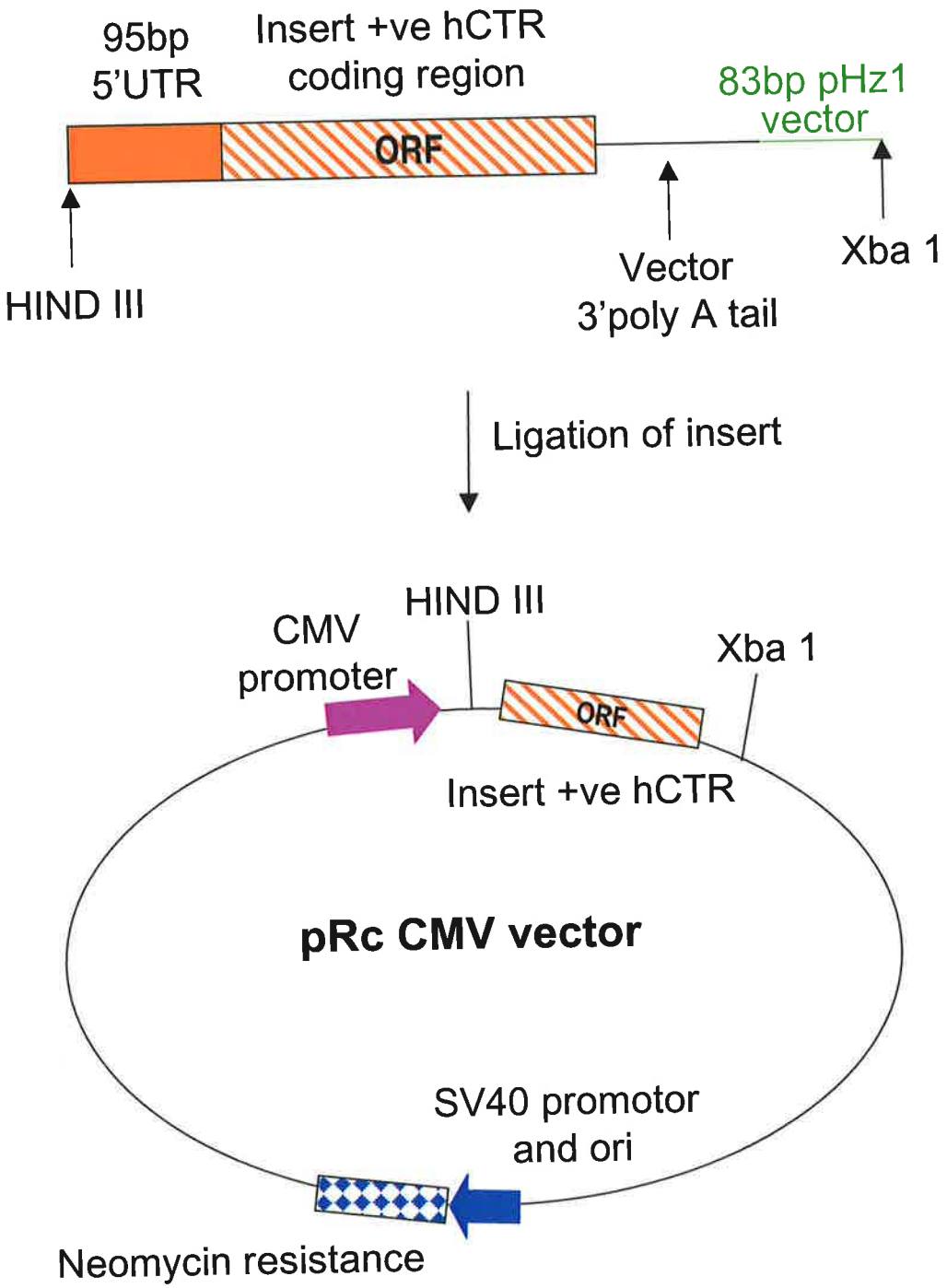


**Figure 3.2 Ligation of the Insert +ve hCTR cDNA into the pRcCMV vector.**

The isolated insert +ve hCTR ORF was ligated into a CMV expression plasmid using Hind III and Xba I restriction sites.

3.1). The fragment containing the insert +ve hCTR DNA was then religated into Hind III and Xba I sites of the pRc-CMV vector (figure 3.2).

#### *3.2.1.2 Sequencing of the insert +ve hCTR pRc-CMV expression plasmid*

To confirm the integrity of the insert +ve hCTR cDNA, the newly generated expression plasmid was sequenced (described in section 2.2.4) (raw sequencing data can be found in appendix I, II and III). The generated sequences were then compared to the published sequence of the insert +ve hCTR *(Gorn et al., 1992)*. Figure 3.3A shows alignment of the insert +ve hCTR sequence with the sequence generated using the 5' CMV primer and indicates the presence of the ATG initiation codon and approximately the first 260 base pairs of the sequence. A sequence was also generated using a 3' CMV primer. This was aligned with the published insert +ve hCTR sequence and was shown to contain a TGA termination codon and approximately 220 base pairs of the 3' sequence (Figure 3.3B). The size of the excised insert +ve hCTR insert together with sequencing from the initiation codon to the stop codon in the newly generated expression vector indicate the presence of the entire open reading frame. To confirm the presence of the 48 bp insert, unique to the insert +ve hCTR, in this ORF an internal 5' hCTR primer was used to sequence this internal region of the newly generated plasmid. Figure 3.3C shows the alignment of the insert +ve hCTR sequence and the sequence generated using the internal hCTR primer, and it includes approximately 600 bp of sequence, including the underlined 48 bp insert.

### 3.2.2 Binding assessment of the insert +ve and insert –ve clones

HEK-293 cells were transfected with hCTR insert-ve and hCTR insert +ve vectors (described in 2.2.5). Following antibiotic selection of individual HEK-293 clones, binding experiments were performed (described in section 2.2.6.2) to assess

**Figure 3.3A** Sequence alignment of published insert +ve hCTR sequence [top] (Gorn *et al.,* 1992) with the insert +ve hCTR pRcCMV expression vector sequence, generated using a primer complementary to the 5' region of the CMV vector [bottom].

**Published insert +ve hCTR sequence (top), sequence generated from insert +ve hCTR pRc-CMV expression plasmid (bottom).**

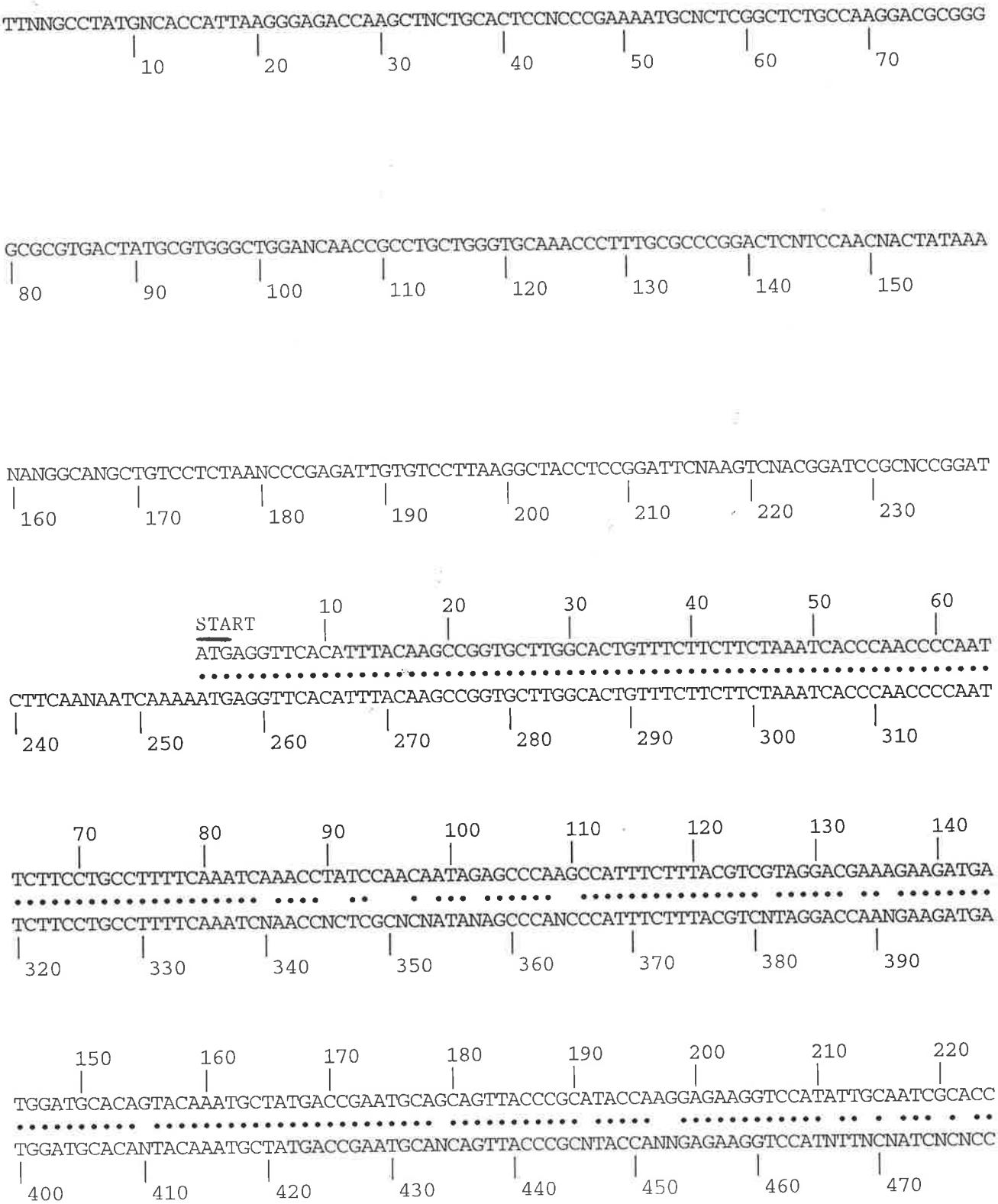

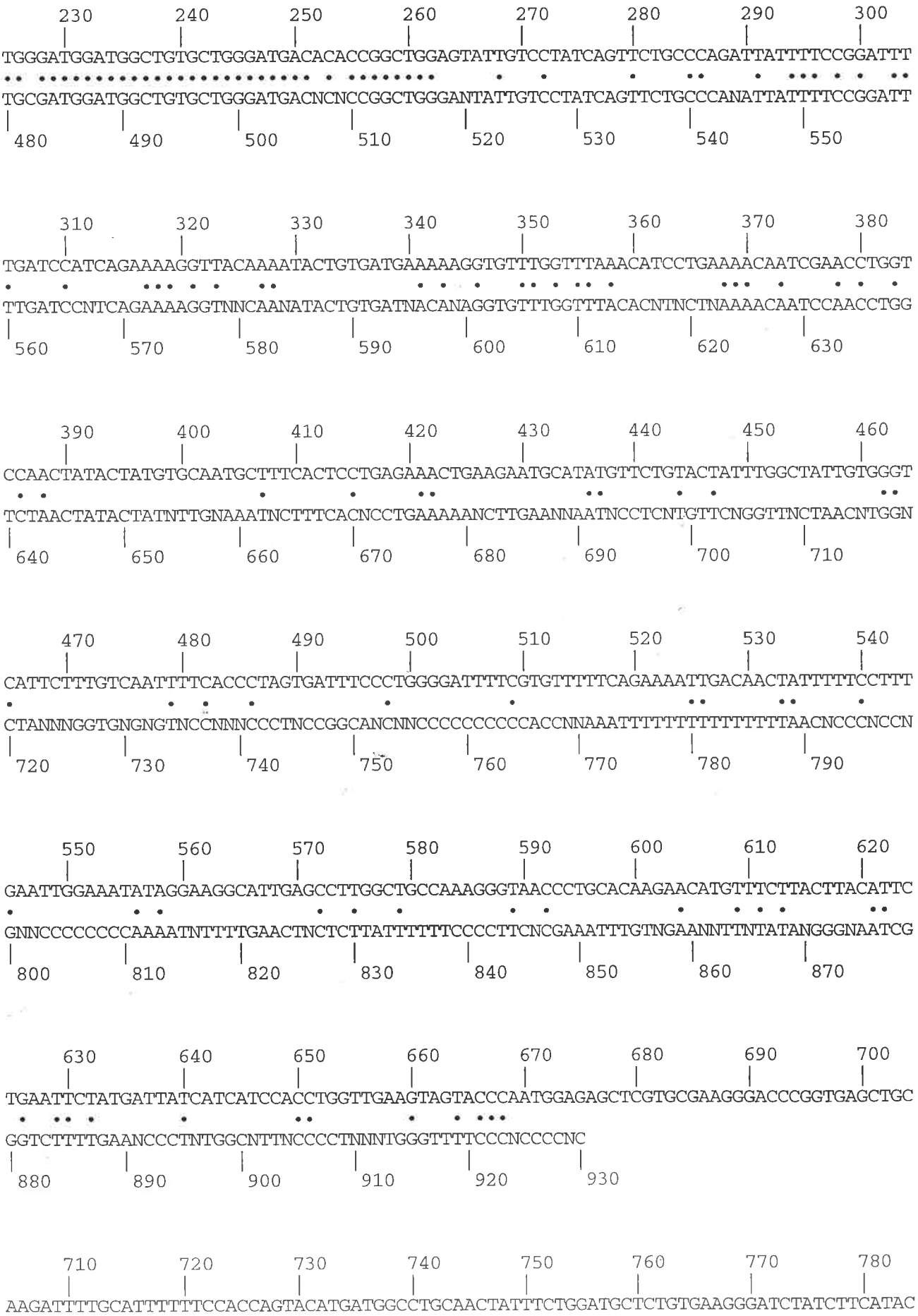
230 240 250 260 270 280 290 300
TGGGATGGATGGCTGTGCTGGGATGACACACCGGCTGGAGTATTGTCCTATCAGTTCTGCCCAGATTATTTTCCGGATTT
TGCGATGGATGGCTGTGCTGGGATGACNCNCCGGCTGGGANTATTGTCCTATCAGTTCTGCCCANATTATTTTCCGGATT
480 490 500 510 520 530 540 550
310 320 330 340 350 360 370 380
TGATCCATCAGAAAAGGTTACAAAATACTGTGATGAAAAAGGTGTTTGGTTTAAACATCCTGAAAACAATCGAACCTGGT
TTGATCCNTCAGAAAAGGTNNCAANATACTGTGATNACANAGGTGTTTGGTTTACACNTNCTNAAAACAATCCAACCTGG
560 570 580 590 600 610 620 630
390 400 410 420 430 440 450 460
CCAACTATACTATGTGCAATGCTTTCACTCCTGAGAAACTGAAGAATGCATATGTTCTGTACTATTTGGCTATTGTGGGT
TCTAACTATACTATNTTGNAAATNCTTTCACNCCTGAAAAANCTTGAANNAATNCCTCNTGTTCNGGTTNCTAACNTGGN
640 650 660 670 680 690 700 710
470 480 490 500 510 520 530 540
CATTCTTTGTCAATTTTCACCCTAGTGATTTCCCTGGGGATTTTCGTGTTTTTCAGAAAATTGACAACTATTTTTCCTTT
CTANNNGGTGNGNGTNCCNNNCCCTNCCGGCANCNNCCCCCCCCCCACCNNAAATTTTTTTTTTTTTTTAACNCCCNCCN
720 730 740 750 760 770 780 790
550 560 570 580 590 600 610 620
GAATTGGAAATATAGGAAGGCATTGAGCCTTGGCTGCCAAAGGGTAACCCTGCACAAGAACATGTTTCTTACTTACATTC
GNNCCCCCCCCCAAAATNTTTTGAACTNCTCTTATTTTTTCCCCTTCNCGAAATTTGTNGAANNTTNTATANGGGNAATCG
800 810 820 830 840 850 860 870
630 640 650 660 670 680 690 700
TGAATTCTATGATTATCATCATCCACCTGGTTGAAGTAGTACCCAATGGAGAGCTCGTGCGAAGGGACCCGGTGAGCTGC
GGTCTTTTGAANCCCTNTGGCNTTNCCCCTNNNTGGGTTTTCCCNCCCCNC
880 890 900 910 920 930
710 720 730 740 750 760 770 780
AAGATTTTGCATTTTTTCCACCAGTACATGATGGCCTGCAACTATTTCTGGATGCTCTGTGAAGGGATCTATCTTCATAC

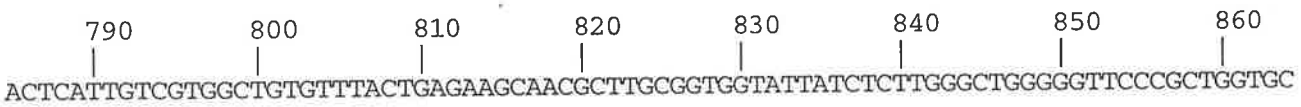
790
800
810
820
830
840
850
860
ACTCATTGTCGTGGCTGTGTTTACTGAGAAGCAACGCTTGCGGTGGTATTATCTCTTGGGCTGGGGGTTCCCGCTGGTGC

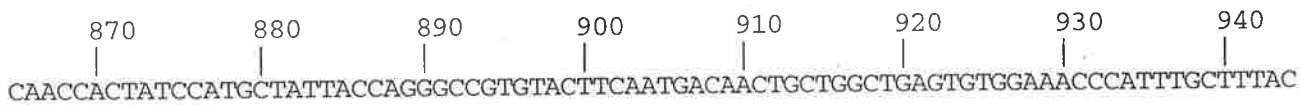
870
880
890
900
910
920
930
940
CAACCACTATCCATGCTATTACCAGGGCCGTGTACTTCAATGACAACTGCTGGCTGAGTGTGGAAACCCATTTGCTTTAC


950
960
970
980
990
1000
1010
1020
ATAATCCATGGACCTGTCATGGCGGCACTTGTGGTCAATTTCTTCTTTTTGCTCAACATTGTCCGGGTGCTTGTGACCAA

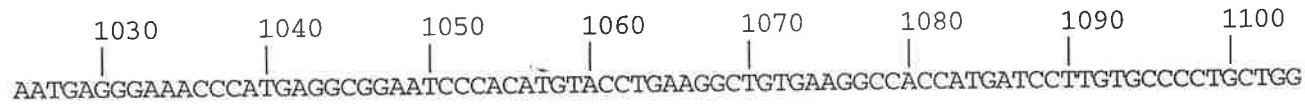
1030
1040
1050
1060
1070
1080
1090
1100
AATGAGGGAAACCCATGAGGCGGAATCCCACATGTACCTGAAGGCTGTGAAGGCCACCATGATCCTTGTGCCCCTGCTGG

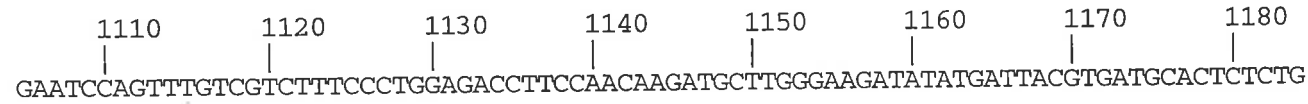
1110
1120
1130
1140
1150
1160
1170
1180
GAATCCAGTTTGTCGTCTTTCCCTGGAGACCTTCCAACAAGATGCTTGGGAAGATATATGATTACGTGATGCACTCTCTG

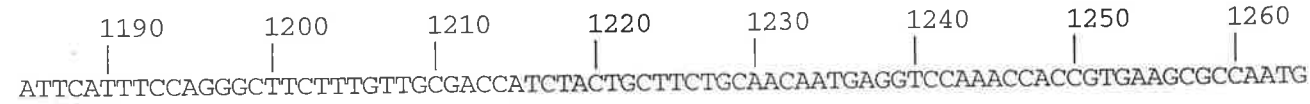
1190
1200
1210
1220
1230
1240
1250
1260
ATTCATTTCCAGGGCTTCTTTGTTGCGACCATCTACTGCTTCTGCAACAATGAGGTCCAAACCACCGTGAAGCGCCAATG

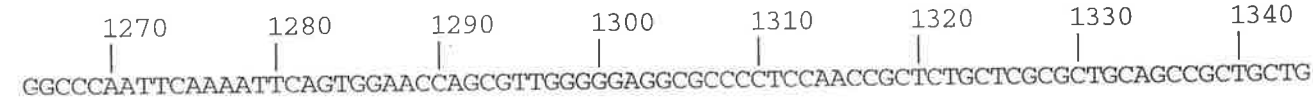
1270
1280
1290
1300
1310
1320
1330
1340
GGCCCAATTCAAAATTCAGTGGAACCAGCGTTGGGGGAGGCGCCCCTCCAACCGCTCTGCTCGCGCTGCAGCCGCTGCTG

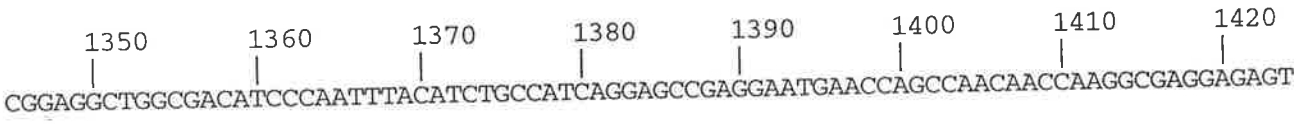
1350
1360
1370
1380
1390
1400
1410
1420
CGGAGGCTGGCGACATCCCAATTTACATCTGCCATCAGGAGCCGAGGAATGAACCAGCCAACAACCAAGGCGAGGAGAGT

STOP
GCTGA

**Figure 3.3B** Alignment of the published insert +ve hCTR sequence (Gorn *et al.,* 1992) with the sequence generated from the insert +ve hCTR CMV vector, using a primer complementary to the 3' CMV vector.

**Published insert +ve hCTR sequence (top), sequence generated from insert +ve hCTR pRc-CMV expression plasmid (bottom).**

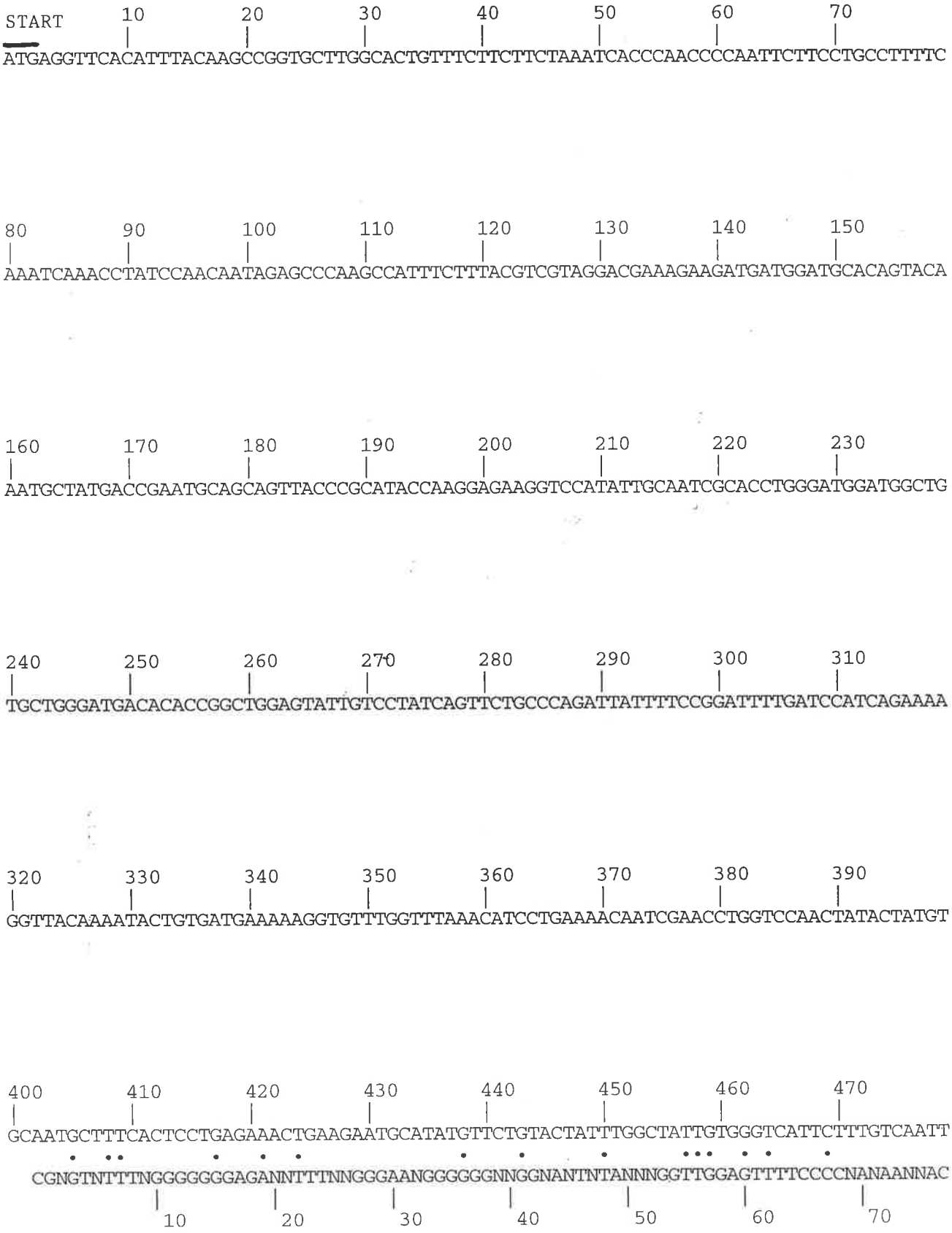

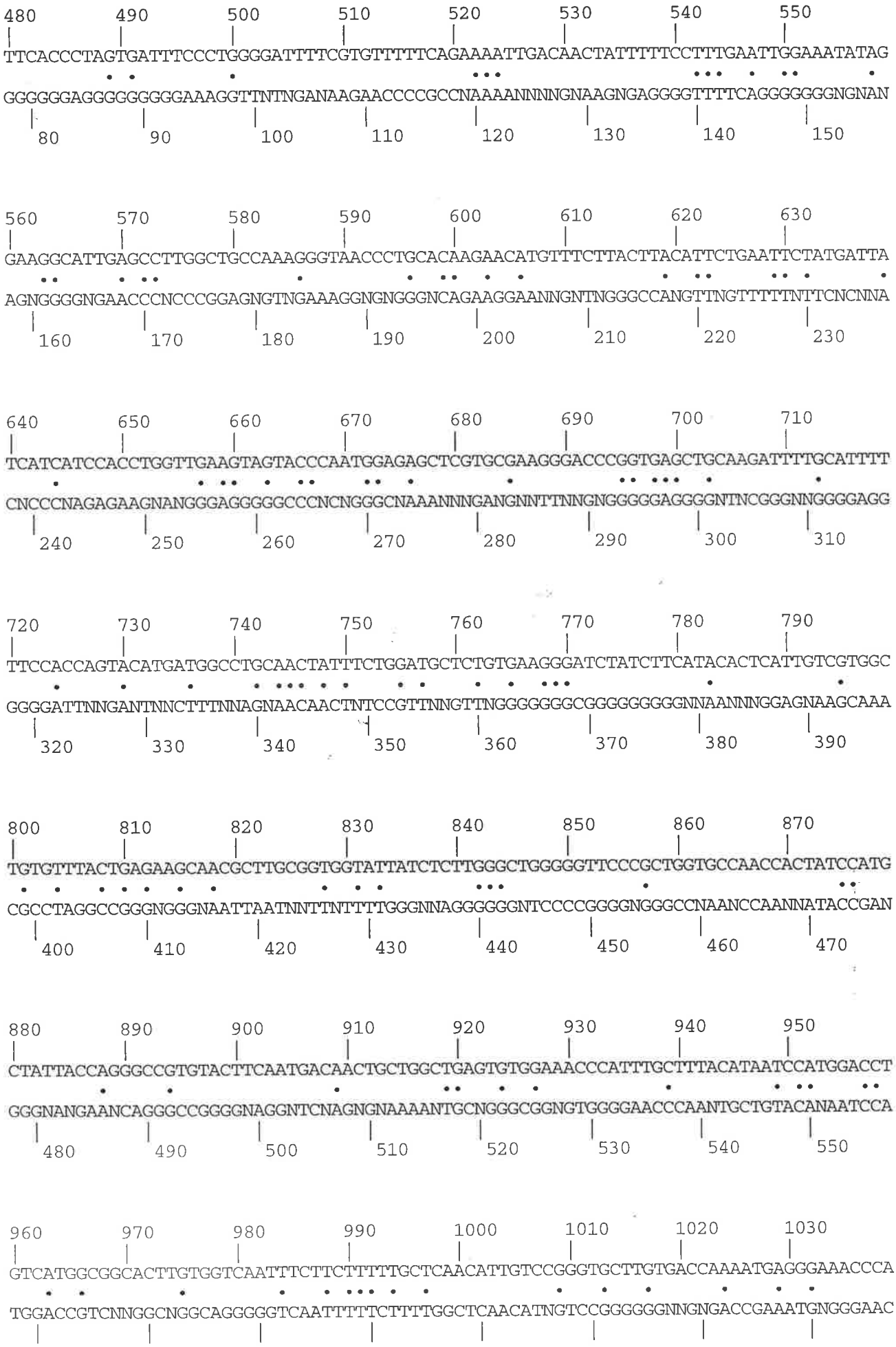
480 490 500 510 520 530 540 550
TTCACCCTAGTGATTTCCCTGGGGATTTTCGTGTTTTTCAGAAAATTGACAACTATTTTTCCTTTGAATTGGAAATATAG
GGGGGGAGGGGGGGGGAAAGGTTNTNGANAAGAACCCCGCCNAAAANNNNGNAAGNGAGGGGTTTTCAGGGGGGGNGNAN
80 90 100 110 120 130 140 150
560 570 580 590 600 610 620 630
GAAGGCATTGAGCCTTGGCTGCCAAAGGGTAACCCTGCACAAGAACATGTTTCTTACTTACATTCTGAATTCTATGATTA
AGNGGGGNGAACCCNCCCGGAGNGTNGAAAGGNGNGGGNCAGAAGGAANNGNTNGGGCCANGTTNGTTTTTNTTCNCNNA
160 170 180 190 200 210 220 230
640 650 660 670 680 690 700 710
TCATCATCCACCTGGTTGAAGTAGTACCCAATGGAGAGCTCGTGCGAAGGGACCCGGTGAGCTGCAAGATTTTGCATTTT
CNCCCNAGAGAAGNANGGGAGGGGGCCCNCNGGGCNAAANNNGANGNNTTNNGNGGGGGAGGGGNTNCGGGNNGGGGAGG
240 250 260 270 280 290 300 310
720 730 740 750 760 770 780 790
TTCCACCAGTACATGATGGCCTGCAACTATTTCTGGATGCTCTGTGAAGGGATCTATCTTCATACACTCATTGTCGTGGC
GGGGATTNNGANTNNCTTTNNAGNAACAACTNTCCGTTNNGTTNGGGGGGGCGGGGGGGGGNNAANNNGGAGNAAGCAAA
320 330 340 350 360 370 380 390
800 810 820 830 840 850 860 870
TGTGTTTACTGAGAAGCAACGCTTGCGGTGGTATTATCTCTTGGGCTGGGGGTTCCCGCTGGTGCCAACCACTATCCATG
CGCCTAGGCCGGGNGGGNAATTAATNNTTNTTTTGGGNNAGGGGGGNTCCCCGGGGNGGGCCNAANCCAANNATACCGAN
400 410 420 430 440 450 460 470
880 890 900 910 920 930 940 950
CTATTACCAGGGCCGTGTACTTCAATGACAACTGCTGGCTGAGTGTGGAAACCCATTTGCTTTACATAATCCATGGACCT
GGGNANGAANCAGGGCCGGGGNAGGNTCNAGNGNAAAANTGCNGGGCGGNGTGGGGAACCCAANTGCTGTACANAATCCA
480 490 500 510 520 530 540 550
960 970 980 990 1000 1010 1020 1030
GTCATGGCGGCACTTGTGGTCAATTTCTTCTTTTTGCTCAACATTGTCCGGGTGCTTGTGACCAAAATGAGGGAAACCCA
TGGACCGTCNNGGCNGGCAGGGGGTCAATTTTTCTTTTGGCTCAACATNGTCCGGGGGGNNGNGACCGAAATGNGGGAAC

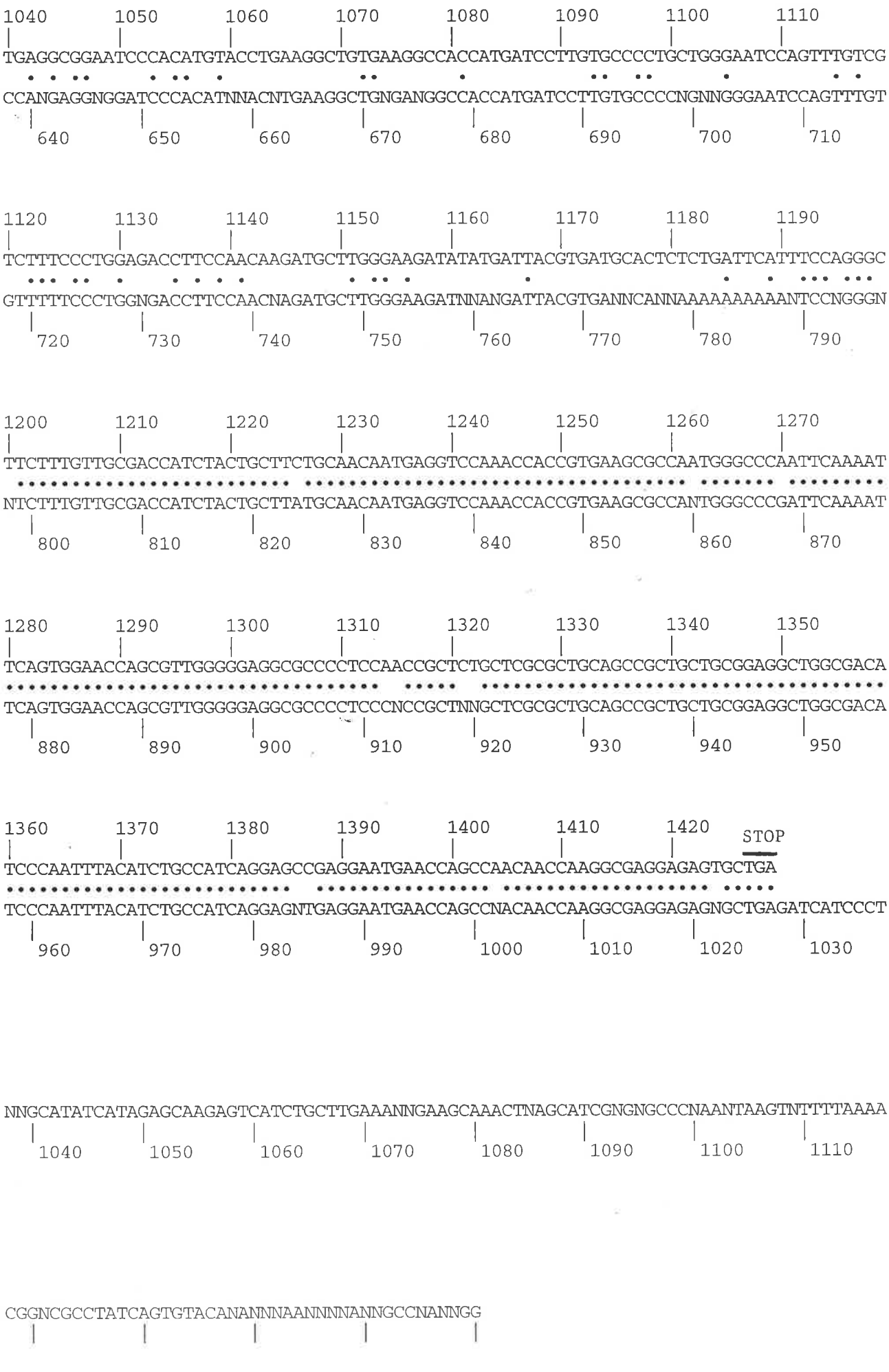
1040 1050 1060 1070 1080 1090 1100 1110
TGAGGCGGAATCCCACATGTACCTGAAGGCTGTGAAGGCCACCATGATCCTTGTGCCCCTGCTGGGAATCCAGTTTGTCG
CCANGAGGNGGATCCCACATNNACNTGAAGGCTGNGANGGCCACCATGATCCTTGTGCCCCNGNNGGGAATCCAGTTTGT
640 650 660 670 680 690 700 710
1120 1130 1140 1150 1160 1170 1180 1190
TCTTTCCCTGGAGACCTTCCAACAAGATGCTTGGGAAGATATATGATTACGTGATGCACTCTCTGATTCATTTCCAGGGC
GTTTTTCCCTGGNGACCTTCCAACNAGATGCTTGGGAAGATNNANGATTACGTGANNCANNAAAAAAAAAANTCCNGGGN
720 730 740 750 760 770 780 790
1200 1210 1220 1230 1240 1250 1260 1270
TTCTTTGTTGCGACCATCTACTGCTTCTGCAACAATGAGGTCCAAACCACCGTGAAGCGCCAATGGGCCCAATTCAAAAT
NTCTTTGTTGCGACCATCTACTGCTTATGCAACAATGAGGTCCAAACCACCGTGAAGCGCCANTGGGCCCGATTCAAAAT
800 810 820 830 840 850 860 870
1280 1290 1300 1310 1320 1330 1340 1350
TCAGTGGAACCAGCGTTGGGGGAGGCGCCCCTCCAACCGCTCTGCTCGCGCTGCAGCCGCTGCTGCGGAGGCTGGCGACA
TCAGTGGAACCAGCGTTGGGGGAGGCGCCCCTCCCNCCGCTNNGCTCGCGCTGCAGCCGCTGCTGCGGAGGCTGGCGACA
880 890 900 910 920 930 940 950
1360 1370 1380 1390 1400 1410 1420
STOP
TCCCAATTTACATCTGCCATCAGGAGCCGAGGAATGAACCAGCCAACAACCAAGGCGAGGAGAGTGCTGA
TCCCAATTTACATCTGCCATCAGGAGNTGAGGAATGAACCAGCCNACAACCAAGGCGAGGAGAGNGCTGAGATCATCCCT
960 970 980 990 1000 1010 1020 1030
NNGCATATCATAGAGCAAGAGTCATCTGCTTGAAANNGAAGCAAACTNAGCATCGNGNGCCCNAANTAAGTNTTTTAAAA
1040 1050 1060 1070 1080 1090 1100 1110
CGGNCGCCTATCAGTGTACANANNNAANNNNANNGCCNANNGG

**Figure 3.3C** Alignment of the published insert +ve hCTR sequence (Gorn et al,. 1992) with the sequence generated using a 5' primer complementary to the internal region of the hCTR. The sequence complementary to the primer is underlined, as are the 48-bp corresponding to the hCTR insert.

**Published insert +ve hCTR sequence (top), sequence generated from insert +ve hCTR pRc-CMV expression plasmid (bottom).**

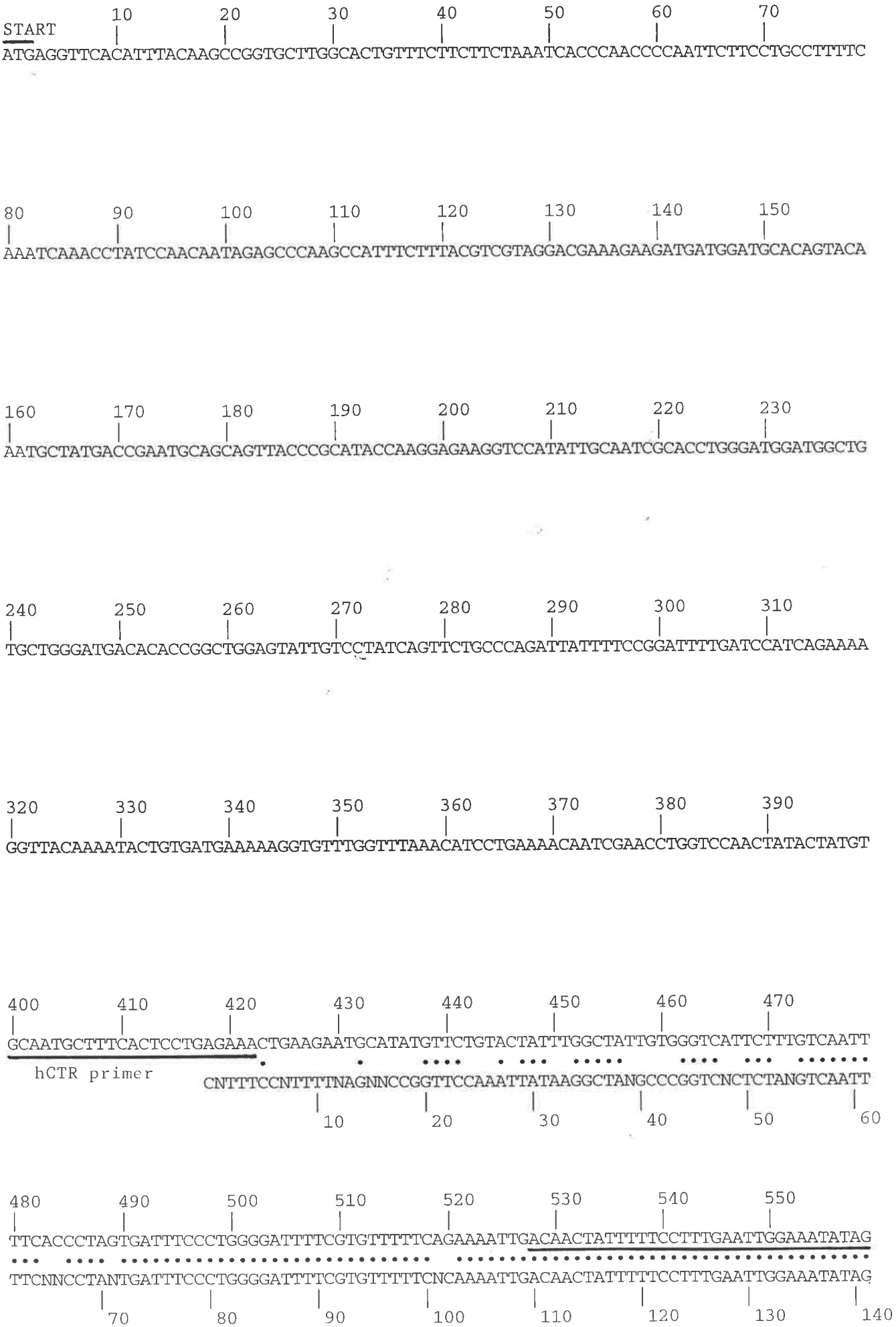

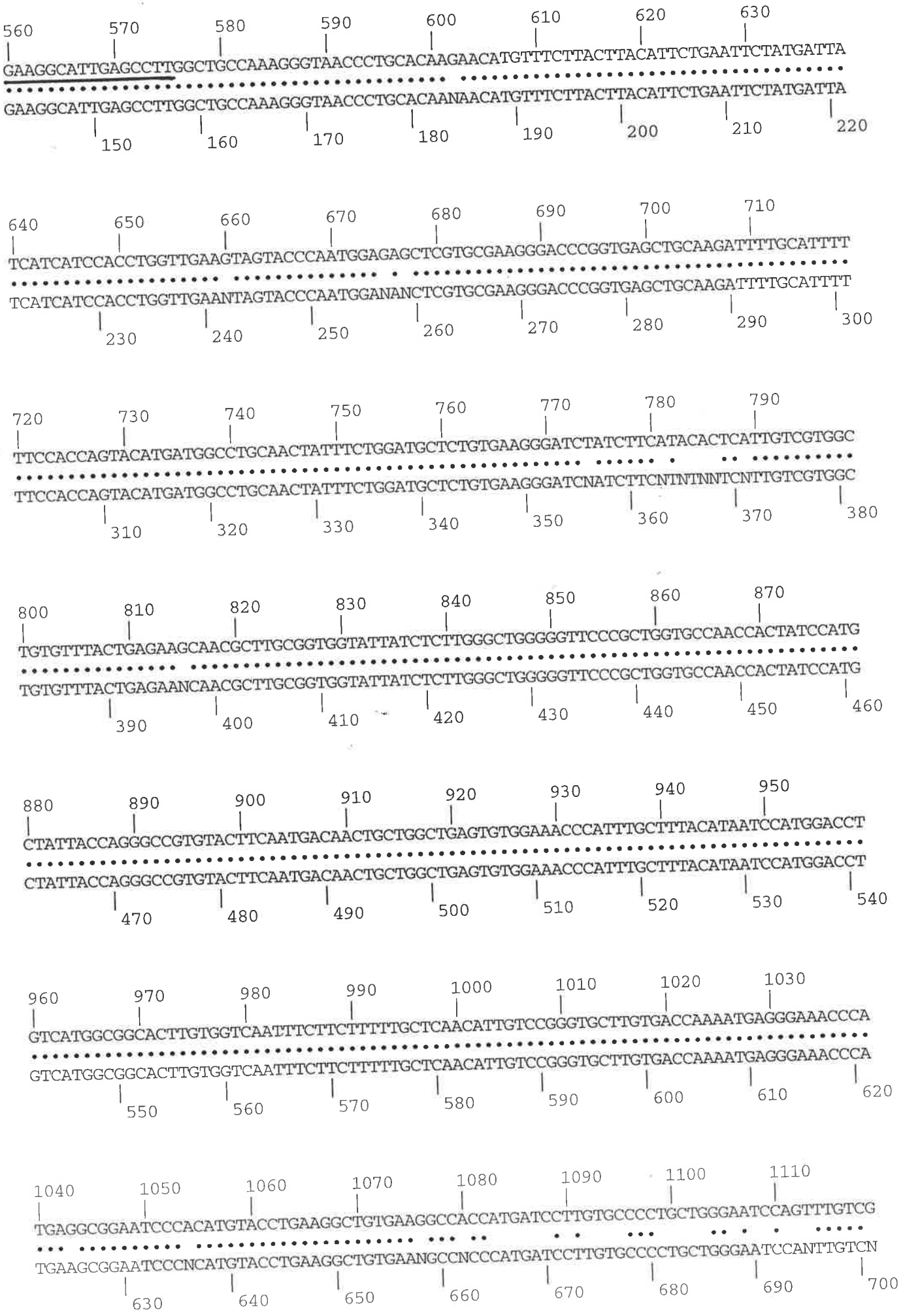
560 570 580 590 600 610 620 630
GAAGGCATTGAGCCTTGGCTGCCAAAGGGTAACCCTGCACAAGAACATGTTTCTTACTTACATTCTGAATTCTATGATTA
GAAGGCATTGAGCCTTGGCTGCCAAAGGGTAACCCTGCACAANAACATGTTTCTTACTTACATTCTGAATTCTATGATTA
150 160 170 180 190 200 210 220
640 650 660 670 680 690 700 710
TCATCATCCACCTGGTTGAAGTAGTACCCAATGGAGAGCTCGTGCGAAGGGACCCGGTGAGCTGCAAGATTTTGCATTTT
TCATCATCCACCTGGTTGAANTAGTACCCAATGGANANCTCGTGCGAAGGGACCCGGTGAGCTGCAAGATTTTGCATTTT
230 240 250 260 270 280 290 300
720 730 740 750 760 770 780 790
TTCCACCAGTACATGATGGCCTGCAACTATTTCTGGATGCTCTGTGAAGGGATCTATCTTCATACACTCATTGTCGTGGC
TTCCACCAGTACATGATGGCCTGCAACTATTTCTGGATGCTCTGTGAAGGGATCNATCTTCNTNTNNTCNTTGTCGTGGC
310 320 330 340 350 360 370 380
800 810 820 830 840 850 860 870
TGTGTTTACTGAGAAGCAACGCTTGCGGTGGTATTATCTCTTGGGCTGGGGGTTCCCGCTGGTGCCAACCACTATCCATG
TGTGTTTACTGAGAANCAACGCTTGCGGTGGTATTATCTCTTGGGCTGGGGGTTCCCGCTGGTGCCAACCACTATCCATG
390 400 410 420 430 440 450 460
880 890 900 910 920 930 940 950
CTATTACCAGGGCCGTGTACTTCAATGACAACTGCTGGCTGAGTGTGGAAACCCATTTGCTTTACATAATCCATGGACCT
CTATTACCAGGGCCGTGTACTTCAATGACAACTGCTGGCTGAGTGTGGAAACCCATTTGCTTTACATAATCCATGGACCT
470 480 490 500 510 520 530 540
960 970 980 990 1000 1010 1020 1030
GTCATGGCGGCACTTGTGGTCAATTTCTTCTTTTTGCTCAACATTGTCCGGGTGCTTGTGACCAAAATGAGGGAAACCCA
GTCATGGCGGCACTTGTGGTCAATTTCTTCTTTTTGCTCAACATTGTCCGGGTGCTTGTGACCAAAATGAGGGAAACCCA
550 560 570 580 590 600 610 620
1040 1050 1060 1070 1080 1090 1100 1110
TGAGGCGGAATCCCACATGTACCTGAAGGCTGTGAAGGCCACCATGATCCTTGTGCCCCTGCTGGGAATCCAGTTTGTCG
TGAAGCGGAATCCCNCATGTACCTGAAGGCTGTGAANGCCNCCCATGATCCTTGTGCCCCTGCTGGGAATCCANTTGTCN
630 640 650 660 670 680 690 700

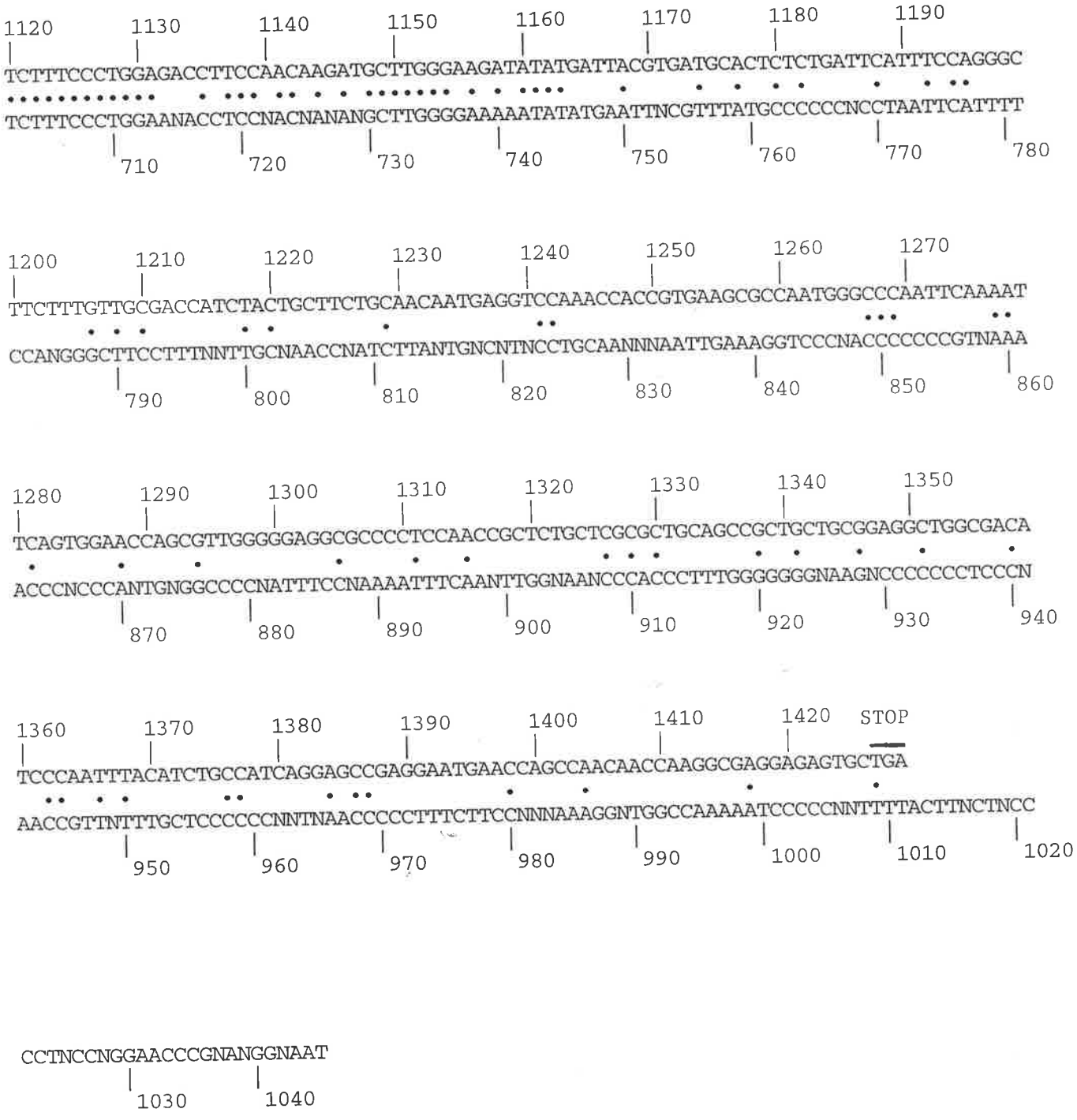
1120 1130 1140 1150 1160 1170 1180 1190
TCTTTCCCTGGAGACCTTCCAACAAGATGCTTGGGAAGATATATGATTACGTGATGCACTCTCTGATTCATTTCCAGGGC
TCTTTCCCTGGAANACCTCCNACNANANGCTTGGGGAAAAATATATGAATTNCGTTTATGCCCCCCNCCTAATTCATTTT
710 720 730 740 750 760 770 780
1200 1210 1220 1230 1240 1250 1260 1270
TTCTTTGTTGCGACCATCTACTGCTTCTGCAACAATGAGGTCCAAACCACCGTGAAGCGCCAATGGGCCCAATTCAAAAT
CCANGGGCTTCCTTTNNTTGCNAACCNATCTTANTGNCNTNCCTGCAANNNAATTGAAAGGTCCCNACCCCCCCGTNAAA
790 800 810 820 830 840 850 860
1280 1290 1300 1310 1320 1330 1340 1350
TCAGTGGAACCAGCGTTGGGGGAGGCGCCCCTCCAACCGCTCTGCTCGCGCTGCAGCCGCTGCTGCGGAGGCTGGCGACA
ACCCNCCCANTGNGGCCCCNATTTCCNAAAATTTCAANTTGGNAANCCCACCCTTTGGGGGGGGNAAGNCCCCCCCTCCCN
870 880 890 900 910 920 930 940
1360 1370 1380 1390 1400 1410 1420 STOP
TCCCAATTTACATCTGCCATCAGGAGCCGAGGAATGAACCAGCCAACAACCAAGGCGAGGAGAGTGCTGA
AACCGTTNTTTGCTCCCCCCNNTNAACCCCCTTTCTTCCNNNAAAGGNTGGCCAAAAATCCCCCNNTTTTACTTNCTNCC
950 960 970 980 990 1000 1010 1020
CCTNCCNGGAACCCGNANGGNAAT
1030 1040

receptor expression on the cell surface. Several clonal cell lines were generated that had varying ability to bind [$^{125}$I] sCT, when compared to the previously described D11 cell line *(Houssami et al., 1994)*, which expresses the rat C1a isoform of the rat CTR (Table 3.1). To compare ligand-receptor interactions in HEK-293 clones stably expressing either the insert –ve or insert +ve hCTR, binding competition curves (described in section 2.2.6.3) were constructed using [$^{125}$I] sCT as the radioligand, with increasing concentrations of unlabeled sCT. Binding competition in two cell lines expressing the insert –ve form of the hCTR (designated HR12 and HR9) were compared to D11 cells expressing the rat C1a CTR. There were no consistent differences between the binding ability of the insert –ve hCTR isoform or the rCTR isoform (Figure 3.4). Scatchard analysis was performed to determine the number of receptors expressed by each clone and the binding affinity (Kd) of the receptors (Figure 3.4 insert). The HR12 cell line expressed 1.4±0.4x10$^6$ receptors per cell (mean ± SEM, n=3), and bound [$^{125}$I]sCT with a Kd of 2.0±0.4nM (mean ± SEM, n=3). A second cell line investigated, HR9, had similar binding kinetics to the HR12, expressing 1.2x10$^6$ receptors per cell (n=2), with a Kd of 2.6nM (n=2).

Similarly, ligand-receptor interactions were compared between clones expressing the insert –ve and insert +ve hCTR, using binding competition curves (figure 3.5). Binding competition of the HR12 cell line expressing the insert –ve hCTR was compared with two cell lines stably transfected with the insert +ve hCTR (designated Hi12 and Hi5). There were no significant differences between the binding ability of these hCTR isoforms (figure 3.5). Scatchard analysis showed that the Hi12 cells expressed 2.3x10$^6$ receptors per cell (n=2) and bound [$^{125}$I]sCT with a Kd of 3.3nM (n=2) (figure 3.5 insert). The Hi5 cell line had comparable binding

**Comparison of [$^{125}$I] sCT binding in parental HEK-293 cells or individual HEK-293 clones expressing either the insert –ve hCTR or Cla rCTR.**

Experiment 1

| Clone | CTR expression | Specific Binding Counts per $10^6$ cells |
|---|---|---|
| HEK | - | 1621 |
| D11 | rCTR | 23815 |
| HR3 | insert -ve hCTR | 13516 |
| HR8 | insert -ve hCTR | 13733 |
| HR1 | insert -ve hCTR | 14837 |
| HR2 | insert -ve hCTR | 14163 |
| HR5 | insert -ve hCTR | 13434 |

Experiment 2

| Clone | CTR expression | Specific Binding Counts per $10^6$ cells |
|---|---|---|
| HEK | - | 550 |
| D11 | rCTR | 27372 |
| HR12 | insert -ve hCTR | 37405 |
| HR13 | insert -ve hCTR | 48323 |
| HR11 | insert -ve hCTR | 25844 |
| HR10 | insert -ve hCTR | 53819 |
| HR9 | insert -ve hCTR | 13408 |

**Table 3.1** Clonal cell lines stably expressing either the C1a rCTR or the insert –ve hCTR were incubated with [$^{125}$I] sCT alone or [$^{125}$I] sCT and 100 nM unlabeled sCT for 1h at 37°C. Cells were then washed twice with PBS and solublised with 0.5 ml of 0.5 M NaOH. Cell associated radioactivity was determined by counting in a $\gamma$-counter. Results are means of duplicate determinations from two independent experiments.

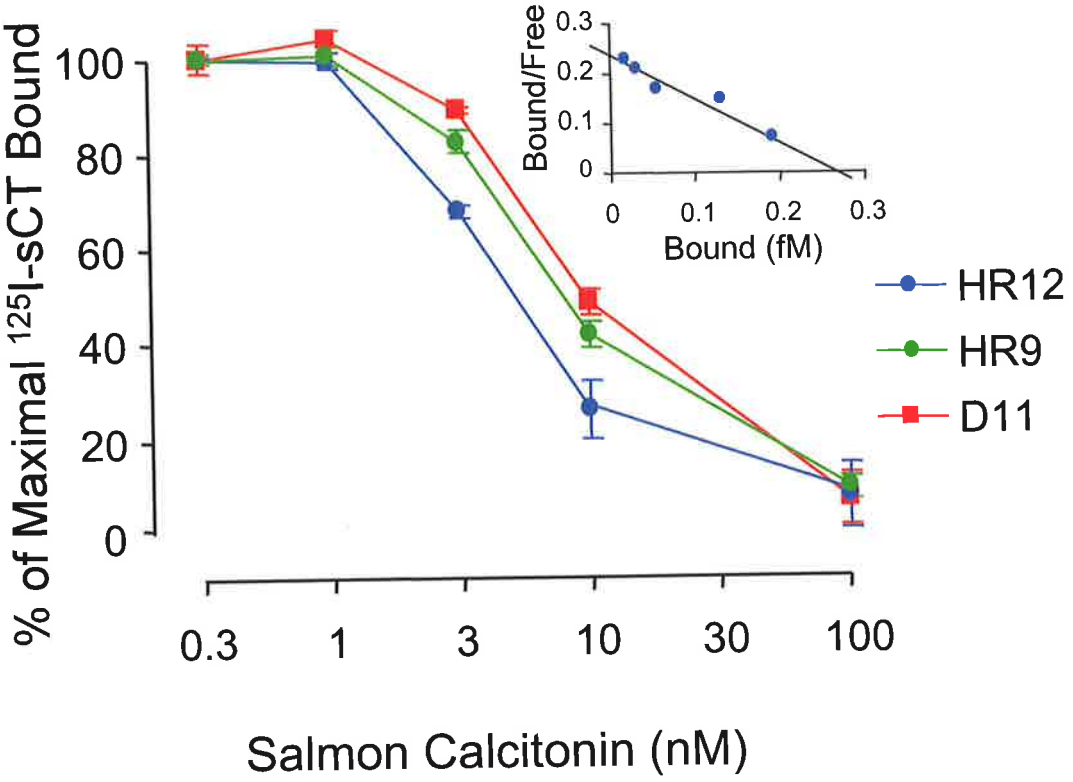


**Figure 3.4 Binding of [$^{125}$I]sCT in HEK-293 cells expressing the C1a rCTR or the insert –ve hCTR.**

Cells stably expressing the C1a rCTR D11 clone (■), the insert –ve hCTR HR12 clone (●), HR9 clone (●) were incubated with [$^{125}$I]sCT and increasing concentrations of unlabeled sCT for 1 h at 37° C. Cells were then washed twice with PBS and solublised in 0.5ml of 0.5M NaOH. Cell associated radioactivity was determined by counting in a γ-counter. Results are mean ± SEM of triplicate determinations, expressed as a percent of maximal bound [$^{125}$I]sCT, and these results are representative of three independent experiments for D11 and HR12 cells and two independent experiments for the HR9 cells. The insert is a representative example of the Scatchard analysis of sCT binding to HEK-293 cells expressing the insert –ve hCTR, HR12 clone, performed as described in the *Experimental materials and methods.*

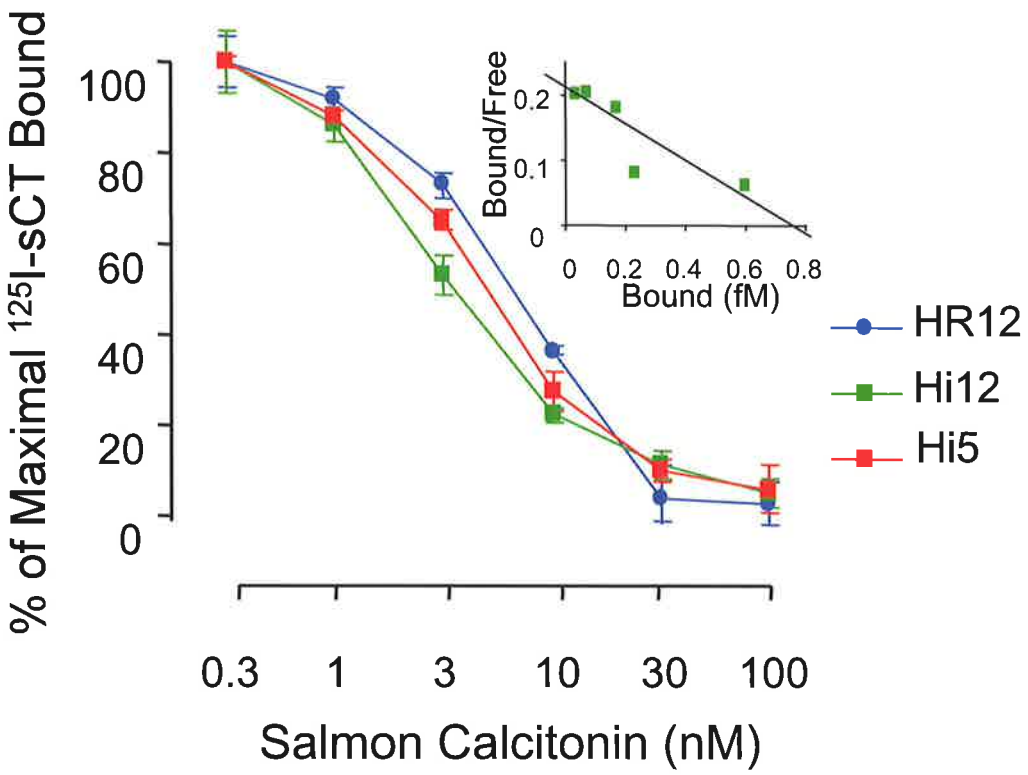


**Figure 3.5 Binding of [$^{125}$I]sCT in HEK-293 cells expressing the insert –ve or the insert +ve hCTR.**

Cells stably expressing the insert –ve hCTR HR12 clone (●), the insert +ve hCTR Hi12 clone (■), or Hi5 clone (■) were incubated with [$^{125}$I]sCT and increasing concentrations of unlabeled sCT for 1 h at 37°C. Cells were then washed twice with PBS and solubilised in 0.5 ml of 0.5 M NaOH. Cell associated radioactivity was determined by counting in a γ-counter. Results are mean ± SEM of triplicate determinations expressed as a percent of maximal bound [$^{125}$I]sCT, and these results are representative of two independent experiments. The insert is a representative example of the Scatchard analysis of sCT binding to HEK-293 cells, expressing the insert +ve hCTR, Hi12 clone, performed as described in the *Experimental materials and methods*.

kinetics, expressing $3.6x10^6$ receptors per cell (n=2) and binding [$^{125}$I]sCT with a Kd of 3.3nM (n=2).

### 3.2.3 Internalisation of hCTR isoforms

The internalisation of the ligand receptor complex is known to occur following the binding of [$^{125}$I]sCT to rat *(Houssami et al., 1994)*, pig *(Findlay et al., 1994)* and human *(Moore et al., 1995)* CTR receptors. On the cell surface, receptor-bound CT is sensitive to removal by low pH buffer, but in a time and energy dependent manner translocates to an acid resistant state, which is consistent with receptor internalisation *(Findlay et al., 1984)*. Previously, the insert –ve and insert +ve hCTR receptor isoforms have been shown to internalise at very different rates in response to binding of [$^{125}$I]sCT, when stably expressed in BHK cells *(Moore et al., 1995)*. Those data indicated another clear functional difference between these receptor isoforms, and suggested a link between the ability of the receptor to signal and to induce down regulation. In the current experiments (described in section 2.2.6.4) the pattern of internalisation observed in HEK-293 cells expressing either the insert –ve or +ve hCTR was different from that previously observed in the BHK cells. The amount of cell surface-bound [$^{125}$I]sCT was assessed by the ability of an acidic buffer to remove the radioactivity from the surface of intact cells. To assess the ligand-induced receptor internalisation, cells were first incubated for 30 min with [$^{125}$I]sCT, prior to measurement of acid elutability at the different time points thereafter. Figure 3.6 shows 22% and 28 % of the insert –ve and +ve hCTR, respectively, were internalised during the incubation process. During the 240 min following the [$^{125}$I]sCT incubation, the insert +ve hCTR maintained a relatively constant sensitivity to acid elution. A maximum of 30% of surface-associated radioactivity was internalised by cells expressing the insert +ve hCTR during the experimental time frame, most of

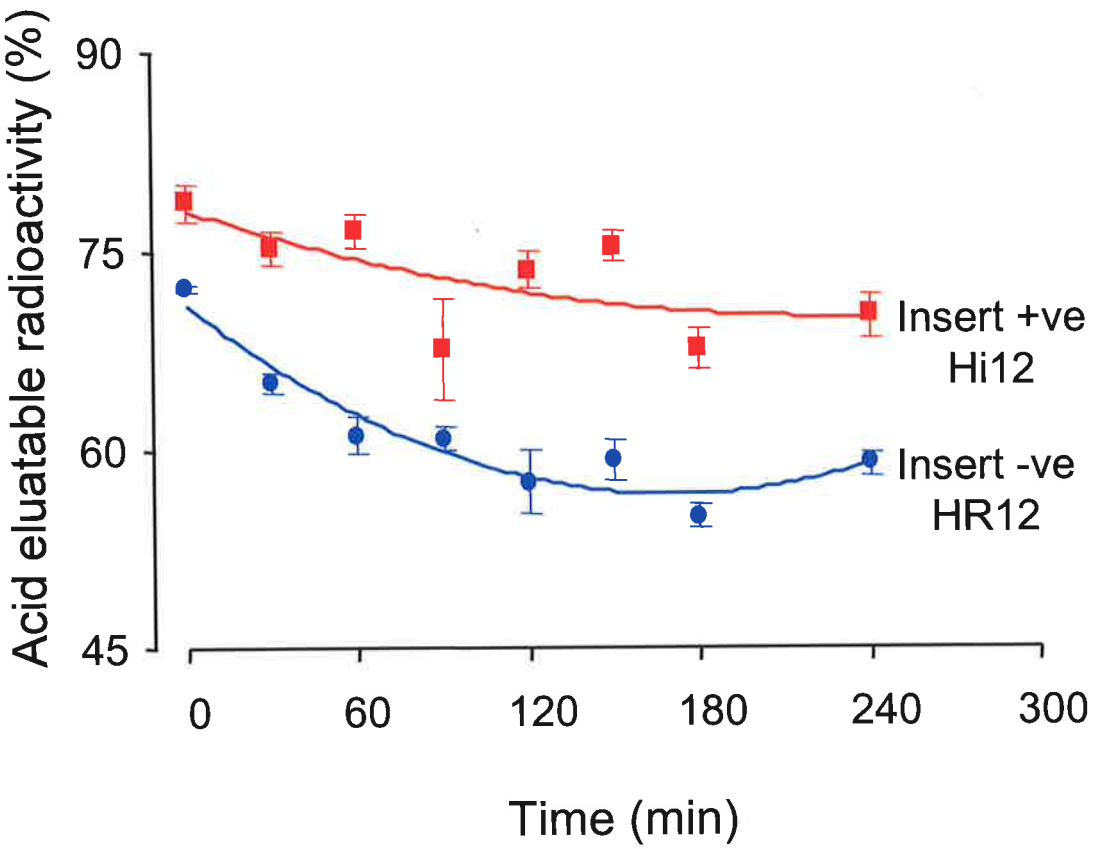


**Figure 3.6 Acid elution of [$^{125}$I]sCT from cells expressing either the insert –ve or +ve hCTR.**

Cells were incubated with [$^{125}$I]sCT for 30 min at 37 C, the medium was removed, cells were washed once with 1x PBS and fresh medium containing no sCT was added. At the times indicated, the cells were washed with 1x PBS, followed by 0.5ml ice cold 0.15 M NaCl-0.05 glycine (pH 2.5). The cells were then solubilised in 0.5ml of 0.5 M NaOH. The elutable and cell associated radioactivity was then measured using a $\gamma$-counter. The results show the percentage of cell associated radioactivity eluted by acid at each time. Each Data point is the mean $\pm$ SEM of triplicate determinations and the experiment is representative of two experiments.

experimental time frame, most of which occurred in the first hour following the incubation. The HEK-293 cells expressing the insert –ve hCTR exhibited a similar pattern of receptor internalisation to the Hi12 cells, with a greater amount of cell surface receptor internalised. The amount of acid-elutable radioactivity increased from 28%-40% during the first hour post [$^{125}$I]sCT incubation, and then plateaued and remained approximately at this level over the next 240 min. Thus a qualitatively similar functional difference between the internalisation of the receptor isoforms was seen in HEK-293 cells as BHK cells although with a reduced magnitude.

### 3.2.4 cAMP accumulation

CT stimulates cAMP accumulation in BHK cells transfected with either the insert -ve or the insert +ve hCTR *(Moore et al., 1995)*. However BHK cells transfected with the insert +ve hCTR cells responded with greatly reduced sensitivity *(Moore et al., 1995)*. The results of experiments performed in HEK-293 cells (described in section 2.2.7) were quite different. Treatment with sCT resulted in an accumulation of cAMP in cells expressing the insert –ve hCTR, with an $EC_{50}$ of approximately $3x10^{-9}$M (Figure 3.7). In contrast, insert +ve hCTR transfected cells were essentially unresponsive to CT, even at concentrations that were saturating or near-saturating for the insert -ve hCTR (Figure 3.7).

### 3.2.5 Free calcium mobilisation

Nanomolar concentrations of sCT have been shown to induce a transient rise in intracellular calcium in BHK cells transfected with the insert-ve hCTR *(Stroop et al., 1993)*, and HEK-293 cells stably transfected with the rat C1a CTR *(Houssami et al., 1994)*. However, BHK cells expressing the insert +ve hCTR *(Moore et al., 1995)* were found to be unresponsive to CT with respect to $Ca^{2+}$ mobilisation. It was therefore of interest to compare the ability of the hCTR isoforms to induce

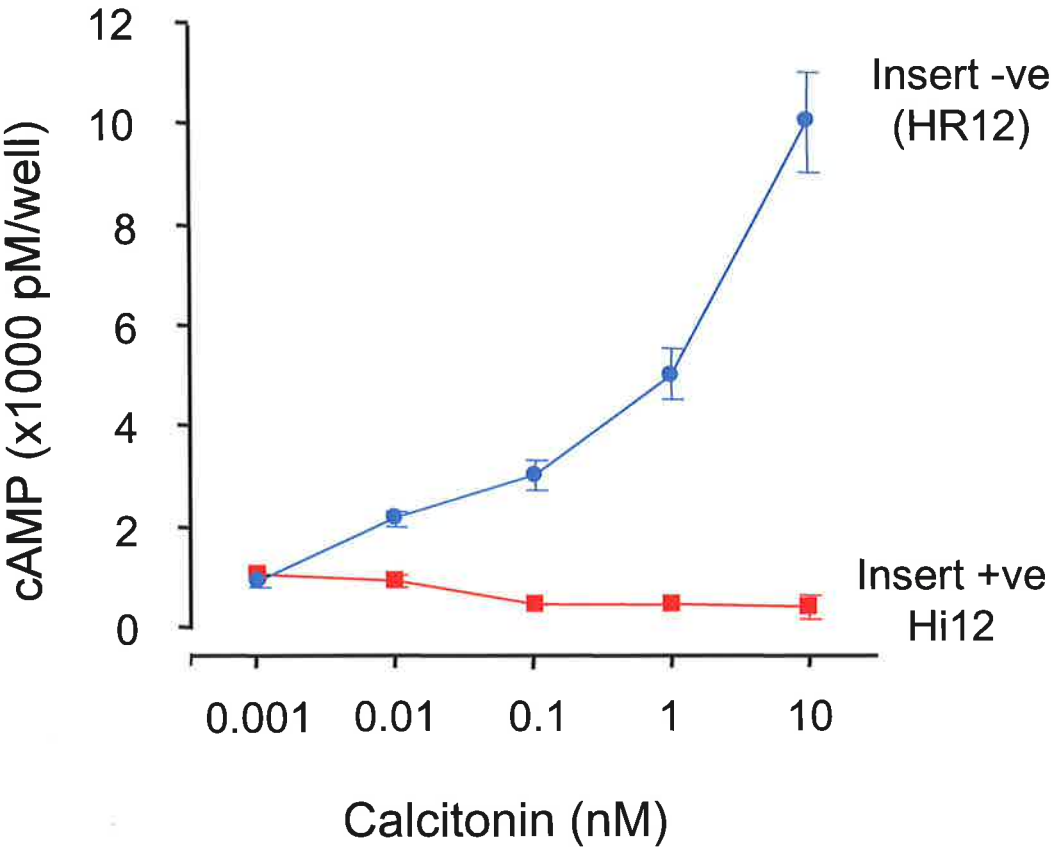


**Figure 3.7 CT induction of intracellular cAMP accumulation.**
HEK-293 cells stably expressing the insert –ve (●) or insert +ve hCTR (■) were treated with the indicated concentrations of sCT for 15 min at 37°C. Cells were then lysed and assayed for intracellular cAMP content as described in the *Experimental materials and methods*. The results are mean ± SEM of triplicate determinations and are representative of two independent experiments.

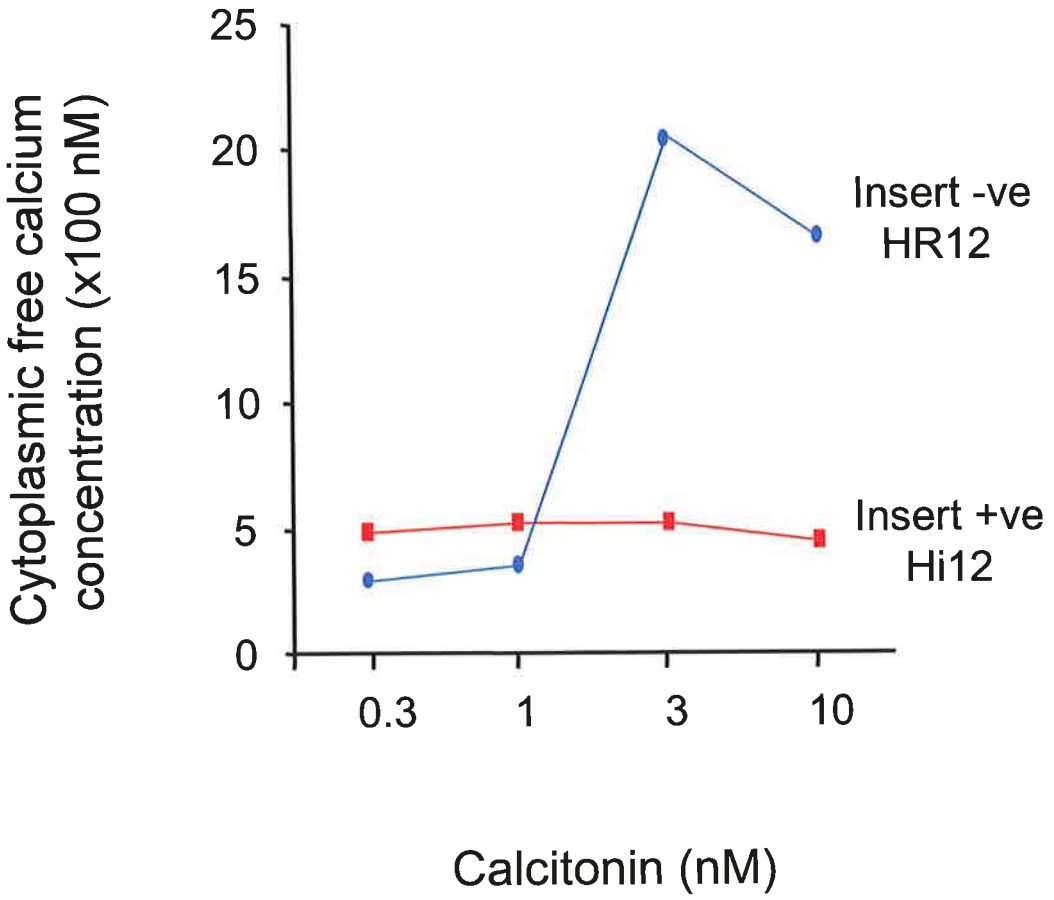


**Figure 3.8 Intracellular calcium mobilisation.**

Suspensions of fura-2AM loaded HEK-293 cells, expressing the insert –ve hCTR HR12 clone (●) or insert +ve hCTR Hi12 clone (▮), were exposed to increasing concentrations of sCT. Cytoplasmic free calcium was calculated as described in the *Experimental material and methods.* This data is representative of two independent experiments.

intracellular calcium in HEK-293 cells (as described in section 2.2.8). Treatment of cells transfected with the insert-ve hCTR with sCT induced a rapid, dose-responsive increase in intracellular calcium, similar to that shown in BHK cells (Figure 3.8). This increase in intracellular calcium was receptor isoform specific since concentrations of CT that were maximally effective for the insert –ve hCTR had no effect on intracellular calcium concentrations in cells transfected with the insert +ve hCTR (Figure 1.8). As expected in HEK-293 cells transfected with the vector alone, CT had no effect on intracellular calcium concentration (data not shown).

### 3.2.6 Sustained activation of Erk1/2 MAPK by CT

To examine the effect of CT on activation of the Erk1/2 MAPK pathway, we determined the effect of CT on phosphorylation of Erk1/2 in HEK-293 cells stably expressing either the insert –ve or insert +ve hCTR (described in section 2.2.9). Treatment with CT resulted in a minor and transient phosphorylation of Erk1/2 in the first hour of treatment. However, a marked induction of Erk1/2 phosphorylation was seen at 24h that was sustained for up to 48h and 72h in cells stably expressing the insert –ve hCTR (Figure 3.9A and Figure 8.8). Cells expressing the insert +ve hCTR, or vector alone, showed no change in the phosphorylation state of Erk1/2 in response to CT treatment (Figure 3.9B & C). Phosphorylation of Erk1/2 by CT was ligand-dependent and was not seen in cells incubated in the absence of CT (Figure 3.9A, B and C).

### 3.2.7 Changes in extracellular pH

An interesting phenomenon was observed after CT treatment of HEK-293 cells transfected with either the insert -ve hCTR or the insert +ve hCTR. Despite the presence of both sodium bicarbonate and hepes buffering agents, there was a time-dependent increase in the acidity of the growth media, in response to sCT treatment

**Figure 3.9 CT activation of ERK1/2 is CTR isoform specific.**

Sub-confluent HEK-293 cells stably expressing the insert –ve hCTR, HR12 clone, (panel A), insert +ve hCTR Hi12 clone (panel B) or vector alone (panel C) were treated for the indicated times with 10 nM sCT, or for 5 min with 10 ng/ml EGF as a positive control. Cells were washed once in PBS and lysed in lysis buffer. Total cell extracts were processed, as described in the *Experimental materials and methods,* for immunoblotting with anti-phospho-Erk1/2 antibody to determine the phosphorylation state of Erk1/2 (upper panel) or anti-Erk1 antibody, to determine the total amount of protein in each sample (lower panel). These results are representative of three independent experiments.

A

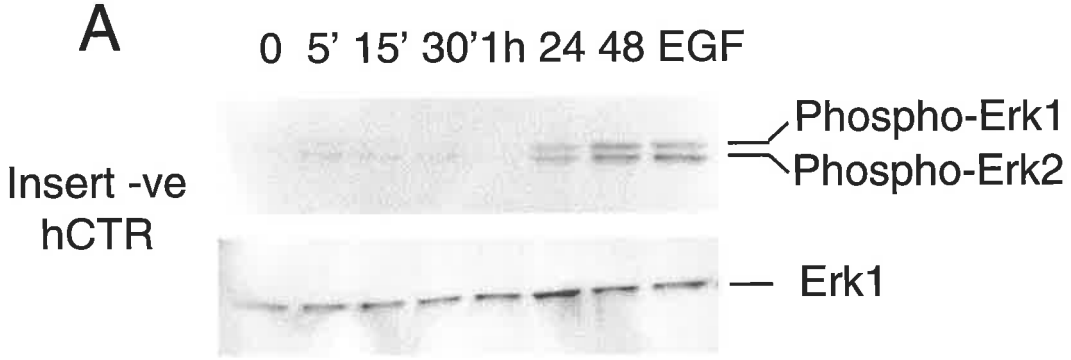
0 5' 15' 30'1h 24 48 EGF
Phospho-Erk1
Phospho-Erk2
Insert -ve
hCTR
Erk1

B

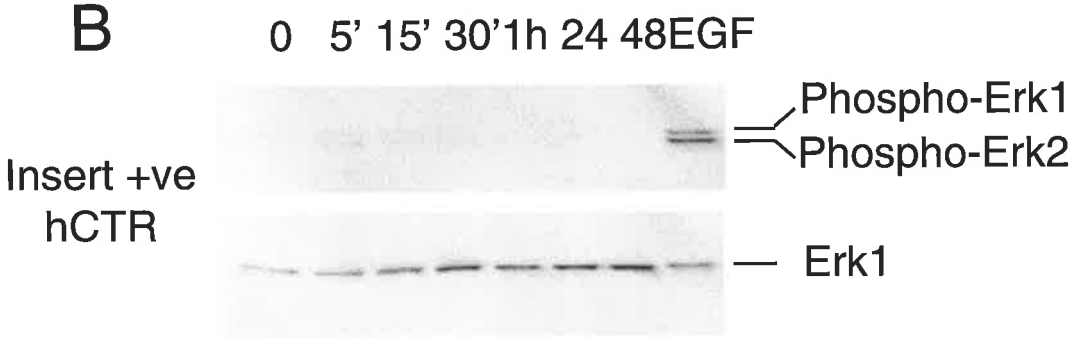
0 5' 15' 30'1h 24 48EGF
Phospho-Erk1
Phospho-Erk2
Insert +ve
hCTR
Erk1

C

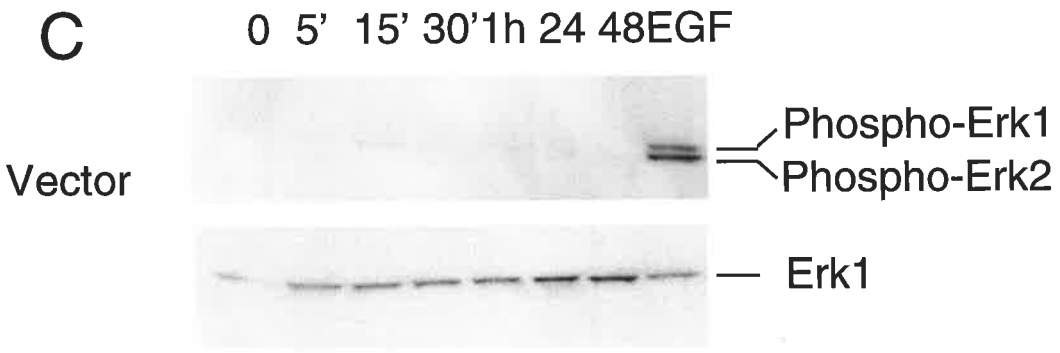
0 5' 15' 30'1h 24 48EGF
Phospho-Erk1
Phospho-Erk2
Vector
Erk1

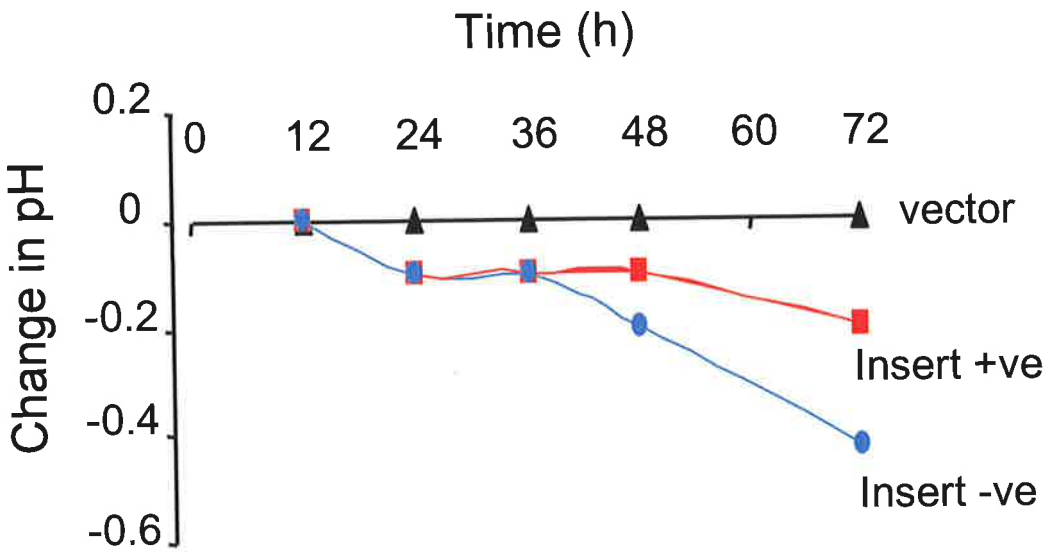


**Figure 3.10 CT-induced extracellular acidification.**

HEK-293 cells stably expressing the insert –ve hCTR clone HR12 (●), the insert ve hCTR clone Hi12 (■) or vector alone (▲) were treated 48 h after plating with 10 nM sCT. At the indicated times the media pH of triplicate wells was measured. These results are mean ± SEM, with error bars obscured by the data points, and the data is representative of 3 independent experiments.

(described in section 2.2.10) (figure 1.10). This novel effect was of greater magnitude for cells transfected with the insert –ve hCTR. Treatment of cells transfected with the vector alone showed no change in extracellular pH after sCT treatment (figure 1.10).

## 3.3 Discussion

In reconsidering the physiology of CT, it is necessary to understand the significance of the CTR isoforms that result from alternative splicing of the primary transcript and that are expressed in a tissue-specific manner *(Kuestner et al., 1994)*. In particular, transcripts corresponding to the insert +ve isoform of the hCTR are expressed as a minor product in most tissues examined, relative to the insert -ve transcript and not at all in stomach and brain, but are well expressed in ovary and placenta *(Kuestner et al., 1994)*. Interestingly, the insert +ve isoform appears to be always expressed together with the insert -ve isoform, although the converse is not true *(Kuestner et al., 1994)*. This pattern of expression would make possible modulation of the insert –ve isoform by the insert +ve isoform. Although there is no evidence for such an action as yet, this possibility is discussed in chapter 9.

Two HEK-293 clones expressing the insert –ve hCTR isoform displayed similar binding characteristics for [$^{125}$I]CT to the previously reported D11 clone, which expresses the C1a isoform of the rat CTR. The C1a isoform bears 78% homology with the insert -ve hCTR *(Gorn et al., 1992)*, and has similar binding kinetics to the human homologue. The second isoform of the rat CTR contains an extracellular insert, which consequently reduces the affinity of the receptor for [$^{125}$I]sCT *(Sexton et al., 1993)*. The insert +ve hCTR has a 16 amino acid insert in the first intracellular loop of the receptor *(Gorn et al., 1992)*. The insert did not alter the binding ability of

the two HEK-293 clones expressing the insert positive hCTR, as they have binding characteristics indistinguishable from the HR12 clone. This observation agrees with previous reports on the binding kinetics of these receptors in non-human BHK cells *(Moore et al., 1995)*.

The pattern of ligand mediated receptor internalisation for both the insert +ve and -ve hCTR isoforms in the HEK-293 transfection model, was different from that observed in the BHK system *(Moore et al., 1995)*. However the pattern of internalisation for the insert –ve hCTR was similar to that reported when the C1a rCTR was expressed in HEK cells *(Houssami et al., 1994)*, where acid elutability plateaued following internalisation of 40% of surface radioactivity. Interpretation of receptor internalisation kinetics in HEK cells is confounded by a recent report that this cell line is deficient in the molecular machinery required for agonist-induced receptor internalisation *(Barlic et al., 1999)*. Internalisation of the CXCR1 receptor in response to IL-8 activation was shown to require GPCR kinase 2 (GRK2), β-arrestins and dynamin. HEK-293 cells have significantly reduced endogenous levels of β-arrestin 2 and GRK2 and thus have impaired internalisation of CXCR1 receptor *(Barlic et al., 1999)*. With the abundant cell surface expression of hCTR in a transfected cell model, it is probable that the internalisation machinery becomes saturated when all (GRK2) and β-arrestin molecules are in use, thus inducing the plateau effect observed when C1a rCTR and hCTR are expressed in these cells.

Although the presence of the 16 amino acid insert does not alter the binding capacity of the hCTR receptors, the signalling ability was affected *(Moore et al., 1995)*. The results shown here suggest that the insert -ve hCTR isoform, when expressed in HEK-293 cells, couples to αs and αq G-proteins inducing a rise in intracellular cAMP and cytosolic calcium. In contrast, the insert +ve hCTR isoform

did not activate αs or αq mediated signalling pathways in HEK-293 cells. This result, together with previous reports on the ability of the insert +ve hCTR isoform to activate Gαs-mediated signalling pathways *(Moore et al., 1995)*, indicates that this activity is cell-type dependent. For example, when the insert +ve hCTR was expressed in COS *(Nussenzveig et al., 1994)* and BHK *(Moore et al., 1995)* cells, the $EC_{50}$ for CT to stimulate adenylate cyclase was several orders of magnitude greater than that required for the same cells expressing the insert –ve hCTR. In addition to the relative ability of the isoforms to activate adenylate cyclase being cell type dependent, the maximal activation of adenylate cyclase by the insert +ve hCTR was also cell specific. In COS cells expressing the insert +ve hCTR, the maximal activation of adenylate cyclase by CT was greatly reduced compared to COS cells expressing the insert -ve hCTR *(Nussenzveig et al., 1994)*. However in BHK cells there was no difference in the maximal activation of adenylate cyclase by the insert –ve or +ve hCTR *(Moore et al., 1995)*. These differences in hCTR receptor signalling are not fully understood at present, but are likely due to the species specificity of the transfected cells used. To date, human, hamster and monkey transfected models have been used. Knowledge of the molecular complexes involved in GPCR signalling, for example G-proteins, arrestins, receptor kinases and RAMPS, is increasing and thus the specific pattern of expression a cell has of these proteins is likely to dictate the signalling pathway ultimately activated by a receptor.

In addition to investigating the ability of the insert –ve and +ve hCTR isoforms to activate classical signalling pathways in HEK cell, we have explored the ability of CT to activate the MAPK pathway. CT treatment of HEK-293 cells expressing the hCTR induced a delayed and sustained phosphorylation of Erk1/2 in an isoform specific manner. In response to CT treatment, cells expressing the insert

–ve hCTR phosphorylated Erk1/2, while CT treatment of cells expressing the insert +ve hCTR or vector transfected cells alone failed to phosphorylate Erk1/2. Recently CT was reported to cause transient activation of Erk1/2 in HEK-293 cells transfected with the rabbit CTR *(Chen et al., 1998)*, although the authors did not link this activation with later events in the cells, in particular cell growth. It is important to note that the experiments performed by Chen *et al. (Chen et al., 1998)* using the rabbit CTR were performed in low serum (0.5%) conditions. The experiments described here were conducted under optimal mitogenic conditions, in medium containing 10% FCS. In the current experimental conditions we observed a minor early and transient activation of Erk1/2, followed by a delayed and prolonged activation.

Thus far, the insert +ve hCTR isoform appears to be relatively inert with respect to activation of signalling pathways in the HEK system, however CT treatment of HEK-293 cells stably transfected with either hCTR isoform lowered media pH. This suggests that the insert +ve hCTR is not simply a decoy receptor but has functional significance in the cells. The mechanism of this acidification is unknown, however this finding suggests that the insert +ve hCTR may activate previously unrecognised signalling pathways. The action by which CT induces acidification of the extracellular media may be similar to the reported extracellular acidification by the parathyroid hormone receptor in SaOS2 cells. PTH induces a receptor-mediated, concentration dependent increase in extracellular acid, which was mediated through the PKC signalling cascade *(Barrett et al., 1997)*. Alternatively the mechanism of hCTR extracellular acidification may be independent of G-protein activation. Recently the $\beta_2$-adrenergic 7TMD receptor was shown to interact with the $Na^+/H^+$ exchanger regulatory factor (NHERF), a protein, which activates the $Na^+/H^+$ exchanger 3 (NHE3) *(Hall et al., 1998b)*. The NHERF interacts with the cytoplasmic

tail of the $\beta_2$ receptor through a direct binding of a PDZ-domain. Site-specific mutagenesis of the $\beta_2$ terminal tail has identified the optimal NHERF binding motif to be D-S/T-X-L *(Hall et al., 1998a)*. Replacement of the terminal leucine with an alanine abolished $\beta_2$ interaction with NHERF, uncoupling the $\beta_2$- receptor regulation of NHE3 without altering the $\beta_2$-receptor activation of adenylate cyclase. Although the hCTR terminal cytoplasmic tail sequence, Glu-S-S-A, shows only 50% homology to the required NHERF binding motif, the exact sequence requirements for this function have not been determined, allowing the possibility that the hCTR mediates extracellular acidification through NHERF regulation of NHE or *via* an as yet unidentified mechanism.

h RAMP 3 has NHERF sequence !

# Chapter 4

# Growth inhibitory effects of CT on HEK-293 cells transfected with either the C1a rCTR, the insert –ve or insert +ve hCTR.

## 4.1 Introduction

Cell growth regulation has until recently been viewed primarily as an action of phosphotyrosine kinase receptors such as the EGF receptor (discussed in section 1.3.2). The intracellular kinase domain of these single transmembrane spanning receptors has intrinsic catalytic activity, which is activated upon extracellular ligand binding (discussed in section 1.3.3.1). The CTR is a member of a subclass of the large seven transmembrane domain (7TMD) G-protein coupled receptor (GPCR) family, that includes receptors for the parathyroid hormone/parathyroid hormone related peptide PTH/PTHrP, glucagon, vasoactive intestinal peptide and pituitary adenylate cyclase activity peptide *(Spengel and Eva 1994).* The implication of GPC receptors in growth regulation is relatively recent, beginning with the identification of gain-of-function mutations in both the receptors themselves and the G-protein subunits they activate *(Dhanasekaran et al., 1995; Dhanasekaran et al., 1998).* The thyroid stimulating receptor (TSH) is an example, as approximately 30% of hyperfunctioning thyroid adenomas have GTPase inhibiting mutations in the Gαs subunit that increase cAMP production. A similar frequency of thyroid adenomas have mutated (TSH) receptors, inducing constitutive activation of adenylate cyclase, and thus continuous cAMP production. In addition to transducing growth promoting signals, GPC receptors can transfer growth inhibitory signals. For example in Jansen's metaphyseal chondrodysplasia, constitutive activity of the PTH/PTHrP receptor results in impairment of chondrocyte growth and differentiation in the developing long bone growth plates *(Schipani et al., 1995).*

CT is best known for its ability to inhibit osteoclastic bone resorption *(Chambers 1982).* However the identification of CTR and CT production in extraskeletal sites implies that the CT/CTR system may have additional actions,

---

Growth inhibitory effects of CT on HEK-293 cells transfected with either the C1a rCTR, the insert –ve or the insert +ve hCTR

unrelated to calcium homeostasis, including regulation of cell growth (as discussed in 1.2.4.4). Particularly relevant to the present studies, are the previous reports that CT regulates the growth of human breast *(Ng et al., 1983)* and prostate *(Shah et al., 1994; Ritchie et al., 1997)* cancer cells *in vitro*. These findings were paradoxical, in that CT down regulated the growth of T47D breast cancer cells *(Ng et al., 1983)* and up regulated the growth of prostate cancer cells *(Shah et al., 1994)*. These reports highlight this less considered action of CT in regulating cell proliferation and the more general involvement of the 7TMD GPCR family in cell growth regulation.

A confounding factor in understanding the growth modulating actions of the CTR, is the expression of multiple human CTR isoforms (discussed in section 1.2.1) throughout the body tissues and cells (discussed in section 1.2.3). The human CTR is principally expressed as two functionally different isoforms, the insert –ve form and a form that contains 16 additional amino acid inserted into the first putative intracellular loop, known as the insert +ve isoform. The receptor isoforms result from the alternative splicing of the primary mRNA transcript *(Moore et al., 1995)* and are expressed in a tissue-specific manner (refer to figure 1.2) *(Kuestner et al., 1994)*. Transcripts corresponding to the insert +ve hCTR are expressed as a minor product in most tissues examined, relative to the insert -ve transcript and not at all in the stomach and brain, but are well expressed in ovary and placenta *(Kuestner et al., 1994)*. Interestingly, the insert +ve isoform appears to be always expressed together with the insert –ve isoform, although the converse is not always true *(Kuestner et al., 1994)*.

The aims of the present experiments were to use HEK-293 transfected cell models to investigate the actions of the insert –ve and +ve hCTR, independently, on growth regulation. The CTR-mediated growth suppression was found to be isoform

---

Growth inhibitory effects of CT on HEK-293 cells transfected with either the C1a rCTR, the insert –ve or the insert +ve hCTR

specific, occurring in cells expressing the hCTR insert –ve hCTR and C1a rCTR, but not the insert +ve hCTR.

## 4.2 Results

### 4.2.1 Anti-proliferative actions of sCT in transfected HEK-293 cells

sCT treatment of parental HEK-293 cells (described in section 2.2.11.1), which do not endogenously express the CTR, did not influence the proliferation of the cells at any concentration of sCT used (figure 4.1A). A single addition of sCT *in vitro* under optimal mitogenic conditions (10%FCS) profoundly inhibited the subsequent proliferation [$p<0.001$] of HEK-293 cells stably transfected with either the C1a isoform of the rCTR (D11 clone) or the insert –ve isoform of the hCTR (clone HR12), in a concentration dependent manner (figure 4.1A & B). Interestingly the $ED_{50}$ of sCT, while in the nM range for both receptors, was 10-fold higher for the insert –ve hCTR compared to the C1a rCTR. Consequently a treatment concentration of 10 nM, which significantly inhibited cell proliferation of cells expressing either the C1a rCTR or insert –ve hCTR, was used in the subsequent growth experiments.

The sCT-induced inhibition of growth was time dependent, as shown in figure 4.2A & B. Treatment of parental HEK-293 cells (described in section 2.2.11.1) with 10 nM sCT over a 96 h period did not effect the growth of the cells (figure 4.1A). In comparison, HEK-293 cells stably transfected with either the C1a rCTR or the insert –ve hCTR showed a significant decrease in growth [$p<0.001$] 48 h following a single treatment with 10 nM sCT (figure 4.1A &B respectively). It is notable that while sCT significantly inhibited the growth of cells in all experiments, the specific time at which the inhibition was detectable varied between experiments. For example, growth inhibition was significant 24 h after sCT addition in the experiment shown in figure

Growth inhibitory effects of CT on HEK-293 cells transfected with either the C1a rCTR, the insert –ve or the insert +ve hCTR

**Figure 4.1 The effect of salmon calcitonin concentration on cell proliferation.**

A. HEK-293 cells transfected with the rat C1a CTR (D11) (■), or untransfected HEK-293 cells (◆), were plated at $5x10^4$ cells per well in 24 well plates. After 24 h, sCT was added once at the indicated concentrations and cells were incubated for a further 72 h. ✱ signifies significantly different from treatment with 0.01 nM and 0.1 nM sCT ($p<0.001$) and # indicates significantly different from treatment with 0.01, 0.1 and 1 nM of sCT ($p<0.001$), as determined by one–way ANOVA.

B. HEK-293 cells transfected with the human CTR (HR12) (●) were treated with sCT as described in A. Cells were harvested and counted using a haemocytometer. Each data point indicates the mean ± SEM of triplicate determinations and these results are representative of 4 independent experiments. ✱ denotes significantly different from treatment with 0.01, 0.1 and 1 nM sCT ($p<0.001$) and # denotes significantly different from treatment with all other concentrations of sCT ($p<0.001$) as determined by one-way ANOVA.

A

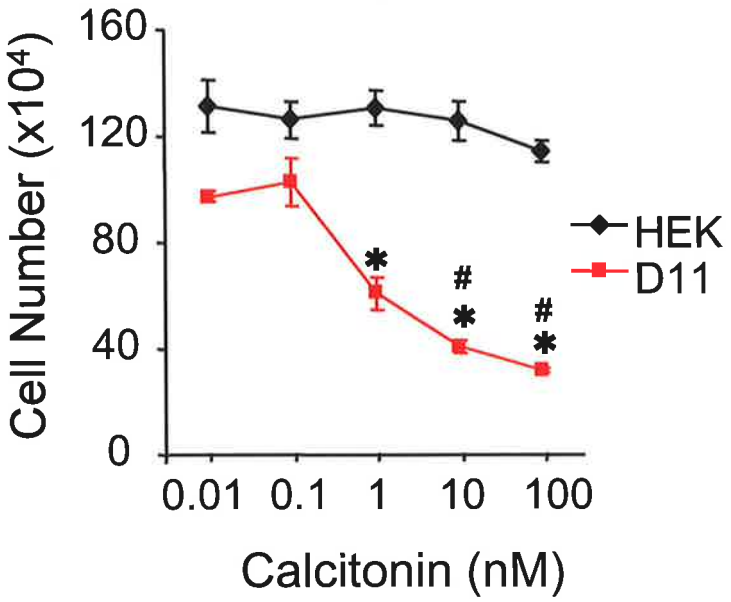
160
120
80
40
0
Cell Number (x10⁴)
0.01
0.1
1
10
100
Calcitonin (nM)
HEK
D11
*
#
*
#
*

B

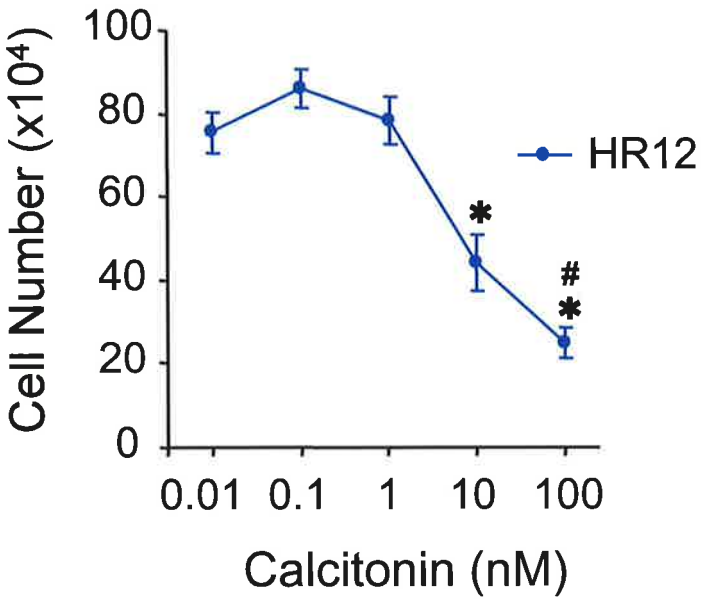
100
80
60
40
20
0
Cell Number (x10⁴)
0.01
0.1
1
10
100
Calcitonin (nM)
HR12
*
#
*

**Figure 4.2 The effect of salmon calcitonin on cell proliferation.**

HEK-293 (◆), D11 (■) and HR12 (●) cells were seeded at $2x10^4$ cells per well in 24 well plates. 24 hours after seeding, cells remained untreated (open symbols) or were treated with one addition of 10 nM sCT (closed symbols). Cells were harvested and counted using a haemocytometer at 24, 48, 72 and 96 h after sCT addition. Data points represent the mean ± SEM of triplicate determinations, and the results are representative of 3 experiments. a, b, c, signify significant difference from the respective control at each time point, with $p<0.001$, as determined by two-way ANOVA.

A

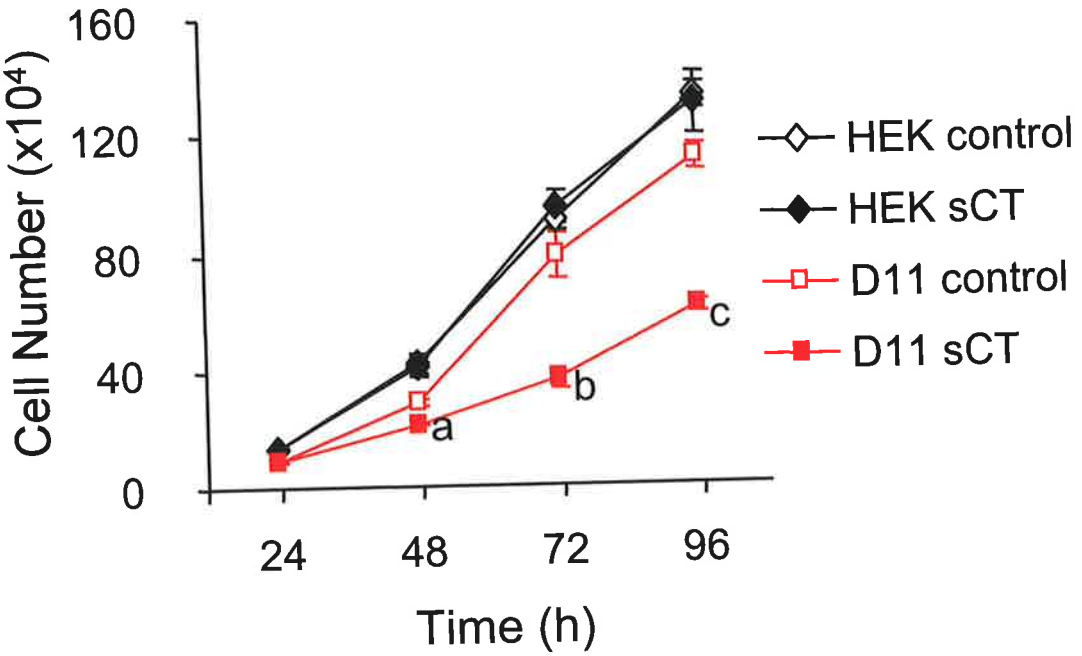
160
120
80
40
0
Cell Number (x10⁴)
24
48
72
96
Time (h)
a
b
c
HEK control
HEK sCT
D11 control
D11 sCT

B

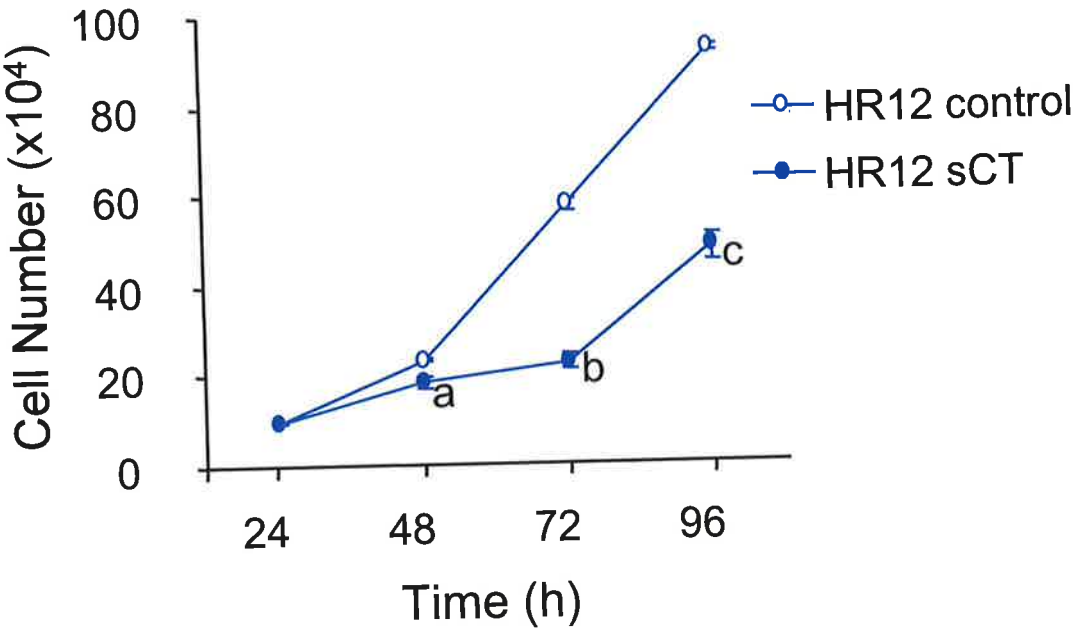
100
80
60
40
20
0
Cell Number (x10⁴)
24
48
72
96
Time (h)
a
b
c
HR12 control
HR12 sCT

4.2A & B, but was not detectable until 48 h post treatment in the experiments shown in figure 4.5A & B. The difference in the time at which growth inhibition was detected in the experiments may have been due to variability in the lag phase of cell growth, which occurred between experiments.

### 4.2.2 Recovery of cells from CT-induced growth suppression

At later times (72-96 h) of the growth experiments (figure 4.2A & B), it appeared possible that the cells were recovering from the CT-induced growth inhibition and this effect was explored further. sCT has a very low dissociation rate once bound to the C1a rCTR *(Houssami et al., 1994)* or the insert –ve hCTR *(Kuestner et al., 1994)*. Thus, to investigate the ability of the D11 cells to recover from sCT treatment, an acid wash protocol was used (described section 2.2.11.3). The acid wash removes the sCT from the receptor and thus signalling by the ligand *(Wada et al., 1995)*. In figure 4.3, the control cells remained untreated over the 6 day time course, the sCT treated cells were exposed to 10nM sCT for the 6 day period, the sCT wash cells were treated with sCT for 3 days before the sCT was removed by acid wash, so that they remained untreated for the final 3 days of the experiment. Removal of the sCT appeared to partially reverse the growth inhibitory effects of sCT, as there were significantly more cells ($p<0.001$) on day 5 and 6 in the sCT wash compared to the sCT treatment (figure 4.3). Due to experimental constraints, in particular the confluency of the control cells, it was not possible to extend the experiment to days 7 & 8, which may have established more clearly the ability of the cells to recover from sCT exposure.

---

Growth inhibitory effects of CT on HEK-293 cells transfected with either the C1a rCTR, the insert –ve or the insert +ve hCTR

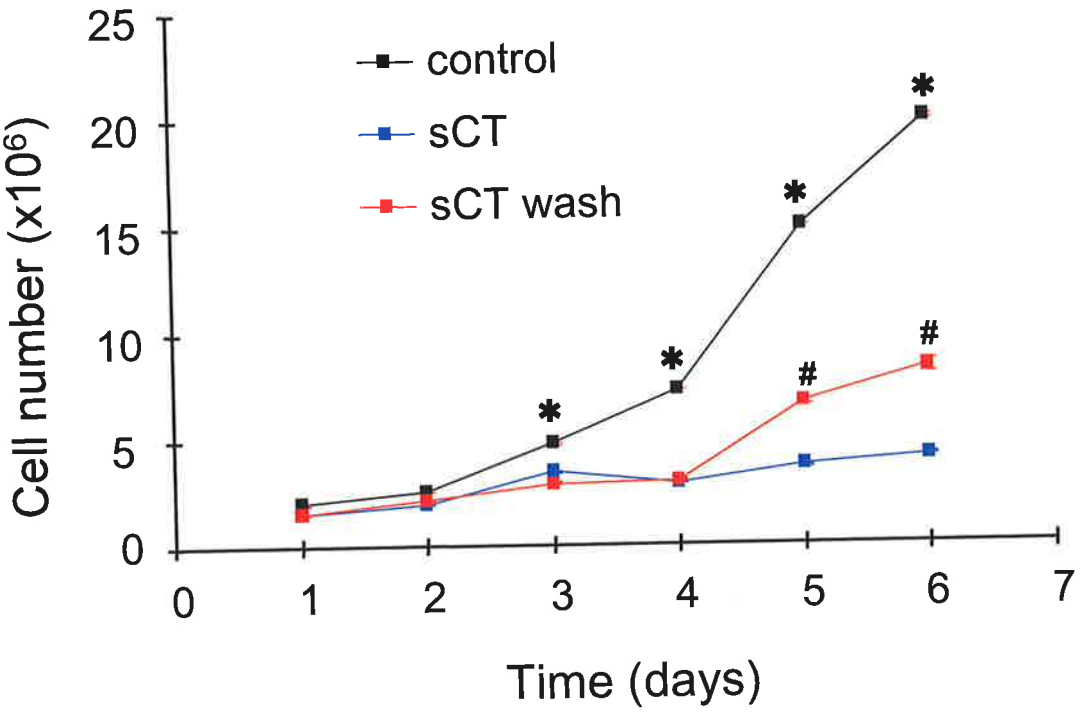


**Figure 4.3 Growth recovery following the removal of salmon calcitonin.**

HEK-293 cells transfected with the C1a rat CTR (D11), were seeded at $3x10^5$ cells per flask in T25cm$^2$ culture flasks. 48 hours after seeding (day 0), the cells remained untreated (■) or were treated with one addition of 10 nM sCT (■, ■). On day 3 all cells were washed once with 2ml of acid wash solution (0.15 M NaCl-0.05 M glycine (pH 2.5)), followed by 2ml PBS, and media was then replaced such that cells remained untreated (■, ■) or were treated once with one addition of 10nM sCT (■). At day 6, the cells were harvested and counted using a haemocytometer. Data points represent the mean ± SEM of triplicate determinations, and the results are representative of 3 experiments. * denotes significant difference from sCT and sCT wash treated cells $p<0.001$ and # denotes significant difference from continuously sCT treated cells $p<0.001$, as determined by the ANOVA described in the *Experimental materials and methods*.

### 4.2.3 The CT-induced inhibition of cell growth occurred in a number of HEK-293 clones expressing the insert –ve hCTR

A number of HEK-293 clones expressing the insert –ve hCTR were generated and screened for surface receptor expression using iodinated sCT (see Table 3.1). sCT treatment of the HR11, HR9 and HR10 clones significantly inhibited the growth of these cells in a concentration dependent manner [$p<0.001$ (figure 4.5A, B & C)], confirming that the growth inhibitory action of sCT on the HR12 cells was not a clonal artefact. The growth inhibition was qualitatively evident in all clones, however the extent of inhibition did vary between cell lines and between experiments. Under the experimental conditions used here, a significant decrease in cell growth [$p<0.001$] was consistently recorded following a 72 h treatment with 0.1nM sCT (HR9 and HR11 clones) and 1nM sCT (clone HR10) (figure 4.3). This growth inhibitory effect in these clones occurred at 10-100 fold lower concentrations of sCT than was required to produce a similar effect in HR12 clone (figure 4.2B). In addition to confirming this growth inhibitory effect in several HEK-293 clonal lines expressing the insert –ve hCTR, a second HEK-293 clone expressing the C1a rat CTR (F12) also displayed growth inhibition in response to sCT treatment (data not shown). The growth suppressive actions of sCT in multiple HEK-293 cells transfected with either the rCTR or the insert –ve hCTR, show that the ability of the CTR to modulate cell growth is not species dependent, with respect to the CTR.

### 4.2.4 Anti-proliferative actions of other hCT and sCT[8-32] analogues

The growth suppression observed was dependent on receptor activation since the sCT[8-32] analog, which binds to rat and human CTR's but does not elicit intracellular signalling *(Houssami et al., 1995)*, had no effect on the rate of cell growth (Table 4.1). Interestingly, human CT (hCT) treatment, even at very high

Growth inhibitory effects of CT on HEK-293 cells transfected with either the C1a rCTR, the insert –ve or the insert +ve hCTR

**Figure 4.4 Salmon calcitonin inhibition of HEK-293 cells expressing the insert –ve hCTR is not a clonal artefact.**

Three HEK-293 cell lines expressing the insert –ve hCTR, HR9, HR10, HR11 were seeded at $5x10^4$ cells per well in 24 well plates. After 24 h, sCT was added once at the indicated concentrations and cells were incubated for a further 72 h. Cells were harvested and counted using a haemocytometer. Each data point indicates the mean ± SEM of triplicate determinations. These results are representative of 2 independent experiments. ✱ denotes significantly different from control ($p<0.001$), # denotes significantly different from 0.1 nM and 1 nM $p<0.001$ and § denotes significantly different from 0.1nM $p<0.001$, as determined by one-way ANOVA.

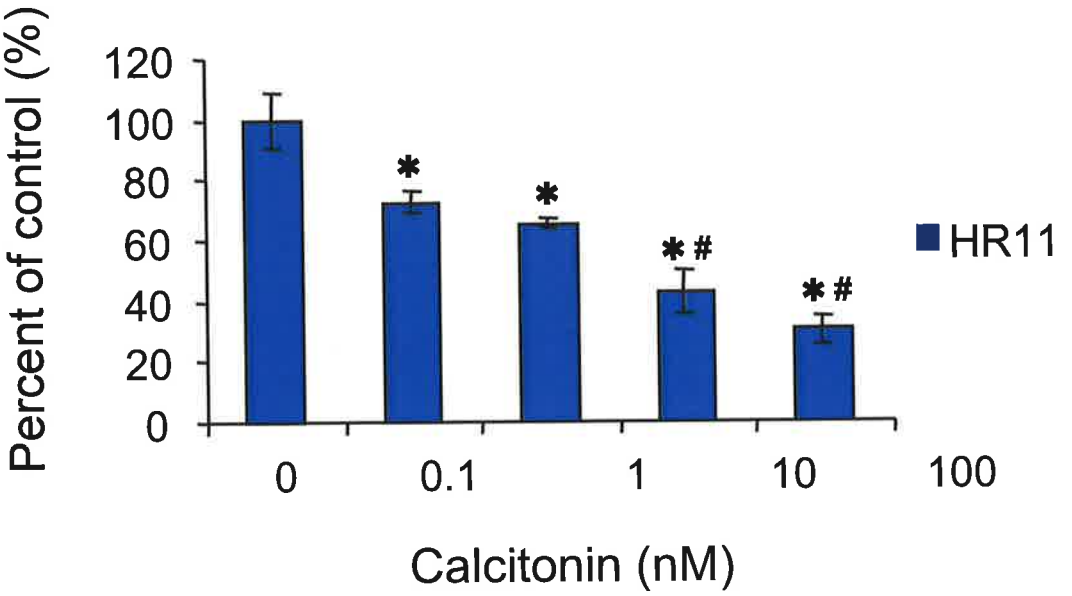
Percent of control (%)
120
100
80
60
40
20
0
*
*
*#
*#
0
0.1
1
10
100
Calcitonin (nM)
HR11

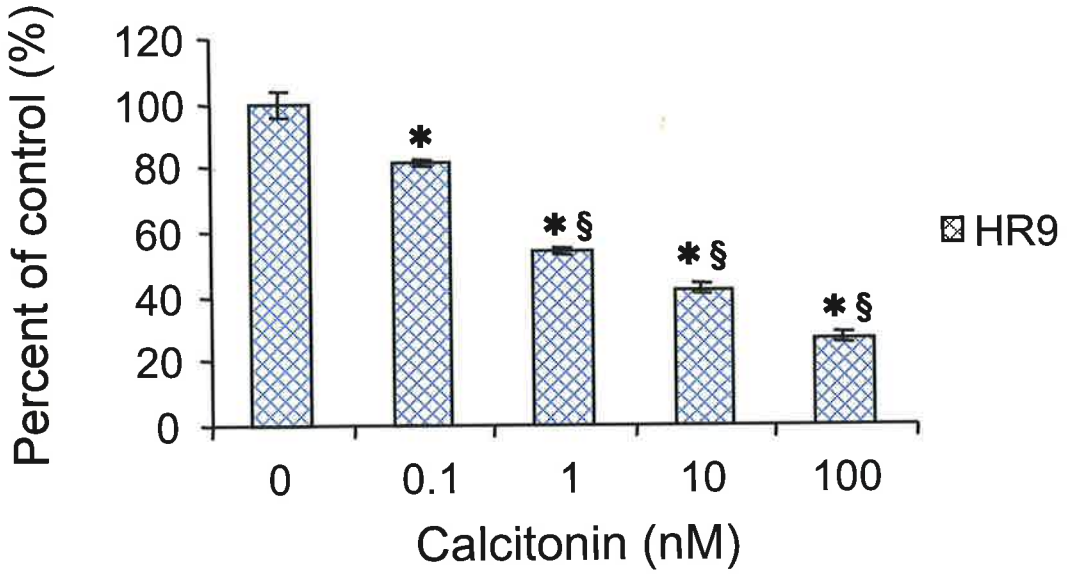
Percent of control (%)
120
100
80
60
40
20
0
*
*§
*§
*§
0
0.1
1
10
100
Calcitonin (nM)
HR9

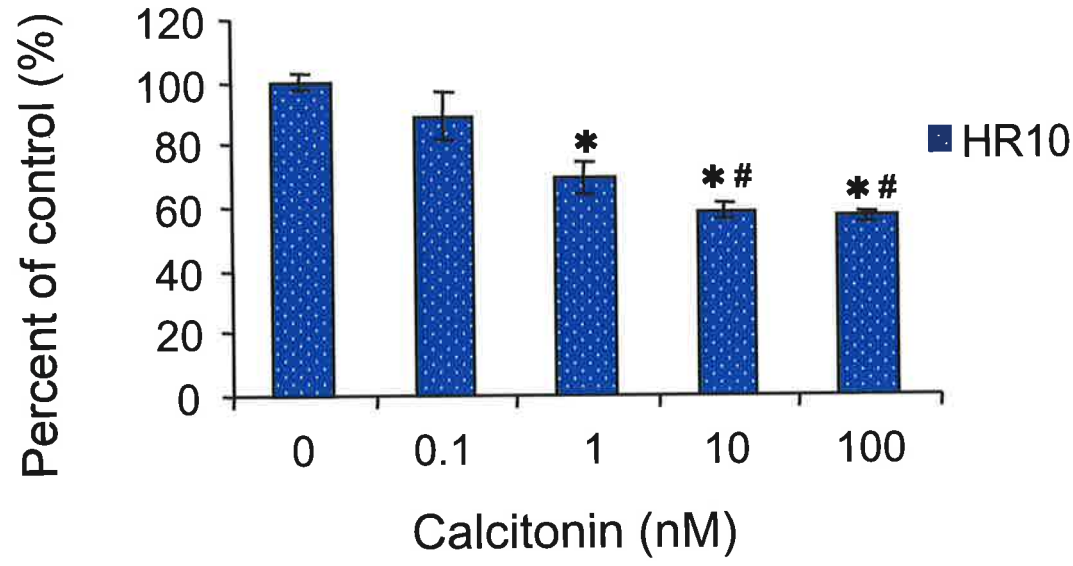
Percent of control (%)
120
100
80
60
40
20
0
*
*#
*#
0
0.1
1
10
100
Calcitonin (nM)
HR10

| Comparison of sCT, hCT, and [8-32]sCT on cell proliferation | | | |
|---|---|---|---|
| | Cell Count (% Untreated) | | |
| | HEK | D11 (C1a rat CTR) | HR12 (insert –ve hCTR) |
| Untreated | 100 | 100 | 100 |
| sCT | 92.7 ± 7.7 | 53.9 ± 2.4 * | 61.2 ± 6.5 * |
| hCT | 92.7 ± 1.4 | 95.1 ± 2.5 | 86.0 ± 2.8 * |
| [8-32]sCT | 98.2 ± 3.7 | 94.8 ± 2.4 | 99.0 ± 1.9 |

**Table 4.1** HEK-293 cells, D11 cells, or HR12 cells were plated at $2x10^4$ cells per well in 24-well plates. After 24 h, sCT (10nM), hCT (1μM), or [8-32]sCT (10nM) was added, and cells were incubated for a further 72 h. Cells were harvested and counted in triplicate using a haemocytometer. Cell numbers in each case are mean ± SEM of triplicate determinations, represented as a percent of untreated (control) cell numbers. These results are representative of three similar experiments. ✱ denotes significant difference from untreated cells $p<0.001$.

**Figure 4.5 Salmon calcitonin-induced growth suppression is calcitonin receptor isoform-specific.**

HEK-293 cells transfected with the insert –ve (o,●), insert +ve hCTR (□,■), or vector alone (△, ▲) were plated at $2x10^5$ cells per T25 flask. 48 h following plating, cells remained untreated (closed symbols) or were treated once with 10 nM sCT (open symbols). At the indicated times following commencement of treatment, cells were harvested and counted. Panel A shows vector alone vs insert –ve hCTR cells and panel B compares insert –ve and insert +ve hCTR cells. Data points represent the mean ± SEM of triplicate determinations and this data is representative of 3 independent experiments. a and b denote significant difference from the respective control at each time, with $p<0.001$, as determined by two-way ANOVA.

A

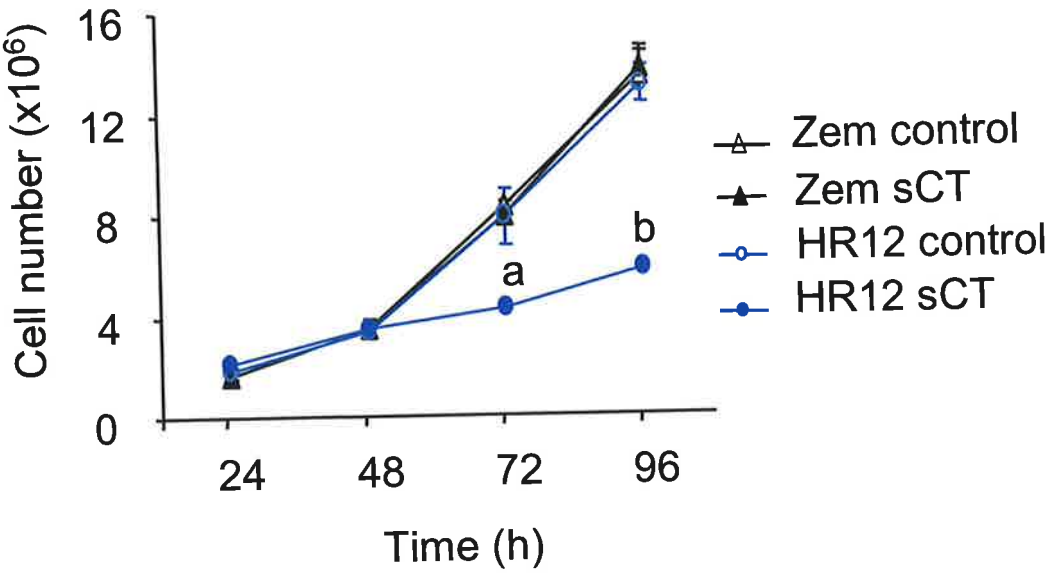
Cell number (x10^6)
16
12
8
4
0
24
48
72
96
Time (h)
a
b
Zem control
Zem sCT
HR12 control
HR12 sCT

B

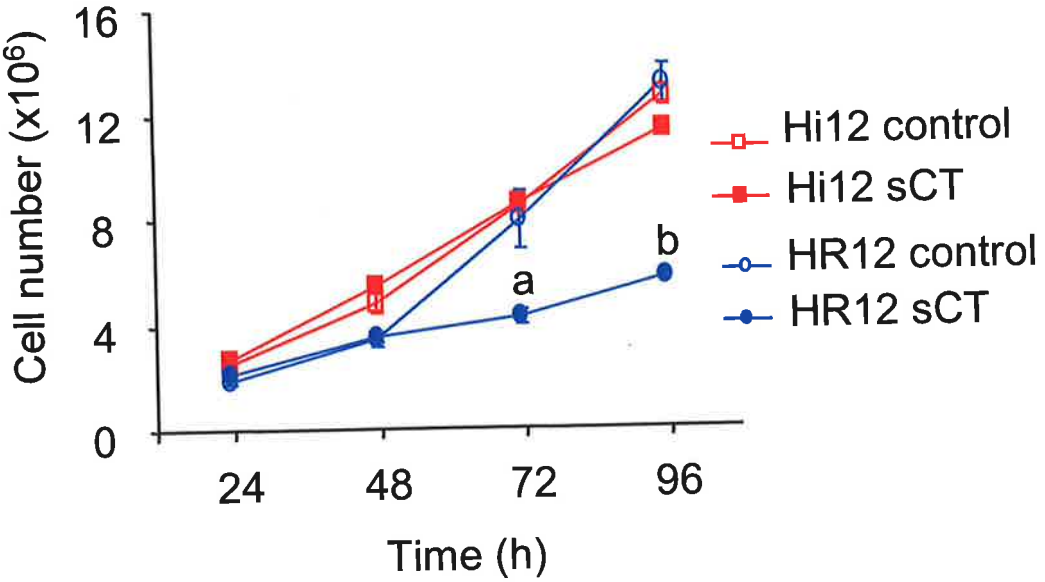
Cell number (x10^6)
16
12
8
4
0
24
48
72
96
Time (h)
a
b
Hi12 control
Hi12 sCT
HR12 control
HR12 sCT

**Effect of sCT on growth of HEK-293 clones expressing the insert +ve hCTR**

| | Cell Count (% Untreated) | | |
|---|---|---|---|
| | Hi12 | Hi8 | Hi5 |
| Untreated | 100 | 100 | 100 |
| 10 nM sCT | 96.1 ± 1.4 | 101.5 ± 4.0 | 101.7 ± 2.8 |
| 100 nM sCT | 99.7 ± 3.0 | 108.2 ± 4.3 | 96.1 ± 4.7 |
| 1 μM sCT | 100 ± 3.8 | 102.3 ± 5.6 | 98.5 ± 1.9 |

**Table 4.2** Three HEK-293 clones expressing the insert +ve hCTR, designated Hi12, Hi8 and Hi5 were plated in 12 well plates at a density of $3x10^4$ cells. After 72 h cells remained untreated or were treated once with 10 nM, 100 nM or 1 μM of sCT, and incubated for a further 72 h. Cells were harvested and counted in triplicate using a haemocytometer. Cell numbers in each case are mean ± SEM of triplicate determinations, represented as a percent of untreated (control) cell numbers. These results are representative of two similar experiments.

concentration (1 μM), had no effect on the growth of D11 cells. However hCT had a significant anti-proliferative effect on HR12 cells (Table 4.1) despite being a potent activator of adenylate cyclase activation at both the rat and human CTR *(Houssami et al., 1995)*.

### 4.2.5 Anti-proliferative action of sCT on hCTR is isofoms specific

To compare the mitogenic effect of sCT on the insert +ve and –ve isoforms of the hCTR, HEK-293 cells stably transfected with the insert-ve (HR12 clone) or insert +ve (Hi12 clone) isoforms of the hCTR, were treated with sCT under conditions of optimal mitogenic stimulus (10 % foetal calf serum - FCS) (described section 2.2.11.2). Consistent with figure 4.1B, a single addition of sCT to cells expressing the insert –ve hCTR profoundly inhibited cell proliferation, while cells transfected with vector alone were not influenced by sCT (figure 4.3A). In contrast to cells expressing the insert-ve hCTR, CT-treatment had no effect on the growth of cells expressing the insert +ve hCTR isoform (Figure 4.3B). In confirmation of this result, sCT also failed to alter the growth of other cell clones stably expressing the insert +ve hCTR (Table 4.2).

### 4.2.6 Anti-proliferative actions of CT in breast cancer cell lines

The original demonstration of the anti-proliferative effect of CT was in the T47D human breast cancer cell line *(Ng et al., 1983)*. In that report, a significant decrease in cell growth was observed 5 days after treatment with 0.3 nM sCT. Interestingly, these experiments were performed in sub-optimal mitogenic conditions, in the absence of FCS with 0.1% BSA supplement. In considering CT as a potential therapeutic cancer agent, it is important to address the anti-proliferative actions of the hormone under mitogenic conditions, more relevant to the physiological environment.

---

Growth inhibitory effects of CT on HEK-293 cells transfected with either the C1a rCTR, the insert –ve or the insert +ve hCTR

**Figure 4.6 CT-induced growth suppression of breast cancer cell lines.**

A. T47D and MCF7 cells were plated at $2x10^4$ cells per well in 6 well plates. After 24 h cells remained untreated (open symbol) or were treated once with 10 nM sCT (closed symbol). At the indicated times following treatment, cells were harvested and counted using a haemocytometer Each data point represents the mean ± SEM of triplicate determinations and the results are representative of 2 experiments. a denotes significant difference from the respective control at each time, with $p<0.001$ by two way ANOVA.

B. MCF7 cells and T47D cells were incubated with [$^{125}$I]-sCT alone, (total binding, T), or in the presence of 100 nM sCT, (non-specific binding, NS), for 1 h at 37 C. Cells were washed twice with PBS and solubilised in 0.5 ml of 0.5 M NaOH. Cell-associated radioactivity was counted in a γ-counter. Results are mean ± SEM of triplicate determinations, expressed as [$^{125}$I]-sCT bound per $10^6$ cells, and are representative of 2 independent experiments. ✱ denotes significant difference from NS treatment, $P<0.001$, by students t-test.

A

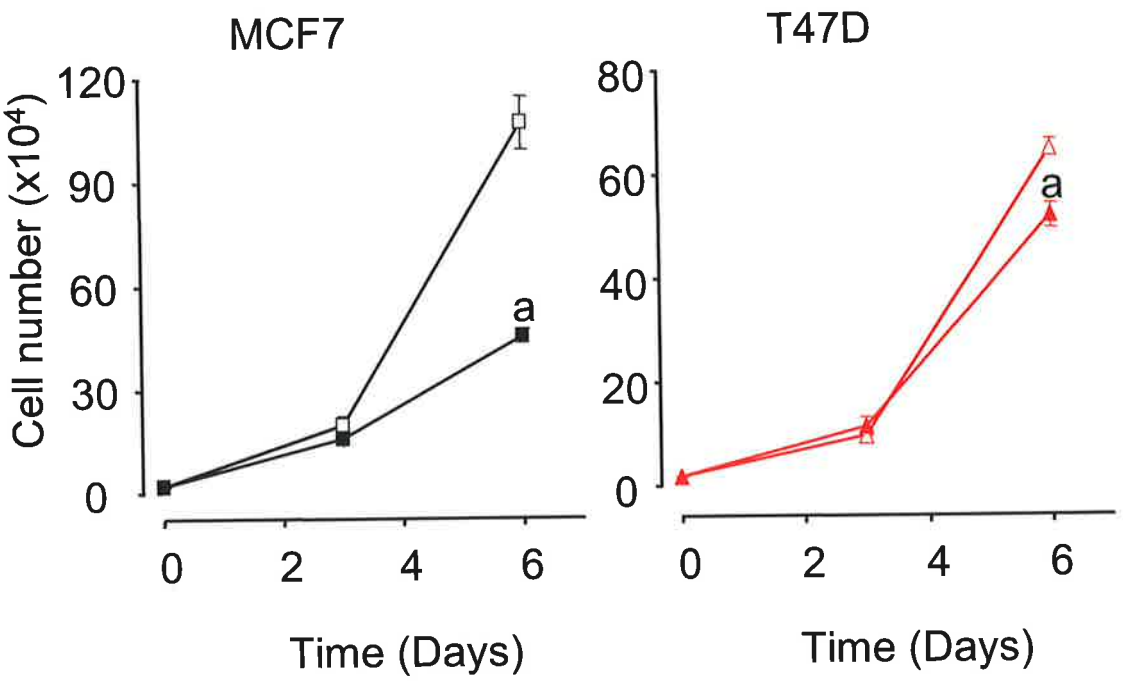
MCF7
T47D
Cell number (x10⁴)
120
90
60
30
0
80
60
40
20
0
a
a
0
2
4
6
Time (Days)
Time (Days)

B

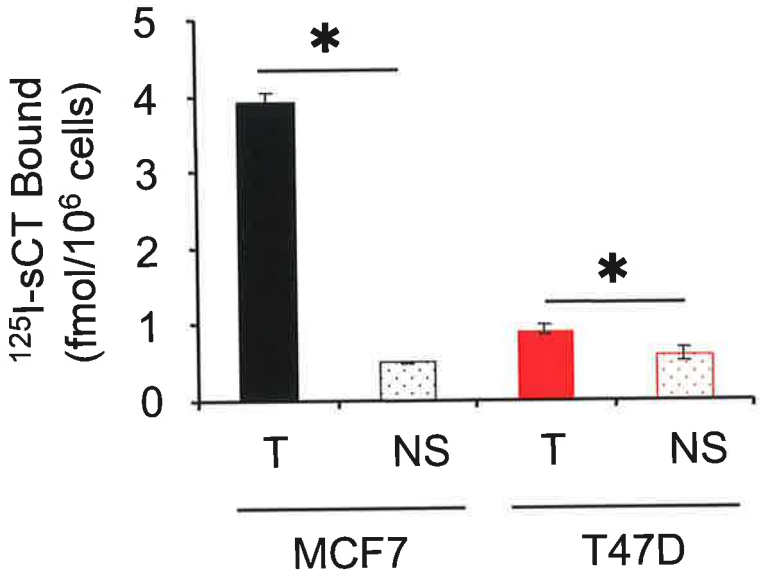
¹²⁵I-sCT Bound
(fmol/10⁶ cells)
5
4
3
2
1
0
*
*
T
NS
T
NS
MCF7
T47D

Experiments were performed in T47D and MCF7 cells, nominally the same as those used in the original experiments, albeit from different sources. Although we found that both cell types expressed hCTR mRNA by RT/PCR, the T47D cells had very low binding capacity for [$^{125}$I]-sCT (figure 4.6B). Both cell lines expressed multiple isoforms of the hCTR (data not shown). Cells were treated with 10nM sCT under conditions of optimal mitogenic stimulus (10 % FCS) (Figure 4.6A) (described in section 2.2.11.2). CT treatment inhibited the growth of both MCF7 and T47D breast cancer cells. The growth inhibitory effect of CT was delayed in comparison to the transfected HEK cells, only becoming evident after 4 or more days exposure to CT. However the growth inhibitory effect of CT was more pronounced in the MCF7 than the T47D cells, consistent with the greatly reduced receptor expression in T47D cells (figure 4.6B) (protocol described in section 2.2.6.2).

## 4.3 Discussion

The present study showed that sCT treatment of HEK-293 cells stably transfected with the rat C1a CTR, or the insert –ve hCTR isoform, dramatically decreased cell proliferation. This reduction in cell growth in response to treatment with sCT appeared partially reversible, as cells re-established growth following the removal of the sCT stimulus by acid washing. The growth inhibitory effect observed with CT treatment was dependent on the CT ligand used. The teleost CT, sCT, potently inhibited the growth of cells expressing either the C1a rCTR or the insert –ve hCTR. However treatment with hCT had a minimal effect on the growth of D11 cells expressing the rat C1a CTR and a significant but a much lesser effect than sCT, on the growth of HR12 cells, expressing the insert –ve hCTR. There are several possible implications of this finding. Firstly, human CT may be antiproliferative only

Growth inhibitory effects of CT on HEK-293 cells transfected with either the C1a rCTR, the insert –ve or the insert +ve hCTR

at the hCTR, as seen also in T47D breast cancer cells *(Ng et al., 1983)*. In those experiments, hCT was added repeatedly and inhibition of cell growth occurred over a longer time course than the present experiments. The species-specific ligand activation of intracellular signalling pathways, specifically cAMP, supports this data and the possibility of species-specific ligand/receptor functions. The potency of hCT as an activator of cAMP is indistinguishable from sCT when acting through the insert -ve hCTR *(Moore et al., 1995)*. However hCT is 100 fold less effective than sCT in stimulating cAMP when coupling to the C1a rCT *(Houssami et al., 1994)*. This highlights the potential for species-specific ligand and receptor interactions inducing species-specific cellular responses. Secondly, the teleost or fish-like CTs may be more potent than hCT in terms of growth inhibition. This potency effect may be related to the higher affinity of sCT for both the C1a rCTR and insert –ve hCTR, compared to hCT *(Moore et al., 1995; Houssami et al., 1994)*. The increased affinity of sCT for the CTR would prolong G-protein signalling, which might in turn modify the cellular response. The relevance of this is that there is good evidence for the presence of fish-like CTs in several mammalian tissues, including brain *(Sexton et al., 1992)* and pituitary *(Hilton et al., 1998)*, although their physiological role in these tissues is not yet understood.

These data show for the first time that the growth inhibitory effect of sCT is specific with respect to the CTR isoform, occurring only in cells expressing the C1a rCTR and the homologous insert –ve hCTR. Cells expressing the insert +ve hCTR showed no change in growth rate in response to treatment with sCT.

Our attempts to confirm the anti-proliferative actions of sCT in the T47D breast cancer cell line showed a greatly reduced response from that previously reported by Ng *et al* (1983). The present experiments were performed using different conditions

---

Growth inhibitory effects of CT on HEK-293 cells transfected with either the C1a rCTR, the insert –ve or the insert +ve hCTR

to those of Ng *et al.* Specifically we utilized optimal mitogenic conditions, in order to more closely mimic the physiological *in vivo* environment. All previous investigations on the growth regulating actions of sCT have been performed in low mitogenic conditions, without FCS. These altered conditions are unlikely to be responsible for these divergent results, as we were able to demonstrate CT-induced growth inhibition in the MCF7 breast cancer cell line. On investigation, the T47D cells were shown to express only low levels of CTR as assessed by [$^{125}$I]-sCT binding studies, while MCF7 cells displayed plentiful cell surface CTR. Thus it appeared the T47D cells used here had a different phenotype to those used by Ng *et al (Ng et al., 1983).* This divergence of phenotype is a common experience when using cell lines from different sources, many years apart.

The characteristics of CT-induced growth inhibition differed between the MCF7 cells and those observed in HEK-293 cells transfected with the insert –ve hCTR. Specifically, the required ligand exposure time was increased and the magnitude of the growth inhibition was reduced. The difference in the cellular response to CT exposure was perhaps due to the different levels of surface CTR expression with HR12 cells having a 9-fold greater binding capacity for [$^{125}$I]-sCT compared to MCF7 cells. Alternatively, or in conjunction with this, it may be that the reduced responsiveness of MCF7 cells to sCT is associated with the ratio of expression of their CTR isoforms *(Gillespie et al., 1997).* There is growing evidence that cell surface receptors are able to cross-talk and cross-modulate each other's activity *(Liu et al., 2000).* This, taken together with the inability of sCT to regulate cell growth through the insert +ve hCTR, suggests that the latter receptor isoform may be able to modulate the activity of the insert –ve isoform, although there is no direct evidence for such an action as yet (discussed further in chapter 9).

---

Growth inhibitory effects of CT on HEK-293 cells transfected with either the C1a rCTR, the insert –ve or the insert +ve hCTR

# Chapter 5

# Characterisation of the CT-induced growth inhibition of HEK-293 cells transfected with the C1a rCTR or the insert –ve hCTR

## 5.1 Introduction

The cellular mechanisms by which 7TMD receptors influence cell growth are not well understood. Work to date has focussed on the involvement of immediate post-receptor signalling events and the subsequent G-protein pathways that regulate cell growth and differentiation, reviewed in van Biesen *et al* (1996) and Gutkind (1998) and discussed in chapter 8. There has been only limited work to identify the mechanisms by which 7TMD G-protein coupled receptor/ligand signalling alter more distal events, including those controlling the eukaryotic cell cycle, in order to regulate cell growth.

There are a number of mechanisms by which the growth of eukaryotic cells can be regulated. There may be induction of cell death *via* cellular necrosis or apoptosis (programmed cell death) *(Auer et al., 1998)*. Alternatively, cell cycling may be prevented, producing quiescence, or cells may undergo the phenotypic changes of differentiation *(Coffman et al., 1999)*. There are now reported examples, including those in the family of receptors to which the CTR belongs, demonstrating such changes in cell growth patterns mediated by 7TMD G-protein coupled receptors. For example, the PTHrP deficient mouse showed an important role for the PTHrP receptor, a member of the same subfamily of the 7TMDR as the CTR, in regulating the growth of chondrocytes in the endochondral bone plate *(Lee et al., 1996)*. The PTHrP deficient animals have shorter endochondral bones than their wild type litter mates, indicating a reduction in the number of chondrocytes in the proliferative zone of the growth plate *(Lee et al., 1996)*. Analysis of the cells in the proliferative zone failed to identify changes in the distribution of cells through the cell cycle. However an increase in chondrocyte differentiation, assessed by the amount of cellular hypertrophy, apoptosis and mineralisation, was evident in the PTHrP deficient mice.

These findings show a specific requirement for PTHrP in delaying chondritic differentiation and thus allowing elongation of the endochondral bones during development of the mouse *(Lee et al., 1996)*. Alternatively, the PTH/PTH receptor system can cause cell cycle arrest. Treatment of osteoblast-like UMR106 osteogenic sarcoma cells with PTH caused cells to accumulate in the G1 phase of the cell cycle, an event that may be physiologically relevant to the process of osteoblastic differentiation and bone formation *(Onishi et al., 1997)*. Thus, the ability of the PTHrP and PTH ligands to induce either cell cycle arrest or cell proliferation shows that the regulation of cell growth by 7TMDR is dependent on the cellular context.

VIP and PACAP receptors, which are also in the same sub-family as the CTR, regulate cell growth and differentiation. Both VIP and PACAP inhibit proliferation of the glioblastoma cell line T986 *(Vertongen et al., 1996)*. The specific mechanism by which these peptides inhibit cell growth has not been determined. However treatment of cells with either VIP or PACAP did not change the distribution of cells in the cell cycle, indicating that there was no induction of cell cycle arrest. The authors did not investigate the possibility that VIP or PACAP were inducing apoptosis *(Vertongen et al., 1996)*. The possibility that PACAP was inducing apoptosis in T986 cells, highlights the cellular specificity of these growth regulating events. PACAP can also activate anti-apoptotic pathways in human pituitary adenoma cells (HP75) to prevent induction of apoptosis *(Oka et al., 1999)*. Alternatively, PACAP can induce growth inhibition and cellular differentiation in rat embryonic cortical brain precursor cells *(Lu et al., 1997)*. In the broader context of GPCR, these findings again highlight the importance of these receptor/ligand systems in directing cellular decisions relating to growth and differentiation.

---

Characterisation of CT-induced growth inhibition of HEK-293 cells transfected with the C1a rCTR or the insert –ve hCTR

To date the cellular process by which CT inhibits cellular proliferation has not been characterised. Thus the aim of the experiments reported in this chapter was to identify how CT changes the eukaryotic cell cycle to inhibit cell proliferation in HEK-293 cells stably expressing different hCTR isoforms.

## 5.2 Results

### 5.2.1 Morphological changes associated with CT treatment

Treatment of HR12 cells with CT was associated with a distinct set of morphological changes. After 24 h of treatment with 10 nM sCT, HR12 cells took on a more retracted appearance (figure 5.1 panel B) having lost the sharp fibroblastic shape that is characteristic of untreated HR12 cells (figure 5.1 panel A). As was expected from growth studies, there were fewer HR12 cells visible in a given field of view of cells treated with sCT for 48 h compared to untreated cells (figure 5.1 panel C & D). In addition, the treated cells appeared to be detaching from the substratum, as indicated by the arrows in figure 5.1 panel D. After 72 h of exposure to sCT, the number of loosely attached cells was dramatically increased (figure 5.1 panel F). Significant agitation was required to remove these rounded cells from the remaining attached cells, indicating they were not free floating in culture, but loosely attached to the substratum and to the remaining attached cells. These morphological changes observed for cells expressing the insert -ve hCTR were also observed in D11 cell expressing the rat C1a CTR (data not shown).

### 5.2.2 Apoptosis Analysis

In order to determine whether the CT-mediated growth suppression was due to induction by CT of apoptosis, cellular DNA was isolated and separated on an agarose gel (described in section 2.2.13). When cells were grown in optimal

**Figure 5.1 Morphological changes associated with sCT treatment.**

HR12 cells were plated at $3x10^4$ cells per well in 12 well plates and allowed to adhere. 48 h after plating, the cells remained untreated or were treated with 10 nM sCT. Cells were photographed, 24, 48 and 72 h after treatment as described in the *Experimental material and methods* to record cell morphology. The white arrows indicate the rounded cell morphology induced by sCT treatment. This is a view of the cells when using a 20x objective and 10x binoculars.

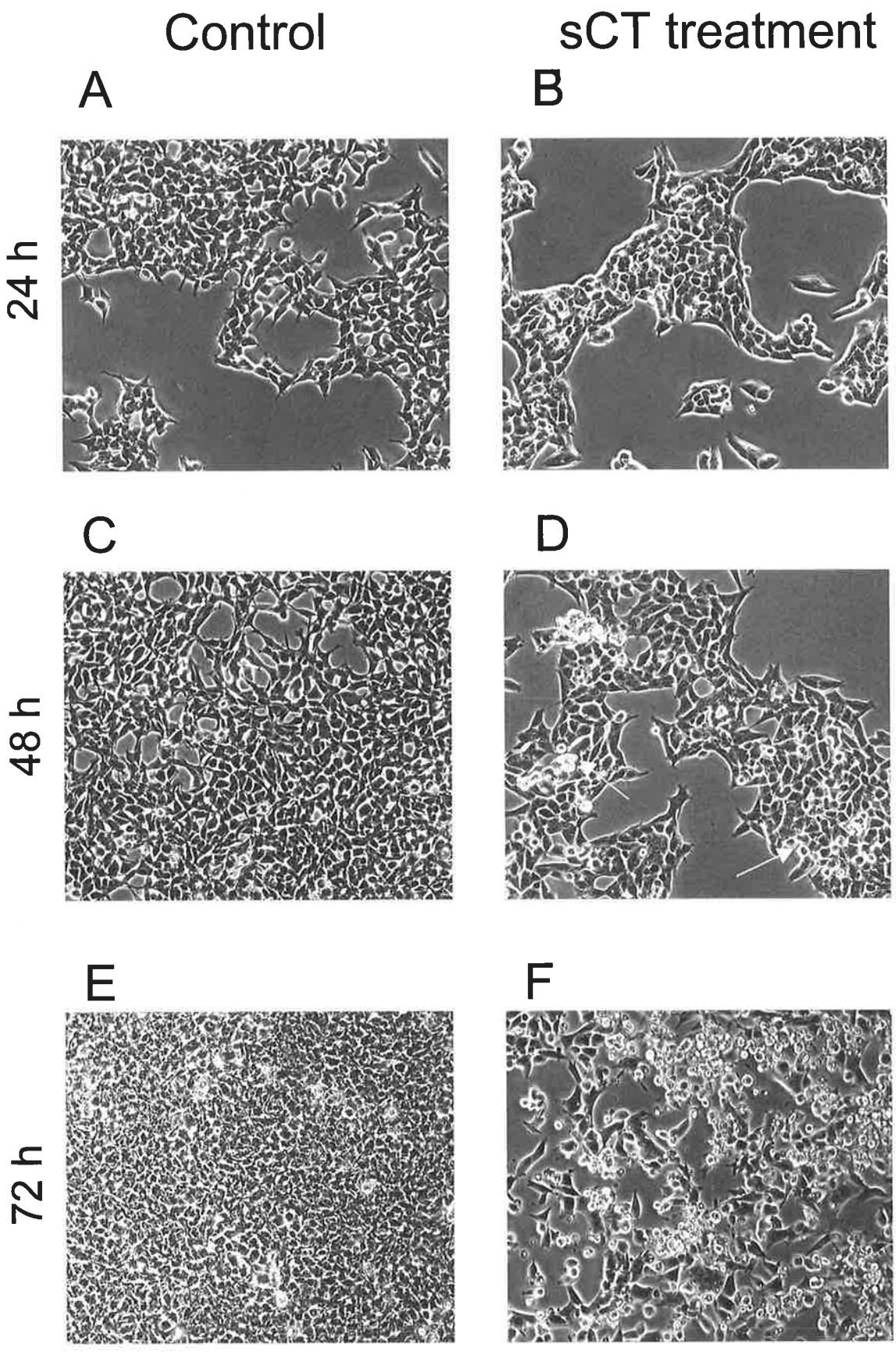
Control
sCT treatment
A
B
C
D
E
F
24 h
48 h
72 h

**Figure 5.2 Detection of DNA fragmentation after treatment with CT.**

Parental HEK-293 cells, D11 and HR12 cells were untreated or treated once with 10 nM sCT, hCT or sCT[8-32]. After 48 h, DNA was isolated and subjected to agarose electrophoresis. No internucleosomal DNA fragmentation was observed when cells were grown in the presence of 10% serum. However, a low molecular-size DNA ladder, which is characteristic of cells undergoing apoptosis, was observed when in D11 and HR12 cells grown in the presence of sCT and 0.5% serum.

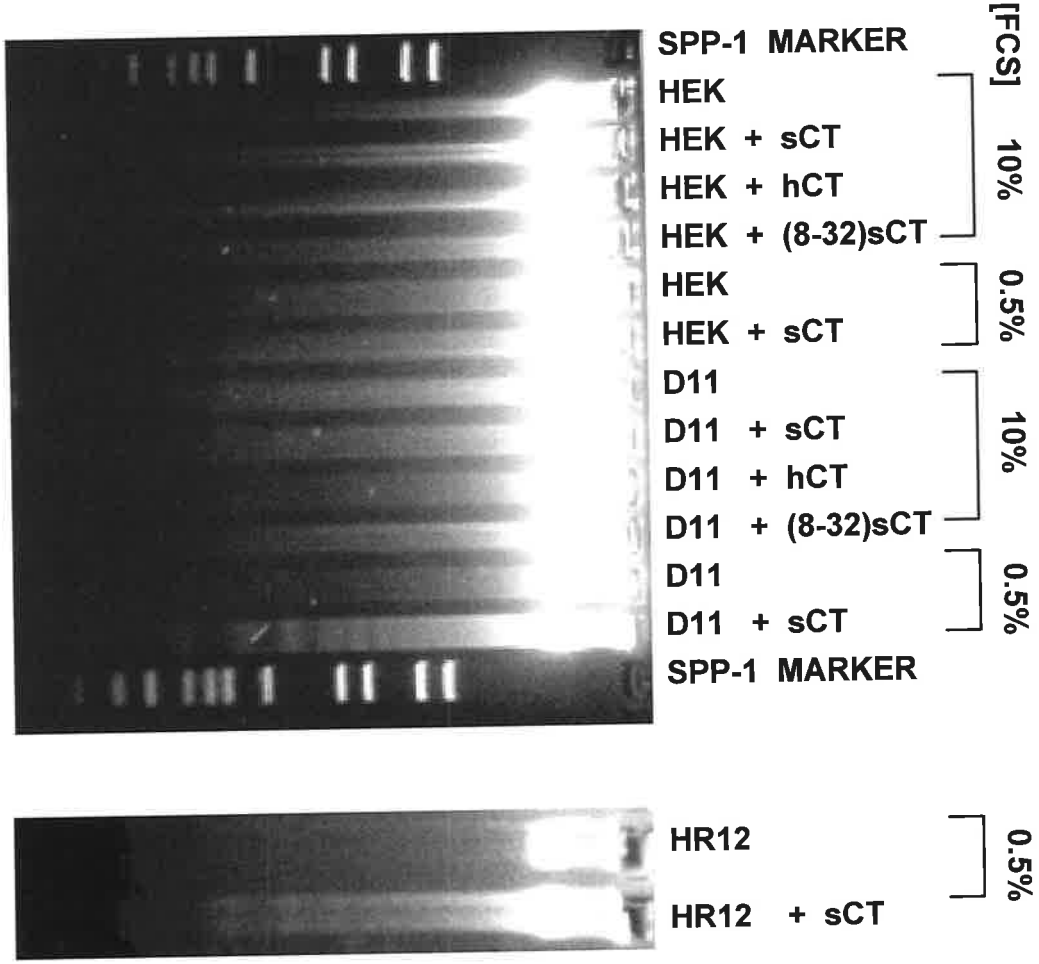
SPP-1 MARKER
HEK
HEK + sCT
HEK + hCT
HEK + (8-32)sCT
HEK
HEK + sCT
D11
D11 + sCT
D11 + hCT
D11 + (8-32)sCT
D11
D11 + sCT
SPP-1 MARKER
HR12
HR12 + sCT
[FCS]
10%
0.5%
10%
0.5%
0.5%

mitogenic conditions of 10% FCS and treated with either the inactive 8-32 sCT peptide or the active hCT or sCT peptides, no nucleosomal DNA fragmentation was detected in HEK-293 cells transfected with the C1a rCTR (figure 5.2). Treatment of parental HEK-293 cells under the same conditions also failed to induce the characteristic DNA "ladder", which is visible when cells are undergoing apoptosis. Under optimal growth conditions, CT-treatment inhibited cell proliferation (figure 5.2), however no evidence of apoptotic DNA "laddering" was detected, indicating that an alternative mechanism was responsible for the CT-induced growth suppression.

When D11 and HR12 cells grown in low serum (0.5% FCS) conditions were treated with sCT, DNA fragmentation, indicative of apoptosis, was observed (figure 5.2 lanes 13 and 16 respectively). This was CTR-mediated, since no apoptosis was detected in parental HEK-293 cells grown in low serum conditions with sCT (figure 5.2 lane 7). These data indicate that sCT does not induce apoptosis in HEK-293 cells expressing CTR when they are grown in serum replete conditions. However, sCT was able to increase the susceptibility of the cells to apoptosis when used in conjunction with growth factor deprivation.

### 5.2.3 Evaluation of cell viability following CT-treatment

To assess the effect of sCT treatment on cell viability, cells were stained with 0.4% trypan blue following sCT treatment (described in section 2.2.12). Viable cells are able to exclude the dye, where as non-viable cells are unable to do so and thus become blue in colour. There was no change in the percent of viable D11 (figure 5.3A) or HR12 (figure 5.3B) cells following 24 h or 48 h treatment with sCT. In contrast, a 72 h exposure to sCT decreased the percent of viable D11 (figure 5.3A) and HR12 (figure 5.3B) cells by 6.6% and 11.7% respectively. The reduction in viable D11 and HR12 cells was unable to account for the difference in cell numbers

**Figure 5.3 The effect of CT on cell viability.**

D11 cells expressing the C1a rCTR (panels A & C) and HR12 cells expressing the insert –ve hCTR (panels B & D) were plated at $2x10^5$ cells per well in 12 well plates. After 48 h the cells either remained untreated (closed bars) or were treated with 10 nM sCT (spotted bars). At the time points indicated the cells were harvested, stained with 0.4% trypan blue such that viable and non viable cells could be counted using a haemocytometer. In panels A and B the data is representative of the percent of viable cells at the indicated time points and the mean ± SEM of triplicate determinations is shown. In C and D the mean ± SEM of the total number of cells counted at each time point is recorded. These results are representative of two independent experiments in which similar results were obtained.

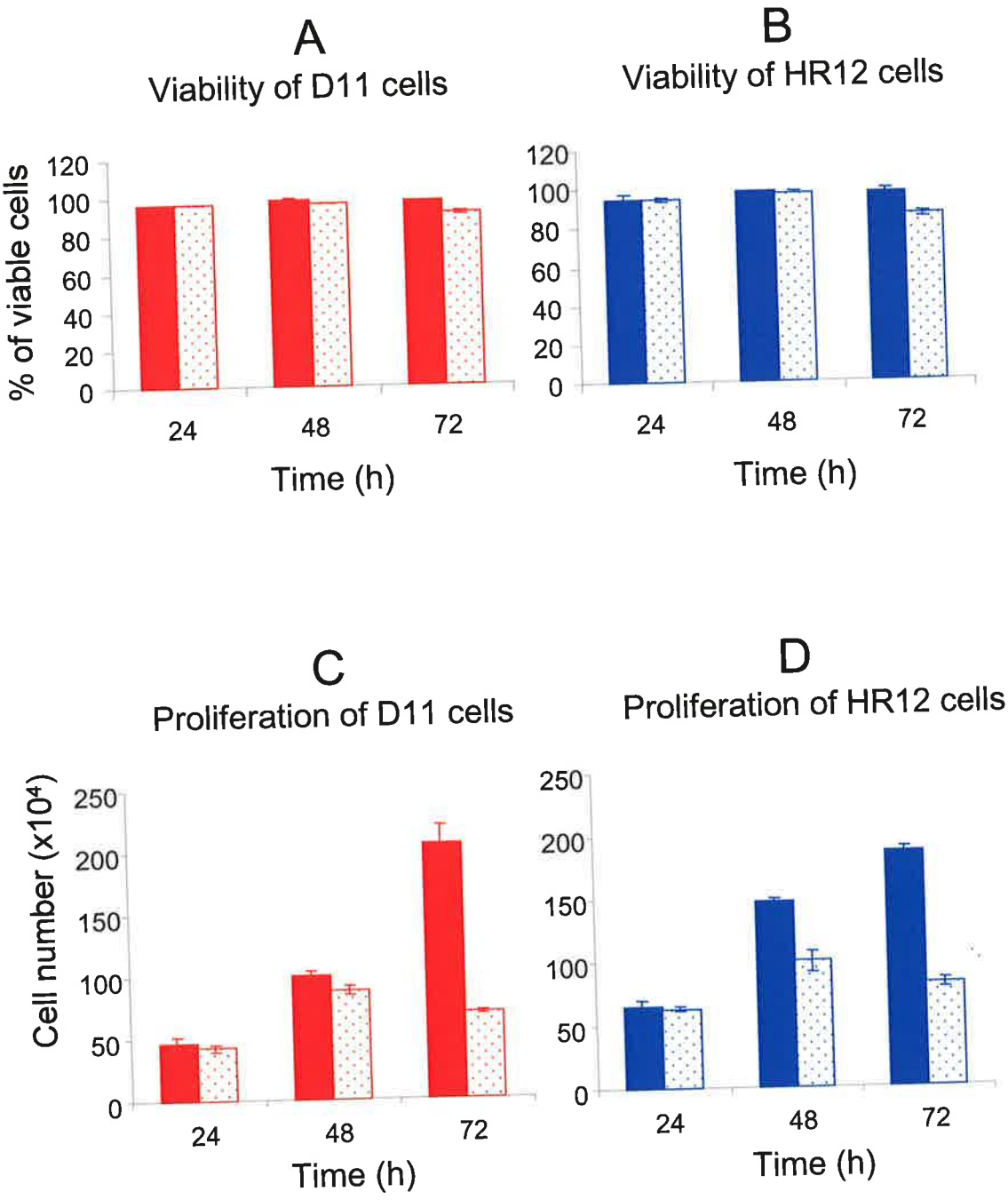
A
Viability of D11 cells
% of viable cells
120
100
80
60
40
20
0
24
48
72
Time (h)
B
Viability of HR12 cells
120
100
80
60
40
20
0
24
48
72
Time (h)
C
Proliferation of D11 cells
Cell number (x10⁴)
250
200
150
100
50
0
24
48
72
Time (h)
D
Proliferation of HR12 cells
250
200
150
100
50
0
24
48
72
Time (h)

observed after 72 h exposure to sCT, which were 63% and 57.9%, respectively (figure 5.3C and 5.3D). These results indicate that CT suppressed cell growth *via* a mechanism that did not primarily involve cellular necrosis.

### 5.2.4 CT effects on cell cycle

Since CT only minimally influenced the viability of cells, this suggested that it might inhibit passage of the cells through the cell cycle. To examine the quantity of nucleosomal DNA in each cell and thus the relative distribution of cells in each phase of the cell cycle, cell nuclei were stained with propidium iodide and fluorescence-activated cell scanning (FACS) was performed (as described in section 2.2.14). Figure 5.4 shows the FACS histogram analysis of D11 and HR12 cells, expressing the Cla rCTR or the insert –ve hCTR receptor, respectively, which were treated with 10nM sCT for 48 h. Each histogram represents a scan of at least 50,000 cells, showing the number of cells at each level of fluorescence. The fluorescence is an indicator of the cellular DNA content, increasing as cells progress from G1 to G2/M phase of the cell cycle replicating their nuclear DNA. The first and second peaks denote cells in the G1 and G2/M phase, respectively (figure 5.4), while the intermediate region represents S phase cells currently undergoing DNA replication (figure 5.4). The proportion of cells in each phase of the cell cycle is represented as a percent of the total number of cells scanned (figure 5.4). There was a prominent accumulation of cells in G2/M phase of the cell cycle and a concomitant reduction in the number of D11 and HR12 cells in the G1 phase of the cell cycle in response to sCT treatment (figure 5.4). In comparison parental HEK-293 cells showed no change in the distribution of cells through the cell cycle (figure 5.4). These data indicate that CT-treatment caused arrest of the cells in the G2/M phase of the cell cycle. To characterise the time course of the cell cycle changes in response to CT-

**Figure 5.4 Fluorescence activated cell scanning (FACS) analysis of sCT-treated cells.**

HEK-293, D11 and HR12 cells remained untreated or were treated with one addition of sCT (10nM). Cells were harvested 72 h later, fixed, stained and analyzed for DNA content, as described in the *Experimental materials and methods*. Shown is the distribution and percentage of cells in the G1, S, and G2 phase of the cell cycle, respectively.

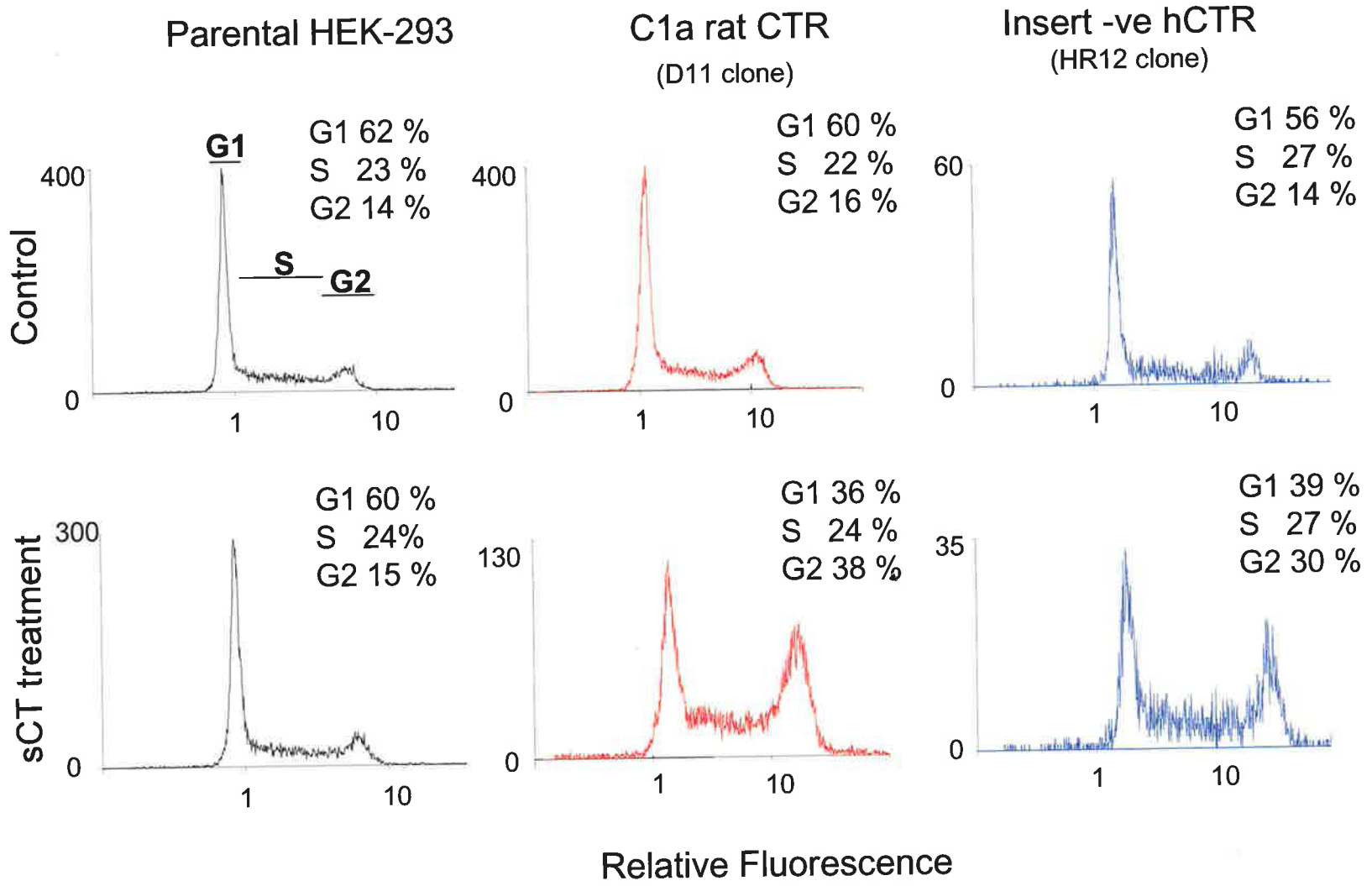
Parental HEK-293
C1a rat CTR
(D11 clone)
Insert -ve hCTR
(HR12 clone)
Control
sCT treatment
G1
S
G2
G1 62 %
S 23 %
G2 14 %
G1 60 %
S 22 %
G2 16 %
G1 56 %
S 27 %
G2 14 %
G1 60 %
S 24%
G2 15 %
G1 36 %
S 24 %
G2 38 %
G1 39 %
S 27 %
G2 30 %
400
0
1
10
60
300
130
35
Relative Fluorescence

**Figure 5.5 The effect of CT on the progression of HEK-293 and D11 cells through the cell cycle.**

HEK-293 (◆,◇) and D11 (■,□) cells were plated in six-well plates at $8x10^4$ cells per well. 48 h after plating, the cells were left untreated (open symbols) or were treated once with 10 nM sCT (closed symbols). Cells were harvested and fixed at the indicated times after sCT addition, then stained and analysed for DNA content, as described in the *Experimental materials and methods.* Each data point represents the percent of cells in the G1, S or G2 phase of the cell cycle, respectively, from a scan of approximately 50,000 cells. The results are representative of two independent experiments.

**Parental HEK-293 cells**
(untransfected)

**D11 cells**
(C1a rCTR)

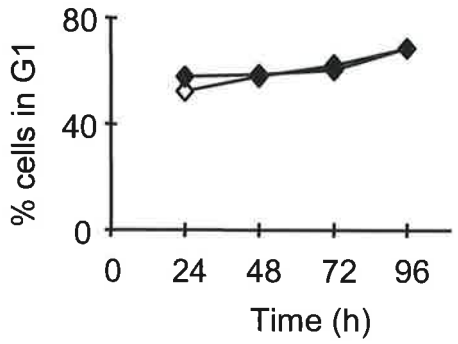


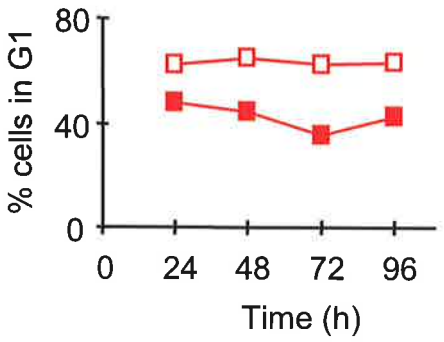


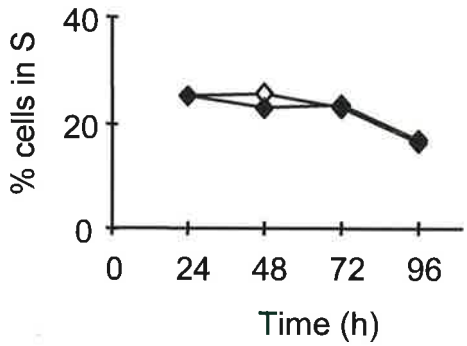


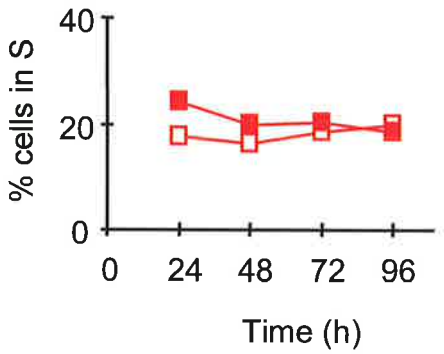


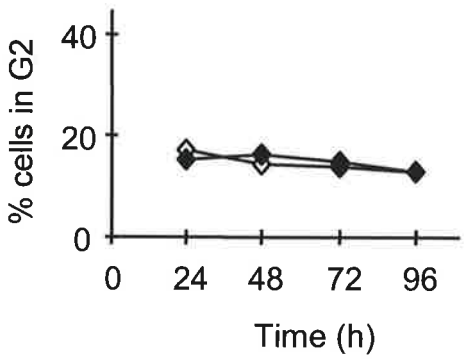


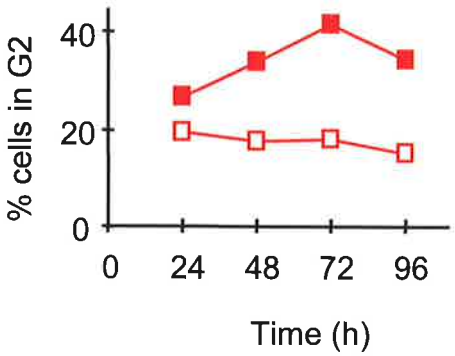

**Figure 5.6 The effect of CT on the progression of vector-transfected HEK-293 cells and HR12 cells through the cell cycle.**

Vector transfected HEK-293 cells – zem (▲, Δ) and HR12 (●, o) cells were plated in six-well plates at $8x10^4$ cells per well. 48 h after plating the cells were left untreated (open symbols) or were treated once with 10 nM sCT (closed symbols). Cells were harvested and fixed at the indicated times after sCT addition, then stained and analysed for DNA content, as described in the *Experimental materials and methods*. Each data point represents the percent of cells in the G1, S or G2 phase of the cell cycle, respectively, from a scan of approximately 50,000 cells. The results are representative of two independent experiments.

**Zem cells**
(vector transfected)

**HR12 cells**
(Insert -ve hCTR)

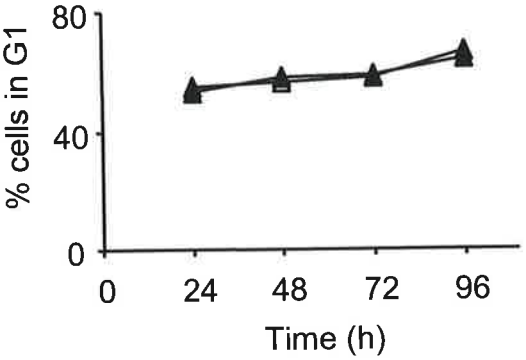


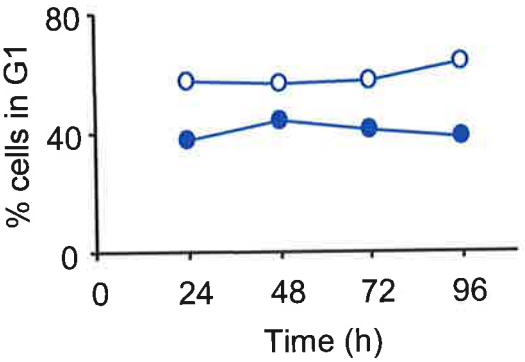


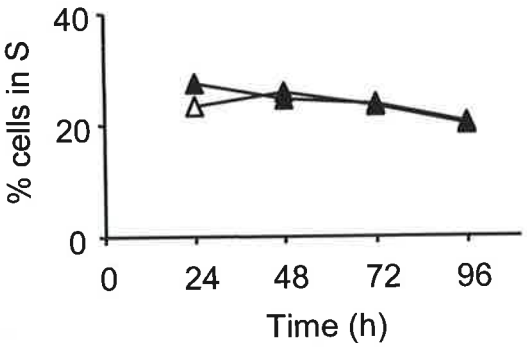


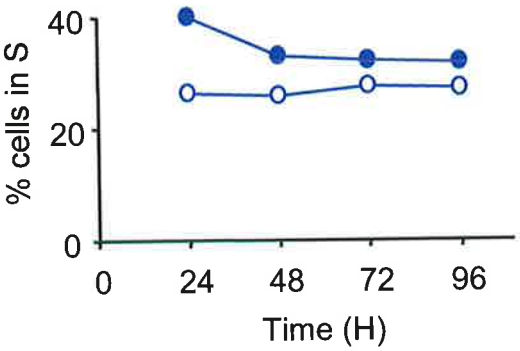


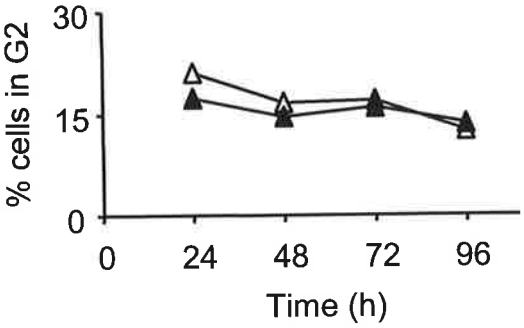


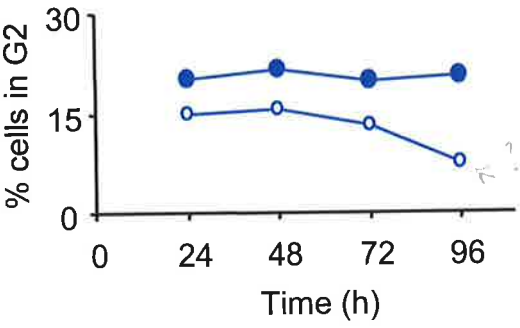

treatment, the percent of cells in each phase of the cell cycle was plotted as a function of time. Figures 5.5 and 5.6 show characterisation of the time course of the cell cycle changes in response to CT-treatment. Once again, untransfected HEK-293 cells showed no change in cell cycle distribution in response to CT-treatment over 96 h (figure 5.5). In contrast, D11 cells expressing the rCTR experienced substantial changes in the cell cycle distribution in response to sCT-treatment. Figure 5.5 illustrates a dramatic increase in the percent of D11 cells in G2/M, a decrease in the percent of cells in G1, but an unchanged S phase population of cells. The increase in G2/M and decrease in G1 paralleled each other, commencing at 24 h post-treatment and continued consistently over the next 48 h, with a peak occurring 72 h post sCT treatment. This CT-induced arrest in G2/M was CTR-dependent because cells transfected with vector alone (figure 5.6), like parental HEK cells (figure 5.5), failed to respond to CT treatment and thus showed no change in the distribution of cells through the cell cycle in response to CT. However the response was not a species-specific phenomenon, with respect to the CTR, as HEK-293 cells expressing the insert –ve hCTR also accumulated in G2/M in response to CT treatment (figure 5.6).

### 5.2.5 CT-induced G2/M cell cycle arrest is CTR isofom specific

Cells expressing the insert +ve hCTR did not experience growth changes in response to CT-treatment (figure 4.5), consequently CT was not expected to change cell cycle parameters of these cells. In order to confirm this, cell cycle distribution of cells expressing either the insert –ve or +ve hCTR were compared. In contrast to HEK-293 cells transfected with the insert –ve hCTR, those expressing the insert +ve hCTR showed no significant changes in cell cycle distribution in response to CT treatment (figure 5.7). Thus, the inability of CT to alter the cell cycle distribution of

Characterisation of CT-induced growth inhibition of HEK-293 cells transfected with the C1a rCTR or the insert –ve hCTR

**Figure 5.7 The effect of CT on the cell cycle progression of cells transfected with the insert –ve hCTR (HR12) or insert +ve hCTR (Hi12).**

HR12 cells expressing the insert -ve hCTR (●,o) and Hi12 cells expressing the insert +ve hCTR (■,□) were plated in six-well plates at $8x10^4$ cells per well. 48 h after plating the cells were left untreated (open symbols) or were treated once with 10 nM sCT (closed symbols). Cells were harvested and fixed at the indicated times after sCT addition, then stained and analysed for DNA content, as described in the *Experimental materials and methods*. Each data point represents the percent of cells in the G1, S or G2 phase of the cell cycle, respectively, from a scan of approximately 50,000 cells. The results are representative of two independent experiments.

**HR12 cells**
(Insert -ve hCTR)

**Hi12 cells**
(Insert +ve hCTR)

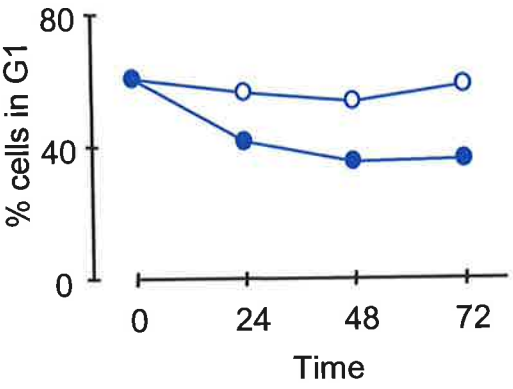


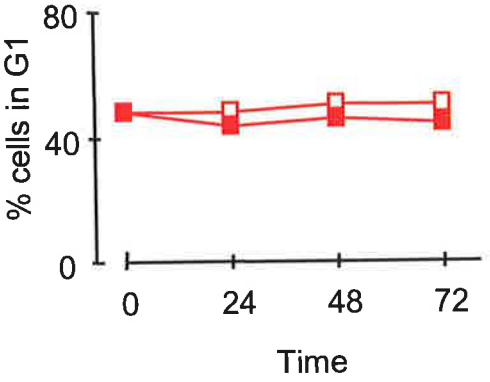


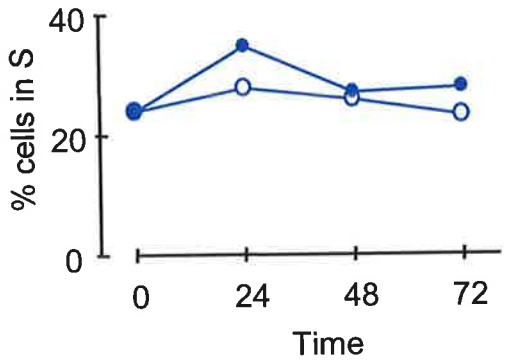


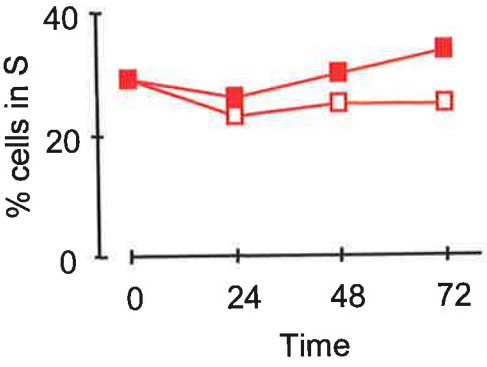


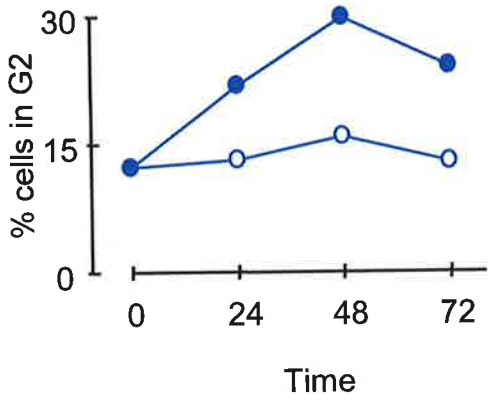


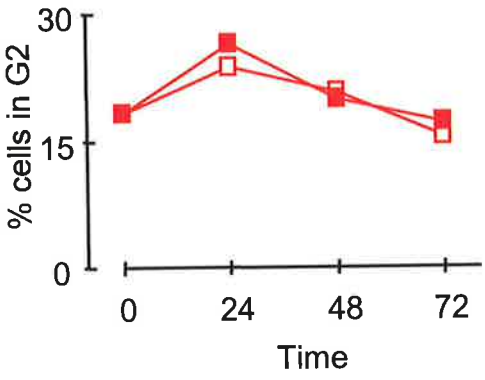

**Figure 5.8 The effect of sCT treatment on mitotic index of HR12 cells.** HR12 cells stably expressing the insert –ve hCTR were treated for 24 h with 10 nM sCT. Cells were then trypsinised, and fixed onto glass slides, as described in the *Experimental materials and methods.* This is a view of the cells when viewed using a 40x objective and 10x binoculars. Cells that have progressed from G2 and entered mitosis have condensed chromosomes (metaphase chromosomes), as indicated by the arrows in panel A. The mitotic indicies are expressed as the average number of cells ± SEM with condensed chromosomes per 3000 cells, calculated from 10 random fields of view. These results are representative of two independent experiments.

A

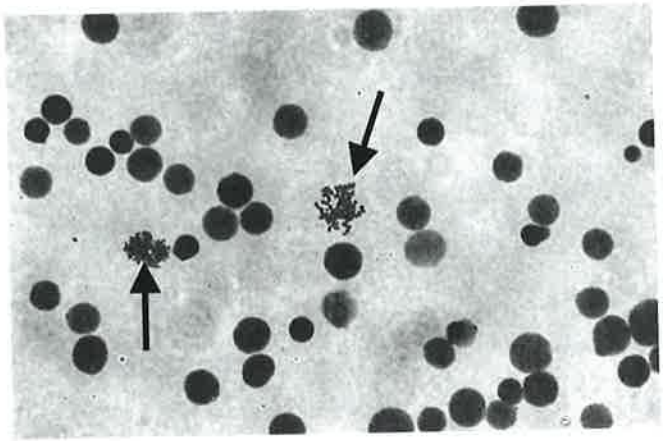

B

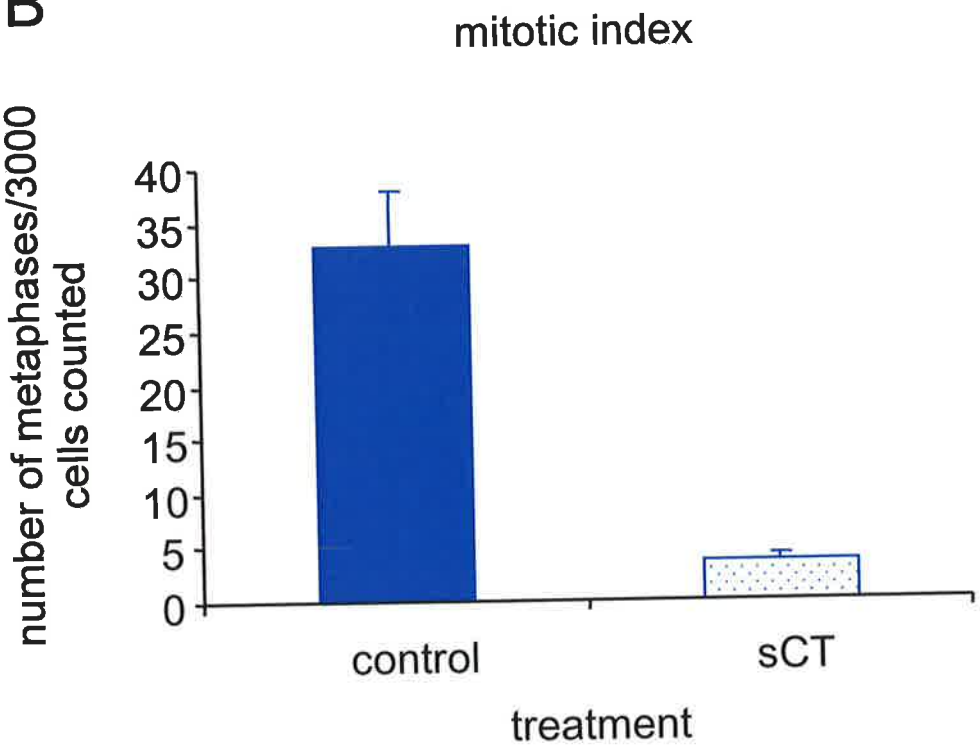
mitotic index
number of metaphases/3000 cells counted
40
35
30
25
20
15
10
5
0
control
sCT
treatment

cells expressing the insert –ve hCTR, is consistent with the growth data discussed in Chapter 4, specifically the lack of anti-proliferative activity shown in HEK-293 cells expressing the insert +ve hCTR in response to CT-treatment.

### 5.2.6 CT-effect on mitotic index

To investigate whether the CT-induced G2/M accumulation was due to a specific block in G2 or in M phase, the mitotic index of CT-treated cells was evaluated 24 h after CT treatment (described in section 2.2.15). Figure 5.8A shows a characteristic metaphase spread of chromosomes, observed when cells leave G2 phase of the cell cycle and enter mitosis. The number of mitotic cells, as determined by the number of cells with chromosomes in metaphase, was 10-fold lower in the CT-treated cells compared with controls (figure 5.8B), indicative of a specific block in G2 and failure of cells to enter mitosis.

## 5.3 Discussion

The data presented in this chapter showed that the CT-mediated inhibition of HEK-293 cells over 72 h is not due to an induction of apoptosis and involves minimal cell death. However, the anti-proliferative action of CT was due to induction of cell cycle arrest. CT-treatment arrested cells in the G2/M phase of the cell cycle, following DNA replication and prior to mitotic division. Associated with the timing of the CT induced G2 arrest, was an increase in the number of rounded loosely attached cells. Loss of cell adherence in some cells, leads to reduced cell viability (McGill et al., 1997; Okuda et al., 1999). The loss of adherence in HR12 cells following 72 h of treatment with sCT is therefore a possible explanation for the observed reduction in cell viability. However further investigation is required to confirm this proposal.

The G2/M check-point is not characterised or understood as well as the G1/S check-point. The G2 arrest is described as a DNA damage check–point, which is activated in response to the cell detecting DNA damage (Aguda 1999). The use of DNA damaging agents to induce G2 arrest in human cancer cell lines has been reported (Lallemand et al., 1999; Li et al., 1999; Panagiotou et al., 1999), and may be a potential therapeutic approach to cancer treatment. The G2 cell cycle arrest also has a role in cell development and differentiation, being employed in the process of oocyte maturation (Cross et al., 1998). It has been suggested that the G2 arrest is involved in the differentiation of megakaryocytes and osteoclasts (Coffman et al., 1999). This opinion is in contradiction to the current understanding, which indicates that osteoclasts are formed by a process of cell fusion. Despite cell fusion being an "accepted" mechanism of osteoclast formation, there is limited published material documenting the process of multinucleation, and thus it remains possible that both endoreduplication and cell fusion are involved in the generation of osteoclasts.

In agreement with the CT-induced G2 cell cycle arrest presented in this chapter, the G-protein coupled alpha-1B- adrenergic receptor ($\alpha$1BAR) was also able to induce G2/M arrest in a transfected cell model of human hepatoma cells (Auer et al., 1998). The authors speculated that the ability of this receptor to induce such an arrest may explain the lack of $\alpha$1BAR expression in transformed hepatocytes. In searching for a physiological significance of this observed G2 arrest, it cannot be disregarded that the effect seen with both the $\alpha$1BAR and CTR is non-physiological, and simply due to the over-expression of the receptors in the transfected cell model. However, the CTR has a reported role in influencing cellular decisions, being essential in the process of blastocyst implantation in the

mouse endometrium (Wang et al., 1998; Zhu et al., 1998a; Zhu et al., 1998b). These reports provide evidence that CT has an *in vivo* role in growth regulation and cellular differentiation.

The observation that sCT-treatment can induce apoptosis when cells are grown in sub-optimal mitogenic conditions, suggests a potential pharmacological use for the peptide, in cancer therapy. Primary cancers commonly express CTR (as discussed in section 1.2.2.4) and the growth of cancer cell lines can be regulated by CT (as discussed in section 1.2.4.4). Therefore it may be possible to induce apoptosis in cancer cells by treating the cells with CT in conjunction with a chemotherapeutic agent, instead of using the low serum conditions. The potential may exist to use CT as an adjunct cancer therapy and while not explored further here, this is a fertile area of future study.

# Chapter 6

# Molecular mechanisms for the CT-induced G2 arrest in HEK-293 cells

## 6.1 Introduction

Proliferation of eukaryotic cells requires progression through the cell cycle, which is regulated by proteins that act at cell cycle check-points (discussed in section 1.3.2). Specifically, the cyclin dependent kinase (CDK) inhibitors (CKIs) are involved in regulating cell growth, arrest and differentiation at cell cycle check points. CKIs are classified into two groups on the basis of their sequence homology *(Pines 1997)*. The INK4 family specificallly inhibit CDK4 and CDK6 activity *(Hirai et al., 1995)*, by disrupting their ability to bind cyclin D *(Hall et al., 1995)*. The control of cyclin D CDK4 *(Tam et al., 1994)* / CDK6 *(Meyerson et al., 1994)* complexes is vital to controlling progression through the G1 phase, thus the INK4 inhibitors have well recognised roles in the G1/S phase check-point. The second CKI category is the Kip/Cip family which includes $p21^{CIP1/WAF1/SDI1}$, $p27^{KIP1}$ and $p57^{KIP2}$ *(Pines 1997)*. The Kip/Cip CKIs inhibit a wider variety of CDK-cyclin complexes by directly binding to the complex *(Hall et al., 1995)* and thus have been associated with G1/S (discussed in section 1.3.2.1) and the G2/M check-points.

Growth inhibition specifically, has been reported to be accompanied by a rapid and sustained increase in the CKIs p21 and p27 *(Coats et al., 1996)*. Both p21 and p27 have been extensively studied with respect to their inhibition of G1 CDK/cyclin complexes, cyclin D/CDK and cyclin E/CDK *(LaBaer et al., 1997; Santra et al., 1997; Toyoshima et al., 1994)*, and thus induction of G1 cell cycle arrest. In comparison to the G1 checkpoint, considerably less is known about the G2/M cell cycle checkpoint, particularly the CKIs involved. However the initial reports described p21 as a universal inhibitor of cyclin kinases *(Xiong et al., 1993)*, implying a potential regulatory role throughout the cell cycle. In addition, p21 mRNA has a biphasic periodicity in human fibroblasts, peaking in both G1 and G2/M *(Li et al., 1994)*,

suggesting a role for p21 in both the G1 and G2/M cell cycle check points. Recent reports have implicated p21 in G2/M cell cycle arrest. Niculescu *et al* overexpressed p21 in a diverse panel of cell lines and found that this induced both G1 and G2 cell cycle arrest *(Niculescu et al., 1998)*. In a more physiological setting, using non-transformed fibroblasts, ionising radiation induced an accumulation of nuclear p21. This p21 accumulation occurred prior to the G2/M phase transition and was associated with cyclin A-CDK and cyclin B1-CDK complexes *(Dulic et al., 1998)*. The involvement of p21 in the G2/M pause is further supported by the p21 gene knock out mouse. Murine embryonic fibroblasts from the p21 -/- animals have a significantly reduced proportion of premitotic cells containing cyclin B1 compared to cells from wild type littermates.

In the G1 checkpoint, induction of p21 is frequently found to be dependent on up-regulation of p53 *(Polyak et al., 1996)*, but has also been reported to occur independently of p53 *(Michieli et al., 1994)*. The p21/p53 relationship is equally ambiguous in the G2 checkpoint, as p21 has been shown to be both p53-dependent *(Bunz et al., 1998)* and independent *(Bates et al., 1996)*. In addition to the mechanism of p21 regulation being multi dimensional, there are at least two methods by which p21 can control the G2-M transition. The transition of a cell from G2 to M phase requires activation of the cdc2-cyclin B1 complex (discussed in section 1.3.2.2.2). Current evidence indicates that p21 can prevent activation of the cdc2-cyclin B1 complex either through direct association with the complex *(Bunz et al., 1998)* or *via* an indirect mechanism *(Bates et al., 1996)*.

The aim of the experiments described in this chapter was to elucidate the nuclear mechanisms by which CT induces a G2 cell cycle arrest in transfected HEK-293 cells expressing the insert –ve hCTR. I would like to acknowledge Dr Evdokiou's

guidance, supervision and involvement in the experiments presented in this chapter. The results indicated that CT up-regulates p21 *via* a p53-independent mechanism to induce a G2 cell cycle arrest. This block in cell progression was due to inhibition by CT of cdc2 kinase activity. However we were unable to conclude that this involved direct interaction between p21 and the cdc2/cyclin B1 complex.

## 6.2 Results

### 6.2.1 CT elevates p21 mRNA and protein

To examine the nuclear events underlying CTR-mediated growth arrest in G2/M, the effect of CT on the expression of the cyclin-dependent kinase inhibitor p21 was examined by northern blot (described in section 2.2.16) (figure 6.1) and western blot (described section 2.2.9) (figure 6.2) analysis. Acknowledgement and thanks are extended to Dr Helena Richardson for kindly providing the human $p21^{WAF1/CIP1}$ cDNA, used in the Northern blot analysis. D11 cells expressing the C1a isoform of the rCTR showed an increase in $p21^{WAF1/CIP1}$ mRNA in response to a 4 h treatment with 10nM sCT. This single addition of CT induced a further increase in $p21^{WAF1/CIP1}$ mRNA, which was sustained over the 48 h treatment period. A similar effect was seen in the HR12 cells expressing the insert -ve hCTR isoform, with slightly altered kinetics, as p21 mRNA levels did not increase until 24 h following CT-treatment. There was no effect of CT on the p21 mRNA levels in untransfected HEK-293 cells, however in all cells there was an increase in p21 mRNA with increasing cell density, independent of CT-treatment. Western blot analysis allowed determination of whether the increase in p21 mRNA was reflected in the cellular p21 protein. Corresponding to the mRNA levels, a large increase in p21 protein was also observed in D11 cells, after treatment with CT (figure 6.2A). This elevation in p21 protein decreased 24 h post-treatment,

**Figure 6.1 Expression of p21 and p53 mRNA following treatment with calcitonin.**

Parental HEK-293 cells and cells stably transfected with either C1a isoform of the rat CTR (clone D11) or the insert negative isoform of the human CTR (clone HR12) were cultured for the times indicated in the absence or presence of 10 nM sCT, added once. Total RNA was extracted and Northern blot analysis performed. Panel A: 10 μg of total RNA was electrophoresed through a 1% agarose formaldehyde gel, transferred to nylon membrane and hybridised with cDNA probes for p21 and p53 as indicated. Blots were rehybridised with a cDNA probe specific for GAPDH to indicate RNA loading. Results were analysed by densitometry and expressed as a ratio of p21 mRNA/GAPDH mRNA, panel B and p53 mRNA/GAPDH mRNA, panel C.

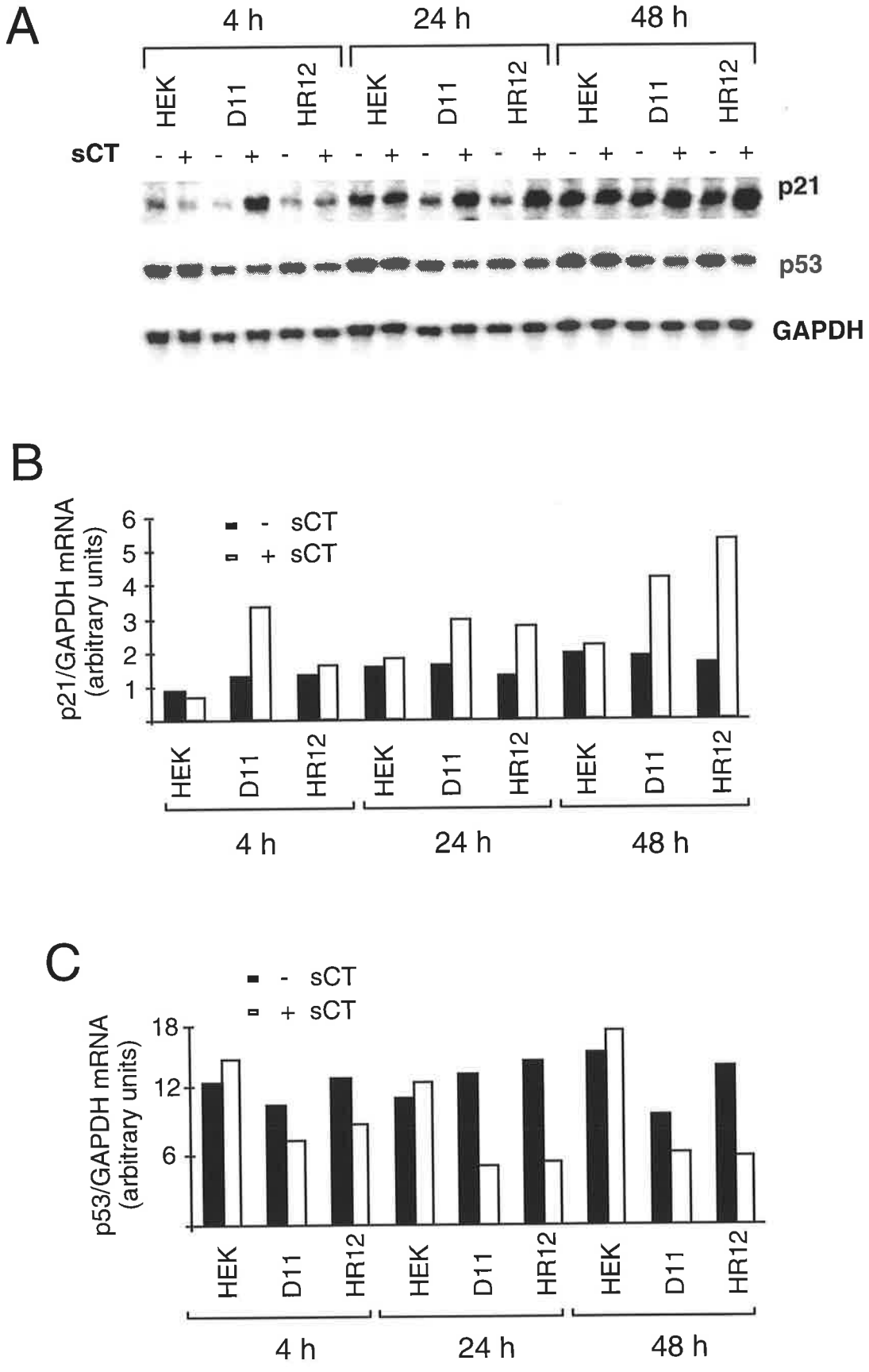
A
4 h
24 h
48 h
HEK
D11
HR12
sCT
- + - + - + - + - + - + - + - + - + - +
p21
p53
GAPDH
B
p21/GAPDH mRNA (arbitrary units)
- sCT
+ sCT
6
5
4
3
2
1
HEK
D11
HR12
4 h
24 h
48 h
C
p53/GAPDH mRNA (arbitrary units)
- sCT
+ sCT
18
12
6
HEK
D11
HR12
4 h
24 h
48 h

**Figure 6.2. Western blot analysis of p21 and p27 protein following treatment with calcitonin.**

Parental HEK-293 and D11 cells were untreated or treated once with 10 nM sCT for the times indicated. Total cell lysates were prepared and equal amounts of total cell protein (50 μg) were separated by SDS-PAGE, transferred to PVDF membrane and immunoblotted with mouse monoclonal antibodies against p21 protein, panel A, p27 protein, panel B and p53 protein panel C. In each case, results were analysed by densitometry and are expressed as bar charts.

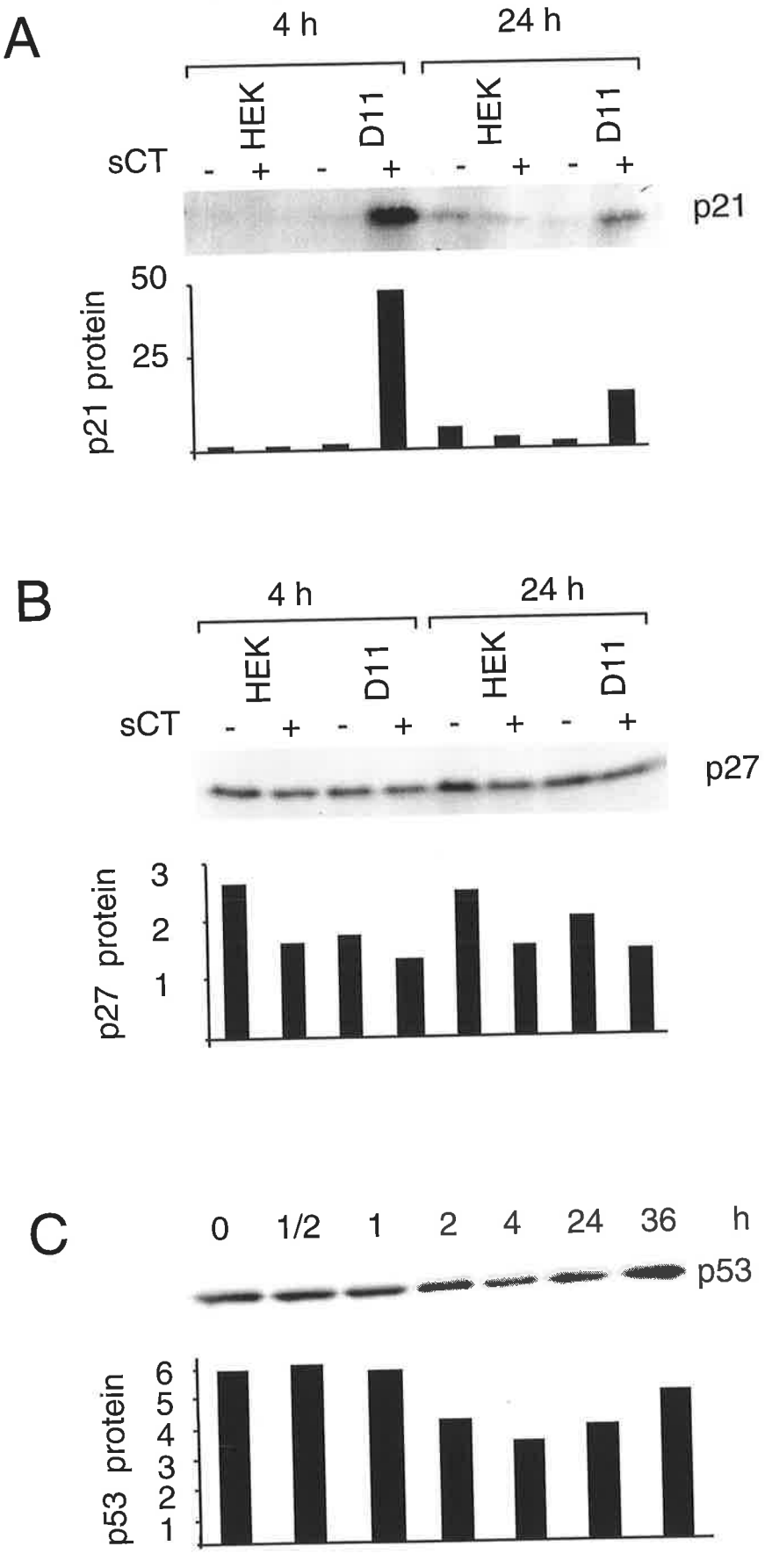
A
4 h
24 h
HEK
D11
HEK
D11
sCT
- + - + - + - +
p21
50
25
p21 protein
B
4 h
24 h
HEK
D11
HEK
D11
sCT
- + - + - + - +
p27
3
2
1
p27 protein
C
0 1/2 1 2 4 24 36 h
p53
6
5
4
3
2
1
p53 protein

but remained higher than untreated cells (Figure 6.2A). CT-treatment did not influence the p21 levels in untransfected cells. The protein level of p27, another CDK inhibitor belonging to the cip/kip family, was also examined, and no appreciable effect was seen with CT-treatment (figure 6.2B). In several cell systems, the mechanism of p21 inhibition of cell cycle is dependent on the p53 protein. Elevation of the p53 transcription factor increases p21 levels, such that p21 can then inhibit the activity of the CDK2/cyclin B1 complex. Analysis of steady-state levels of p53 mRNA in both D11 and HR12 cells following CT-treatment showed a consistent decrease in p53 mRNA levels (Figure 6.1C). The decrease in the steady-state levels of p53 mRNA occurred within 2 h of CT-treatment and persisted for up to 48 h. The obvious change in cellular p53 levels was reflected in the amount of cellular p53 protein, which decreased rapidly within 2 h of CT treatment of HR12 cells (Figure 6.2C).

### 6.2.2 Effects of p21 on cell growth following CT-treatment

The up-regulation of p21 mRNA and protein occurring early after CT-treatment, suggested that p21 may be involved in the CT-induced G2 arrest. To investigate this, antisense oligonucleotide experiments were performed (described in section 2.2.17). The ability of CT to induce growth inhibition was assessed in the presence of p21 sense or antisense oligonucleotide. The sense oligonucleotide had no effect on the CT-induced increase in p21 mRNA (Figure 6.3A), protein (Figure 6.3B) or the CT-mediated inhibition of cell growth. In contrast, treatment of the cells with p21 antisense oligonucleotides substantially prevented the CT–induced p21 mRNA increase at 24 and 48 h (Figure 6.3A), as well as the protein increase at 48 h (figure 6.3B). Most convincing, however, was the ability of antisense oligonucleotides to completely reverse the CT-induced growth suppression (Figure 6.3C). There was no significant difference between cell numbers in the control, sense or antisense

**Figure 6.3 Effect of antisense p21 on the growth of HR12 cells after CT treatment.**

HR12 cells were untreated (-) or treated (+) with CT in the presence or absence of either the sense or antisense p21 oligonucleotide. Northern blot analysis was performed to assess the levels of p21 mRNA at 24 and 48 h after treatment with CT, panel A. Cell extracts were collected 48 h after CT treatment and p21 protein levels were assessed by western blotting using a p21 specific antibody, panel B. HR12 cells were trypsinised and counted 48 h post CT treatment, panel C. These results are representative of four independent transfection experiments.

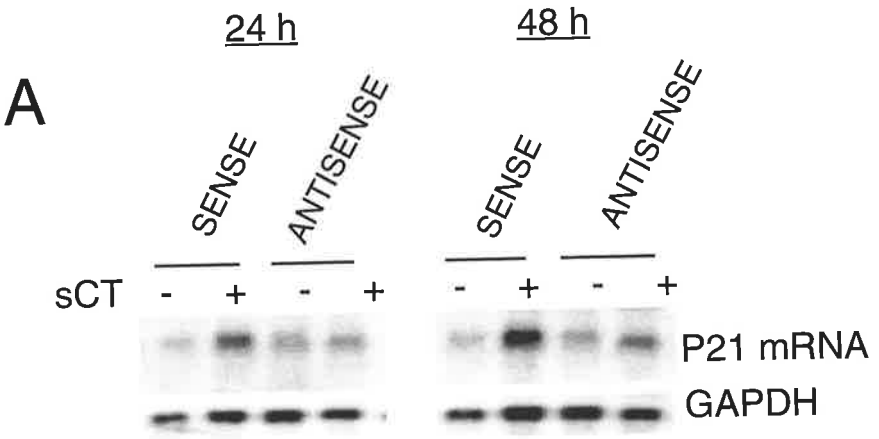
A
24 h
48 h
SENSE
ANTISENSE
SENSE
ANTISENSE
sCT - + - + - + - +
P21 mRNA
GAPDH

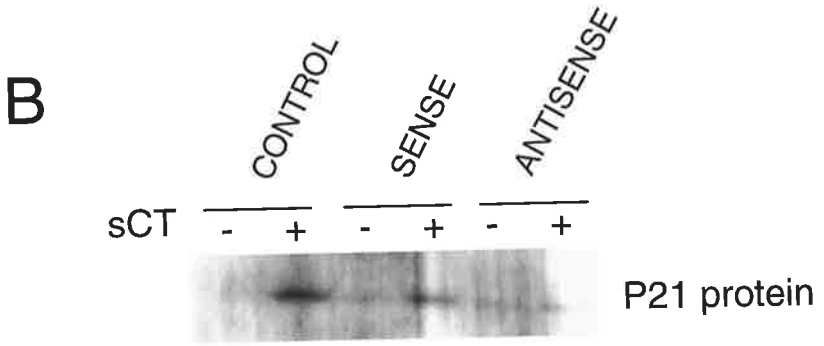
B
CONTROL
SENSE
ANTISENSE
sCT - + - + - +
P21 protein

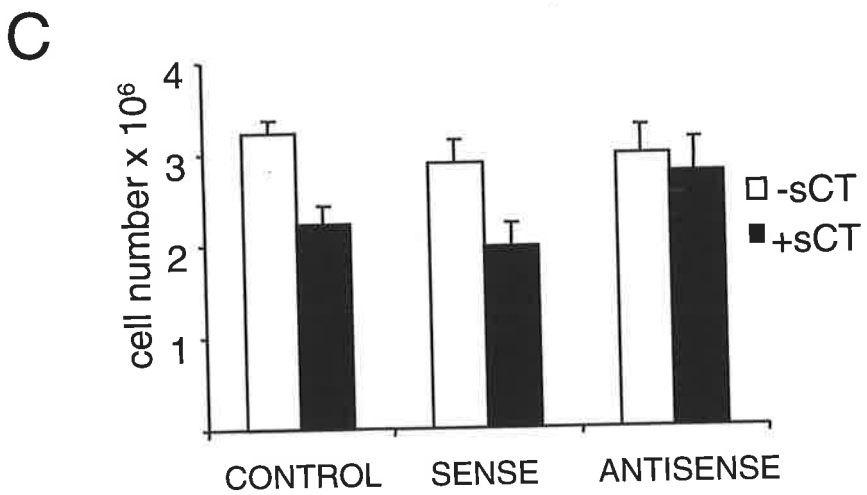
C
cell number x 10⁶
4
3
2
1
-sCT
+sCT
CONTROL
SENSE
ANTISENSE

oligonucleotide treated cells in the absence of CT, indicating that the oligonucleotides were not having any non-specific toxic effects. The results suggest a causative relationship between CT-induction of p21 and CT-mediated growth suppression.

### 6.2.3 The effect of CT on cdc2/cyclin B1 kinase activity

To further define the molecular mechanisms of CT-induced growth arrest, the properties of the G2-specific cyclin dependent kinase/cyclin complex (cdc2/CyclinB1) in HEK-293 cells expressing the insert –ve hCTR were investigated. The generation of the cdc2/CyclinB1 complex requires an accumulation of cyclin B1 as the cells approach M phase *(Nurse 1990)*, and thus levels of cyclin B1 protein in HR12 cells in the presence and absence of sCT were determined (described in section 2.2.9). As shown in figure 6.4A, the cyclin B1 levels increased with increasing sCT exposure, such that at 48h, a time coinciding with maximal accumulation of cells in late G2 (Chapter 5 Figure 5.5), there was significantly more cyclin B1 protein present. Progression of cells from G2 into M phase requires an accumulation of cdc2/cyclin B1, but is dependent on activation of the cdc2 kinase activity (refer section 1.3.2.2.2 & figure 1.9B). Thus we examined the kinase activity of the cdc2/cyclin B1 complex in response to sCT treatment (described in section 2.2.18). Figure 6.4B, upper panel, shows cdc2-immunoprecipitate resolved by electrophoresis and assayed for cdc2 by western blotting. Cdc2 was detected in all immunocomplexes and its levels were not changed with CT-treatment. The kinase activity of cdc2 was evaluated following CT-treatment, by analysing the ability of cdc2 (figure 6.4B) and cyclin B1 (figure 6.4C) immunoprecipitates, from HR12 cells, to phosphorylate the substrate histone H1. Cdc2 cyclin B1 kinase activity increased transiently in the first 24 h after CT-treatment, then declined dramatically and was lowest at 48 and 72 h, times when the G2 arrest was prominent (Chapter 5 figure 5.5). In contrast, when HR12 cells

**Figure 6.4. Effect of CT on cyclin B1 protein levels and on Cdc2 protein kinase activity in HR12 cells.**

HR12 cells were untreated or treated with sCT for different times and total cell extracts (50 μg) were assayed for cyclin B1 by western blotting, using a Fluorimager (panel A). To determine cdc2 kinase activity, cells were treated with CT for the indicated times or treated with the drug nocodazole for 24 hr. Immune complexes were resolved by electrophoresis and assayed for cdc2 by western blotting using a Fluorimager (panel B, Upper panel). The cdc2 immunoprecipitated complexes were also assayed for their ability to phosphorylate histone H1 *in vitro* using a phosphorImager (panel B lower panel). For cyclin B1 associated kinase activity, extracts were immunoprecipitated with a cyclin B1 polyclonal antibody and kinase activity assessed as previously described in the *Experimental material and methods* (panel C). Phosphorylation of Cdc2 Tyr15 in total cell lysates (50 μg) treated with CT or nocodazole was detected by western blotting using a phospho-Cdc2 (Tyr15) specific antibody, on a Fluorimager (panel D).

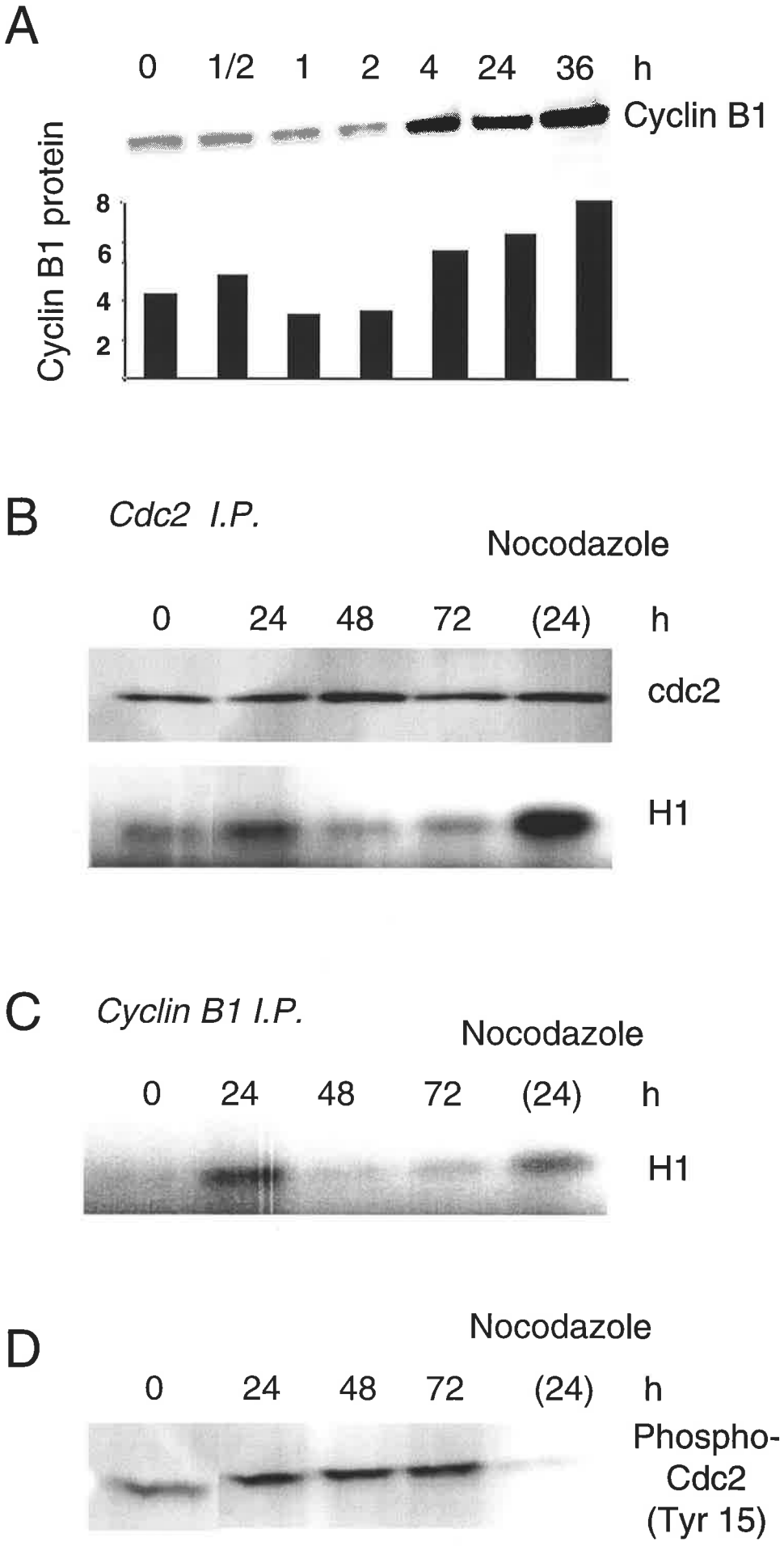
A
0 1/2 1 2 4 24 36 h
Cyclin B1
Cyclin B1 protein
8
6
4
2
B
Cdc2 I.P.
Nocodazole
0 24 48 72 (24) h
cdc2
H1
C
Cyclin B1 I.P.
Nocodazole
0 24 48 72 (24) h
H1
D
Nocodazole
0 24 48 72 (24) h
Phospho-
Cdc2
(Tyr 15)

were treated with the microtubule-depolymerising drug, nocodazole, which specifically arrests cells in mitosis, the kinase activity associated with cdc2 (figure 6.4B) and cyclin B1 (figure 6.4C) immunoprecipitates was dramatically higher than in CT-treated cells. The specific activation of cdc2 occurs through de-phosphorylation of the tyrosine 15 residue (Tyr15). To investigate the inactivation of cdc2 by CT on Tyr15 phosphorylation, cell extracts were immuno blotted with a phospho-cdc2Try15 antibody that detects cdc2 when it is catalytically inactivated by phosphorylation at Try15. As shown in figure 6.4D, CT treatment resulted in a modest but reproducible increase in cdc2-Tyr15 phosphorylation, which occurred at 48 and 72 h post-treatment, consistent with inactive cdc2 and G2 arrest. In contrast, cells treated with Nocodazole had unphosphorylated cdc2-Tyr15. These data indicate that when M phase was blocked by activation of the spindle microtubule-assembly checkpoint using nocodazole, cdc2 complexes were held in an active state manifested by the lack of cdc2-Tyr15 phosphorylation (figure 6.4D). However, when cells were arrested in G2 with CT, the kinase activity of cdc2 complexes was low and cdc2 Tyr15 was maintained in the phosphorylated and inactive state. Taken together, these results clearly demonstrate that CT inhibits the kinase activity of the cdc2/cyclin B1 complex which may therefore block progression into mitosis.

### 6.2.4 p21 interaction with cdc2/cyclin B1

The CDK-inhibitor p21 has been reported to inhibit activation of cdc2/cyclinB1, *via* direct association with the complex. To explore the kinetics of p21 up-regulation, western blot analysis of p21 immunoprecipitates isolated from HR12 cells were assayed for p21 protein (described in section 2.2.18). p21 was barely detectable in immunoprecipitates of untreated cells but increased significantly within 2 h after CT-treatment, peaking at 4 h, but remaining elevated in CT-treated cells (figure 6.5A).

**Figure 6.5 The effect of CT-treatment on the interaction of p21 with the cdc2/cyclin B1 complex.**

HR12 cells remained untreated or were treated with CT for the indicated times, and total cell lysates were prepared. Aliquots of cell lysate were immunoprecipitated with p21 or cdc2 polyclonal antibody, and the immune complexes were resolved by electrophoresis and assayed for p21 panel A. Aliquots of the same lysates were immunoprecipitated with p21 or Rb (in the case of the –ve control [-ve]) polyclonal antibody. The immune complexes and one track of total cell lysate [lysate], were resolved by electrophoresis and assayed for cdc2 immunoreactivity panel B.

A *p21 IP*

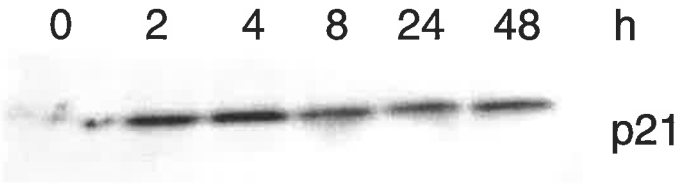


*Cdc2 IP*


B *p21 IP*

This induction of p21 prior to the G2 arrest indicated that p21 may be binding to, and inhibiting the activation of cdc2/cyclin B1 complex. Thus cdc2-immunoprecipitates from cells were assayed for p21 protein using p21 monoclonal antibody (figure 6.5B). There was no detectable p21 protein associated with the cdc2 immunoprecipitates. In the converse experiments we were unable to detect cdc2 protein in p21 immunoprecipitates (figure 6.5C). The inability to detect p21 associated with the cdc2-cyclin B1 complex indicates that the CT-inactivation of cdc2 kinase activity and consequent G2 arrest does not involve direct interaction between p21 and the cdc2/cyclin B1 complex. Alternatively the affinity of p21 for binding to the cdc2/cyclin B1 complex may be too low to survive the immunoprecipitation process.

## 6.3 Discussion

In the present experiments, we found that CT treatment of HEK-293 cells expressing insert -ve hCTR resulted in a prominent increase in p21 mRNA and protein, which occurred concomittantly with the G2 arrest. The CT induced elevation of the p21 CKI was highly specific, as CT treatment had no appreciable effect on another CIP family CKI, p27. The CIP family of CKI's, are up-regulated by a number of GPCR to induce cell cycle arrest. For example the PTH receptor, which is in the same sub-family of 7TMDR as the CTR, is able to induce osteoblast differentiation in response to ligand stimulation (discussed in chapter 5). The osteoblast differentiation process is accompanied by inhibition of cell proliferation, elevated levels of the CDK inhibitor $p27^{kip1}$, and accumulation of cells in G1 phase of the cell cycle *(Onishi et al., 1997)*. This association between p27 up-regulation and G1 arrest is not restricted to the CT sub-family of 7TMDR, but has also been reported to occur *via* activation of the

number 2 human somatostatin receptor (hSSTR 2) in chinese hamster ovary cells *(Pagès et al., 1999)*.

The p21 anti-sense oligonucleotides were able to prevent the increase in p21 protein and the G2 arrest induced by CT, indicating a causative relationship between the two events. There are many reports in the literature, which support this association between p21 and the G2 arrest. For example, treatment of breast cancer cell lines with conditioned media from myoepithelial cells significantly inhibited the proliferation of the cancer cells, *via* induction of a G2/M cell cycle arrest. Associated with the G2/M arrest was an increase in cellular p21 levels *(Shao et al., 1998)*. Similarly the sodium butyrate-induced G2 arrest in MDA-MB-231 breast cancer cells was associated with an elevation in p21 protein *(Lallemand et al., 1999)*. However to date this is the first report of a 7TMDR up-regulating p21 to induce a G2 cell cycle arrest. Although there are reports of 7TMDR inducing G1 cell cycle arrest (discussed in chapter 5), for example the human somatostatin receptor number 5 (hSSTR5) induces a G1 arrest, which is associated with an increase in cellular p21 *(Sharma et al., 1999)*.

The p21 promoter contains several p53-response elements *(Nakano et al., 1997)* and p21 up-regulation in G1 arrest was first reported to be p53-dependent *(Wu et al., 1997; Sheikh et al., 1994)*. Subsequently, p21 induction has also been shown to occur independently of p53 *(Li et al., 1994)*. In HEK-293 cells transfected with the insert –ve hCTR, the increase in p21 mRNA and protein is unlikely to depend on p53, as p53 mRNA levels decreased in response to CT-treatment. This inverse relationship between p21 and p53 regulation by CT is interesting and the specific involvement of reduced p53 levels in response to a G2 arrest remains to be investigated. In some cells, up-regulation of p53 is associated with induction of

apoptosis *(Bates et al., 1996)*. In the present experiments the CT induced G2 arrest in serum replete conditions did not precede cell apoptosis (discussed in chapter 5). It is speculative to propose, but possible, that the decrease in p53 levels is a protective mechanism allowing the cells to avoid apoptosis.

The activation of cdc2/cyclin B1 complex is critical in allowing mammalian cells to progress from G2 into M phase *(Pines 1993)*. The activity of the cdc2 kinase is dependent on it being phosphorylated on threonine 161 *(Norbury et al., 1992)* and de-phosphorylated on tyrosine 15 and threonine 14 *(Nurse 1990)*. The phosphatase cdc25 removes the inhibitory phosphates on Tyr 15 and Thr 14 and allows the cell to commence mitotic division. The results presented here show that CT blocked mitosis in HEK-293 cells by preventing activation of the cdc2/cyclin B1 complex by maintaining phosphorylation on Tyr 15. P21 has been reported to inhibit activation of cdc2/cyclin B1 kinase activity *(Guadagno et al., 1996)*. However there was no evidence to indicate a direct interaction between p21 and cdc2/cyclin B1 complex in HEK-293 cells, despite the dramatic decrease in kinase activity. These results indicate that p21 has a causative role in the CT-induction of G2 arrest, however we were unable to conclude whether this was due to the direct interaction of p21 with the cdc2/cyclin B1 complex. It is possible that p21 prevents activation of cdc2/cyclin B1 *via* direct interaction with the complex, but that this association is too weak to survive the cell lysis and immunoprecipitation process.

# Chapter 7

# Identification of novel CT receptor elements in the promoter of the human $p21^{WAF1/CIP1}$ gene

## 7.1 Introduction

In most cases, the mechanism by which CT exerts its effects has not been elucidated. The action most intensively studied to date is the CT-induced receptor down regulation in mouse *(Ikegame et al., 1996; Wada et al., 1995; Wada et al., 1996a; Rakopoulos et al., 1995)* and human osteoclasts *(Takahashi et al., 1988; Inoue et al., 1999)* (discussed in section 1.2.6). In mouse osteoclasts, CTR activation caused a rapid and sustained down regulation of the CTR mRNA, due to a cAMP-mediated destabilization of receptor mRNA *(Rakopoulos et al., 1995)* with perhaps an effect on transcription also *(Inoue et al., 1999)*. In contrast, glucocorticoid treatment of osteoclasts increased their expression of the CTR, by increasing transcription from the CTR gene *(Wada et al., 1997)*. There is currently no information on the manner by which CT affects gene transcription, and no identification of the promoter elements involved.

The promoter of the p21 gene contains multiple p53-response elements and induction of p21 has been shown to occur under p53 dependent conditions *(Wu et al., 1997; Li et al., 1994)*. However, a number of diverse agents have been described, which activate transcription of p21 by p53-independent mechanisms. These include phorbol esters, okadaic acid, transforming growth factor β (TGFβ), extracellular calcium, butyrate, histone deacetylase inhibitor, trichostatin A and NGF *(Biggs et al., 1996; Datto et al., 1995; Prowse et al., 1997; Nakano et al., 1997; Sowa et al., 1997; Yan et al., 1997)*. These agents act through multiple signal transduction pathways, which modulate transcription of p21 by facilitating binding of different transcription factors to specific elements located within the p21 promoter. The proximal region between –122 and the start of transcription of the human p21 promoter contains multiple binding sites for members of the Sp1 family of transcription factors and plays

an important role in the p53-independent regulation of p21 transcription *(Gartel et al., 1999)*. Sp1 is a member of a multigene family of GC box-binding transcription factors that include Sp1, Sp2, Sp3 and Sp4, which share extensive structural and sequence homology, reviewed in Courey *et al* (1992). Three members of this family recognize the same DNA response motif, while Sp2 recognizes a distinct site. Whereas Sp1 is exclusively an activating transcription factor, Sp3 was shown to act as either a transcriptional activator or repressor in a manner dependent on the particular promoter and cell type *(Kennett et al., 1997)*. The Sp1 transcription factor is found in glycosylated and phosphorylated forms, but little is known about how these modifications affect function. Because Sp1 is constitutively expressed and Sp1 binding sites have been described in many promoters, it was long thought that its activity is necessary only for basal transcription *(Courey et al., 1992)*. However, the increasing number of studies demonstrating that Sp1-dependent transcription is regulated by activation of different signaling pathways, in response to a variety of signals, suggests that it may regulate expression by facilitating the interaction of other differentially expressed transcription factors.

To determine the mechanism, by which CT activates p21 expression and thus exerts its antiproliferative effect, detailed deletion and mutational analyses of the p21 promoter were performed. I would like to acknowledge Dr Evdokiou for his involvement in and supervision of the experiments presented in this chapter. The results show that transcriptional activation of p21 by CT is p53-independent and is mediated by a region of the promoter between –82 and –69, relative to the transcription start site. This sequence contains two binding sites for the transcription factor Sp1, which are required for transcriptional activation of the p21 gene. Further, the CTR-mediated transcriptional activation of p21 was shown to be receptor-isoform

specific in that the presence of a 16 amino acid insert in the first intracellular loop of hCTR abolished promoter activity in response to CT.

## 7.2 Results

### 7.2.1 Transcriptional activation of p21 by calcitonin

The induction of p21 mRNA by CT in HEK-293 cells stably transfected with the insert –ve hCTR (refer chapter 6) could be due to altered mRNA stability and/or increased transcription of the p21 gene. To determine whether CT stimulates transcription from the p21 promoter, a construct containing the wild type full-length p21 promoter cloned in front of a luciferase reporter gene pWWP-Luc plasmid (kindly provided by Dr B Vogelstein, John Hopkins Medical School) was transiently transfected (as described in section 2.2.19.2) into D11 and HR12 cells. Each set of transfected cells was split into equal aliquots that were treated with sCT or left untreated as controls. As shown in figure 7.1A, treatment with 10 nM sCT for 24 h resulted in a significant increase in luciferase activity (more than 5.0-fold in D11 cells and up to 6-fold in HR12 cells) when compared to untreated cells or untransfected parental HEK cells. In agreement with the p21 Northern blot data (figure 6.1B), there was no increase in luciferase activity in cells treated with [8-32]sCT. These results indicate that the up-regulation of p21 by CT in HEK-293 cells is due, at least in part, to transcriptional stimulation. In addition, these experiments demonstrated that transcriptional activation of the p21 promoter by CTR is independent of the receptor species, since p21 promoter activation was seen equally in both the rat (D11) and human (HR12) CTR-expressing cells. To determine if p21 transcriptional activation is receptor-isoform specific, the effect of CT on p21 promoter activity was compared in cells expressing either the insert -ve hCTR isoform or the insert +ve hCTR isoform.

**Figure 7.1 p21 promoter activity in D11 and HR12 cells treated with sCT.**

Parental HEK-293, D11 and HR12 cells (panel A) were plated at $1x10^5$ cells per well in six well plates. After 48 h, cells were transiently transfected with the WWP-Luc reporter plasmid containing the full-length p21 promoter and luciferase activity was analyzed 24 h after treatment with 10 nM sCT or [8-32]sCT. Untreated cells indicate basal activity. Relative luciferase activity is shown as raw light units (RLU) in cell lysates standardized to protein concentration. These results are representative of three independent experiments. These data represent the means ± S.D. *(bars)* of triplicate samples. Experiments using stably transfected cells produced similar results (not shown).

Parental HEK-293, HR12 and Hi12 cells were plated and transiently transfected with pWWP-Luc reporter plasmid, as described above. Luciferase activity was analysed 24 h after treatment with 10 nM sCT. Untreated cells indicate basal activity. Relative luciferase activity is shown as raw light units (RLU) in cell lysates standardized to protein concentration. These results are representative of three independent experiments. These data represent the means ± S.D. *(bars)* of triplicate samples.

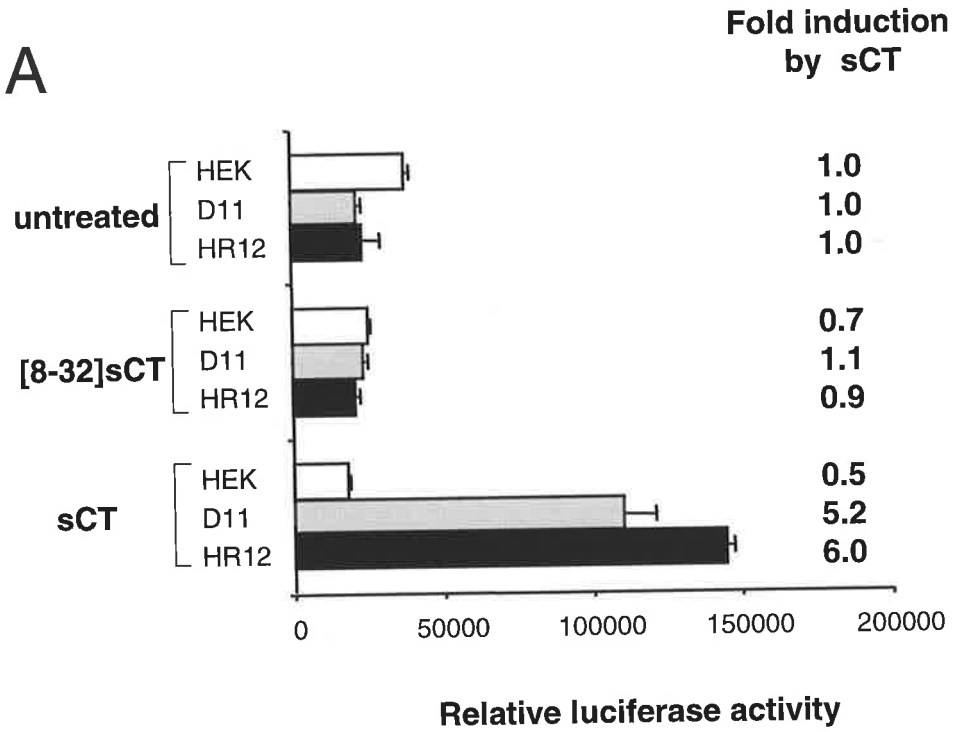
A
Fold induction by sCT
untreated
HEK
D11
HR12
1.0
1.0
1.0
[8-32]sCT
HEK
D11
HR12
0.7
1.1
0.9
sCT
HEK
D11
HR12
0.5
5.2
6.0
0
50000
100000
150000
200000
Relative luciferase activity

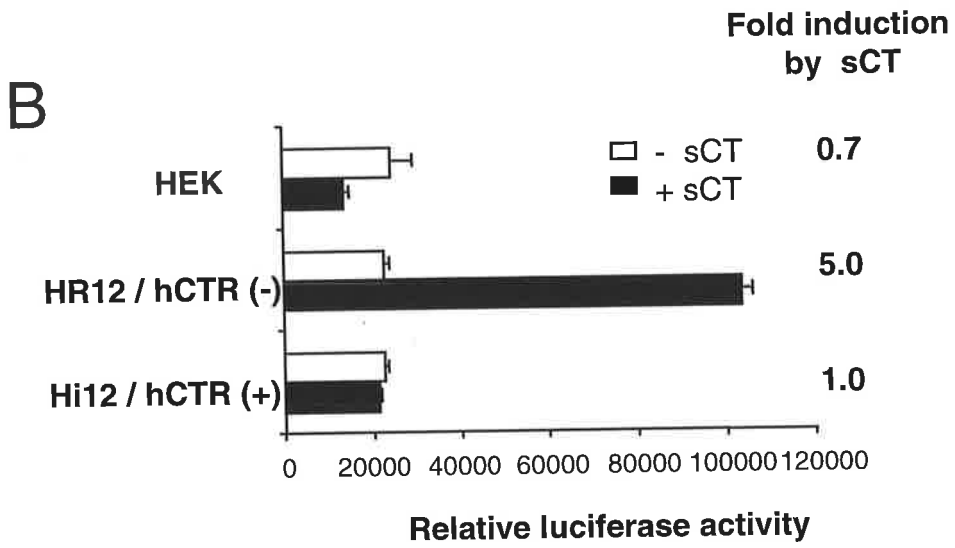
B
Fold induction by sCT
- sCT
+ sCT
HEK
0.7
HR12 / hCTR (-)
5.0
Hi12 / hCTR (+)
1.0
0
20000
40000
60000
80000
100000
120000
Relative luciferase activity

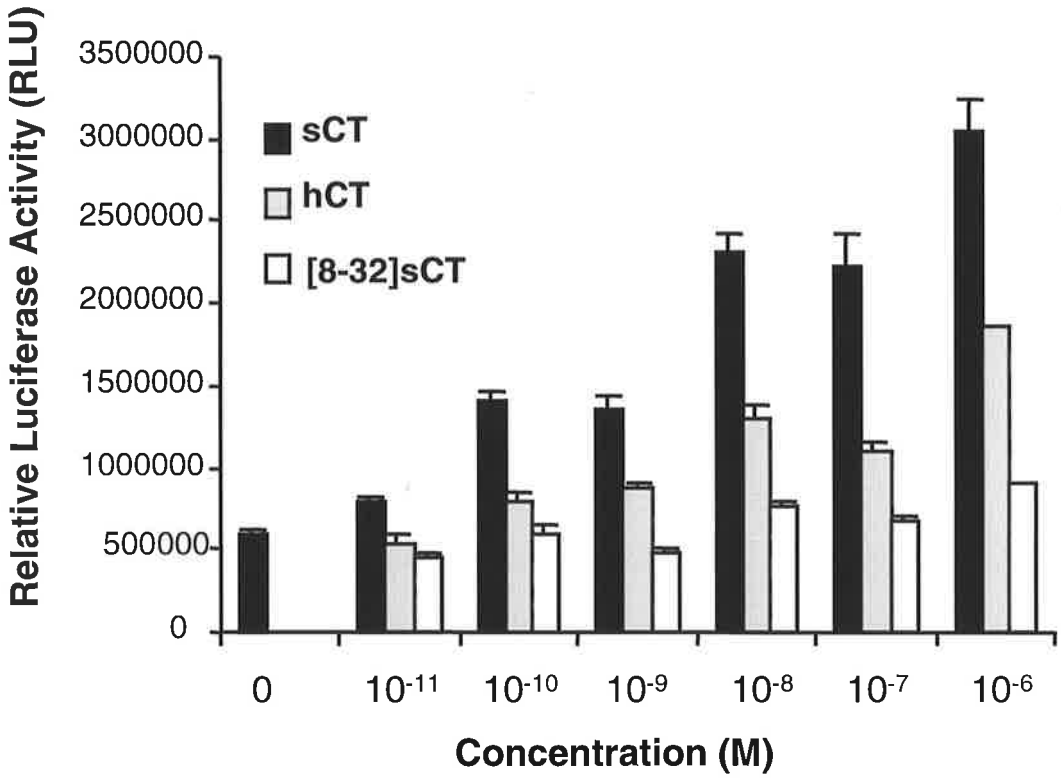


**Figure 7.2 Comparison of p21 promoter activity in HR12 cells treated with sCT, hCT and sCT[8-32].**

HR12 cells were plated at $2x10^4$ cells per well in 24 well plates. After 48 h, cells were transiently transfected with the WWP-Luc reporter plasmid containing the full length p21 promoter. Cells were treated for 24 h treatment with increasing concentrations of sCT, hCT or sCT[8-32] as indicated and cell lysates were then prepared for analysis of luciferase activity. Untreated cells were also used as a control for basal activity. Relative luciferase activity is shown as raw light units (RLU) in cell lysates standardized to protein concentration. These results are representative of 2 independent experiments. These data represent the means ± S.D. *(bars)* of triplicate samples. Experiments using stably transfected cells produced similar results (not shown).

As shown in figure 7.1B, CT-treatment consistently activated the p21 promoter by about 5 fold in HR12 cells, whereas CT treatment of Hi12 cells failed to cause activation of the p21 promoter.

The dose response relationship with respect to sCT or hCT treatment was determined in HR12 cells transiently transfected with the full-length p21 promoter construct, pWWP-Luc. As shown in Figure 7.2, the luciferase activity increased in a dose-dependent manner, up to 6-fold, by treatment with sCT when compared to untreated cells. The $EC_{50}$ for sCT was approximately $10^{-9}$ M. Similarly, treatment with hCT, also resulted in a dose-dependent increase in luciferase activity with a maximum stimulation 3-fold above basal at the highest concentration used. The $EC_{50}$ for hCT was also approximately $10^{-9}$ M. [8-32]sCT showed no effect on p21 promoter activity, even at high concentrations of peptide.

### 7.2.2 Deletion analysis of the p21 promoter

To determine the regions of the p21 promoter that respond to CT *via* CTR-mediated activation, we used a series of 5' deletion promoter constructs (figure 7.4) which were kindly provided by Dr Sakai Sowa, Kyoto Prefectural University of Medicine, Kyoto). The deletion series, which spanned the 2.4 kb full-length p21 promoter, were transiently transfected (as described in section 2.2.19.2) into HR12 cells and luciferase activities (as described in section 2.2.19.3) were measured 24 h following treatment with sCT. The full-length p21 promoter construct, pWWP-Luc, was activated 8.0 fold by sCT when compared to untreated cells (figure 7.3). The promoter for the p21 gene contains two p53-response elements in close proximity and induction of p21 has been shown to occur under p53-dependent conditions *(Wu et al., 1997; Li et al., 1994)*. However, induction in other situations appears not to require p53 *(Sheikh et al., 1994)*. The pWP124-Luc construct, which lacks the two p53 binding sites, was consistently activated by sCT up to 10-fold, a level slightly

**Figure 7.3 Deletion analysis of the p21 promoter.**

Full-length pWWP and deletion p21 promoter reporter constructs pW124, pWP101 and pWPdel-SmaI were transiently transfected into HR12 cells stably expressing the insert negative isoform of the human CTR. Luciferase activities were measured after 24 h treatment with 10 nM sCT. Fold induction shown on the right was calculated by comparing the luciferase activity of cells treated with sCT and untreated controls. In each experiment triplicate transfections were performed. These results are from a representative experiment. These data represent the means ± S.D. *(bars)* of triplicate samples All transfections included a cytomegalovirus/β-galactisidase plasmid; cell extracts were assayed for β-galactisidase activity to ensure equal transfection efficiency and luciferase activities were normalized to protein concentration and galactosidase activity as described in *Experimetnal materials and methods*. The constructs are shown schematically on the left highlighting the p53, Sp1 sites and TATA box.

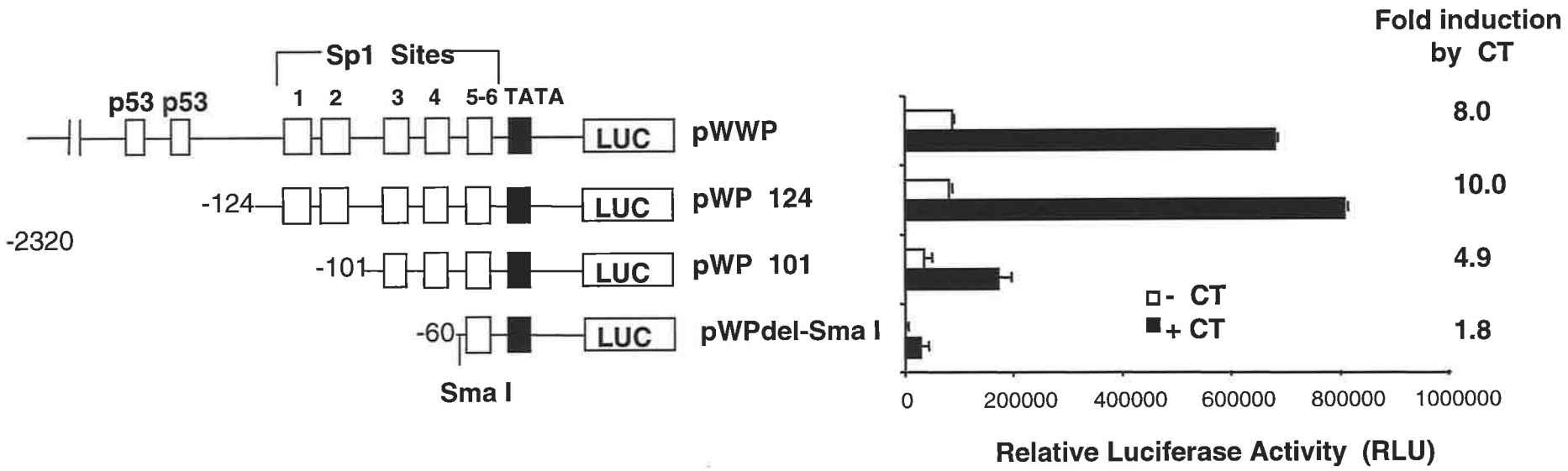
Sp1 Sites
p53 p53
1 2 3 4 5-6 TATA
LUC
pWWP
-124
pWP 124
-2320
-101
pWP 101
-60
pWPdel-Sma I
Sma I
Fold induction by CT
8.0
10.0
4.9
1.8
- CT
+ CT
0
200000
400000
600000
800000
1000000
Relative Luciferase Activity (RLU)

higher than the full length p21 promoter (pWWP), suggesting that activation of p21 promoter by CT is independent of p53 activity. This finding is consistent with the earlier observations, which showed that CT treatment of CTR-expressing cells in fact decreases the levels of p53 mRNA (chapter 6, figure 6.1). Similarly, the pWP101-Luc construct, which contains the promoter fragment 101-bp up-stream of the transcription initiation site, was also activated by CT up to 5-fold (figure 7.3). In contrast, the minimal promoter construct, pWPdel-SmaI, which contains a fragment spanning 60-bp from the transcription start site, was significantly less activated by CT (1.8-fold). Furthermore, the basal promoter activity of pWPdel-SmaI decreased to only 6.5% of pWWP, whereas that of pWP124 and pWP101 were comparable to that of the full length promoter construct (pWWP). These results suggest that the region from 101 bp to the transcription start site harbors a putative CT response element and defines the minimal region of the p21 promoter responsible for induction by CT.

### 7.2.3 Mutational analysis of the p21 promoter

The 101-bp fragment, which defines the minimal region of the p21 promoter for induction by CT, contains two independent and two overlapping consensus Sp1 binding sites *(Nakano et al., 1997)*. These are termed Sp1-3, Sp1-4 and Sp1-5-6 (figure 7.4). To define precisely the region of the p21 promoter necessary for induction by CT, and to determine whether these Sp1 binding sites are involved in activation, a series of constructs carrying mutations (developed and provided by Dr Sakai Sowa, Kyoto Prefectural University of Medicine, Kyoto) in each of the Sp1 consensus binding sites was used. In addition, a construct containing mutations in the TATA box was included. The mutant constructs are shown schematically in figure 7.5 and are identical to the wild type pWP101 except for the mutations indicated in lower case letters. The mutant constructs were transiently transfected (as described in section 2.2.19.2) into HR12 cells and CT-induced luciferase activity was measured

**Figure 7.4 Mutational analysis of the p21 promoter.**

Mutants pWP101-mt Sp1-3, pWP101-mt Sp1-4, pWP101-mt Sp1-5-6 and pWP101-mt TATA are identical to the wild type pWP101 with the exception of the sequences shown for each mutant construct. These constructs were transiently transfected into HR12 cells and sCT-induced luciferase activity was measured 24 hr later. Luciferase activity was normalized to protein concentration and β-galactisidase activity. Fold induction shown on the right was calculated by comparing the luciferase activity of cells treated with 10 nM sCT and untreated controls. In each experiment triplicate transfections were performed. These results are representative of three independent experiments. These data represent the means ± S.D. *(bars)* of triplicate samples

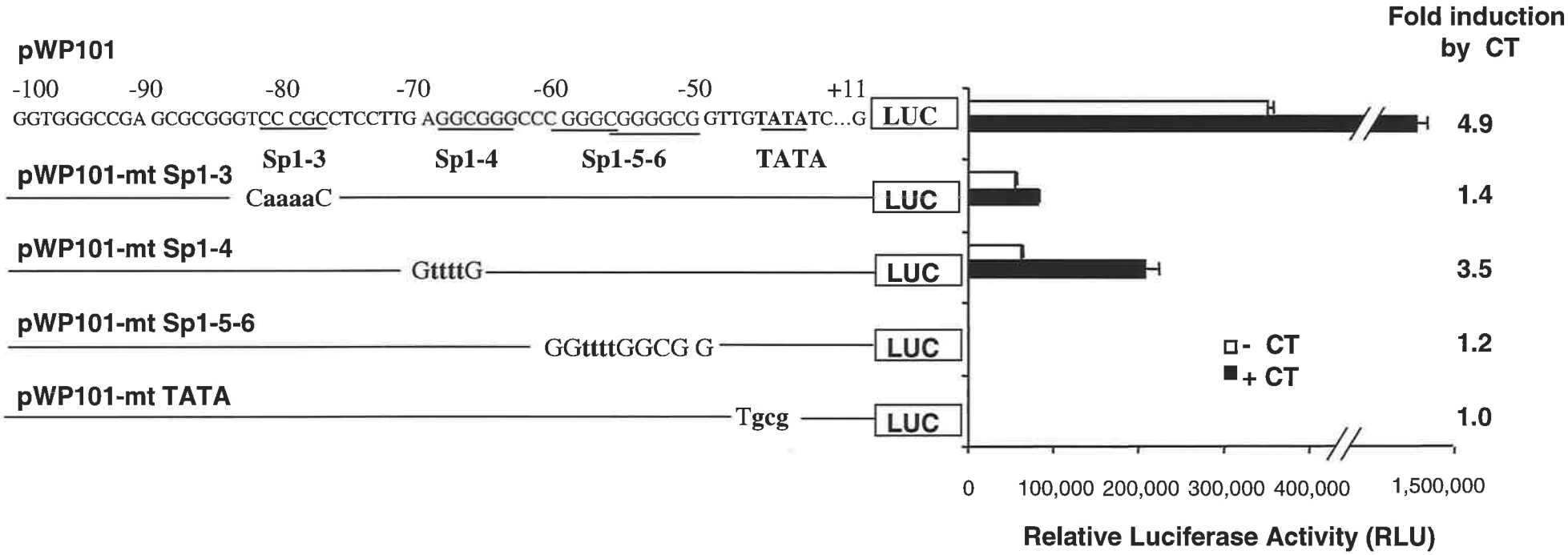
pWP101
-100 -90 -80 -70 -60 -50 +11
GGTGGGCCGA GCGCGGGTCC CGCCTCCTTG AGGCGGGCCC GGGCGGGGCG GTTGTATATC...G
Sp1-3
Sp1-4
Sp1-5-6
TATA
LUC
pWP101-mt Sp1-3
CaaaaC
pWP101-mt Sp1-4
GttttG
pWP101-mt Sp1-5-6
GGttttGGCG G
pWP101-mt TATA
Tgcg
Fold induction by CT
4.9
1.4
3.5
1.2
1.0
- CT
+ CT
0
100,000
200,000
300,000
400,000
1,500,000
Relative Luciferase Activity (RLU)

(as described in section 2.2.19.3) 24 h after CT treatment. All mutant constructs had decreased basal activity in the absence of CT when compared to the wild type pWP101 construct. In addition only one of these Sp1 mutant constructs, pWP101-mt-Sp1-4, retained the ability to be activated by CT in a manner similar to that of the wild type pWP101. pWP101-mt-Sp1-3, pWP101-mt-5-6 and pWP101-mt-TATA had completely lost the ability to be activated by CT. These results suggest that the sequence of the p21 promoter between –77 and –82 relative to the transcription start site, and which comprises the Sp1-3 binding site, is required for activation by CT. However, the two overlapping Sp1 binding sites (pWP101-mt-Sp1-5-6) between –60 and –51 and TATA box may also be required for induction by CT, because mutation of these completely abolished sCT-induced luciferase activity. Furthermore, the effect of mutation in the two overlapping Sp1 consensus sites and the TATA box resulted in complete loss of activity even in the absence of CT, suggesting that transcription factor(s) binding to these sites are important in both CT-mediated transcription and basal activity of the p21 promoter.

### 7.2.4 CT regulates transcription of the p21 promoter through Sp1

The above results suggest that Sp1 transcription factors are important in the activation of the p21 promoter in response to CT. To confirm that Sp1 elements are indeed activated by CT, a wild-type reporter plasmid, pGL2-Sp1-luc, which contains only three consensus Sp1 binding sites derived from the SV40 promoter and no TATA box (kindly provided by Dr Peggy J Farnham, McArdle Laboratory for Cancer Research, University of Wisconsin, Madison) was used. A reporter construct, pGL2-mt-Sp1-luc that contains mutations in these Sp1 sites (developed and provided by Dr Sakai Sowa, Kyoto Prefectural University of Medicine, Kyoto), and a vacant vector pGL2-Basic lacking Sp1 sites, were used as controls. When transiently transfected (as described in section 2.2.19.2) into HR12 cells, the wild-type construct was

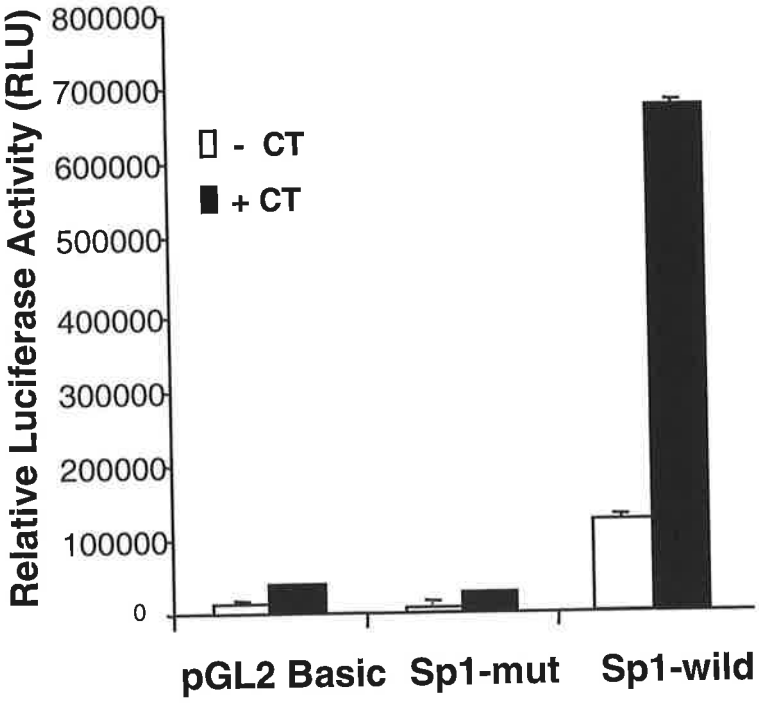


**Figure 7.5 Transcription of a reporter plasmid containing three Sp1 binding sites and no TATA box is induced by sCT in HR12 cells.**

HR12 cells were transiently transfected with either the Sp1-luc reporter plasmid, mt-Sp1-luc or control reporter plasmid pGL2-Basic. Luciferase activities were calculated by comparing the luciferase activity of cells treated with 10 nM sCT and untreated controls 24 hr after treatment. Luciferase activity was normalized to protein concentration. These results are representative of two independent experiments. These data represent the means ± S.D. *(bars).*

significantly activated by CT about 6-fold, whereas, neither the vacant vector nor the Sp1 mutant construct, were activated by CT above background levels. In fact, the latter two constructs demonstrated near complete loss of promoter activity in the presence or absence of CT (figure 7.5). These results strongly suggest that Sp1 plays important roles in both the basal transcriptional and CT-induced activity of the p21 promoter.

### 7.2.5 CT co-operates synergistically with butyrate to activate p21 transcription.

The results thus far clearly demonstrate that Sp1-3 is critical for the CT-induced promoter activity, whereas Sp1-5 and Sp1-6 are required for basal activity. Similarly, this GC-rich region has also been shown previously to be required during p53-independent induction of p21 by a number of other agents. Recently, Nakano *et al* (1997) demonstrated that the same region containing Sp1-3 is also critical for butyrate-mediated activation of p21 promoter in colorectal cancer cells. To determine whether butyrate also activates transcription of p21 *via* the same mechanism, HR12 cells were transiently transfected with each of the p21 promoter constructs and luciferase activity was measured 24 h after treatment with 4 mM butyrate. Figure 7.6A shows that in HR12 cells, butyrate activated the p21 promoter in a manner similar to CT. In fact, when compared to the CT-induced pattern of promoter activation (figure 7.3 and 7.4), butyrate displayed an identical pattern across all promoter constructs. These findings suggest that CT and butyrate may work through common signaling pathways that converge onto the same Sp1-3 binding site to activate transcription of p21. To determine if both agents work through the same or alternate signaling pathways to induce p21 transcription, HR12 cells were transfected (as described in section 2.2.19.2) with the full-length p21 construct and luciferase activity was compared following treatment with either CT or butyrate alone or in

**Figure 7.6 Combination of CT and butyrate results in co-operative transcriptional activation of the p21 promoter.**

HR12 cells were transiently transfected with each of the luciferase p21 constructs as indicated (panel A) and luciferase activity was measured 24 hr after treatment with 4.0 mM sodium butyrate. Luciferase activity was normalized to protein. Fold induction shown on the right was calculated by comparing the luciferase activity of cells treated with 4 mM butyrate and untreated controls. These data represent the means ± S.D. *(bars)*.

HR12 cells (panel B) were transiently transfected with the full length p21 promoter construct pWWP-luc. Following transfection, cells were treated with either 10 nM sCT, 4 mM sodium butyrate or a combination of both and luciferase activity measured 24 hr after treatments. Luciferase activity was normalized to protein concentration and β-galactosidase activity. Fold induction shown on the right was calculated by comparing the luciferase activity of treated cells and untreated controls. In each experiment triplicate transfections were performed. These results are representative of at least three independent experiments. These data represent the means ± S.D. *(bars)* of triplicate samples.

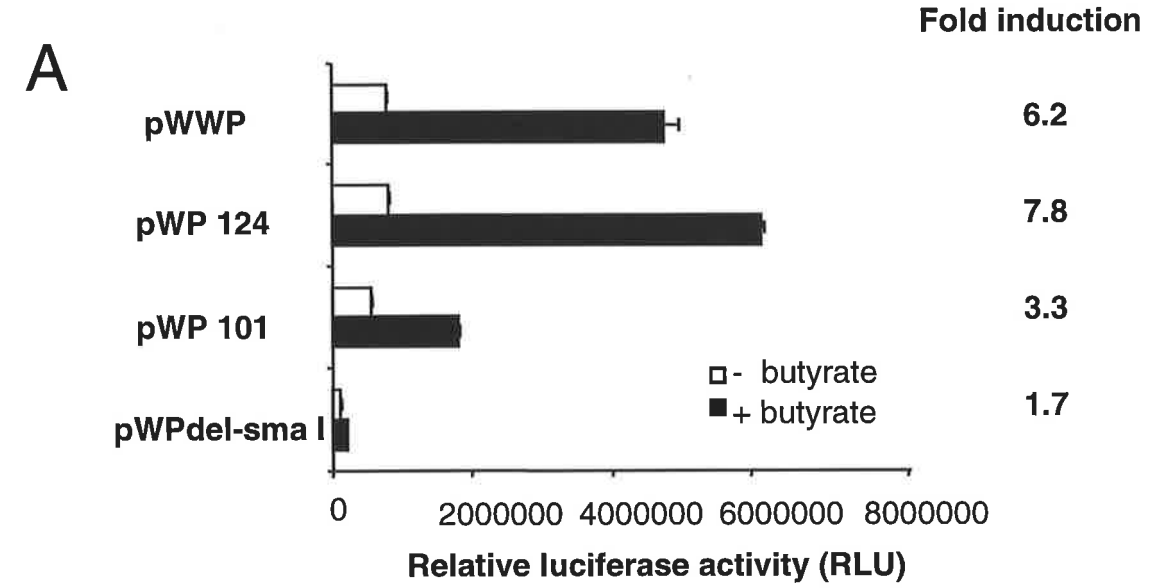
A
Fold induction
pWWP
pWP 124
pWP 101
pWPdel-sma I
6.2
7.8
3.3
1.7
- butyrate
+ butyrate
0
2000000
4000000
6000000
8000000
Relative luciferase activity (RLU)

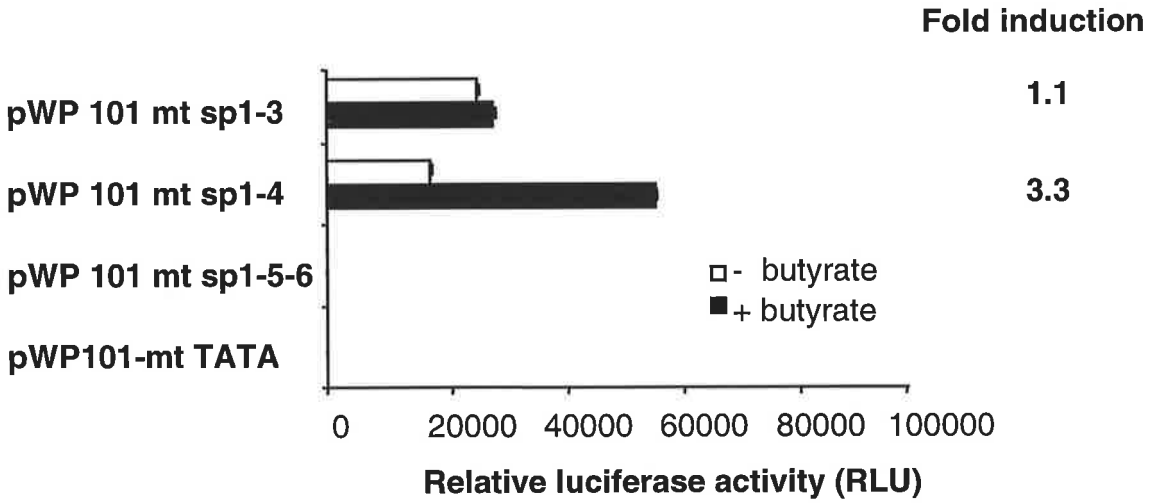
Fold induction
pWP 101 mt sp1-3
pWP 101 mt sp1-4
pWP 101 mt sp1-5-6
pWP101-mt TATA
1.1
3.3
- butyrate
+ butyrate
0
20000
40000
60000
80000
100000
Relative luciferase activity (RLU)

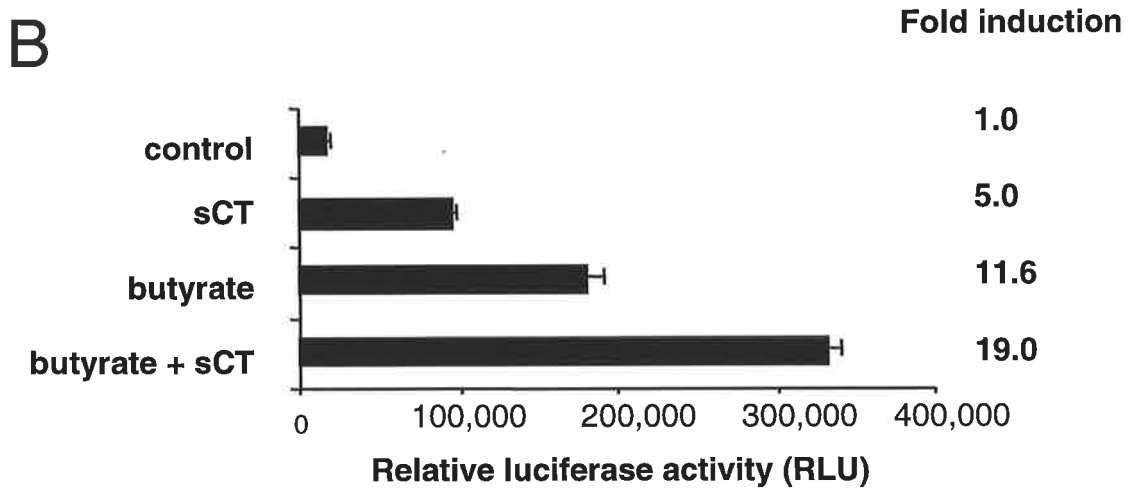
B
Fold induction
control
sCT
butyrate
butyrate + sCT
1.0
5.0
11.6
19.0
0
100,000
200,000
300,000
400,000
Relative luciferase activity (RLU)

combination. The rationale for this was that if each agent alone maximally activates the same pathway, then additional activation by the combined treatment through this mechanism would be impossible. Alternatively, if each agent activates separate signaling pathways, then the combined treatment of CT and butyrate should result in a synergistic effect on p21 promoter induction. Figure 7.6B shows that while CT and butyrate when used individually were able to activate the p21 promoter (5 fold for CT and 11 fold for butyrate), a combination of CT and butyrate consistently resulted in a more than additive response of up to 20 fold. These findings suggest that the synergistic activity may result from the differential expression and interplay of additional transcription factors mediated by alternate signaling mechanisms that converge onto the same Sp1 binding site to increase p21 transcription.

## 7.3 Discussion

To determine the mechanisms by which induction of p21 mRNA expression occurs during CT-treatment in CTR expressing cells, a detailed functional analysis of the p21 promoter was performed. Through deletion analysis it was shown that induction of p21 by CT occurs *via* a p53-independent mechanism since deletion of the two p53 response elements upstream of the promoter did not influence promoter activity. It was also shown that the minimal region of the p21 promoter required for its induction maps to a stretch of 77 bp relative to the transcriptional start site. This GC-rich region harbors two independent (Sp-1-3, Sp1-4) and two overlapping (Sp1-5-6) binding sites for the transcription factor Sp1, as well as a TATA box. By mutation analysis of each of these Sp1 sites, a major CT-responsive element was identified, defined by one of the four Sp1 binding sites (Sp1-3) present in this region. In addition, the finding that CT is capable of activating transcription from a wild-type

reporter plasmid, which contains only three consensus Sp1 binding sites derived from the SV40 promoter and no TATA box, provides further evidence that Sp1 or Sp1 related proteins are involved in the transcriptional activation of the p21 promoter in response to CT.

The same region comprising Sp1-3 was previously shown to be critical for p21 induction by a number of other agents including, transforming growth factor β (TGF-β calcium, NGF, the histone deacetylase inhibitors, trichostatin A and butyrate *(Datto et al., 1995; Prowse et al., 1997; Nakano et al., 1997; Sowa et al., 1997)*. Taken together, these findings suggest that regulation of Sp-1-related factors could be part of a common mechanism to induce expression of p21. However, since each of these agents activate distinct signal transduction pathways, it is likely that several differentially expressed transcription factors, including activators and co-activators, may converge onto the same Sp1-3 binding site to regulate p21 transcription. The interplay of such factors and the way in which they interact with the general transcriptional machinery is likely to be important in determining the degree of activation. The observation that CT cooperates synergistically with butyrate to increase p21 promoter activity further supports this notion.

The mechanisms by which Sp1 or Sp1-related transcription factors mediate p21 induction are largely unknown. Regulation of Sp1-dependent transcription was shown previously to be affected by phosphorylation and glycosylation events. Phosphorylation has been shown to influence DNA binding and transactivation activities *(Black et al., 1999)*, whereas glycosylation confers resistance to proteosome-dependent degradation by increasing the stability of the Sp1 protein *(Han et al., 1997)*. In addition, Sp1 was shown to associate directly with members of the general transcriptional machinery such as TFIID and the co-integrator CBP/p300

*(Gill et al., 1994; Owen et al., 1998).* Furthermore, Sp1 physically interacts and functionally cooperates with several other transcription factors including NF-kB, GATA, YY1, E2F1, SREBP-1 pRb, Smad proteins *(Lee et al., 1993; Udvadia et al., 1995; Lin et al., 1996; Hirano et al., 1998; Kardassis et al., 1999)* and more recently c-jun *(Moustakas et al., 1998).* Therefore, Sp1-regulated p21 gene transcription by multiple signaling pathways appears to be mediated by the interaction of several differentially expressed factors.

The human CTR is primarily expressed as two functionally different isoforms, comprising an insert-negative form and a form that contains 16 additional amino acids inserted in the first intracellular loop *(Kuestner et al., 1994; Gorn et al., 1992).* Unlike the insert-negative form, which was shown to mediate transcriptional activation of p21 in response to CT, the insert-positive form did not. This finding is consistent with earlier observations (chapter 4) showing that CT induces growth inhibition, specifically in cells expressing the insert negative isoform of the hCTR, whereas cells expressing the insert positive isoform are essentially resistant to the antiproliferative effects of CT (Chapter 4). This is despite the fact that both cell lines display similar binding characteristics for CT (Chapter 3).

In summary, the results support the conclusion that CT induces p21 transcription *via* a p53 independent mechanism, mediated through specific activation of Sp1 binding sites in the promoter of the p21 gene. The main CT-response element is defined by the Sp1-3 site in the p21 promoter and this sequence is essential for the CT-mediated p21 transcription. Further, the CTR-mediated activation of p21 promoter is receptor-isoform specific and the presence of the 16 amino acid insert in the first intracellular loop of the hCTR, which comprises the insert positive isoform, was without effect on p21 promoter. There is currently no information on the manner by which CT affects gene transcription, and no identification of the promoter elements

involved. Therefore, this is the first demonstration that CT induces gene transcription through the constitutively expressed transcription factor Sp1 and suggests that other Sp1 responsive genes might be similarly regulated by CT. These findings, together with the potent antiproliferative function of CT mediated by induction of the cyclin dependent kinase inhibitor, p21, defines a novel signaling pathway for CT.

# Chapter 8

# Investigation of the intracellular signalling pathways involved in the inhibition of cell growth by CT

## 8.1 Introduction

The CTR activates heterotrimeric G-proteins, specifically the $\alpha_s$, $\alpha_i$ and $\alpha_q$, subunits and their subsequent second messenger systems, as discussed in section 1.2.6.2. Both the cAMP and calcium intracellular signalling pathways have been implicated in CT-mediated cell growth. CT activation of the type II cAMP dependent PKA isoenzyme was shown to be associated with growth inhibition of the T47D human breast cancer cell line *(Ng et al., 1983)*. Both intracellular cAMP and free calcium are increased by CT treatment of prostate cancer cells, in association with the CT-mediated growth of prostate cell lines *(Shah et al., 1994)*. It has been shown that the CTR can activate additional intracellular signalling pathways, including phospholipase D *(Naro et al., 1998)* and tyrosine kinases *(Zhang et al., 1999)*. In particular, activation of the rabbit CTR transfected into HEK-293 cells caused a rapid, but transient activation of the MAPK pathway, by mechanisms involving Gi and pertussis toxin-insensitive PKC activation *(Chen et al., 1998)*. However CT activation of the Erk1/2 MAPK pathway has not been associated with any cellular function, including regulation of cell growth.

Activation of the Erk1/2 MAPK signalling pathway is centrally involved in cell growth regulation *(Gutkind 1998)*. Initially, activation of the MAPK pathways was shown to be a function of the membrane bound tyrosine kinase receptors (refer to section 1.3.3). However the CTR and other GPCRs are now recognised as activators of MAPK pathways, through a number of G-protein-mediated mechanisms (refer section 1.3.3.2). These findings, together with the paradoxical reports that activation of the Erk1/2 MAPK pathway can lead to either cell proliferation *(Mansour et al., 1994)* or growth suppression *(Pumiglia et al., 1997)*, have identified the potential

importance of the Erk1/2 MAPK pathway in mediating the suppression of growth by CT.

The aim of the experiments in this chapter was to develop an understanding of the intracellular signalling pathways involved in the CT-induced inhibition of growth, and specifically the involvement of the Erk1/2 MAPK pathway in CTR-mediated growth suppression. HEK-293 cells transfected with the insert –ve hCTR, were treated with chemical activators and inhibitors of specific signalling molecules. Chemical inhibitors of Erk1/2 activation abrogated both the CT-induced induction of $p21^{WAF1/CIP1}$ and cell growth suppression, suggesting that the Erk1/2 MAPK pathway has an integral role in the CT-regulation of cell growth in HEK-293 cells.

## 8.2 Results

### 8.2.1 Involvement of the adenylate cyclase and cAMP signalling pathway in the CT-growth cascade

The CTR activates the cAMP signalling pathway in many cellular systems, including the current transfected system (refer chapter 3 figure 3.7), and has been implicated in the CT-inhibition of growth in T47D cells *(Ng et al., 1983)*. To investigate the involvement of the $\alpha_s$ G-protein signalling pathways in the CT-induced inhibition of cell growth, cells expressing the insert –ve hCTR (HR12) were treated with specific activators or inhibitors of these pathways in an attempt to mimic or reverse the inhibition of growth. sCT treatment of HR12 cells significantly reduced cell proliferation [$p<0.001$ (figure 8.1C)], however treatment of HR12 cells with the synthetic cAMP analogue 8-Br cAMP (figure 8.1A) did not alter the growth of the HR12 cells (figure 8.1C). The adenylate cyclase activator, forskolin (figure 8.1A) was also used. Although forskolin did slow cell growth significantly $p<0.001$, the

**Figure 8.1 Involvement of the adenylate cyclase and cAMP signalling pathway in the CT-growth inhibition in HEK-293 cells.**

A. Schematic diagram of the CT-induced regulation of the adenylate cyclase/cAMP pathway, and the chemical activators and inhibitors used. Forskolin activates adenylate cyclase and 8-Br cAMP mimics cAMP to activate PKA without ligand activation. H-89 is a chemical inhibitor that blocks activation of PKA.

B. HEK-293 cells transfected with the insert –ve hCTR (HR12 cell) were plated at $3x10^4$ cells/well in 12 well plates, and allowed to adhere. 4 days following plating the cells remained untreated or were treated with 10 nM sCT, 10 mM 8-Br cAMP, 200 μM Forskolin, 10 μM H89, 10 μM H89 and 10 nM sCT, 1 ng/ml PTX or 1 ng/ml PTX and 10 nM sCT. 72 h after treatment cells were harvested and counted. Data points represent mean ± SEM of triplicate determinations and are representative of 3 separate experiments. ✱ indicates significantly different from control [$p<0.001$], and # indicates significantly different from all other treatments [$p<0.001$].

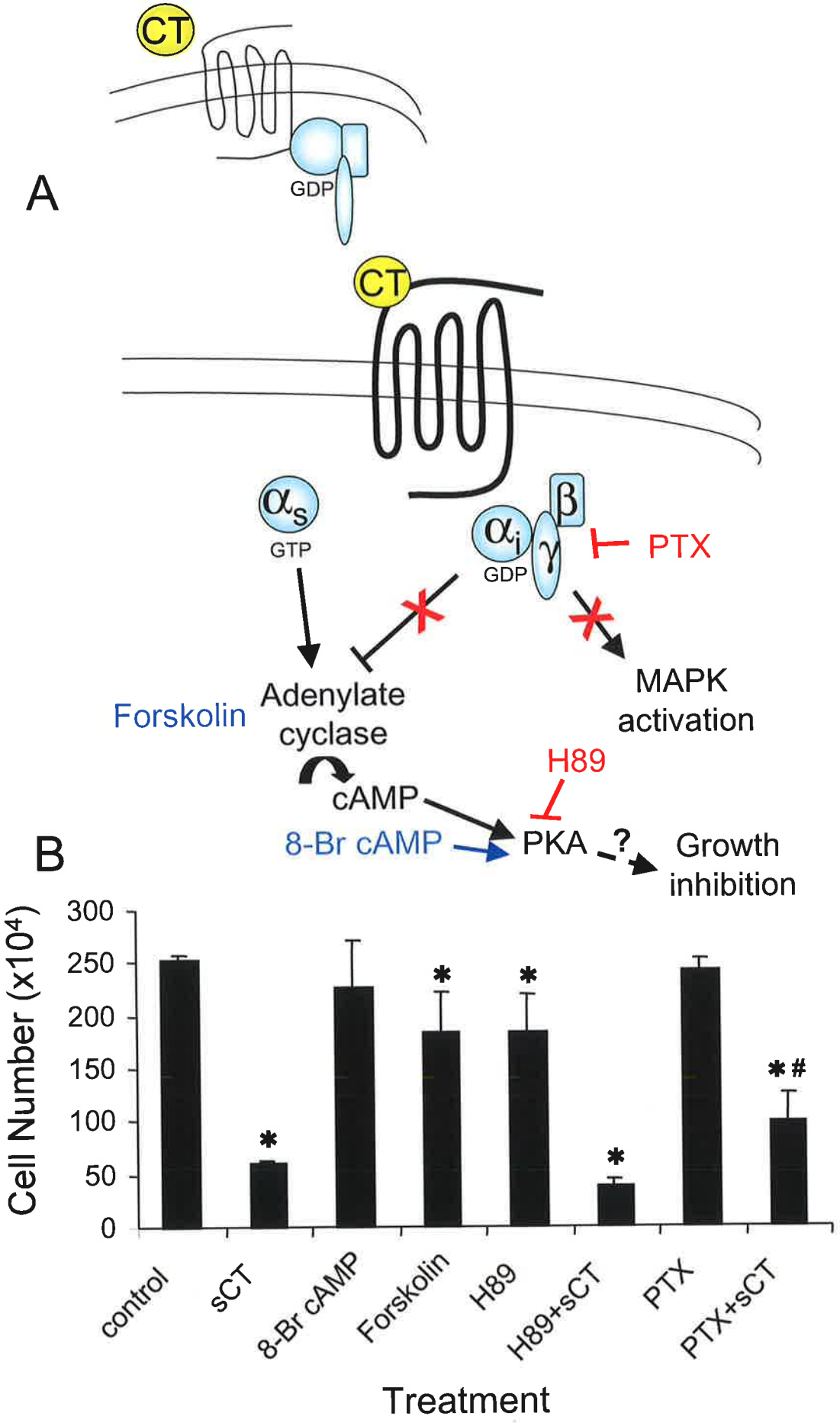
A
CT
GDP
CT
$\alpha_s$
GTP
$\alpha_i$
GDP
$\beta$
$\gamma$
PTX
Forskolin
Adenylate cyclase
MAPK activation
H89
cAMP
8-Br cAMP
PKA
?
Growth inhibition
B
Cell Number (x10⁴)
300
250
200
150
100
50
0
control
sCT
8-Br cAMP
Forskolin
H89
H89+sCT
PTX
PTX+sCT
Treatment

C. Following treatment, and prior to the trypsinisation process described in B, cells were photographed as described in the *Experimental materials and methods*, to record cell morphology. The cell treatment is recorded above each photograph. This is a view of the cells when viewed using a 20x objective and 10x binoculars.

C

Control

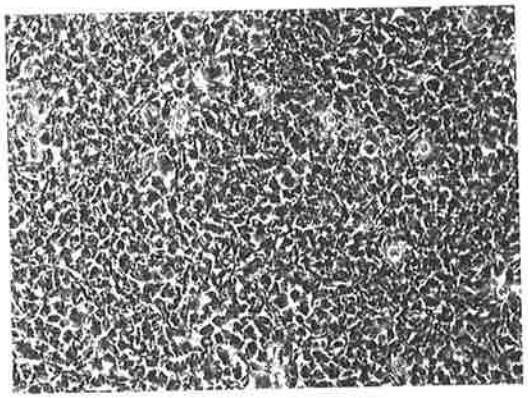

sCT

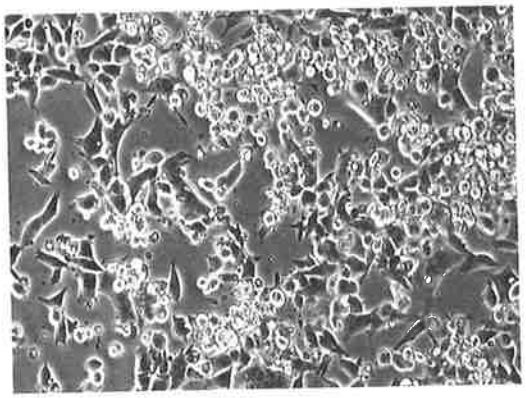

8-Br cAMP

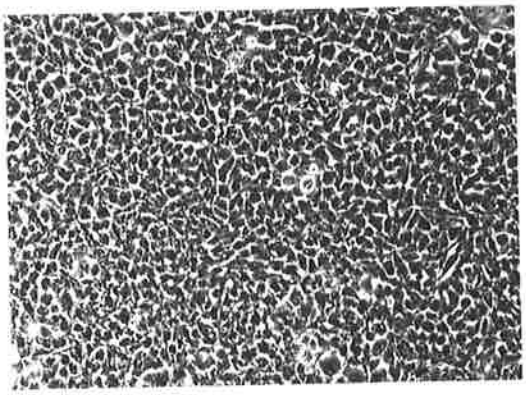

Forskolin

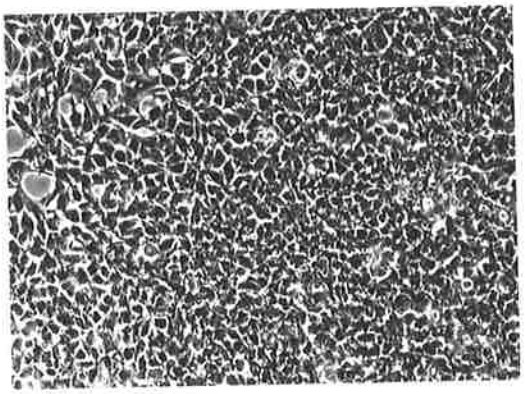

H89

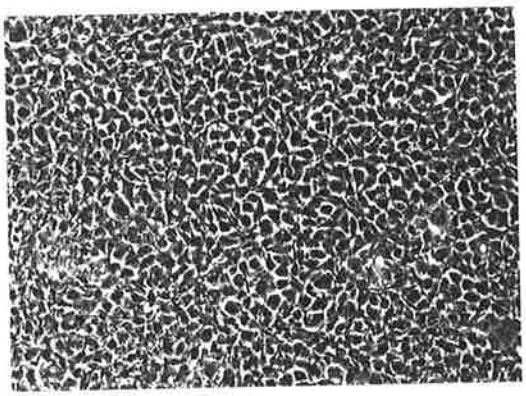

H89 + sCT

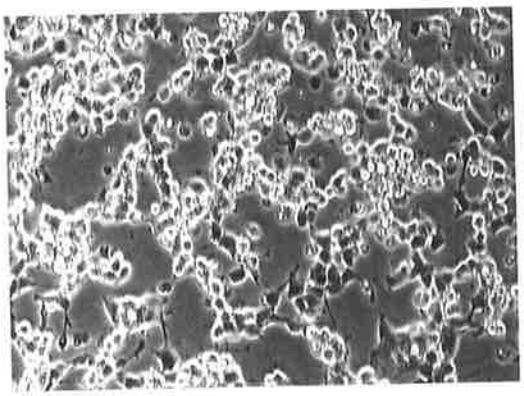

PTX

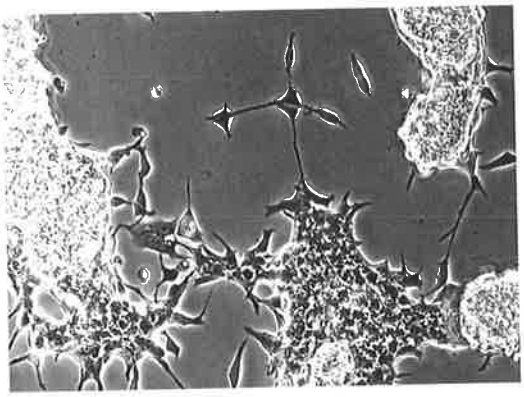

PTX + sCT

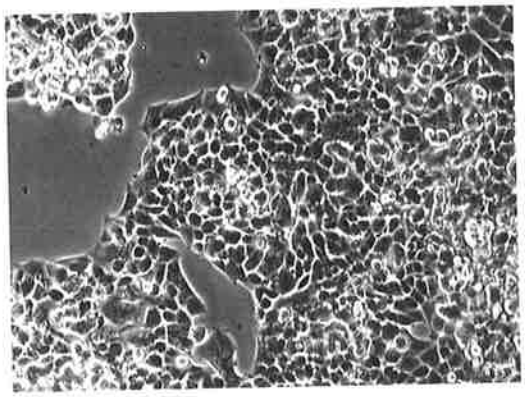

magnitude of this effect was much less than that of CT (Figure 8.3B). Neither 8-Br cAMP nor forskolin induced the changes in cell morphology seen with CT-treatment (figure 8.3C). To confirm that the $G\alpha_s$ signalling pathways were not involved in the CT-induced growth changes, CT treatment was applied in the presence or absence of a chemical inhibitor of PKA, H89 (Figure 3.1A). Treatment of HR12 cells with the PKA inhibitor H89 alone did significantly reduce the growth of HR12 cells [$p<0.001$ (figure 8.1B)], and in conjunction with exposure to 10 nM sCT the growth inhibition was significantly greater [$p<0.001$ (figure 8.1B)] than when cells were treated with sCT alone. However when the slight growth retarding influence of H89 was accounted for, the cumulative effect of H89 and sCT was comparable to that of sCT alone, sCT reducing cell growth by 77% when used alone and by 79% when used in combination with H89. Thus, disruption of the $\alpha_s$ G-protein signalling pathway did not alter the growth regulating action of CT, indicating that the signalling cascade by which sCT regulates growth is independent of the cAMP and PKA pathway.

CT also activates the $\alpha_i$ G-protein and is able consequently to inhibit activation of adenylate cyclase (figure 8.1A). PTX is a potent and specific inhibitor of the $\alpha_i\beta\gamma$ complex, preventing dissociation of the trimer and the subsequent activation of $\alpha_i$ subunit. Treatment of HEK-293 cells expressing the insert -ve hCTR with PTX alone, had no effect on the growth of HR12 cells (figure 8.1B), indicating this pathway is not involved in normal proliferation of these cells. However, co-treatment of the cells with sCT and PTX significantly prevented the CT-induced inhibition of cell growth [$p<0.001$ (figure 8.1B)]. This finding implies that either $\alpha_i$ or $\beta\gamma$ subunits of this G-protein complex are involved in the CT growth cascade. Although, treatment of HR12 cells with PTX alone did not alter the growth of the cells, the chemical inhibitor dramatically altered the morphology of the cells (figure 8.1C). PTX treatment

stopped the cells growing in a monolayer and induced them to grow in cellular colonies (figure 8.1C). The joint treatment of HR12 cells with the PTX and sCT almost completely reversed this clonal cellular growth, with the cells growing once again in a monolayer and appearing much flatter in morphology (figure 8.1C). These morphological changes complicate interpretation of the growth effects of PTX, as discussed below.

### 8.2.2 Involvement of the PLC signalling transduction pathway in the CT growth cascade

CT mediates cellular actions through the PLC signalling pathway (as discussed in section 1.2.7.2.2). Chemical inhibitors of the $\alpha_q$ G-protein signalling pathway were used (described in section 2.2.11.4) to investigate the relationship of this pathway to the growth inhibitory actions of CT. As expected, treatment of HR12 cells with sCT, significantly decreased cell growth [$p<0.001$ (figure 8.2B)] and induced the characteristic rounding up and semi-detachment of cells from the monolayer (figure 8.2D). Treatment of HR12 cells with the specific PLC inhibitor, U73122 alone (figure 8.2A), also significantly decreased the growth of these cells compared to control [$p<0.001$ (figure 8.2B)]. The PLC inhibitor did not alter the morphology of the HR12 cells (figure 8.2D), despite the slight but significant reduction in cell growth. Importantly, the PLC inhibitor was unable to reverse the inhibitory growth actions of sCT (figure 8.2B). Activation of PLC initiates signalling through the PKC and calcium second messenger pathways (figure 8.2C). The PLC inhibitor U73122 did not abrogate the CT induced growth response, consequently the PKC signalling pathway was not expected in be involved in this growth response. A chemical inhibitor of PKC, chelerythrine chloride (CC) was used to confirm this hypothesis. As expected, treatment of HR12 cells with sCT alone reduced the

**Figure 8.2 Involvement of the PLC signalling transduction pathway in the inhibition of cell growth by CT.**

A. A schematic representation of the $G_q$ proteins involved in the CT activation of the PLC pathway, and the two compounds used to explore the involvement of this pathway in the CT-mediated growth response. U73122 is a specific inhibitor of PLC and Chelerythrine chloride is a specific and potent inhibitor of PKC.

B. HR12 cells were plated at 2 $X10^4$ cells/well in 12 well plates and allowed to adhere. 4 days following plating, cells remained untreated or were treated with 10 nM sCT, 10 μM U73122, 10 μM U73122 and 10 nM sCT. 72 h cells were harvested and counted. Data points are representative of mean ± SEM of triplicate determinations and are representative of 3 separate experiments. ✱ indicates significant difference from control [$p<0.001$].

C. HR12 cells were plated at $3x10^4$ cells/well in 12 well plates and allowed to adhere. 3 days after plating the cells remained untreated or were treated with 10 nM sCT, 1 μM Chelerythrine chloride (CC) or 10 nM sCT and 1 μM CC. 72 h after treatment cells were harvested and counted. Data points represent the mean ± SEM of triplicate determinations and are representative of 3 separate experiments. ✱ indicates significant difference from control ($p<0.001$).

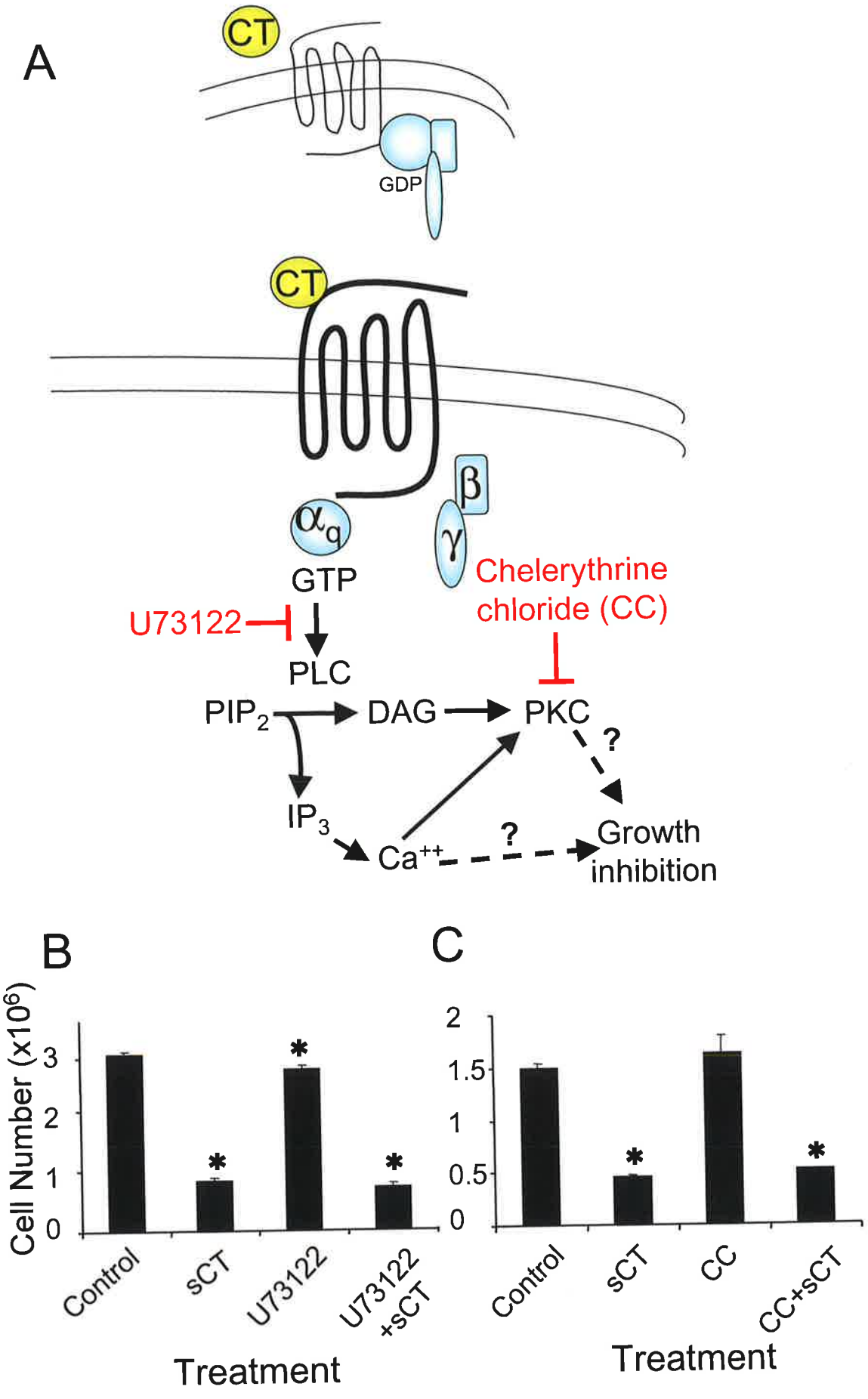
A
CT
GDP
CT
$\alpha_q$
β
γ
GTP
U73122
Chelerythrine
chloride (CC)
PLC
$PIP_2$
DAG
PKC
?
$IP_3$
$Ca^{++}$
?
Growth
inhibition
B
Cell Number (x$10^6$)
3
2
1
0
Control
sCT
U73122
U73122
+sCT
Treatment
C
2
1.5
1
0.5
0
Control
sCT
CC
CC+sCT
Treatment

D. Following treatment, and prior to the trypsinisation process described in B, cells were photographed as described in the *Experimental materials and methods*, to record cell morphology. The cell treatment is recorded above each photograph. This is a view of the cells when viewed using a 20x objective and 10x binoculars.

D

Control

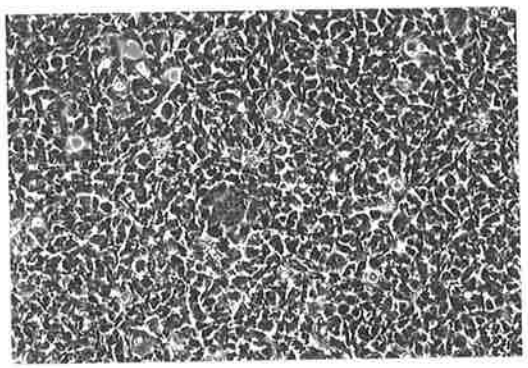

sCT

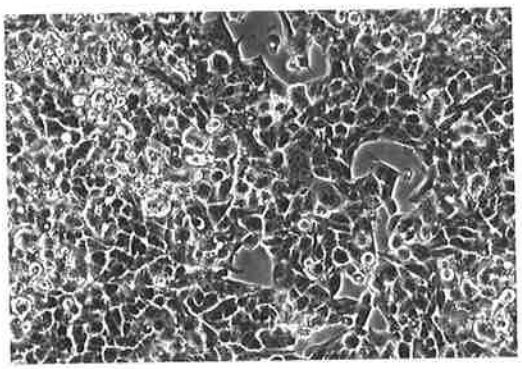

U73122

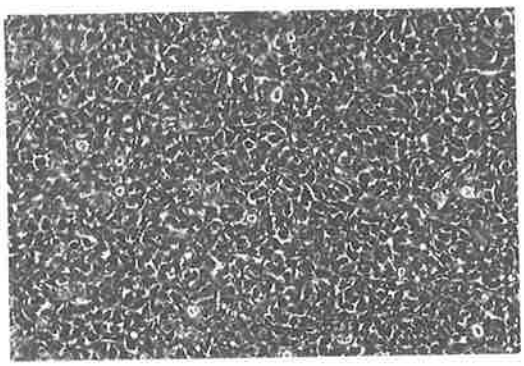

U73122 + sCT

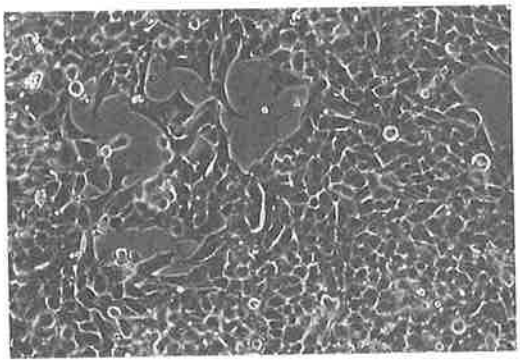

Control

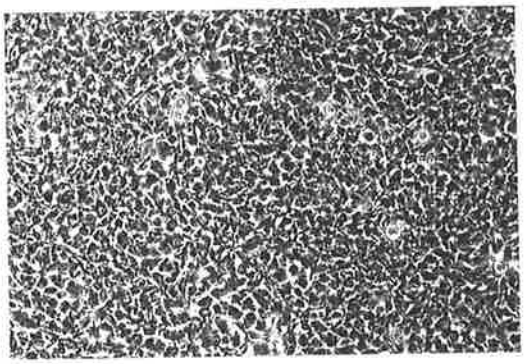

sCT

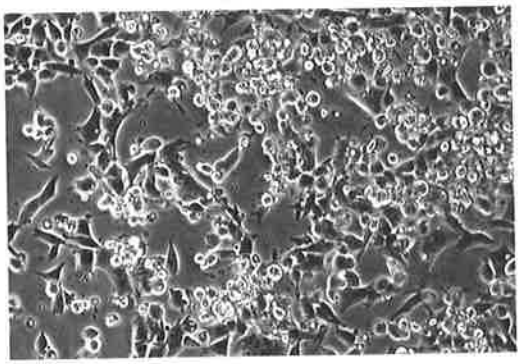

CC

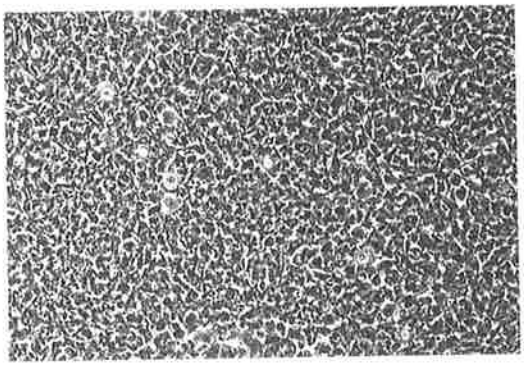

CC + sCT

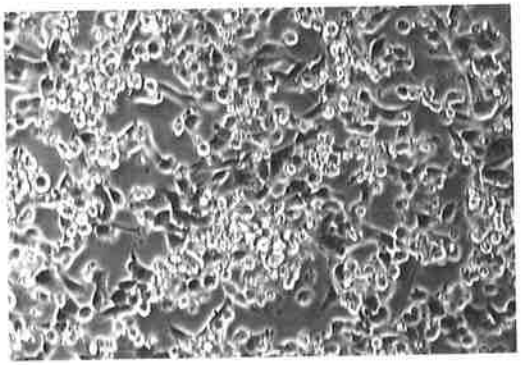

growth of the cells by approximatly 60 % (figure 8.2C) and altered the cell morphology (figure 8.2C). Treatment of HR12 cells with CC alone, had no effect on the growth of the cells, indicating that the inhibitor, at the concentration used was not toxic to the cells (figure 8.2C). The PKC inhibitor CC was unable to abrogate the growth inhibition (figure 8.2B) induced by sCT, confirming that the PKC pathway was not transducing the CT growth signal.

### 8.2.3 Involvement of other growth-regulating pathways in the CT growth cascade

The actin cytoskeleton is essential to the process of cell division *(Hall 1998)* and thus extracellular agents target actin in order to regulate cell growth *(Moustakas et al., 1999)*. Other intracellular signalling pathways are also able to regulate cell growth, for example, the calcium calmodulin pathway *(Sewing et al., 1997; Woods et al., 1997)* and the PI-3 kinase pathway *(Cross et al., 1997; Yuan et al., 2000 May; Ballou et al., 2000 ; Sato et al., 1996)*. Consequently, calcium calmodulin, PI-3 kinase and actin were assessed for their involvement in the CT-mediated inhibition of cell growth, by using specific chemical inhibitors (described in section 2.2.11.4). W7 binds to calmodulin, preventing activation of calmodulin regulated enzymes (figure 8.3A). Treatment of HR12 cells with W7 alone significantly reduced the growth of the cells [$p<0.001$ (figure 8.3B)], however this reduction was not as dramatic as treatment with sCT alone (figure 8.3B) and did not alter cell morphology (figure 8.3C). Treatment of HR12 cells with both sCT and W7 did not prevent the sCT-mediated inhibition of growth. Instead, when the cell number after treatment with sCT and W7 was compared with that after W7 alone, the combination was found to reduce cell growth to a significantly greater extent than sCT alone [$p<0.001$ (figure 8.3B)]. Similar results were obtained when the PI-3 kinase inhibitor LY-294002 (LY) (figure 8.3A) was used to investigate the possible involvement of this pathway in facilitating

**Figure 8.3 Involvement of other growth-regulating pathways in the CT growth cascade.**

A. A schematic representation showing that calcium calmodulin, PI-3 kinase and actin polymerisation can be involved in cell proliferation.

B. HR12 cells were plated at $3X10^4$ cells/well in 12 well plates and allowed to adhere. 4 days following plating, cells remained untreated or were treated with 10 nM sCT, 10 μM W7, 10 μM W7 and 10 nM sCT, LY-94002 (LY), LY and 10 nM sCT, cytochalasin D (cytoD), or cytoD and 10 nM sCT. After 72 h of treatment the cells were harvested and counted. Data points are representative of mean ± SEM of triplicate determinations and are representative of 3 separate experiments. ✱ indicates significant difference from control [$p<0.001$] and # indicates significant difference from treatment with sCT alone [$p<0.001$].

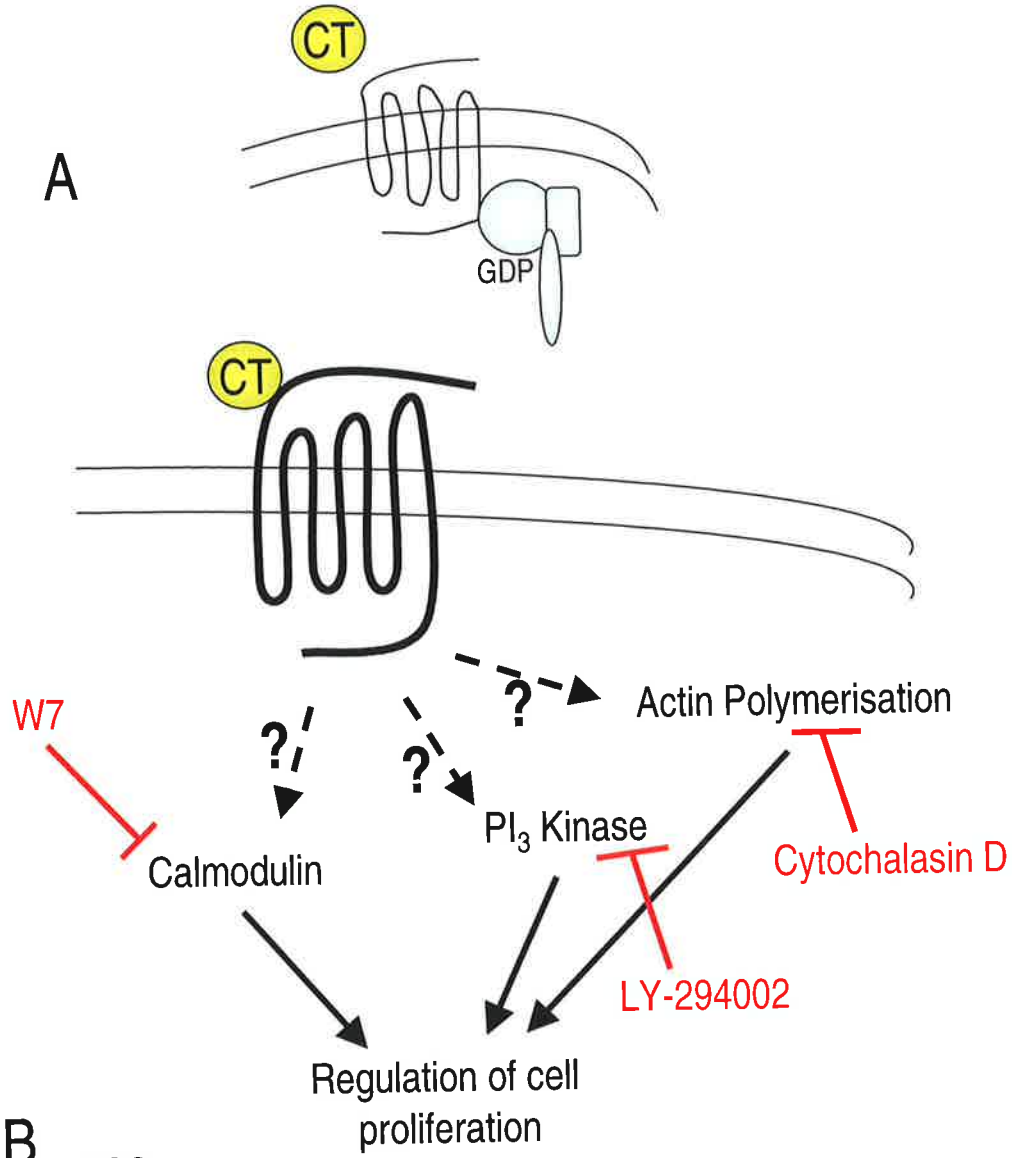
A
CT
GDP
CT
W7
?
?
?
Actin Polymerisation
PI3 Kinase
Calmodulin
Cytochalasin D
LY-294002
Regulation of cell proliferation

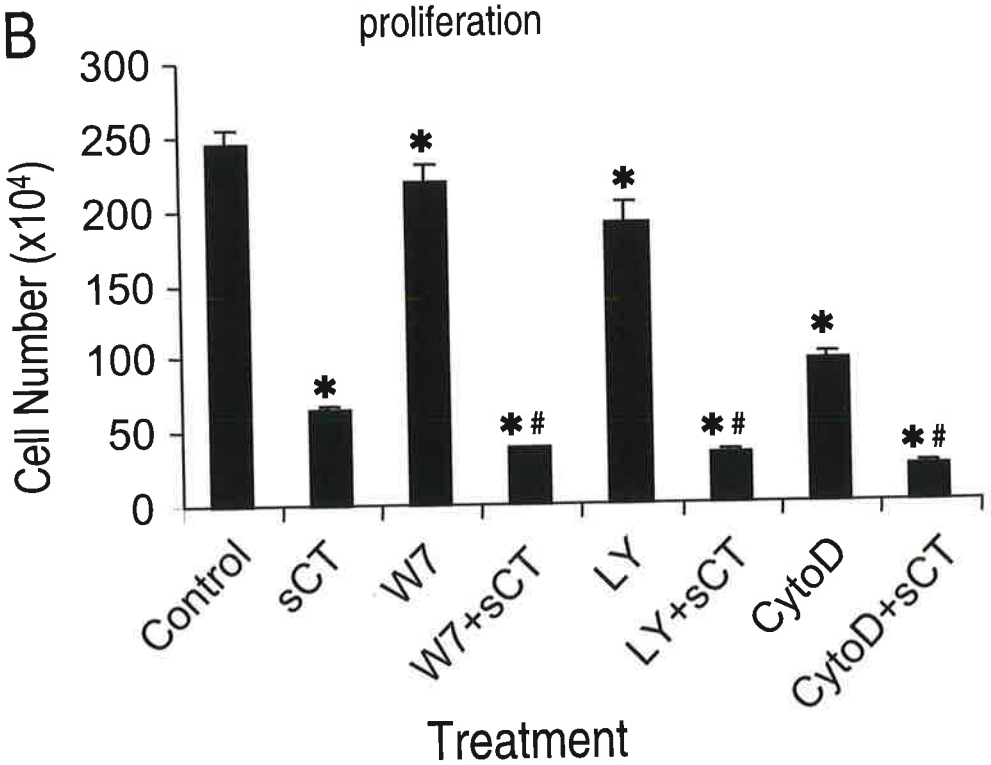
B
Cell Number (x10⁴)
300
250
200
150
100
50
0
Control
sCT
W7
W7+sCT
LY
LY+sCT
CytoD
CytoD+sCT
Treatment

C. Following treatment, and prior to the trypsinisation process described in B, cells were photographed as described in the *Experimental material and methods*, to record cell morphology. The cell treatment is recorded above each photograph. This is a view of the cells when viewed using a 20x objective and 10x binoculars.

C

Control

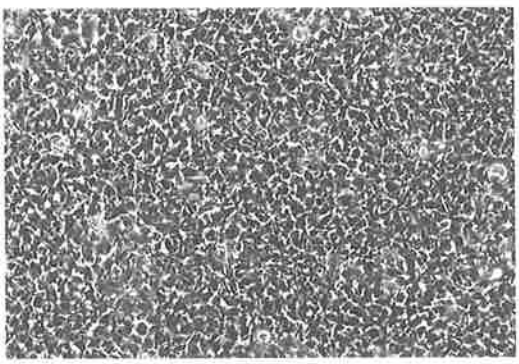

sCT

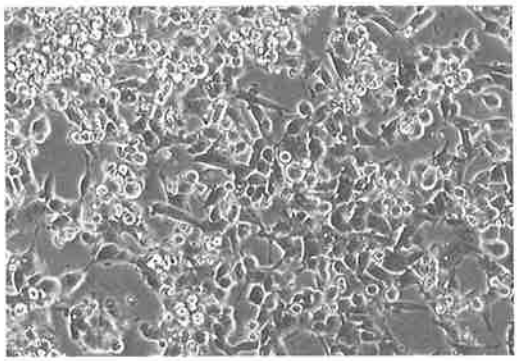

W7

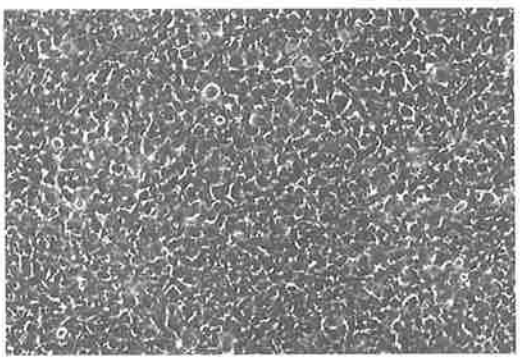

W7 + sCT

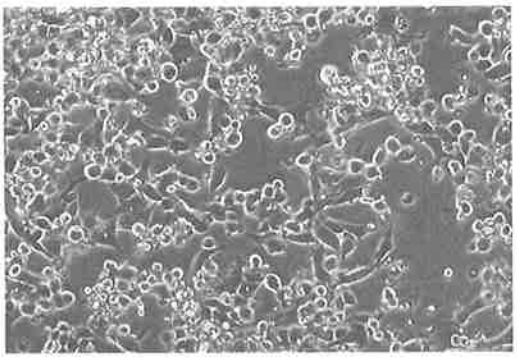

LY-240092

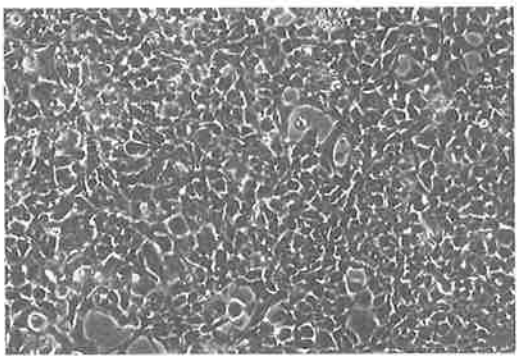

LY-240092 + sCT

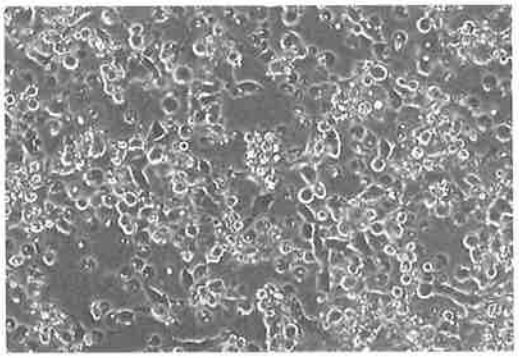

Cytochalasin D

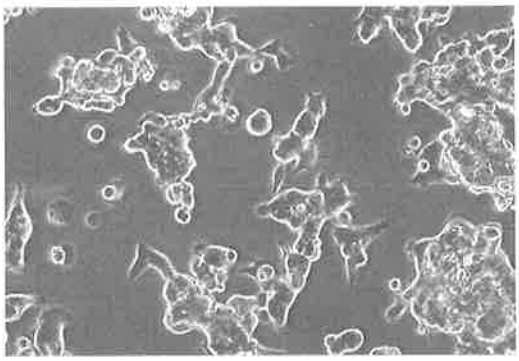

Cytochalasin D + sCT

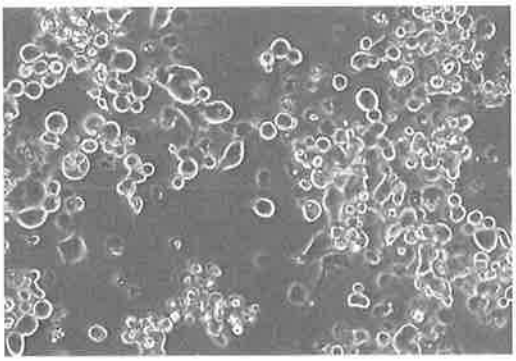

the anti-proliferative actions of CT. Treatment with LY-294002 alone, produced similar results to W7, significantly reducing the growth of HR12 cells $p<0.001$. Comparison of cell numbers following treatment with sCT alone and both sCT and LY-294002 found that the co-treatment reduced cell growth to a significantly greater extent then sCT alone $p<0.001$(figure 8.3B). HR12 cells were also treated with cytochalasin D (CytoD), a chemical inhibitor of actin polymerisation. Treatment with CytoD alone significantly inhibited the growth of the HR12 cells (figure 8.3B), in addition to altering the morphology of the cells (figure 8.3C), making results difficult to interpret. However, unlike W7 and LY-294002, co-administration of CytoD and sCT had no further effects on cell growth than that of sCT alone. Treatment with sCT reduced cell growth by 75%, while co-treatment with both sCT and CytoD reduced cell growth by 74%.

### 8.2.4 Inhibition of Erk1/2 MAPK pathway abrogates the growth inhibitory effects of CT

A number of pathways have been implicated in the CT activation of Erk1/2 *(Chen et al., 1998)*, which are shown schematically in figure 8.3A. To investigate the involvement of the Erk1/2 MAPK pathway in the regulation of cellular proliferation, HR12 cells were treated with the specific MEK inhibitor PD-98059 (figure 8.3A). Proliferation of HR12 cells was significantly decreased by 73%, following a 72 h exposure to 10 nM sCT [$p<0.001$ (figure 8.3B)]. Growth (figure 8.3A) and morphology (figure 8.3D) of the HR12 cells was not altered when the cells were treated with vehicle or PD-98059 alone, however simultaneous treatment with sCT and PD-98059 significantly abrogated (by 33%) the growth inhibitory effects of sCT [$p<0.001$ (figure 8.3B)]. In addition to partial prevention of the inhibition of growth by CT, the cell morphology in the presence of sCT and PD-98059 was more similar to that in control cells, with more cells remaining attached to the culture substrate (figure

**Figure 8.4 Inhibition of Erk1/2 MAPK pathway abrogates the growth inhibitory effects of calcitonin.**

A. A schematic representation of the G protein second messenger pathways putatively involved in the CT activation of the Erk1/2 MAPK pathway, (discussed in section 1.3.3.2.1), and the two compounds used to explore the involvement of this pathway in the CT-mediated growth response. Both PD-98059 and U1026 are specific inhibitors of Mek in the Erk1/2 cascade.

B. HEK-293 cells transfected with the insert –ve hCTR were plated at $1x10^5$ cells/well in 6 well plates. 48 h after plating, cells were treated with vehicle (0.05% DMSO), 10 nM sCT, 50 μM PD-98059 or 50 μM PD-98059 and 10 nM sCT. 72 h after treatment cells were harvested and counted. Data points represent mean ± SEM of triplicate determinations and are representative of three independent experiments. ✱ denotes significant difference from control [$p<0.001$]: # denotes significant difference from sCT treated [$p<0.001$].

C. HR12 cells were plated at $2x10^4$ cells/well in 12 well plates and allowed to adhere. 4 days after plating the cells remained untreated (control) or were treated with 10 nM sCT, 50 μM U1026 or 10 nM and 50 μM U1026. 72 h after plating the cells were harvested and counted. Data points represent mean ± SEM of triplicate determinations and are representative of three independent experiments. ✱ denotes significant

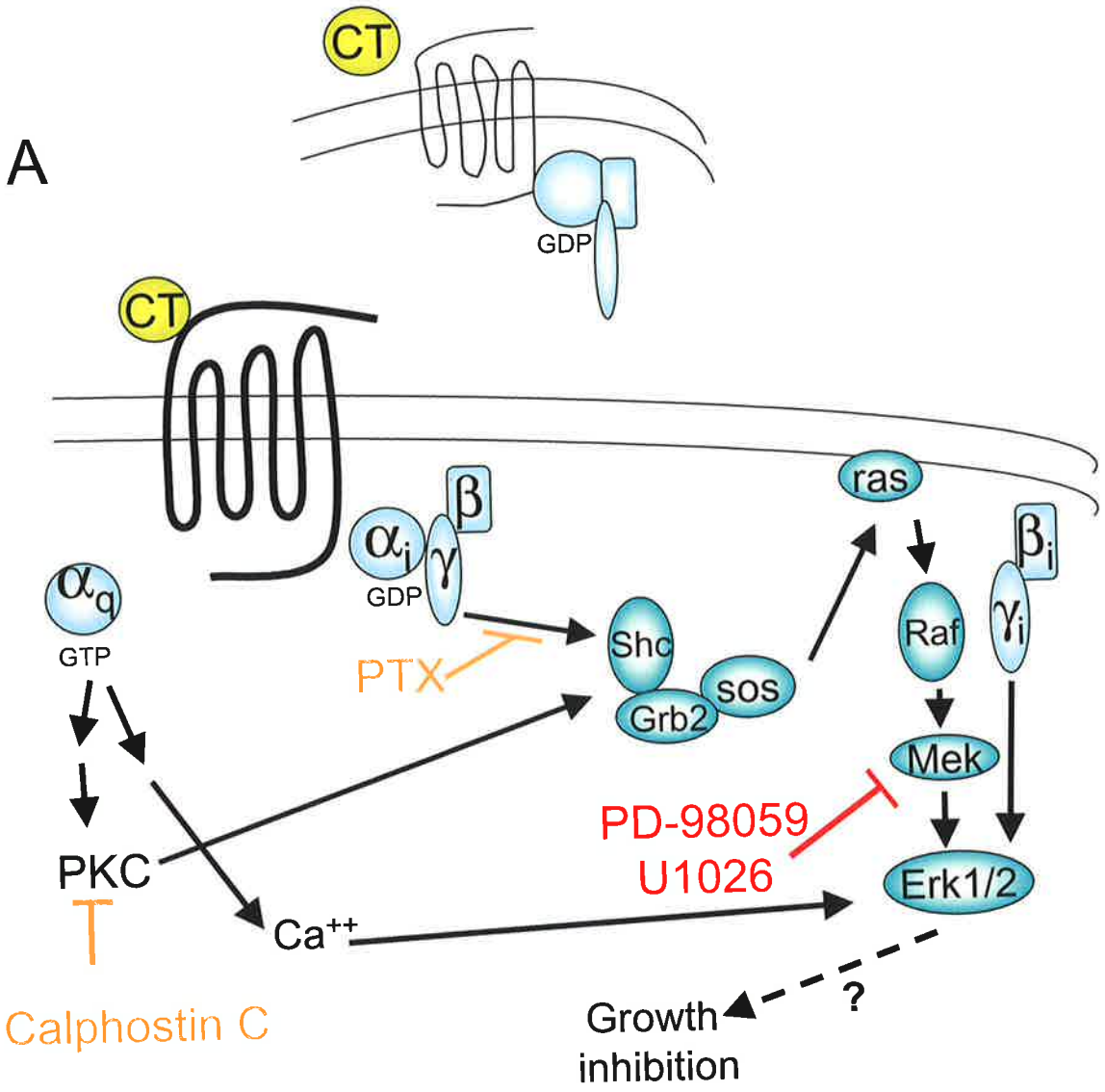
A
CT
GDP
CT
ras
β
$\alpha_i$
γ
GDP
$\alpha_q$
GTP
PTX
Shc
Grb2
sos
Raf
$\beta_i$
$\gamma_i$
Mek
PD-98059
U1026
PKC
Ca++
Erk1/2
Growth
inhibition
?
Calphostin C

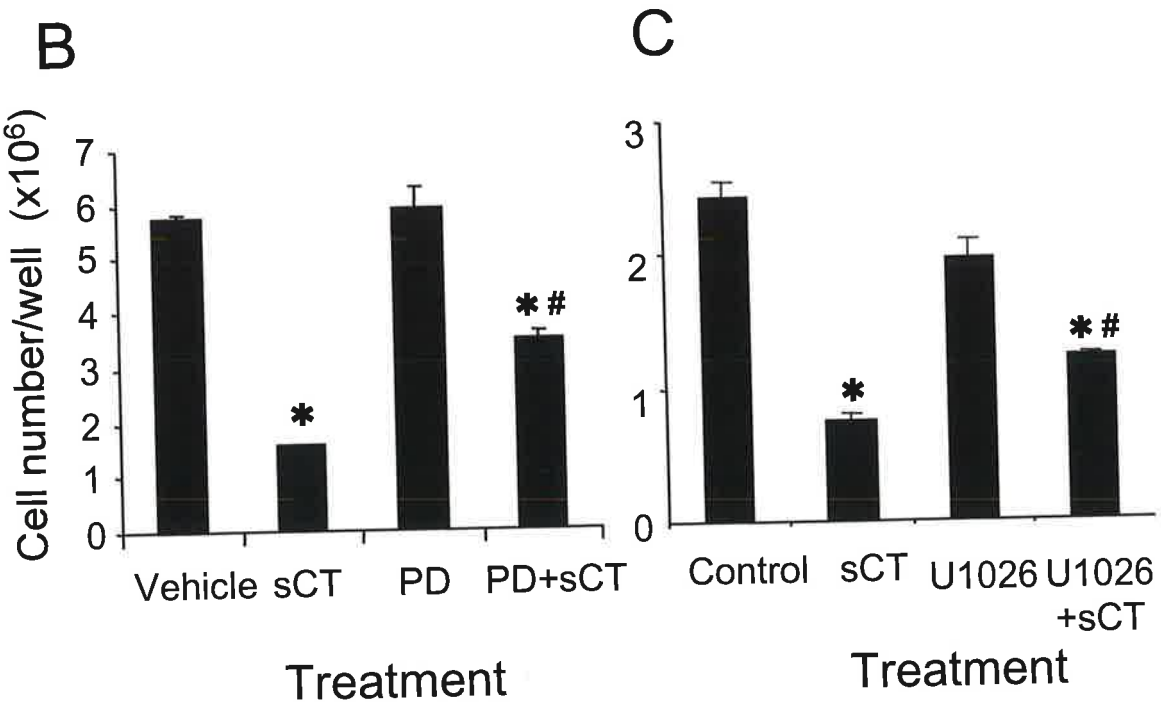
B
Cell number/well (x10⁶)
0
1
2
3
4
5
6
7
*
*#
Vehicle
sCT
PD
PD+sCT
Treatment
C
0
1
2
3
*
*#
Control
sCT
U1026
U1026 +sCT
Treatment

D. Following treatment, and prior to the trypsinisation process described in B, cells were photographed as described in the *Experimental materials and methods*, to record cell morphology. The cell treatment in recorded above each photograph. This is a view of the cells when viewed using a 20x objective and 10x binoculars.

D

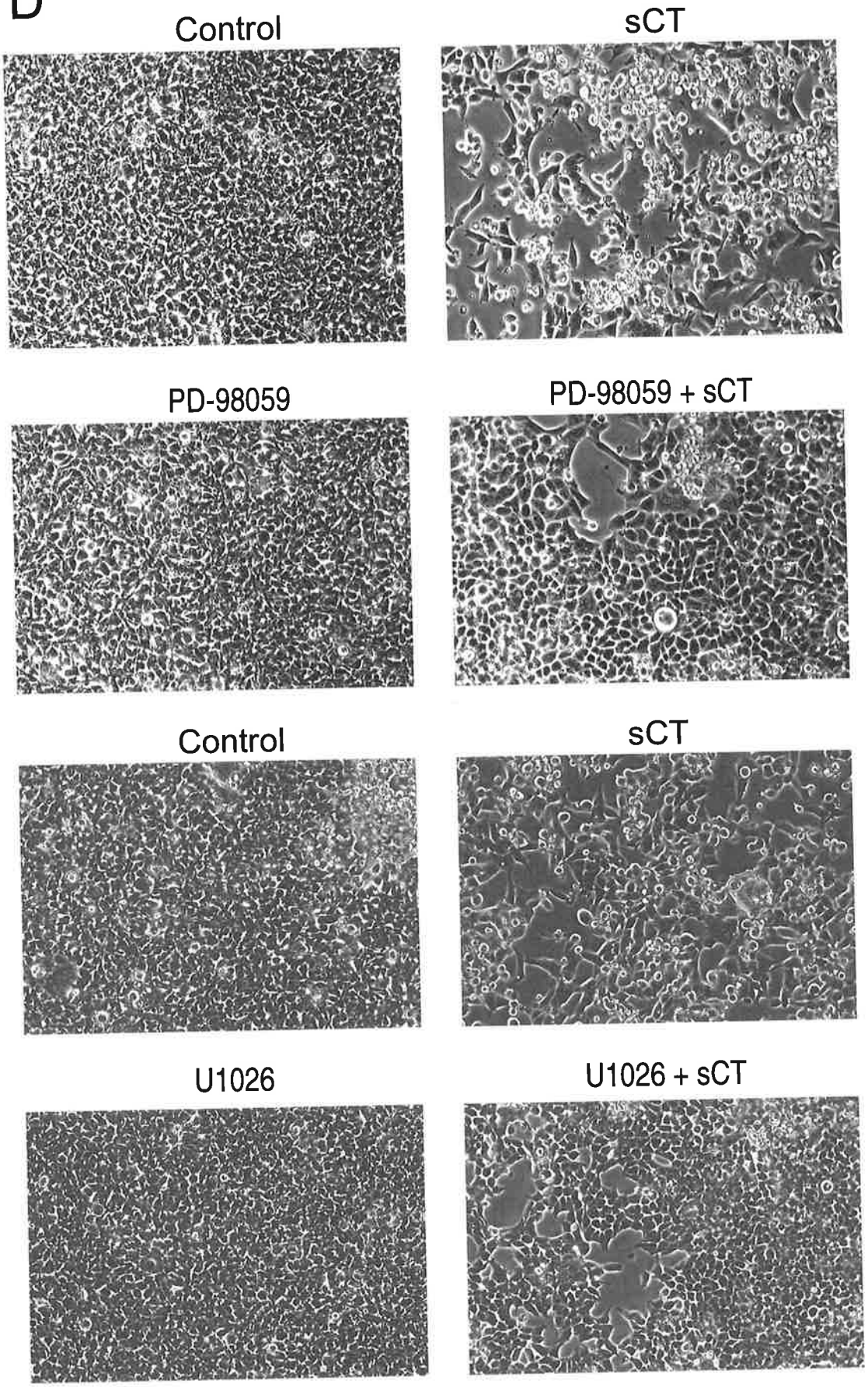
Control
sCT
PD-98059
PD-98059 + sCT
Control
sCT
U1026
U1026 + sCT

8.3D). None of these treatments altered the growth of cells expressing the insert +ve hCTR or those transfected with vector alone (data not shown). HR12 cells were also treated with a second MAPK inhibitor U1026 (figure 8.3). Treatment of cells with U1026 alone significantly inhibited the growth of HR12 cells (figure 8.4C). U1026 did not inhibit cell growth to the same degree as sCT treatment alone (figure 8.3A) and did not alter the morphology of the cells. Co-treatment of HR12 cells with both sCT and U1026 (figure 8.3B) produced a similar profile to those cells treated with PD-98059 and sCT (figure 8.3C). U1026 was able to abrogate (by 30%) the CT-induced inhibition of cell growth [$p<0.001$ (figure 8.3C)], and prevented detachment of cells from the substrate (figure 8.3D), further supporting the involvement of this signalling pathway in this CT-mediated action.

### 8.2.5 Inhibition of Erk1/2 MAPK pathway prevents the CT induced accumulation of cells in G2

To establish the involvement of Erk1/2 MAPK in the CT-induced accumulation of cells in the G2 phase of the cell cycle, HR12 cells were collected 72h after treatment and analysed by FACS (described in section 2.2.14). As shown in figure 8.5A & B, treatment with sCT dramatically altered the cell-cycle parameters, increasing the proportion of cells in the G2 phase. PD-98059 alone did not alter the percentage of cells in G2 (figure 8.5A & B). However simultaneous treatment of cells with PD-98059 and sCT partially prevented the CT-induced accumulation of cells in G2 (Figure 8.5A & B).

### 8.2.6 Effect of calcitonin on expression of p21 is dependent on Erk1/2 MAPK activation

sCT was previously shown to increase the mRNA levels of $p21^{WAF1/CIP1}$ in cells expressing the insert –ve hCTR, as early as 4 h following sCT treatment (chapter 6 figure 6.1). This elevation of $p21^{WAF1/CIP1}$ mRNA was causally related to the CTR

**Figure 8.5 Effect of PD-98059 on CT-induced changes in cell cycle progression.**

HEK-293 cells transfected with the insert –ve hCTR were plated at $1x10^5$ cells/well in 6 well plates. 48 h after plating, cells were treated with vehicle (0.05% DMSO), 10 nM sCT, 50 μM PD-98059 or 50 μM PD-98059 and 10 nM sCT. 72 h after treatment, cells were harvested and fixed, stained and analysed for DNA content, as described in the *Experimental materials and methods*. Panel A shows the distribution of cells in the cell cycle in response to the indicated treatment. Panel B summarises the percent of cells in the G2 phase of the cell cycle in two separate experiments.

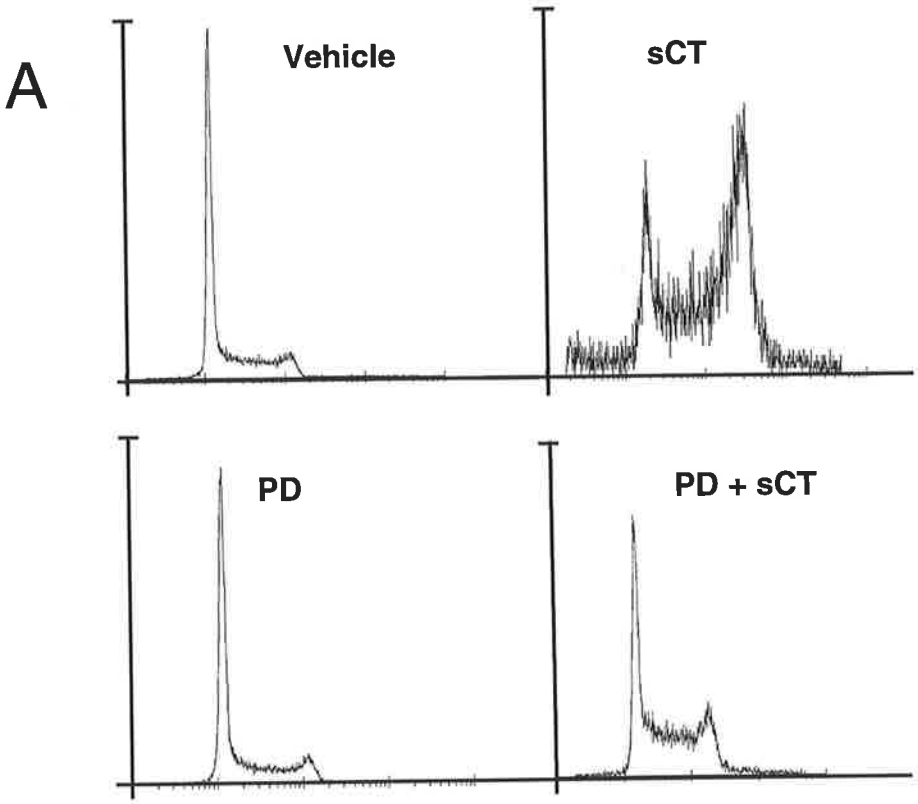
A
Vehicle
sCT
PD
PD + sCT

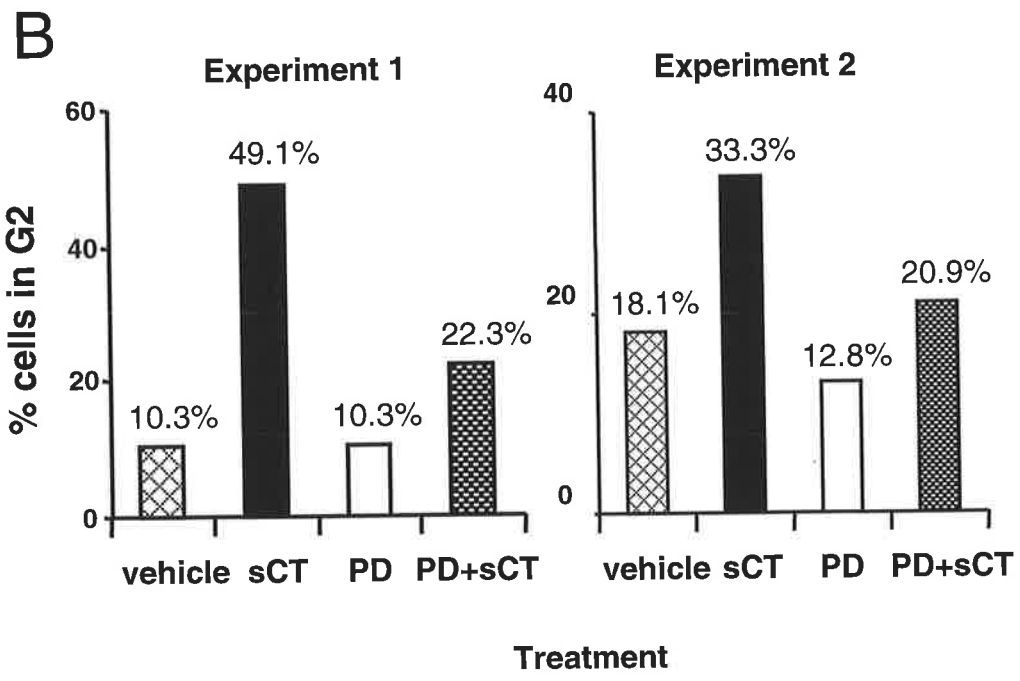
B
Experiment 1
Experiment 2
% cells in G2
60
40
20
0
49.1%
10.3%
10.3%
22.3%
40
20
0
33.3%
18.1%
12.8%
20.9%
vehicle
sCT
PD
PD+sCT
vehicle
sCT
PD
PD+sCT
Treatment

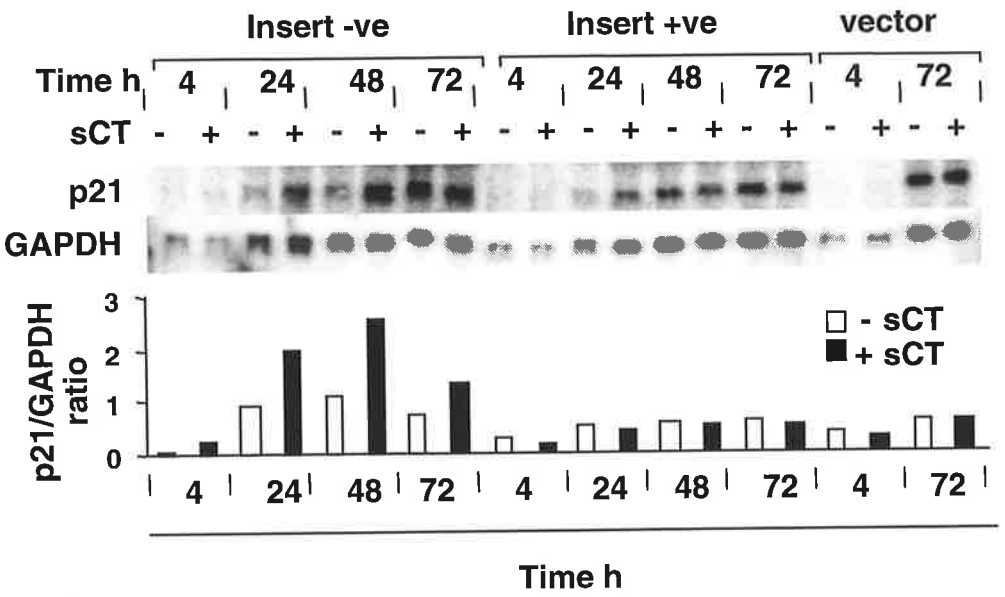


**Figure 8.6 Expression of p21 mRNA after treatment with CT.**

HEK-293 cells stably transfected with the insert -ve, insert +ve hCTR, or vector alone were cultured for the indicated times in the absence or presence of 10 nM sCT, added once 48 h after plating the cells. At the indicated times, total RNA was extracted for Northern blot analysis. RNA was electrophoresed in a 1% agarose formaldehyde gel, transferred to nylon membrane and hybridised with a $^{32}$P-labeled p21 cDNA probe. Blots were rehybridised with a cDNA probe for GAPDH to indicate RNA loading. Signals were analysed by denistometry and expressed in the lower panel as a ratio of p21 mRNA/GAPDH mRNA. These results are representative of 2 independent experiments.

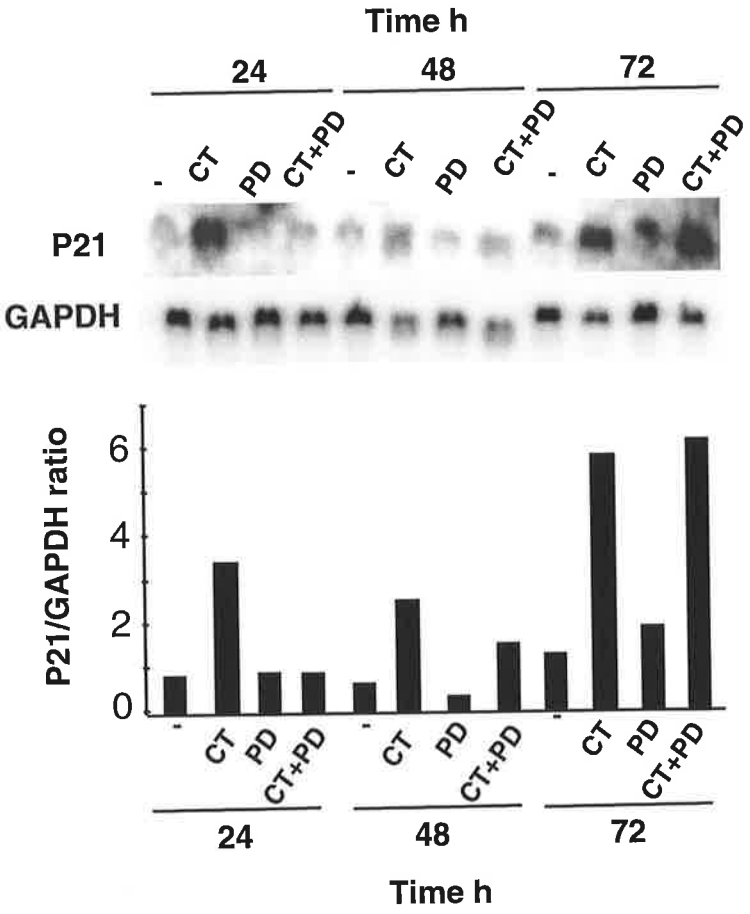


**Figure 8.7 Effect of PD-98059 on p21 mRNA expression.**

HEK-293 cells stably transfected with the insert –ve hCTR were cultured for the indicated times with vehicle (0.05% DMSO), 10 nM sCT, 50 μM PD-98059 or 50 μM PD 98059 and 10 nM sCT. At the indicated times, total RNA was extracted and Northern blot analysis performed. RNA was electrophoresed in a 1% agarose formaldehyde gel, transferred to nylon membrane and hybridised with a $^{32}$P-labeled p21 cDNA probe. Blots were rehybridised with a cDNA probe for GAPDH to indicate RNA loading. Signals were analysed by densitometry and expressed in the lower panel as a ratio of p21 mRNA/GAPDH mRNA.

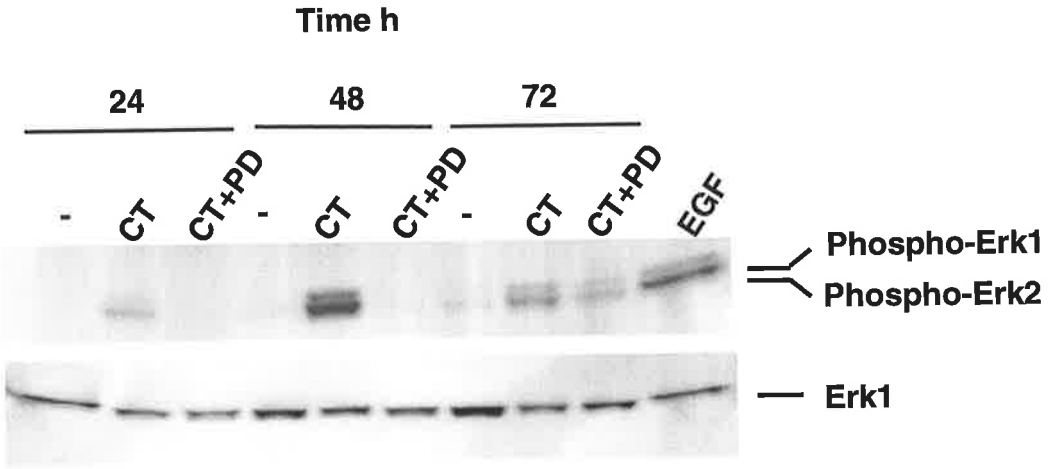


**Figure 8.8 Effect of PD-98059 on CT-induced Erk1/2 phosphorylation.** HEK-293 cells stably transfected with the insert –ve hCTR were treated for the indicated times with vehicle (0.05% DMSO), 10 nM sCT, 50 μM PD-98059 or 50 μM PD 98059 and 10 nM sCT. Total cell extracts were collected, electrophoresed on SDS-page gel, transferred to PVDF membrane as described in the *Experimental material and methods*. Immunoblotting with antiphospho-Erk1/2 was performed to determine the phosphorylation status of Erk1/2 (upper panel) and antiErk1 antibody to determine the total amount of Erk1 protein in each sample (lower panel).

mediated growth inhibition of HEK-293 cells, as p21 antisense oligonucleatides were able to abrogate the inhibition of growth (figure 6.3). This effect of sCT at the insert -ve hCTR is shown again in figure 8.6, which also shows that sCT did not affect the steady state levels of $p21^{WAF1/CIP1}$ mRNA in cells expressing the insert +ve hCTR at any time point investigated. Similarly there was no change in $p21^{WAF1/CIP1}$ mRNA in cells transfected with vector alone (figure 8.6).

To establish the involvement of ERK1/2 MAPK in the calcitonin-induced elevation of $p21^{WAF1/CIP1}$ mRNA levels, cells expressing the insert -ve hCTR were treated with PD-98059. As shown in figure 8.7, sCT treatment of these cells again induced a prolonged increase in the steady state levels of $p21^{WAF1/CIP1}$ mRNA. PD-98059 prevented the CT-induction of $p21^{WAF1/CIP1}$ mRNA at 24 h, although the inhibition was partial at 48 h and was overcome by 72 h.

To determine the ability of PD-98059 to inhibit Erk1/2 activity in culture, cell lysates were analysed for Erk1/2 phosphorylation (described in section 2.2.9). Figure 8.8 shows that PD-98059 completely inhibited the sCT induced Erk1/2 phosphorylation at 24 and 48 h time points. However at the later time point of 72 h, PD-98059 inhibition of the sCT-induced phosphorylation of Erk1/2 was partial (figure 8.8). PD-98059 alone did not affect Erk1/2 phosphorylation compared with control cells (data not shown).

### 8.2.7 The growth abrogating effect of the Mek inhibitor PD-98059 and PTX are not cumulative

Previously, CT activation of Erk1/2 has been shown to be dependent on multiple secondary signalling pathways *(Chen et al., 1998)*. Shc phosphorylation and the subsequent Shc/Grb2 association was shown to require activation of the PTX-sensitive and the PKC G-protein-mediated pathways. In addition, phosphorylation of Erk1/2 was also dependent on mobilisation of the calcium signalling pathway, all of

**Figure 8.9 The effect of PD-98059 and PTX on the inhibition of growth by CT are cumulative.**

A. A schematic representation of the G protein second messenger pathways involved in the CT activation of the Erk1/2 MAPK pathway, (discussed in section 1.3.3.2.1), and the two compounds used to explore the involvement of this pathway in the CT-mediated growth response. Both PD-98059 and U1026 are specific inhibitors of Mek in the Erk1/2 cascade.

B. HR12 cells were plated at $3x10^4$ cells/well in 12 well plates and allowed to adhere. After 4 days, the cells remained untreated or were treated with 10 nM sCT, 1 ng/ml PTX, 1 ng/ml PTX and 10 nM sCT, 50 μM PD-98059, 50 μM PD-98059 and 10 nM sCT, 1 ng/ml PTX and 50 μM PD-98059, or 1 ng/ml PTX, 50 μM PD-98059 and 10 nM sCT. 72 h later cells were harvested and counted. Data points represent mean ± SEM of triplicate determinations. * denotes significant difference from control [$p<0.001$]: # denotes significant difference from sCT alone treatment [$p<0.001$].

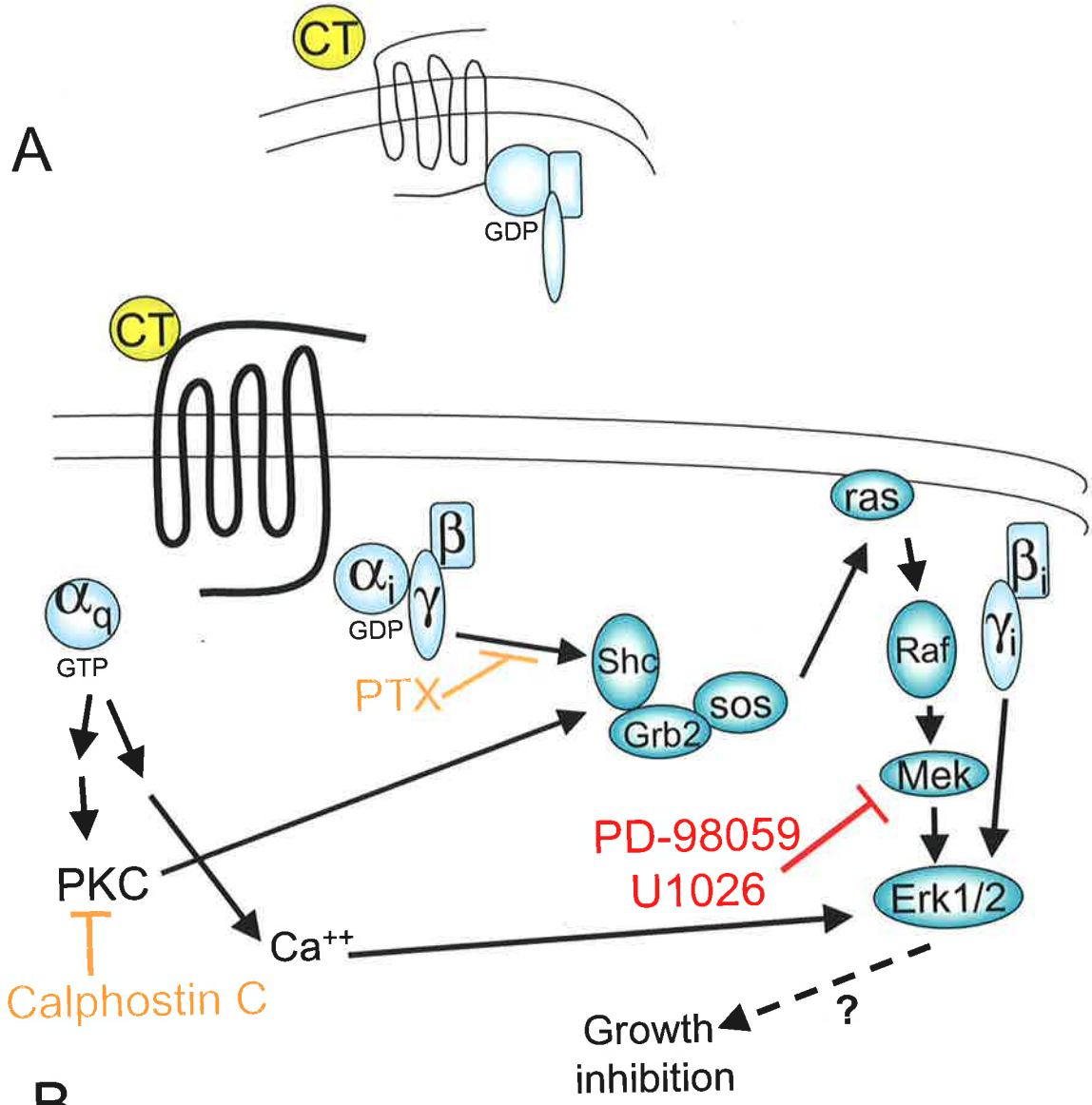
A
CT
GDP
CT
ras
β
$\alpha_i$
γ
GDP
$\alpha_q$
GTP
Shc
Grb2
sos
Raf
$\gamma_i$
$\beta_i$
PTX
Mek
PD-98059
U1026
Erk1/2
PKC
Ca++
Calphostin C
Growth
inhibition
?

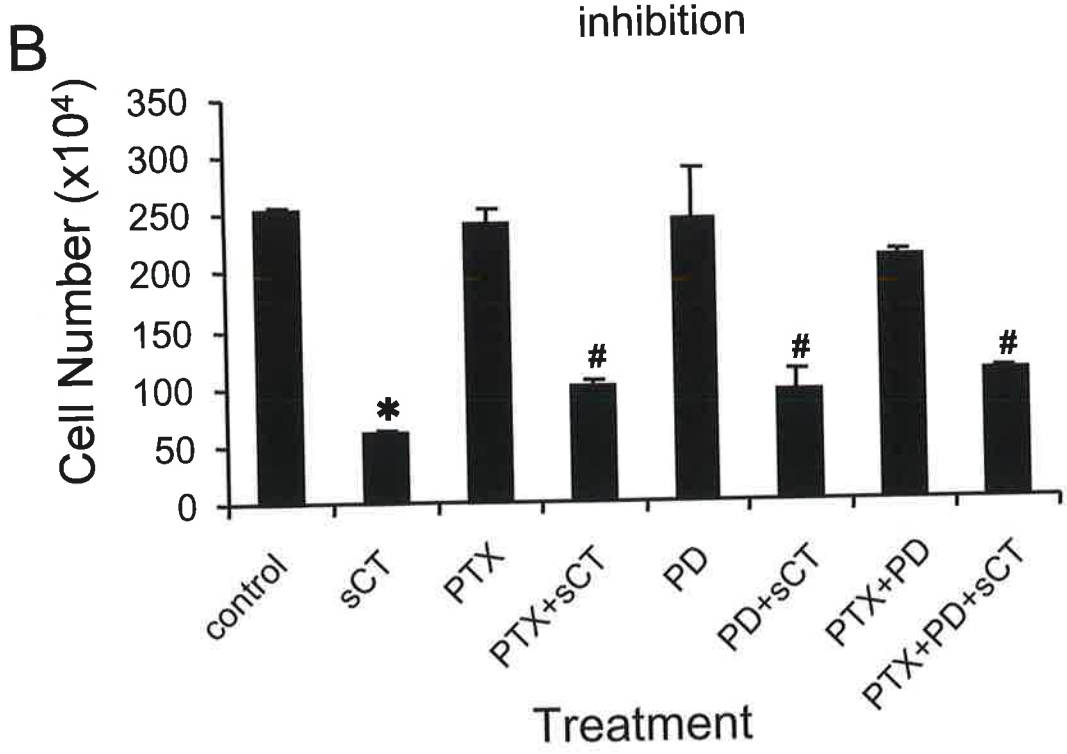
B
Cell Number (x10⁴)
350
300
250
200
150
100
50
0
*
#
#
#
control
sCT
PTX
PTX+sCT
PD
PD+sCT
PTX+PD
PTX+PD+sCT
Treatment

which are depicted schematically in figure 8.9A. As an initial investigation to determine if the growth inhibitory PTX-sensitive intracellular signalling cascade was responsible for the MAPK growth inhibition, cells were treated with both PTX and PD-98059. Teatment of cells with sCT and PTX, or PD-98059 alone abrogated the growth inhibitory effect of sCT to the same degree [$p<0.001$ (figure 8.8B)]. Co-treatment with both PTX and PD-98059 was not cumulative, as it did not abrogate [$p<0.001$ (figure 8.8B)] the growth effect significantly more than treatment with the individual agents alone.

## 8.3 Discussion

The experiments presented in this chapter aimed to explore the intracellular signalling pathways through which the CT growth-regulated signalling is transduced. In the HEK-293 transfected model used here, both the cAMP and PLC pathways are activated in response to CT (refer to chapter 3). However artificial activation or inhibition of these pathways did not mimic or inhibit the CT inhibition of growth, indicating that neither of these signalling cascades is likely to be involved in this growth response. Similarly, no involvement of the PI-3 kinase or calcium/calmodulin pathways was detected, despite both of these pathways being growth regulating. However, activation of Erk1/2 was shown to be important for the insert –ve hCTR-mediated growth effects, since growth suppression of cells expressing the insert –ve hCTR (HR12 cells) by CT was partially blocked by the MEK inhibitor PD-98059. The observation (refer chapter 3, figure 3.2) that CT does not activate Erk1/2 in HEK-293 cells transfected with the insert +ve hCTR isoform (Hi12 cells), coupled with the results (chapter 4) that CT does not affect the growth of Hi12 cells, is consistent with an important role for the Erk1/2 pathway in the growth inhibitory action of CT in HR12

cells. The CT-induced activation of Erk1/2 (chapter 3 figure 3.7) occurred in the same time frame as the induction of $p21^{WAF1/CIP1}$ (chapter 6 figure 6.1) which was shown to be causally related to the inhibition of cell growth (chapter 6 figure 6.3). The work presented in this chapter provides evidence that Erk1/2 activation is in turn responsible for the CT-induced growth suppression and is upstream of $p21^{WAF1/CIP1}$ induction, since inhibition of Erk1/2 abrogated both of these responses.

Although activation of Erk1/2 MAPK is usually associated with growth promotion *(Mansour et al., 1994)*, a number of reports show that activation of Erk1/2 MAPK is also able to arrest cell cycling, and induce cellular differentiation *(Pumiglia et al., 1997; Cowley et al., 1994)*. For example, nerve growth factor (NGF) induces the activation of Erk1/2 MAPK and up-regulates expression of $p21^{WAF1/CIP1}$ in NIH 3T3 cells, resulting in the inhibition of cellular proliferation *(Pumiglia et al., 1997)*. These effects were reversed by direct inhibition of MEK with PD-98059. When an inducible activated form of the Raf-1 protooncogene was expressed in these cells, it resulted in a prolonged increase in Erk1/2 MAPK activity and growth arrest, with a concomitant induction of $p21^{WAF1/CIP1}$ *(Pumiglia et al., 1997)*. However, these events are clearly dependent factors other than just cell type, since transformation of NIH 3T3 cells with a constitutively active MEK induced cellular transformation, allowing the cells to grow on soft agar and to form tumours in nude mice *(Mansour et al., 1994)*. The ability of a signal transduction pathway to induce these conflicting cellular responses in the same cell type has been proposed to depend on the duration of Erk1/2 MAPK activation, with acute activation leading to growth stimulation and DNA synthesis, and chronic activation inhibiting cell cycle progression *(Cowley et al., 1994; Tombes et al., 1998)*. In addition to the duration of the signal being important, there are reports that the intensity of the Erk1/2 MAPK signal may dictate the cellular response. For example, NIH 3T3 cells, expressing an inducible Raf protein that could

be progressively activated, resulted in a G1 arrest and $p21^{WAF1/CIP1}$ induction in response to a strong Raf signal. However, cellular proliferation was evoked in response to a moderate induction of Raf *(Sewing et al., 1997; Woods et al., 1997)*. Thus it is becoming clear that the ultimate cellular response to activation of the Erk1/2 MAPK pathway is determined by the strength and duration of Erk1/2 MAPK signalling and also by the cellular context *(Traverse et al., 1994)*.

In seeking a mechanism for the sustained activation of Erk1/2 MAPK, several issues need to be addressed. In the experiments reported here, a number of intracellular signalling molecules were targeted with chemical activators and inhibitors in an attempt to identify the signalling pathway/s mediating the CT inhibition of cell growth. These experiments required exposing cells for 72 h in cell culture to chemicals that globally activate and inhibit fundamental signalling pathways. In an effort to avoid the complicating effects of long term exposure to these chemicals, we first attempted to use a luciferase reporter system. Chapter 7 showed that CT was able to act on the p21 promoter and activate an attached luciferase reporter gene. Using this system, an attempt was made to modulate the CT-induced luciferase response using chemical activators and inhibitors of intracellular signalling molecules. However the CT-induction of luciferase was not prevented by any of the inhibitors used, and importantly, no effect was observed with the Mek inhibitor PD-98059. Consequently, it was decided to use longer-term growth experiments, although the disadvantage of this was that some chemical treatments alone altered cell growth, making results difficult to interpret. For example, the long term treatment of HR12 cells with PTX alone, dramatically affected the morphology of the cells. Co-treatment of HR12 cells with PTX and sCT also influenced the morphology of the cells compared to that seen with PTX treatment alone. Consequently, it is possible that the ability of PTX to partially reverse the CT inhibition of growth was secondary to the

morphological changes produced by the chemical. Alternatively, as discussed below, the PTX pathway may be fundamental to transducing the CT growth signal.

Elevation of cAMP levels has long been associated with regulation of cell proliferation and differentiation *(Cho Chung 1990)*, and previously it has been shown that inhibition by CT of T47D cell growth occurred in parallel with a selective and sustained activation of the type II isoform of PKA *(Livesey et al., 1984)*. No evidence was found for the involvement of the PKA pathway in the CT-induced early induction of Erk1/2 MAPK activation *(Chen et al., 1998)*. In addition, there was no apparent involvement of the PKA signalling pathway in the CT-inhibition of cell growth in the present experiments. However, the Gi protein inhibitor PTX was found to abrogate the CT-mediated growth effect. Co-treatment of HR12 cells with both PTX and MAPK inhibitor PD-98059 did not abrogate the sCT growth inhibition more than either agent alone, suggesting that they may be acting through a common pathway. This observation, taken together with the previous report that the $\beta\gamma_i$ inhibitor (βARK1ct) was able to partially inhibit the CT-induced phosphorylation of Erk1/2 *(Chen et al., 1998)*, suggests that this G-protein subunit may be integral in the CT-mediated inhibition of growth. However specific targeting of the $\beta\gamma_i$ subunit in growth experiments is required to confirm this proposition (as discussed in chapter 9). Recent reports of a novel mechanism by which $G_i$ proteins can activate the Erk1/2 MAPK pathway *(Auer et al., 1998; Mochizuki et al., 1999; Shefler et al., 1999)* also leaves open the possible involvement of the $G\alpha_i$ subunit. In particular, Mochizuki *et al (Mochizuki et al., 1999)* have shown that, in addition to the free βγ subunits of activated $G_i$ proteins interacting with the Erk1/2 MAPK pathway, the free activated $G\alpha_i$ subunit can independently activate this pathway by binding to and blocking the tonic Erk1/2 inhibitory action of a small GTPase called Rap1. It is possible that

binding at the CTR activates both pathways in HEK-293 cells to control the duration and intensity of the signal through the Erk1/2 MAPK pathway.

In addition to activation of Erk1/2 MAPK *via* the classic tyrosine kinase receptor cascade (refer section 1.3.3.1), phosphorylation of Erk1/2 can occur in response to the assembly of focal adhesion complexes and the subsequent activation of focal adhesion kinases (FAK). GPCR agonists have been reported to phosphorylate FAK. These findings present an alternative explanation for the activation of the Erk1/2 signalling pathway responsible for CT-inhibition of cell growth. As shown in chapter 3, CT treatment of HEK-293 cells transfected with the insert –ve hCTR caused a delayed and sustained activation of Erk1/2 in these cells figure 3.7A. This delay in Erk1/2 phosphorylation is difficult to explain but does correlate with morphological changes observed in the insert –ve cells after CT treatment (Chapter 3 figure 3.8). Cells that accumulated in G2 at 24 and 48 h post-treatment displayed a rounded morphology and were loosely attached to the substratum. It is thus possible that Erk1/2 phosphorylation is a secondary effect of CT treatment following the primary morphological changes, and that focal adhesion complexes initiate the Erk1/2 activation cascade. Interestingly, CT was recently shown to activate focal adhesion kinases and several FAK-associated proteins in HEK-293 cells *(Zhang et al., 1999)*, suggestive of an alternative pathway for CT-activation of Erk1/2 (refer chapter 9).

# Chapter 9

# Future research directions

The development of an HEK-293 transfected cell model expressing either the insert –ve or the insert +ve hCTR (chapter 3) has allowed the growth regulating actions of these receptor isoforms to be assessed (chapter 4). CT activation of the insert –ve hCTR inhibited cell proliferation by arresting the cells in the G2/M phase of the cell cycle (chapter 5). This growth regulating action was isoform-specific, as the insert +ve hCTR did not affect cell growth (chapter 4). The CT-mediated inhibition of cell growth was dependent on an increase in the CKI $p21^{WAF1/CIP1}$ (chapter 6). The specific mechanism by which p21 inhibited activity of the cdc2/cyclin B1 complex was not identified, and possible explanations for this were discussed in chapter 6. In the current study experiments were limited to seeking an association between p21 and the cdc2/cyclin B1 complex. However, p21 has also been reported to interact with other cellular proteins, for example PCNA *(Zhang et al., 1993; Chen et al., 1995; Cayrol et al., 1998)*, to induce cell cycle arrest. An investigation into the association of p21 with PCNA and other cellular proteins, in response to CT treatment, is therefore warranted.

The use of the p21 promoter/luciferase reporter constructs indicated that CT regulates cellular p21 levels *via* regulation of p21 gene transcription (chapter 7). CT elevated p21 transcription independently of p53 and through the constitutively expressed transcription factor Sp1. This finding identifies a number of areas of future study. Firstly, the potential exists for other Sp1 responsive genes to be regulated by CT. Alternatively, it is possible that the regulation of the p21 gene by CT, *via* Sp1 is a specific mechanism and that the specificity arises from one or several co-factors, which either binds directly to Sp1 or to an upstream response element.

The use of chemical activators and inhibitors of intracellular signalling molecules, showed that the Erk1/2 MAPK pathway is an important signalling cascade in transducing the CT-growth inhibition (chapter 8). However inhibition of the Erk1/2

pathway did not completely inhibit the CT-induced inhibition of growth, suggesting that other intracellular signalling pathways may be involved. The PKA, PLC, PI-3 and calicum-calmodulin pathways were investigated in the current study, but appeared not to be involved (chapter 8). However, a limited group of artificial activators and inhibitors were used in this study and a more comprehensive investigation is required to confirm these findings. The preliminary study with PTX suggested that the Erk1/2 activation was *via* the Gi G-protein. Co-treatment of cells with both the Gi inhibitor PTX and the Mek inhibitor PD-98059 did not abrogate the CT-inhibition of growth any more than either agent alone. However a more targeted assessment of the interaction of these two pathways is required to confirm the involvement of Gi in the activation of MAPK, as the approach used here had inherent problems relating to changes in cell morphology, which were discussed in chapter 8. The recent use of conjugated membrane-permeable peptides to identify the G-proteins activated by the $\alpha_{2A}$ adrenergic receptor *(Chang et al., 2000)*, is an example of an alternative approach that may have greater specificity for dissecting intracellular growth signals. The problem with inhibitors of intracellular signalling pathways is that they are rarely completely specific and target normal cellular processes as well as those activated by, in this case CT.

In addressing the other factors which may be involved in the CT-mediated growth inhibition reported here, it will be important to explore further the morphological changes associated with the Erk1/2 activation and the subsequent growth inhibition. CT interacts with FAK *(Zhang et al., 1999)*, which activates Erk1/2 *(Tang et al., 1998; Tapia et al., 1999)*. The possibility therefore exists that the Erk1/2 growth inhibition is actually secondary to the observed morphological changes, which occur with CT-treatment. A study investigating the activation of FAK's by CT using

the optimal mitogenic experimental conditions described here (10% FCS), as apposed to the 0.5% FCS conditions that have been previously used *(Zhang et al., 1999)*, would be required initially. If CT was found to activate FAK, targeting of specific proteins would identify their direct involvement in activating Erk1/2 and the subsequent inhibition of cell growth. Although not reported for the CTR, ligand-independent autophosphorylation of epidermal growth factor receptors (EGFR) is involved in MAPK activation by some GPCR, for example the angiotensin II *(Eguchi et al., 1998)* and $P_{2y2}$ *(Soltoff 1998)* receptors. Trans-activation of the EGFR by a GPCR, allows the EGFR to act as "scaffolding" where Ras complexes can assemble prior to MAPK activation. The PTH receptor is a member of the CTR sub-family of receptors, and regulates MAPK activation *via* a number of signalling pathway, including phosphoylation of the EGFR *(Cole 1999)*. An assessment of the phosphorylation status of the EGFR, in response to CT-treatment, is required to determining the involvement of this mechanism in the activation of MAPK by CT, that is reported here.

The results in chapter 4 identified that the CTR-mediated regulation of cell growth was CTR isoform specific in HEK-293 cells, and raised the question of isoform function. Despite the documented variation in hCTR isoform expression (discussed in section 1.2.1) and signalling potential (discussed in section 1.2.7.3), the physiological function of the hCTR isoforms is currently unknown. There are however, several possibilities. There is now growing evidence to suggest that GRCR's cross-talk and cross-modulate each other's function. For example, non-functional GPCR can heterodimerize to form functional receptors *(Maggio et al., 1993; Monnot et al., 1996)*, suggesting that multimerization is necessary for receptor function. Truncated fragments of the muscurinic acetylcholine receptor form active receptor complexes, able to bind agonists and activate intracellular signalling

pathways when co-expressed in COS-7 cells *(Schoneberg et al., 1995)*. Co-expression of mutant and wild-type platelet-activated factor receptors caused altered ligand binding, cell surface expression and intracellular activation of the wild type receptor *(Le Gouill et al., 1999)*, indicating modulation of the wild-type receptor by the mutant. In addition, heterodimerisation and functional regulation between fully functional GPCR has also been reported *(Jordan et al., 1999)*. Therefore, a potential action for the apparently inert insert +ve hCTR, with respect to signalling, might be to down regulate the activity of the insert -ve hCTR (shown schematically in figure 9.1). This hypothesis, that the insert +ve hCTR may negatively regulate the insert –ve hCTR, is worth investigating because of a recent report showing that hCTR isoform expression varies between healthy postmenopausal women and clinically osteoporotic women *(Beaudreuil et al., 2000)*. Specifically, the postmenopausal women had significantly more insert –ve hCTR mRNA than insert +ve hCTR mRNA in their mononuclear leucocytes, whereas there was no significant difference between the mRNA levels of either hCTR isoform in mononuclear leucocytes isolated from osteoporotic women. It is likely that the significant difference between the mRNA levels of the insert +ve and insert –ve hCTR in postmenopausal women would be reflected in the relative density of cell surface receptors. If, as was postulated above, the insert +ve hCTR negatively regulates the insert –ve hCTR, then a relative increase in the quantity of the insert +ve hCTR receptor isoform may limit the anti-resorptive effect of CT, resulting in a weaker signal from the insert –ve hCTR. In the context of bone, a weaker CTR signal would both decrease the innate protection against bone loss, as well as demonstrating the physiological significance of the CT/CTR system on the skeleton. Rigorous *in vitro* studies addressing the possibility of receptor isoform interactions are required. To date, this has been difficult due to the similarity of the receptor isoforms and the lack of agents able to distinguish them.

A Cross Talk

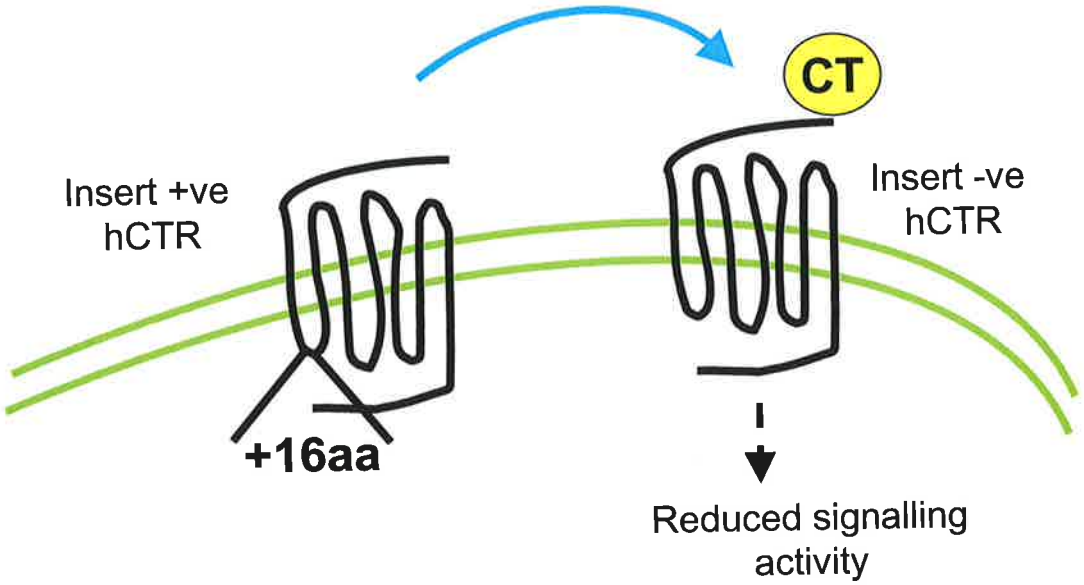


B Altered Ligand Specificity

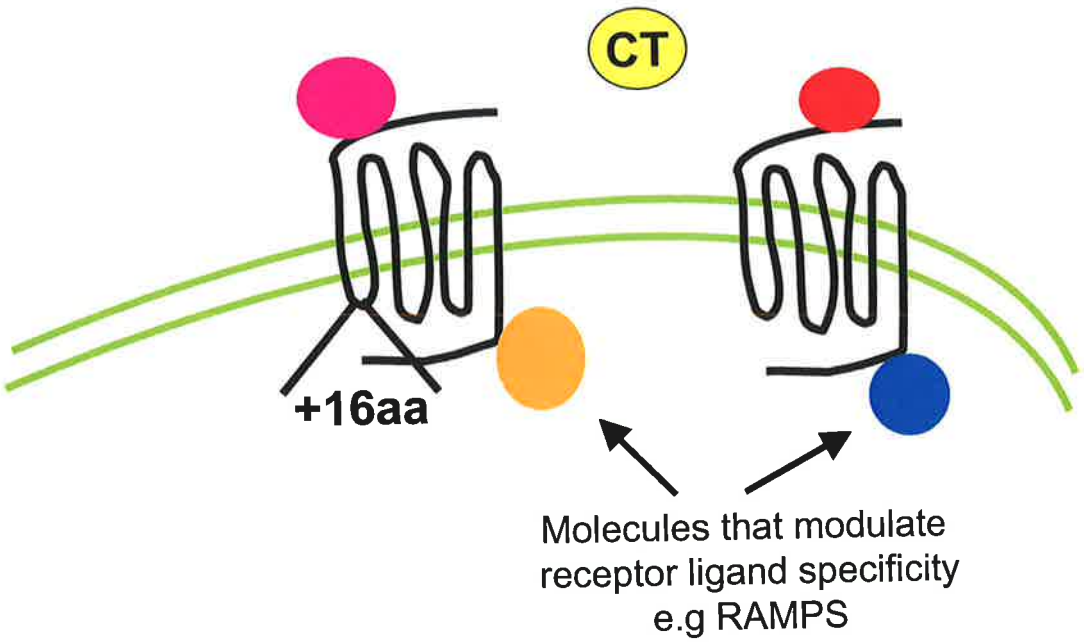

For example, immunoprecipitation studies have not been possible, as they require antibodies that recognise the individual CTR isoforms. Even with such reagents, the question remains as to whether the postulated interaction between the two receptor isoforms would survive immunoprecipitation. An alternative approach to identifying interactions between cell surface receptor, on living cells has recently been reported for the TNF receptor family *(Chan et al., 2000)* and the β2-adrenergic GPCR *(Angers et al., 2000)*. The fluorescence resonance energy transfer technique (FRET) *(Siegel et al., 2000)* involves generating fusion proteins between the receptor of interest and variants of the green fluorescent proteins. Transfection and expression of these constructs in cells, is followed by FACS analysis to identify receptor interactions on the surface of the cells. This technique would be an appropriate way to investigate the postulated interaction between the insert +ve and –ve hCTR isoforms.

The recent identification of molecules that modulate the "phenotype" of GPCR, for example RAMPS (discussed in section 1.2.5 and shown schematically in figure 9.1) is another area of investigation, which may identify novel physiological actions for the specific CTR isoforms.

In summary, the studies presented here have identified novel actions of the CTR with respect to growth regulation, however these growth relationships remain to be examined in other CTR-cells, in particular cancer cells (as discussed in chapter 5). A full understanding of the specific biological significance of the CTR isoforms, including their ability to regulate cell growth within the body, will require a greater appreciation for how the CTR interacts with the increasing number of accessory proteins that regulate GPCR, for example RAMPS, arrestins and GRK's, as well as other yet to be identified molecules.

# Bibliography

Aguda BD. 1999 A quantitative analysis of the kinetics of the G(2) DNA damage checkpoint system. *Proc Natl Acad Sci U S A* 96 (20): 11352-7.

Alam AS, Bax CM, Shankar VS, Bax BE, Bevis PJ, Huang CL, Moonga BS, Pazianas M and Zaidi M. 1993a Further studies on the mode of action of calcitonin on isolated rat osteoclasts: pharmacological evidence for a second site mediating intracellular $Ca^{2+}$ mobilization and cell retraction. *J Endocrinol* 136 (1): 7-15.

Alam AS, Moonga BS, Bevis PJ, Huang CL and Zaidi M. 1993b Amylin inhibits bone resorption by a direct effect on the motility of rat osteoclasts. *Exp Physiol* 78 (2): 183-96.

Albrandt K, Brady EM, Moore CX, Mull E, Sierzega ME and Beaumont K. 1995 Molecular cloning and functional expression of a third isoform of the human calcitonin receptor and partial characterization of the calcitonin receptor gene. *Endocrinology* 136 (12): 5377-84.

Albrandt K, Mull E, Brady EM, Herich J, Moore CX and Beaumont K. 1993 Molecular cloning of two receptors from rat brain with high affinity for salmon calcitonin. *FEBS Lett* 325 (3): 225-32.

Alessandrini A, Brott BK and Erikson RL. 1997 Differential expression of MEK1 and MEK2 during mouse development. *Cell Growth Differ* 8 (5): 505-11.

Almasan A, Yin Y, Kelly RE, Lee EY, Bradley A, Li W, Bertino JR and Wahl GM. 1995 Deficiency of retinoblastoma protein leads to inappropriate S-phase entry, activation of E2F-responsive genes, and apoptosis. *Proc Natl Acad Sci U S A* 92 (12): 5436-40.

Amara SG, Jonas V, Rosenfeld MG, Ong ES and Evans RM. 1982 Alternative RNA processing in calcitonin gene expression generates mRNAs encoding different polypeptide products. *Nature* 298 (5871): 240-4.

Anger S, Salahpour A, Joly E, Hilairet S, Chelsky D, Dennis M and Bouvier M. Detection of beta 2-adrenergic receptor dimerization in living cells using bioluminescence resonance energy transfer (BRET). *Proc Natl Acad Sci USA.* 97 (7): 3684-9.

Auer KL, Spector MS, Tombes RM, Seth P, Fisher PB, Gao B, Dent P and Kunos G. 1998 Alpha-adrenergic inhibition of proliferation in HepG2 cells stably transfected with the alpha1B-adrenergic receptor through a p42MAPkinase/p21Cip1/WAF1-dependent pathway. *FEBS Lett* 436 (1): 131-8.

Ballou LM, Cross M E, Huang S, McReynolds EM, Zhang B X and Lin RZ. 2000 Differential regulation of the phosphatidylinositol 3-kinase/ Akt and p70 S6 kinase pathways by the alpha(1A)-adrenergic receptor in rat-1 fibroblasts. *J Biol Chem* 275 (7): 4803-9.

Barlic J, Khandaker MH, Mahon E, Andrews J, DeVries ME, Mitchell GB, Rahimpour R, Tan CM, Ferguson SS and Kelvin DJ. 1999 beta-arrestins regulate interleukin-8-induced Cxcr1 internalization. *J Biol Chem* 274 (23): 16287-94.

Barrett MG, Belinsky GS and Tashjian AH, Jr. 1997 A new action of parathyroid hormone. Receptor-mediated stimulation of extracellular acidification in human osteoblast- like SaOS-2 cells. *J Biol Chem* 272 (42): 26346-53.

Bates S, Rowan S and Vousden KH. 1996 Characterisation of human cyclin G1 and G2: DNA damage inducible genes. *Oncogene* 13 (5): 1103-9.

Beaudreuil J, Taboulet J, Oracel P, Graulet AM, Denne MA, Baudoin C, Jullienne A and De Vernejoul MC. 2000 Calcitonin receptor mRNA in mononuclear Leucocytes from postmenopausal women: decrease during osteoporosis and link to bone markers with specific isoform involvement. *Bone* 27 (1): 161-168.

Beaumont K, Kenney MA, Young AA and Rink TJ. 1993 High affinity amylin binding sites in rat brain. *Mol Pharmacol* 44 (3): 493-7.

Becker KL, Geelhoed G, W ON, Monaghan KG, Snider RH, Moore CF and Silva OL. 1980 Calcitonin in tissues of thyroidectomized monkey. *Experientia* 36 (5): 609-10.

Becker KL, Snider RH, Moore CF, Monoghan KG and Silva OL. 1979 Calcitonin in extrathyroidal tissues of man. *Acta Endocrinol (Copenh)* 92 (4): 746-51.

Berridge MJ and Irvine RF. 1989 Inositol phosphates and cell signalling. *Nature* 341 (6239): 197-205.

Biggs JR, Kudlow JE and Kraft AS. 1996 The role of the transcription factor Sp1 in regulating the expression of the WAF1/CIP1 gene in U937 leukemic cells. *J Biol Chem* 271 (2): 901-6.

Black AR, Jensen D, Lin SY and Azizkhan JC. 1999 Growth/cell cycle regulation of Sp1 phosphorylation. *J Biol Chem* 274 (3): 1207-15.

Boekhoff I, Inglese J, Schleicher S, Koch WJ, Lefkowitz RJ and Breer H. 1994 Olfactory desensitization requires membrane targeting of receptor kinase mediated by beta gamma-subunits of heterotrimeric G proteins. *J Biol Chem* 269 (1): 37-40.

Born W and Fischer JA (1993). Calcitonin gene products: molecular biology, chemistry and actions. Handbook of Experimental Pharmacology, Physiology and Pharmacology of Bone. Mundy GR and Martin TJ. Berlin, Springer-Verlag: 569-616.

Brewer HB, Jr., Keutmann HT, Potts JT, Jr., Reisfeld RA, Schlueter R and Munson PL. 1968 Isolation and chemical properties of porcine thyrocalcitonin. *J Biol Chem* 243 (21): 5739-47.

Bünemann M and Hosey MM. 1999 G-protein coupled receptor kinases as modulators of G-protein signalling. *J Physiol (Lond)* 517 (Pt 1): 5-23.

Bunz F, Dutriaux A, Lengauer C, Waldman T, Zhou S, Brown JP, Sedivy JM, Kinzler KW and Vogelstein B. 1998 Requirement for p53 and p21 to sustain G2 arrest after DNA damage. *Science* 282 (5393): 1497-501.

Camps M, Hou C, Sidiropoulos D, Stock JB, Jakobs KH and Gierschik P. 1992 Stimulation of phospholipase C by guanine-nucleotide-binding protein beta gamma subunits. *Eur J Biochem* 206 (3): 821-31.

Cayrol C, Knibiehler M and Ducommun B. 1998 p21 binding to PCNA causes G1 and G2 cell cycle arrest in p53-deficient cells. *Oncogene* 16 (3): 311-20.

Chabardes D, Gagnan Brunette M, Imbert Teboul M, Gontcharevskaia O, Montegut M, Clique A and Morel F. 1980 Adenylate cyclase responsiveness to hormones in various portions of the human nephron. *J Clin Invest.* 65 (2): 439-48.

Chabre O, Conklin BR, Lin HY, Lodish HF, Wilson E, Ives HE, Catanzariti L, Hemmings BA and Bourne HR. 1992 A recombinant calcitonin receptor independently stimulates 3',5'-cyclic adenosine monophosphate and $Ca^{2+}$/inositol phosphate signaling pathways. *Mol Endocrinol* 6 (4): 551-6.

Chabre O, Cornillon F, Bottari SP, Chambaz EM and Vilgrain I. 1995 Hormonal regulation of mitogen-activated protein kinase activity in bovine adrenocortical cells: cross-talk between phosphoinositides, adenosine 3',5'-monophosphate, and tyrosine kinase receptor pathways. *Endocrinology* 136 (3): 956-64.

Chai SY, Christopoulos G, Cooper ME and Sexton PM. 1998 Characterization of binding sites for amylin, calcitonin, and CGRP in primate kidney. *Am J Physiol* 274 (1 Pt 2): F51-62.

Chakraborty M, Chatterjee D, Kellokumpu S, Rasmussen H and Baron R. 1991 Cell cycle-dependent coupling of the calcitonin receptor to different G proteins. *Science* 251 (4997): 1078-82.

Chambard JC, Paris S, G LA and Pouysségur J. 1987 Two growth factor signalling pathways in fibroblasts distinguished by pertussis toxin. *Nature* 326 (6115): 800-3.

Chambers TJ, and Magnus, C.J. 1982 Calcitonin alters behaviour of isolated osteoclasts. *J Pathol* 136 27-39.

Chambers TJ and Dunn CJ. 1983 Pharmacological control of osteoclastic motility. *Calcif Tissue Int* 35 (4-5): 566-70.

Chan F, Chun H, Zheng L, Siegel R, Bui K, Lenardo M 2000 A Domain in the TNF Receptor that mediates ligand-independent receptor assembly and signaling *Science* 288: 2351-2354.

Chance WT, Balasubramaniam A, Chen X *et al.,* 1992 Tests od adipsia and conditioned taste aversion following the intrahypothalamic injection of amylin. *Peptides* 13: 961-4.

Chang M, Zhang L, Tam JP and Sanders Bush E. 2000 Dissecting G protein-coupled receptor signaling pathways with membrane-permeable blocking peptides. Endogenous 5- HT(2C) receptors in choroid plexus epithelial cells. *J Biol Chem* 275 (10): 7021-9.

Chao WT and Forte LR. 1983 Rat kidney cells in primary culture: interaction of salmon calcitonin with receptor sites. *Endocrinology* 112 (2): 745-52.

Chausmer AB, Stevens MD and Severn C. 1982 Autoradiographic evidence for a calcitonin receptor on testicular Leydig cells. *Science* 216 (4547): 735-6.

Chen J, Jackson PK, Kirschner MW and Dutta A. 1995 Separate domains of p21 involved in the inhibition of Cdk kinase and PCNA. *Nature* 374 (6520): 386-8.

Chen Y, Shyu JF, Santhanagopal A, Inoue D, David JP, Dixon SJ, Horne WC and Baron R. 1998 The calcitonin receptor stimulates Shc tyrosine phosphorylation and Erk1/2 activation. Involvement of Gi, protein kinase C, and calcium. *J Biol Chem* 273 (31): 19809-16.

Cho Chung YS. 1990 Role of cyclic AMP receptor proteins in growth, differentiation, and suppression of malignancy: new approaches to therapy. *Cancer Res* 50 (22): 7093-100.

Christopoulos G, Paxinos G, Huang XF, Beaumont K, Toga AW and Sexton PM. 1995 Comparative distribution of receptors for amylin and the related peptides calcitonin gene related peptide and calcitonin in rat and monkey brain. *Can J Physiol Pharmacol* 73 (7): 1037-41.

Christopoulos G, Perry KJ, Morfis M, Tilakaratne N, Gao Y, Fraser NJ, Main MJ, Foord SM and Sexton PM. 1999 Multiple amylin receptors arise from receptor activity- modifying protein interaction with the calcitonin receptor gene product. *Mol Pharmacol* 56 (1): 235-42.

Coats S, Flanagan WM, Nourse J and Roberts JM. 1996 Requirement of p27Kip1 for restriction point control of the fibroblast cell cycle. *Science* 272 (5263): 877-80.

Cochran M, Peacock M, Sachs G and Nordin BE. 1970 Renal effects of calcitonin. *Br Med J* 1 (689): 135-7.

Coffman FD and Studzinski GP. 1999 Differentiation-related mechanisms which suppress DNA replication. *Exp Cell Res* 248 (1): 58-73.

Cole J. 1999 Parathyroid hormone activates mitogen activated protein kinase in opossum kidney cells. *Endocrinology* 140 (12): 5771-79

Collins K, Jacks T and Pavletich NP. 1997 The cell cycle and cancer. *Proc Natl Acad Sci U S A* 94 (7): 2776-8.

Cooper C, Hirsch P and Troverud S. 1967 An improved method for the biological assay of thyrocalcitonin. *Endicrinology* 81 610-617.

Copp DH, Cameron EC and Cheney BA. 1962 Evidence for calcitonin - a new hormone from the parathyroid that lowers blood calcium. *Endocrinology* 70 638-649.

Courey A and Tjian R (1992). Transcriptional Regulation. New York, Cold Spring Harbor Press.

Cowley S, Paterson H, Kemp P and Marshall CJ. 1994 Activation of MAP kinase kinase is necessary and sufficient for PC12 differentiation and for transformation of NIH 3T3 cells. *Cell* 77 (6): 841-52.

Cross DA and Smythe C. 1998 PD 98059 prevents establishment of the spindle assembly checkpoint and inhibits the G2-M transition in meiotic but not mitotic cell cycles in Xenopus. *Exp Cell Res* 241 (1): 12-22.

Cross MJ, Hodgkin MN, Plumb JA, Brunton VG, Stewart A, MacAully G, Hill R, Kerr DJ, Workman P and Wakelam MJ. 1997 Inhibition of phospholipid signalling and proliferation of Swiss 3T3 cells by the wortmannin analogue demethoxyviridin. *Biochim Biophys Acta* 1362 (1): 29-38.

Datto MB, Yu Y and Wang XF. 1995 Functional analysis of the transforming growth factor beta responsive elements in the WAF1/Cip1/p21 promoter. *J Biol Chem* 270 (48): 28623-8.

Davis NS, DiSantAgnese PA, Ewing JF and Mooney RA. 1989 The neuroendocrine prostate: characterization and quantitation of calcitonin in the human gland. *J Urol* 142 (3): 884-8.

Dayer JM, Vassalli JD, Bobbitt JL, Hull RN, Reich E and Krane SM. 1981 Calcitonin stimulates plasminogen activator in porcine renal tubular cells: LLC-PK1. *J Cell Biol* 91 (1): 195-200.

Desai D, Gu Y and Morgan DO. 1992 Activation of human cyclin-dependent kinases *in vitro*. *Mol Biol Cell* 3 (5): 571-82.

Dhanasekaran N, Heasley LE and Johnson GL. 1995 G protein-coupled receptor systems involved in cell growth and oncogenesis. *Endocr Rev* 16 (3): 259-70.

Dhanasekaran N, Tsim ST, Dermott JM and Onesime D. 1998 Regulation of cell proliferation by G proteins. *Oncogene* 17 (11): 1383-94.

Dulic V, Stein GH, Far DF and Reed SI. 1998 Nuclear accumulation of p21Cip1 at the onset of mitosis: a role at the G2/M-phase transition. *Mol Cell Biol* 18 (1): 546-57.

Dunlay R and Hruska K. 1990 PTH receptor coupling to phospholipase C is an alternate pathway of signal transduction in bone and kidney. *Am J Physiol* 258 (2 Pt 2): F223-31.

Eguchi S, Numaguchi K, Iwasaki H, Matsumoto T, Yamakawa T, Utsunomiya H, Motley ED, Kawamura M, Owada KM, Hirata Y, Marumo F and Inagami T. 1988 Calcium-dependent epidermal growth factor receptor transactivation mediates the angiotensin II-induced mitogen activated potein kinase activation in vascular smooth muscle cells. *J Biol Chem* 273: 8890-6.

Fabbri A, Fraioli F, Pert CB *et al.* 1985 Calcitonin receptors in the rat mesencephalon mediate its analgesic actions: Autoradiogaphic and behavioural analyses. *Brain Res* 343: 205-15.

Farley JR, Tarbaux NM, Hall SL, Linkhart TA and Baylink DJ. 1988 The anti-bone-resorptive agent calcitonin also acts *in vitro* to directly increase bone formation and bone cell proliferation. *Endocrinology* 123 (1): 159-67.

Farley JR, Wergedal JE, Hall SL, Herring S and Tarbaux NM. 1991 Calcitonin has direct effects on 3[H]-thymidine incorporation and alkaline phosphatase activity in human osteoblast-line cells. *Calcif Tissue Int* 48 (5): 297-301.

Findlay DM, deLuise M, Michelangeli VP, Ellison M and Martin TJ. 1980a Properties of a calcitonin receptor and adenylate cyclase in BEN cells, a human cancer cell line. *Cancer Res* 40 (4): 1311-7.

Findlay DM, Houssami S, Christopoulos G and Sexton PM. 1996 Homologous regulation of the rat C1a calcitonin receptor (CTR) in nonosteoclastic cells is independent of CTR messenger ribonucleic acid changes and cyclic adenosine 3',5'-monophosphate- dependent protein kinase activation. *Endocrinology* 137 (11): 4576-85.

Findlay DM, Houssami S, Lin HY, Myers DE, Brady CL, Darcy PK, Ikeda K, Martin TJ and Sexton PM. 1994 Truncation of the porcine calcitonin receptor cytoplasmic tail inhibits internalization and signal transduction but increases receptor affinity. *Mol Endocrinol* 8 (12): 1691-700.

Findlay DM, Houssami S, Sexton PM, Brady CL, Martin TJ and Myers DE. 1995 Calcium inflow in cells transfected with cloned rat and porcine calcitonin receptors. *Biochim Biophys Acta* 1265 (2-3): 213-9.

Findlay DM and Martin TJ. 1984 Relationship between internalization and calcitonin-induced receptor loss in T47D cells. *Endocrinology* 115 (1): 78-83.

Findlay DM, Michelangeli VP, Eisman JA, Frampton RJ, Moseley JM, MacIntyre I, Whitehead R and Martin TJ. 1980b Calcitonin and 1,25-dihydroxyvitamin D3 receptors in human breast cancer cell lines. *Cancer Res* 40 (12): 4764-7.

Findlay DM, Michelangeli VP, Moseley JM and Martin TJ. 1981 Calcitonin binding and degradation by two cultured human breast cancer cell lines (MCF7 and T47D). *Biochem J* 196 (2): 513-20.

Findlay DM, Michelangeli VP, Orlowski RC and Martin TJ. 1983 Biological activities and receptor interactions of des- Leu16 salmon and des-Phe16 human calcitonin. *Endocrinology* 112 (4): 1288-91.

Firsov D, Bellanger AC, Marsy S and Elalouf JM. 1995 Quantitative RT-PCR analysis of calcitonin receptor mRNAs in the rat nephron. *Am J Physiol* 269 (5 Pt 2): F702-9.

Fischer JA, Sagar SM and Martin JB. 1981a Characterization and regional distribution of calcitonin binding sites in the rat brain. *Life Sci* 29 (7): 663-71.

Fischer JA, Tobler PH, Henke H and Tschopp FA. 1983 Salmon and human calcitonin-like peptides coexist in the human thyroid and brain. *J Clin Endocrinol Metab* 57 (6): 1314-6.

Fischer JA, Tobler PH, Kaufmann M, Born W, Henke H, Cooper PE, Sagar SM and Martin JB. 1981b Calcitonin: regional distribution of the hormone and its binding sites in the human brain and pituitary. *Proc Natl Acad Sci USA* 78 (12): 7801-5.

Flynn JJ, Margules DL and Cooper CW. 1981 Presence of immunoreactive calcitonin in the hypothalamus and pituitary lobes of rats. *Brain Res Bull* 6 (6): 547-9.

Force T, Bonventre JV, Flannery MR, Gorn AH, Yamin M and Goldring SR. 1992 A cloned porcine renal calcitonin receptor couples to adenylyl cyclase and phospholipase C. *Am J Physiol* 262 (6 Pt 2): F1110-5.

Forrest SM, Ng KW, Findlay DM, Michelangeli VP, Livesey SA, Partridge NC, Zajac JD and Martin TJ. 1985 Characterization of an osteoblast-like clonal cell line which responds to both parathyroid hormone and calcitonin. *Calcif Tissue Int* 37 (1): 51-6.

Foster GV, Baghdiantz A and Kumar M. 1964 Thyroidal origin of calcitonin. *Nature* 202 1303.

Foster GV, MacIntyre I and Pearse AGE. 1965 Calcitonin production and the mitochondrion-rich cells of the dog thyroid. *Nature* 202 1029-1031.

Fraser NJ, Wise A, Brown J, McLatchie LM, Main MJ and Foord SM. 1999 The amino terminus of receptor activity modifying proteins is a critical determinant of glycosylation state and ligand binding of calcitonin receptor-like receptor. *Mol Pharmacol* 55 (6): 1054-9.

Fritsch HA, Van Noorden S and Pearse AG. 1979 Localization of somatostatin-, substance P- and calcitonin- like immunoreactivity in the neural ganglion of *Ciona intestinalis L. (Ascidiaceae). Cell Tissue Res* 202 (2): 263-74.

Gartel AL and Tyner AL. 1999 Transcriptional regulation of the p21(WAF1/CIP1) gene. *Exp Cell Res* 246 (2): 280-9.

Gill G, Pascal E, Tseng ZH and Tjian R. 1994 A glutamine-rich hydrophobic patch in transcription factor Sp1 contacts the dTAFII110 component of the Drosophila TFIID complex and mediates transcriptional activation. *Proc Natl Acad Sci U S A* 91 (1): 192-6.

Gillespie MT, Thomas RJ, Pu ZY, Zhou H, Martin TJ and Findlay DM. 1997 Calcitonin receptors, bone sialoprotein and osteopontin are expressed in primary breast cancers. *Int J Cancer* 73 (6): 812-5.

Girgis SI, Galan FG, Arnett TR, Rogers RM, Bone Q, Ravazzola M and MacIntyre I. 1980 Immunoreactive human calcitonin-like molecule in the nervous systems of protochordates and a cyclostome, *Myxine. J Endocrinol* 87 (3): 375-82.

Gorn AH, Lin HY, Yamin M, Auron PE, Flannery MR, Tapp DR, Manning CA, Lodish HF, Krane SM and Goldring SR. 1992 Cloning, characterization, and expression of a human calcitonin receptor from an ovarian carcinoma cell line. *J Clin Invest* 90 (5): 1726-35.

Gorn AH, Rudolph SM, Flannery MR, Morton CC, Weremowicz S, Wang TZ, Krane SM and Goldring SR. 1995 Expression of two human skeletal calcitonin receptor isoforms cloned from a giant cell tumor of bone. The first intracellular domain modulates ligand binding and signal transduction. *J Clin Invest* 95 (6): 2680-91.

Grynkiewicz G, Poenie M and Tsien R.Y. 1985 A new generation of $Ca^{2+}$ indicators with greatly improved fluorescence properties. *J Biol Chem* 260 (6): 3440-60

Guadagno TM and Newport JW. 1996 Cdk2 kinase is required for entry into mitosis as a positive regulator of Cdc2-cyclin B kinase activity. *Cell* 84 (1): 73-82.

Guidobono F, Bettica P, Villa I, Pagani F, Netti C, Sibilia V and Pecile A. 1991 Treatment with pertussis toxin does not prevent central effects of eel calcitonin. *Peptides* 12 (3): 549-53.

Guidobono F, Netti C, Pecile A, Gritti I and Mancia M. 1987 Calcitonin binding site distribution in the cat central nervous system: a wider insight of the peptide involvement in brain functions. *Neuropeptides* 10 (3): 265-73.

Guidobono F, Netti C, Sibilia V and Pecile A. 1985 Eel calcitonin binding site distribution and antinociceptive activity in rats. *Peptides* 7: 315-22.

Gutkind JS. 1998 Cell growth control by G protein-coupled receptors: from signal transduction to signal integration. *Oncogene* 17 (11 Reviews): 1331-42.

Hall A. 1998 Rho GTPases and the actin cytoskeleton. *Science* 279 (5350): 509-14.

Hall M, Bates S and Peters G. 1995 Evidence for different modes of action of cyclin-dependent kinase inhibitors: p15 and p16 bind to kinases, p21 and p27 bind to cyclins. *Oncogene* 11 (8): 1581-8.

Hall RA, Ostedgaard LS, Premont RT, Blitzer JT, Rahman N, Welsh MJ and Lefkowitz RJ. 1998b A C-terminal motif found in the beta2-adrenergic receptor, P2Y1 receptor and cystic fibrosis transmembrane conductance regulator determines binding to the $Na^+/H^+$ exchanger regulatory factor family of PDZ proteins. *Proc Natl Acad Sci USA* 95 (15): 8496-501.

Hall RA, Premont RT, Chow CW, Blitzer JT, Pitcher JA, Claing A, Stoffel RH, Barak LS, Shenolikar S, Weinman EJ, Grinstein S and Lefkowitz RJ. 1998a The beta2-adrenergic receptor interacts with the $Na^+/H^+$ -exchanger regulatory factor to control $Na^+/H^+$ exchange. *Nature* 392 (6676): 626-30.

Halliday DA, McNeil JD, Betts WH and Scicchitano R. 1993 The substance P fragment SP-(7-11) increases prostaglandin E2, intracellular Ca2+ and collagenase production in bovine articular chondrocytes. *Biochem J* 292: 57-62.

Han I and Kudlow JE. 1997 Reduced O glycosylation of Sp1 is associated with increased proteasome susceptibility. *Mol Cell Biol* 17 (5): 2550-8.

Harper JW, Elledge SJ, Keyomarsi K, Dynlacht B, Tsai LH, Zhang P, Dobrowolski S, Bai C, Connell Crowley L, Swindell E and et al. 1995 Inhibition of cyclin-dependent kinases by p21. *Mol Biol Cell* 6 (4): 387-400.

Henke H, Tobler PH and Fischer JA. 1983 Localization of salmon calcitonin binding sites in rat brain by autoradiography. *Brain Res* 272 (2): 373-7.

Henke H, Tschopp FA and Fischer JA. 1985 Distinct binding sites for calcitonin gene-related peptide and salmon calcitonin in rat central nervous system. *Brain Res* 360 (1-2): 165-71.

Herrera R, Hubbell S, Decker S and Petruzzelli L. 1998 A role for the MEK/MAPK pathway in PMA-induced cell cycle arrest: modulation of megakaryocytic differentiation of K562 cells. *Exp Cell Res* 238 (2): 407-14.

Hilton JM, Chai SY and Sexton PM. 1995 *In vitro* autoradiographic localization of the calcitonin receptor isoforms, C1a and C1b, in rat brain. *Neuroscience* 69 (4): 1223-37.

Hilton JM, Mitchelhill KI, Pozvek G, Dowton M, Quiza M and Sexton PM. 1998 Purification of calcitonin-like peptides from rat brain and pituitary. *Endocrinology* 139 (3): 982-92.

Hirai H, Roussel MF, Kato JY, Ashmun RA and Sherr CJ. 1995 Novel INK4 proteins, p19 and p18, are specific inhibitors of the cyclin D-dependent kinases CDK4 and CDK6. *Mol Cell Biol* 15 (5): 2672-81.

Hirano F, Tanaka H, Hirano Y, Hiramoto M, Handa H, Makino I and Scheidereit C. 1998 Functional interference of Sp1 and NF-kappaB through the same DNA binding site. *Mol Cell Biol* 18 (3): 1266-74.

Hirsch PF, Gauthier GF and Munson PL. 1963 Thyroid hypocalcaemic principle and recurrent laryngeal nerve injury as factors affecting response to parathyroidectomy in rats. *Endocrinology* 73: 244-351.

Homma T, Watanabe M, Hirose S, Kanai A, Kangawa K and Matsuo H. 1986 Isolation and determination of the amino acid sequence of chicken calcitonin I from chicken ultimobranchial glands. *J Biochem (Tokyo)* 100 (2): 459-67.

Hoovers JM, Redeker E, Speleman F, JW Hö, Bhola S, Bliek J, van Roy N, Leschot NJ, Westerveld A and Mannens M. 1993 High-resolution chromosomal localization of the human calcitonin/ CGRP/IAPP gene family members. *Genomics* 15 (3): 525-9.

Horie K and Insel PA. Retrovirally-mediated transfer of G protein-coupled receptor dominant-negative mutant enhances endogenous calcitonin receptor signaling in chinease hamster ovary cells. 2000. JBC paper in press manuscript no. M003413200.

Hosking DJ and Gilson D. 1984 Comparison of the renal and skeletal actions of calcitonin in the treatment of severe hypercalcaemia of malignancy. *Q J Med* 53 (211): 359-68.

Houssami S, Findlay DM, Brady CL, Martin TJ, Epand RM, Moore EE, Murayama E, Tamura T, Orlowski RC and Sexton PM. 1995 Divergent structural requirements exist for calcitonin receptor binding specificity and adenylate cyclase activation. *Mol Pharmacol* 47 (4): 798-809.

Houssami S, Findlay DM, Brady CL, Myers DE, Martin TJ and Sexton PM. 1994 Isoforms of the rat calcitonin receptor: consequences for ligand binding and signal transduction. *Endocrinology* 135 (1): 183-90.

Hunt NH, Ellison M, Underwood JC and Martin TJ. 1977 Calcitonin-responsive adenylate cyclase in a calcitonin- producing human cancer cell line. *Br J Cancer* 35 (6): 777-84.

Ikegame M, Rakopoulos M, Martin TJ, Moseley JM and Findlay DM. 1996 Effects of continuous calcitonin treatment on osteoclast- like cell development and calcitonin receptor expression in mouse bone marrow cultures. *J Bone Miner Res* 11 (4): 456-65.

Inoue D, Shih C, Galson DL, Goldring SR, Horne WC and Baron R. 1999 Calcitonin-dependent down-regulation of the mouse C1a calcitonin receptor in cells of the osteoclast lineage involves a transcriptional mechanism. *Endocrinology* 140 (3): 1060-8.

Jacobs JW, Simpson E, Penschow J, Hudson P, Coghlan J and Niall H. 1983 Characterization and localization of calcitonin messenger ribonucleic acid in rat thyroid. *Endocrinology* 113 (5): 1616-22.

Jagger C, Gallagher A, Chambers T and Pondel M. 1999 The porcine calcitonin receptor promoter directs expression of a linked reporter gene in a tissue and developmental specific manner in transgenic mice. *Endocrinology* 140 (1): 492-9.

Jans DA, Gajdas EL, Dierks Ventling C, Hemmings BA and Fahrenholz F. 1987 Long-term stimulation of cAMP production in LLC-PK1 pig kidney epithelial cells by salmon calcitonin or a photoactivatable analogue of vasopressin. *Biochim Biophys Acta* 930 (3): 392-400.

Johnson GL and Vaillancourt RR. 1994 Sequential protein kinase reactions controlling cell growth and differentiation. *Curr Opin Cell Biol* 6 (2): 230-8.

Jonas V, Lin CR, Kawashima E, Semon D, Swanson LW, Mermod JJ, Evans RM and Rosenfeld MG. 1985 Alternative RNA processing events in human calcitonin/calcitonin gene-related peptide gene expression. *Proc Natl Acad Sci USA* 82 (7): 1994-8.

Jordan BA and Devi LA. 1999 G-protein-coupled receptor heterodimerization modulates receptor function. *Nature* 399 (6737): 697-700.

Kahn A, Jr. 1968 Bone metabolism, thyrocalcitonin, and parathyroid hormone. *J Ark Med Soc* 64 (9): 337-8.

Kallio DM, Garant PR and Minkin C. 1972 Ultrastructural effects of calcitonin on osteoclasts in tissue culture. *J Ultrastruct Res* 39 (3): 205-16.

Kalu DN and Foster GV. 1971 Effect of calcitonin on (3H)proline incorporation into bone hydroxyproline in the rat. *J Endocrinol* 49 (2): 233-41.

Kardassis D, Papakosta P, Pardali K and Moustakas A. 1999 c-Jun transactivates the promoter of the human p21(Waf1/ Cip1) gene by acting as a superactivator of the ubiquitous transcription factor Sp1. *J Biol Chem* 274 (41): 29572-81.

Kennett SB, Udvadia AJ and Horowitz JM. 1997 Sp3 encodes multiple proteins that differ in their capacity to stimulate or repress transcription. *Nucleic Acids Res* 25 (15): 3110-7.

Koida M, Nakamuta H, Furukawa S and Orlowski RC. 1980 Abundance and location of 125-I-salmon calcitonin binding site in rat brain. *Jpn J Pharmacol* 30 (4): 575-7.

Krek W and Nigg EA. 1991 Differential phosphorylation of vertebrate p34cdc2 kinase at the G1/S and G2/M transitions of the cell cycle: identification of major phosphorylation sites. *Embo J* 10 (2): 305-16.

Kuestner RE, Elrod RD, Grant FJ, Hagen FS, Kuijper JL, Matthewes SL, PJ OH, Sheppard PO, Stroop SD, Thompson DL and et al. 1994 Cloning and characterization of an abundant subtype of the human calcitonin receptor. *Mol Pharmacol* 46 (2): 246-55.

Kumar MA, Foster GV and MacIntyre I. 1963 Furthur evidence for calcitonin. A rapid-acting hormone which lowers calcium. *Lancet* 2 480-482.

LaBaer J, Garrett MD, Stevenson LF, Slingerland JM, Sandhu C, Chou HS, Fattaey A and Harlow E. 1997 New functional activities for the p21 family of CDK inhibitors. *Genes Dev* 11 (7): 847-62.

Lallemand F, Courilleau D, Buquet Fagot C, Atfi A, Montagne MN and Mester J. 1999 Sodium butyrate induces G2 arrest in the human breast cancer cells MDA-MB-231 and renders them competent for DNA rereplication. *Exp Cell Res* 247 (2): 432-40.

Le Gouill C, Parent JL, Caron CA, Gaudreau R, Volkov L, Rola Pleszczynski M and Stanková J. 1999 Selective modulation of wild type receptor functions by mutants of G-protein-coupled receptors. *J Biol Chem* 274 (18): 12548-54.

Lee CH, Park D, Wu D, Rhee SG and Simon MI. 1992 Members of the Gq alpha subunit gene family activate phospholipase C beta isozymes. *J Biol Chem* 267 (23): 16044-7.

Lee JS, Galvin KM and Shi Y. 1993 Evidence for physical interaction between the zinc-finger transcription factors YY1 and Sp1. *Proc Natl Acad Sci USA* 90 (13): 6145-9.

Lee K, Lanske B, Karaplis AC, Deeds JD, Kohno H, Nissenson RA, Kronenberg HM and Segre GV. 1996 Parathyroid hormone-related peptide delays terminal differentiation of chondrocytes during endochondral bone development. *Endocrinology* 137 (11): 5109-18.

Letterio JJ, Coughlin SR and Williams LT. 1986 Pertussis toxin-sensitive pathway in the stimulation of c-myc expression and DNA synthesis by bombesin. *Science* 234 (4780): 1117-9.

Li W, Fan J, Banerjee D and Bertino JR. 1999 Overexpression of p21(waf1) decreases G2-M arrest and apoptosis induced by paclitaxel in human sarcoma cells lacking both p53 and functional Rb protein. *Mol Pharmacol* 55 (6): 1088-93.

Li Y, Jenkins CW, Nichols MA and Xiong Y. 1994 Cell cycle expression and p53 regulation of the cyclin- dependent kinase inhibitor p21. *Oncogene* 9 (8): 2261-8.

Lin HY, Harris TL, Flannery MS, Aruffo A, Kaji EH, Gorn A, Kolakowski LF, Jr., Lodish HF and Goldring SR. 1991a Expression cloning of an adenylate cyclase-coupled calcitonin receptor. *Science* 254 (5034): 1022-4.

Lin HY, Harris TL, Flannery MS, Aruffo A, Kaji EH, Gorn A, Kolakowski LF, Jr., Yamin M, Lodish HF and Goldring SR. 1991b Expression cloning and characterization of a porcine renal calcitonin receptor. *Trans Assoc Am Physicians* 104: 265-72.

Lin SY, Black AR, Kostic D, Pajovic S, Hoover CN and Azizkhan JC. 1996 Cell cycle-regulated association of E2F1 and Sp1 is related to their functional interaction. *Mol Cell Biol* 16 (4): 1668-75.

Liu F, Wan Q, Pristupa ZB, Yu XM, Wang YT and Niznik HB. 2000 Direct protein-protein coupling enables cross-talk between dopamine D5 and gamma-aminobutyric acid A receptors. *Nature* 403 (6767): 274-80.

Livesey SA, Collier G, Zajac JD, Kemp BE and Martin TJ. 1984 Characteristics of selective activation of cyclic AMP-dependent protein kinase isoenzymes by calcitonin and prostaglandin E2 in human breast cancer cells. *Biochem J* 224 (2): 361-70.

Loffler F, van Calker D and Hamprecht B. 1982 Parathyrin and calcitonin stimulate cyclic AMP accumulation in cultured murine brain cells. *EMBO J* 1: 297-302.

Logothetis DE, Kurachi Y, Galper J, Neer EJ and Clapham DE. 1987 The beta gamma subunits of GTP-binding proteins activate the muscarinic $K^+$ channel in heart. *Nature* 325 (6102): 321-6.

Lu N and DiCicco Bloom E. 1997 Pituitary adenylate cyclase-activating polypeptide is an autocrine inhibitor of mitosis in cultured cortical precursor cells. *Proc Natl Acad Sci USA* 94 (7): 3357-62.

Lu HK, Fern RJ, Luthin D, Linden J, Liu LP, Cohen CJ and Barrett PQ. 1996 Angiotensin II stimulates T-type $Ca^{2+}$ channel currents *via* activation of a G protein, $G_i$. *Am J Physiol* 271 (4): C1340-9.

Maggio R, Vogel Z and Wess J. 1993 Coexpression studies with mutant muscarinic/adrenergic receptors provide evidence for intermolecular "cross-talk" between G-protein-linked receptors. *Proc Natl Acad Sci USA* 90 (7): 3103-7.

Malgaroli A, Meldolesi J, Zallone AZ and Teti A. 1989 Control of cytosolic free calcium in rat and chicken osteoclasts. The role of extracellular calcium and calcitonin. *J Biol Chem* 264 (24): 14342-7.

Mansour SJ, Matten WT, Hermann AS, Candia JM, Rong S, Fukasawa K, Vande Woude GF and Ahn NG. 1994 Transformation of mammalian cells by constitutively active MAP kinase kinase. *Science* 265 (5174): 966-70.

Martin TJ, Findlay DM, MacIntyre I, Eisman JA, Michelangeli VP, Moseley JM and Partridge NC. 1980 Calcitonin receptors in a cloned human breast cancer cell line (MCF7). *Biochem Biophys Res Commun* 96 (1): 150-6.

Martin TJ and Melick RA. 1969 The acute effects of porcine calcitonin in man. *Australas Ann Med* 18 (3): 258-63.

Martin TJ, Robinson CJ and MacIntyre I. 1966 The mode of action of thyrocalcitonin. *Lancet* 1 (7443): 900-2.

Martin TJ, Findaly DM, Moseley JM, Sexton PM (1998). Calcitonin (chapter 4). Metabolic Bone Disease and Clinically Related Disorders. Avioli LV and Krane SM. San Diego, Academic Press.

Marx SJ and Aurbach GD. 1975 Renal receptors for calcitonin: coordinate occurrence with calcitonin-activated adenylate cyclase. *Endocrinology* 97 (2): 448-53.

Marx SJ, Aurbach GD, Gavin JRd and Buell DW. 1974 Calcitonin receptors on cultured human lymphocytes. *J Biol Chem* 249 (21): 6812-6.

Marx SJ, Woodward CJ and Aurbach GD. 1972 Calcitonin receptors of kidney and bone. *Science* 178 (64): 999-1001.

Matthews J, Martin J and Collins A (1972). Immediate changes in the ultrastructure of bone cells following thyrocalcitonin administration. Calcium, Parathyroid Hormone and the Calcitonins. Talmage R and Munson P. Amsterdam, Excerpta Medica: 375-382.

McGill G, Shimamura A, Bates RC, Savage RE and Fisher DE. 1997 Loss of matrix adhesion triggers rapid transformation-selective apoptosis in fibroblasts. *J Cell Biol* 138 (4): 901-11.

McLatchie LM, Fraser NJ, Main MJ, Wise A, Brown J, Thompson N, Solari R, Lee MG and Foord SM. 1998 RAMPs regulate the transport and ligand specificity of the calcitonin-receptor-like receptor. *Nature* 393 (6683): 333-9.

Meyerson M and Harlow E. 1994 Identification of G1 kinase activity for cdk6, a novel cyclin D partner. *Mol Cell Biol* 14 (3): 2077-86.

Michelangeli VP, Findlay DM, Moseley JM and Martin TJ. 1983 Mechanisms of calcitonin induction of prolonged activation of adenylate cyclase in human cancer cells. *J Cyclic Nucleotide Protein Phosphor Res* 9 (2): 129-41.

Michelangeli VP, Livesey SA and Martin TJ. 1984 Effects of pertussis toxin on adenylate cyclase responses to prostaglandin E2 and calcitonin in human breast cancer cells. *Biochem J* 224 (2): 371-7.

Michieli P, Chedid M, Lin D, Pierce JH, Mercer WE and Givol D. 1994 Induction of WAF1/CIP1 by a p53-independent pathway. *Cancer Res* 54 (13): 3391-5.

Mochizuki N, Ohba Y, Kiyokawa E, Kurata T, Murakami T, Ozaki T, Kitabatake A, Nagashima K and Matsuda M. 1999 Activation of the ERK/MAPK pathway by an isoform of rap1GAP associated with G alpha(i). *Nature* 400 (6747): 891-4.

Monnot C, Bihoreau C, Conchon S, Curnow KM, Corvol P and Clauser E. 1996 Polar residues in the transmembrane domains of the type 1 angiotensin II receptor are required for binding and coupling. Reconstitution of the binding site by co-expression of two deficient mutants. *J Biol Chem* 271 (3): 1507-13.

Moonga BS, Alam AS, Bevis PJ, Avaldi F, Soncini R, Huang CL and Zaidi M. 1992 Regulation of cytosolic free calcium in isolated rat osteoclasts by calcitonin. *J Endocrinol* 132 (2): 241-9.

Moore EE, Kuestner RE, Stroop SD, Grant FJ, Matthewes SL, Brady CL, Sexton PM and Findlay DM. 1995 Functionally different isoforms of the human calcitonin receptor result from alternative splicing of the gene transcript. *Mol Endocrinol* 9 (8): 959-68.

Morimoto T, Okamoto M, Koida M, Nakamuta H and Orlowski RC. 1984 Calcitonin-induced analgesia: an unusual hormone specificity. *Jpn J Pharmacol* 36 (4): 538-9.

Moseley JM, Findlay DM, Gorman JJ, Michelangeli VP and Martin TJ. 1983 The calcitonin receptor on T47D breast cancer cells. Evidence for glycosylation. *Biochem J* 212 (3): 609-16.

Mosselman S, JW Hö, Zandberg J, van Mansfeld AD, Geurts van Kessel AH, Lips CJ and Jansz HS. 1988 Islet amyloid polypeptide: identification and chromosomal localization of the human gene. *FEBS Lett* 239 (2): 227-32.

Moustakas A and Kardassis D. 1998 Regulation of the human p21/WAF1/Cip1 promoter in hepatic cells by functional interactions between Sp1 and Smad family members. *Proc Natl Acad Sci U S A* 95 (12): 6733-8.

Moustakas A and Stournaras C. 1999 Regulation of actin organisation by TGF-beta in H-ras-transformed fibroblasts. *J Cell Sci* 112 (Pt 8): 1169-79.

Muff R, N Bü, Fischer JA and Born W. 1999 An amylin receptor is revealed following co-transfection of a calcitonin receptor with receptor activity modifying proteins-1 or -3. *Endocrinology* 140 (6): 2924-7.

Murad F, Brewer HB, Jr. and Vaughan M. 1970 Effect of thyrocalcitonin on adenosine 3':5'-cyclic phosphate formation by rat kidney and bone. *Proc Natl Acad Sci U S A* 65 (2): 446-53.

Murayama A, Takeyama K, Kitanaka S, Kodera Y, Kawaguchi Y, Hosoya T and Kato S. 1999 Positive and negative regulations of the renal 25-hydroxyvitamin D3 1alpha-hydroxylase gene by parathyroid hormone, calcitonin, and 1alpha,25(OH)2D3 in intact animals. *Endocrinology* 140 (5): 2224-31.

Murphy E, Chamberlin ME and Mandel LJ. 1986 Effects of calcitonin on cytosolic $Ca^{2+}$ in a suspension of rabbit medullary thick ascending limb tubules. *Am J Physiol* 251 (4 Pt 1): C491-5.

Nakamoto H, Soeda Y, Takami S, Minami M and Satoh M. 2000 Localization of calcitonin receptor mRNA in the mouse brain: coexistence with serotonin transporter mRNA. *Mol Brain Res* 76 (1): 93-102.

Nakamura A, Yamatani T, Arima N, Yamashita Y, Fujita T and Chiba T. 1992 Calcitonin inhibits the growth of human gastric carcinoma cell line KATO III. *Regul Pept* 37 (3): 183-94.

Nakamura M, Hashimoto T, Nakajima T, Ichii S, Furuyama J, Ishihara Y and Kakudo K. 1995 A new type of human calcitonin receptor isoform generated by alternative splicing. *Biochem Biophys Res Commun* 209 (2): 744-51.

Nakamuta H, Furukawa S, Koida M, Yajima H, Orlowski RC and Schlueter R. 1981 Specific binding of 125I-salmon calcitonin to rat brain: regional variation and calcitonin specificity. *Jpn J Pharmacol* 31 (1): 53-60.

Nakamuta H, Orlowski RC and Epand RM. 1990 Evidence for calcitonin receptor heterogeneity: binding studies with nonhelical analogs. *Endocrinology* 127 (1): 163-9.

Nakano K, Mizuno T, Sowa Y, Orita T, Yoshino T, Okuyama Y, Fujita T, Ohtani Fujita N, Matsukawa Y, Tokino T, Yamagishi H, Oka T, Nomura H and Sakai T. 1997 Butyrate activates the WAF1/Cip1 gene promoter through Sp1 sites in a p53-negative human colon cancer cell line. *J Biol Chem* 272 (35): 22199-206.

Naro F, Perez M, Migliaccio S, Galson DL, Orcel P, Teti A and Goldring SR. 1998 Phospholipase D- and protein kinase C isoenzyme-dependent signal transduction pathways activated by the calcitonin receptor. *Endocrinology* 139 (7): 3241-8.

Neher R, Riniker B, Maier R, Byfield PG, Gudmundsson TV and MacIntyre I. 1968 Human calcitonin. *Nature* 220 (171): 984-6.

Ng KW, Livesey SA, Larkins RG and Martin TJ. 1983 Calcitonin effects on growth and on selective activation of type II isoenzyme of cyclic adenosine 3':5'-monophosphate- dependent protein kinase in T47D human breast cancer cells. *Cancer Res* 43 (2): 794-800.

Niall HD, Keutmann HT, Copp DH and Potts JT, Jr. 1969 Amino acid sequence of salmon ultimobranchial calcitonin. *Proc Natl Acad Sci USA* 64 (2): 771-8.

Nicholson GC, D'Santos CS, Evans T, Moseley JM, Kemp BE, Michelangeli VP and Martin TJ. 1988 Human placental calcitonin receptors. Biochem J 250 (3): 877-82.

Nicholson GC, Horton MA, Sexton PM, CS DS, Moseley JM, Kemp BE, Pringle JA and Martin TJ. 1987 Calcitonin receptors of human osteoclastoma. *Horm Metab Res* 19 (11): 585-9.

Nicholson GC, Livesey SA, Moseley JM and Martin TJ. 1986a Actions of calcitonin, parathyroid hormone, and prostaglandin E2 on cyclic AMP formation in chicken and rat osteoclasts. *J Cell Biochem* 31 (3): 229-41.

Nicholson GC, Moseley JM, Sexton PM, Mendelsohn FA and Martin TJ. 1986b Abundant calcitonin receptors in isolated rat osteoclasts. Biochemical and autoradiographic characterization. *J Clin Invest* 78 (2): 355-60.

Nicosia S, Guidobono F, Musanti M and Pecile A. 1986 Inhibitory effects of calcitonin on adenylate cyclase activity in different rat brain areas. *Life Sci* 39 (23): 2253-62.

Niculescu AB, 3rd, Chen X, Smeets M, Hengst L, Prives C and Reed SI. 1998 Effects of p21(Cip1/Waf1) at both the G1/S and the G2/M cell cycle transitions: pRb is a critical determinant in blocking DNA replication and in preventing endoreduplication. *Mol Cell Biol* 18 (1): 629-43.

Nilsson J, von Euler AM and Dalsgaard CJ. 1985 Stimulation of connective tissue cell growth by substance P and substance K. *Nature* 315 (6014): 61-3.

Norbury C and Nurse P. 1992 Animal cell cycles and their control. *Annu Rev Biochem* 61 441-70.

Nurse P. 1990 Universal control mechanism regulating onset of M-phase. *Nature* 344 (6266): 503-8.

Nussenzveig DR, Mathew S and Gershengorn MC. 1995 Alternative splicing of a 48-nucleotide exon generates two isoforms of the human calcitonin receptor. *Endocrinology* 136 (5): 2047-51.

Nussenzveig DR, Thaw CN and Gershengorn MC. 1994 Inhibition of inositol phosphate second messenger formation by intracellular loop one of a human calcitonin receptor. Expression and mutational analysis of synthetic receptor genes. *J Biol Chem* 269 (45): 28123-9.

Nygaard SC, Kuestner RE, Moore EE and Stroop SD. 1997 Phosphorylation of the human calcitonin receptor by multiple kinases is localized to the C-terminus. *J Bone Miner Res* 12 (10): 1681-90.

Offermanns S, Iida Klein A, Segre GV and Simon MI. 1996 G alpha q family members couple parathyroid hormone (PTH) /PTH-related peptide and calcitonin receptors to phospholipase C in COS-7 cells. *Mol Endocrinol* 10 (5): 566-74.

Oka H, Jin L, Kulig E, Scheithauer BW and Lloyd RV. 1999 Pituitary adenylate cyclase-activating polypeptide inhibits transforming growth factor-beta1-induced apoptosis in a human pituitary adenoma cell line. *Am J Pathol* 155 (6): 1893-900.

Okuda H, Adachi M, Miyazawa M, Hinoda Y and Imai K. 1999 Protein kinase Calpha promotes apoptotic cell death in gastric cancer cells depending upon loss of anchorage. *Oncogene* 18 (40): 5604-9.

Onishi T and Hruska K. 1997 Expression of p27Kip1 in osteoblast-like cells during differentiation with parathyroid hormone. *Endocrinology* 138 (5): 1995-2004.

Orcel P, Tajima H, Murayama Y, Fujita T, Krane S, Ogata E, Goldring S and Nishimoto I. 2000 Multiple Domains Interacting with $G_s$ in the Porcine Calcitonin Receptor. *Mol. Endocrinol.* 14 (1): 170-182.

Otani M, Yamauchi H, Meguro T, Kitazawa S, Watanabe S and Orimo H. 1976 Isolation and characterization of calcitonin from pericardium and esophagus of eel. *J Biochem (Tokyo)* 79 (2): 345-52.

Owen GI, Richer JK, Tung L, Takimoto G and Horwitz KB. 1998 Progesterone regulates transcription of the p21(WAF1) cyclin- dependent kinase inhibitor gene through Sp1 and CBP/p300. *J Biol Chem* 273 (17): 10696-701.

Pagès P, Benali N, Saint Laurent N, Estève JP, Schally AV, Tkaczuk J, Vaysse N, Susini C and Buscail L. 1999 sst2 somatostatin receptor mediates cell cycle arrest and induction of p27(Kip1). Evidence for the role of Shp-1. *J Biol Chem* 274 (21): 15186-93.

Pan ZQ, Reardon JT, Li L, Flores Rozas H, Legerski R, Sancar A and Hurwitz J. 1995 Inhibition of nucleotide excision repair by the cyclin- dependent kinase inhibitor p21. *J Biol Chem* 270 (37): 22008-16.

Panagiotou S, Bakogeorgou E, Papakonstanti E, Hatzoglou A, Wallet F, Dussert C, Stournaras C, Martin PM and Castanas E. 1999 Opioid agonists modify breast cancer cell proliferation by blocking cells to the G2/M phase of the cycle: involvement of cytoskeletal elements. *J Cell Biochem* 73 (2): 204-11.

Pearse AGE and Carvalheira AF. 1967 Cytochemical evidence for an ultimobranchial origin of rodent thyroid C cells. *Nature* 214 929-931.

Pestell RG, Albanese C, Reutens AT, Segall JE, Lee RJ and Arnold A. 1999 The cyclins and cyclin-dependent kinase inhibitors in hormonal regulation of proliferation and differentiation. *Endocr Rev* 20 (4): 501-34.

Pines J. 1993 Cyclins and their associated cyclin-dependent kinases in the human cell cycle. *Biochem Soc Trans* 21 (4): 921-5.

Pines J. 1997 Cyclin-dependent kinase inhibitors: the age of crystals. *Biochim Biophys Acta* 1332 (1): M39-42.

Plotkin LI, Weinstein RS, Parfitt AM, Roberson PK, Manolagas SC and Bellido T. 1999 Prevention of osteocyte and osteoblast apoptosis by bisphosphonates and calcitonin. *J Clin Invest* 104 (10): 1363-74.

Polak JM, Pearse AG, Le Lièvre C, Fontaine J and Le Douarin NM. 1974 Immunocytochemical confirmation of the neural crest origin of avian calcitonin-producing cells. *Histochemistry* 40 (3): 209-14.

Polyak K, Waldman T, He TC, Kinzler KW and Vogelstein B. 1996 Genetic determinants of p53-induced apoptosis and growth arrest. *Genes Dev* 10 (15): 1945-52.

Potts JT, Jr., Niall HD, Keutmann HT, Brewer HB, Jr. and Deftos LJ. 1968 The amino acid sequence of porcine thyrocalcitonin. *Proc Natl Acad Sci USA* 59 (4): 1321-8.

Powers JF, Shahsavari M, Tsokas P and Tischler AS. 1999 Nerve growth factor receptor signaling in proliferation of normal adult rat chromaffin cells. *Cell Tissue Res* 295 (1): 21-32.

Prowse DM, Bolgan L, Molnár A and Dotto GP. 1997 Involvement of the Sp3 transcription factor in induction of p21Cip1/WAF1 in keratinocyte differentiation. *J Biol Chem* 272 (2): 1308-14.

Przepiorka D, Baylin SB, McBride OW, Testa JR, de Bustros A and Nelkin BD. 1984 The human calcitonin gene is located on the short arm of chromosome 11. *Biochem Biophys Res Commun* 120 (2): 493-9.

Pumiglia KM and Decker SJ. 1997 Cell cycle arrest mediated by the MEK/mitogen-activated protein kinase pathway. *Proc Natl Acad Sci USA* 94 (2): 448-52.

Quiza M, Dowton M, Perry KJ and Sexton PM. 1997 Electrophoretic mobility and glycosylation characteristics of heterogeneously expressed calcitonin receptors. *Endocrinology* 138 (2): 530-9.

Rakopoulos M, Ikegame M, Findlay DM, Martin TJ and Moseley JM. 1995 Short treatment of osteoclasts in bone marrow culture with calcitonin causes prolonged suppression of calcitonin receptor mRNA. *Bone* 17 (5): 447-53.

Rao LG, Heersche JN, Marchuk LL and Sturtridge W. 1981 Immunohistochemical demonstration of calcitonin binding to specific cell types in fixed rat bone tissue. *Endocrinology* 108 (5): 1972-8.

Raulais D, Hagaman J, Ontjes DA, Lundblad RL and Kingdon HS. 1976 The complete amino-acid sequence of rat thyrocalcitonin. *Eur J Biochem* 64 (2): 607-11.

Ritchie CK, Thomas KG, Andrews LR, Tindall DJ and Fitzpatrick LA. 1997 Effects of the calciotrophic peptides calcitonin and parathyroid hormone on prostate cancer growth and chemotaxis. *Prostate* 30 (3): 183-7.

Rizzo AJ and Goltzman D. 1981 Calcitonin receptors in the central nervous system of the rat. *Endocrinology* 108 (5): 1672-7.

Robinson CJ, Martin TJ, Matthews EW and MacIntyre I. 1967 Mode of action of thyrocalcitonin. *J Endocrinol* 39 (1): 71-9.

Roos BA, Yoon MJ, Frelinger AL, Pensky AE, Birnbaum RS and Lambert PW. 1979 Tumor growth and calcitonin during serial transplantation of rat medullary thyroid carcinoma. *Endocrinology* 105 (1): 27-32.

Rosenfeld MG, Lin CR, Amara SG, Stolarsky L, Roos BA, Ong ES and Evans RM. 1982 Calcitonin mRNA polymorphism: peptide switching associated with alternative RNA splicing events. *Proc Natl Acad Sci USA* 79 (6): 1717-21.

Samura A, Wada S, Suda S, Yamanaka K, Osuga I, Kawasaki S, Iitaka M and Katayama S (1999). Homologous Regulation of the Calcitonin Receptor in Human Osteoclasts Prepared by ODF and M-CSF. Abstract SA037 Americal Society of Bone and Mineral Research 21st Annual Meeting, St Louis.

Santra M, Mann DM, Mercer EW, Skorski T, Calabretta B and Iozzo RV. 1997 Ectopic expression of decorin protein core causes a generalized growth suppression in neoplastic cells of various histogenetic origin and requires endogenous p21, an inhibitor of cyclin- dependent kinases. *J Clin Invest* 100 (1): 149-57.

Sasayama Y, Ukawa K, Kai Ya H, Oguro C, Takei Y, Watanabe TX, Nakajima K and Sakakibara S. 1993 Goldfish calcitonin: purification, characterization, and hypocalcemic potency. *Gen Comp Endocrinol* 89 (2): 189-94.

Sato M, Bryant HU, Dodge JA, Davis H, Matter WF and Vlahos CJ. 1996 Effects of wortmannin analogs on bone *in vitro* and *in vivo*. *J Pharmacol Exp Ther* 277 (1): 543-50.

Schipani E, Kruse K and Hüppner, J. 1995 A constitutively active mutant PTH-PTHrP receptor in Jansen- type metaphyseal chondrodysplasia. *Science* 268 (5207): 98-100.

Schoneberg T, Liu J and Wess J. 1995 Plasma membrane localization and functional rescue of truncated forms of a G protein-coupled receptor. *J Biol Chem* 270 (30): 18000-6.

Schot L, P.C., Boes HM, Swaab DF *et al.* 1981 Immunocytochemical demonstration of peptidergic neurons in the central nervous system of the pond snail *Lymnaea ofagnalis* with antisera raised to biologically active peptides of vertebrates. *Cell Tissue Res* 216: 273-291

Sebastian B, Kakizuka A and Hunter T. 1993 Cdc25M2 activation of cyclin-dependent kinases by dephosphorylation of threonine-14 and tyrosine-15. *Proc Natl Acad Sci U S A* 90 (8): 3521-4.

Sewing A, Wiseman B, Lloyd AC and Land H. 1997 High-intensity Raf signal causes cell cycle arrest mediated by p21Cip1. *Mol Cell Biol* 17 (9): 5588-97.

Sexton PM, Adam WR, Moseley JM, Martin TJ and Mendelsohn FA. 1987 Localization and characterization of renal calcitonin receptors by *in vitro* autoradiography. *Kidney Int* 32 (6): 862-8.

Sexton PM and Hilton JM. 1992 Biologically active salmon calcitonin-like peptide is present in rat brain. *Brain Res* 596 (1-2): 279-84.

Sexton PM, Houssami S, Hilton JM, LM OK, Center RJ, Gillespie MT, Darcy P and Findlay DM. 1993 Identification of brain isoforms of the rat calcitonin receptor. *Mol Endocrinol* 7 (6): 815-21.

Sexton PM, Paxinos G, Kenney MA, Wookey PJ and Beaumont K. 1994 *In vitro* autoradiographic localization of amylin binding sites in rat brain. *Neuroscience* 62: 553-67.

Sexton PM, Schneider HG, CS DS, Mendelsohn FA, Kemp BE, Moseley JM, Martin TJ and Findlay DM. 1991 Reversible calcitonin binding to solubilized sheep brain binding sites. *Biochem J* 273 (Pt 1): 179-84.

Shah GV, Rayford W, Noble MJ, Austenfeld M, Weigel J, Vamos S and Mebust WK. 1994 Calcitonin stimulates growth of human prostate cancer cells through receptor-mediated increase in cyclic adenosine 3',5'-monophosphates and cytoplasmic $Ca^{2+}$ transients. *Endocrinology* 134 (2): 596-602.

Shao ZM, Nguyen M, Alpaugh ML, JT OC and Barsky SH. 1998 The human myoepithelial cell exerts antiproliferative effects on breast carcinoma cells characterized by p21WAF1/CIP1 induction, G2/M arrest, and apoptosis. *Exp Cell Res* 241 (2): 394-403.

Sharma K, Patel YC and Srikant CB. 1999 C-terminal region of human somatostatin receptor 5 is required for induction of Rb and G1 cell cycle arrest. *Mol Endocrinol* 13 (1): 82-90.

Shefler I, Seger R and Sagi Eisenberg R. 1999 Gi-mediated activation of mitogen-activated protein kinase (MAPK) pathway by receptor mimetic basic secretagogues of connective tissue-type mast cells: bifurcation of arachidonic acid-induced release upstream of MAPK. *J Pharmacol Exp Ther* 289 (3): 1654-61.

Sheikh MS, Li XS, Chen JC, Shao ZM, Ordonez JV and Fontana JA. 1994 Mechanisms of regulation of WAF1/Cip1 gene expression in human breast carcinoma: role of p53-dependent and independent signal transduction pathways. *Oncogene* 9 (12): 3407-15.

Sheriff S, Fischer JE and Balasubramaniam A. 1992 Amylin inhibits insulin-stimulated glucose uptake in C2C12 muscle cell line through a cholera-toxin-sensitive mechanism. *Biochim Biophys Acta* 1136 (2): 219-22.

Sherr CJ. 1994 G1 phase progression: cycling on cue. *Cell* 79 (4): 551-5.

Shinki T, Ueno Y, DeLuca HF and Suda T. 1999 Calcitonin is a major regulator for the expression of renal 25-hydroxyvitamin D3-1alpha-hydroxylase gene in normocalcemic rats. *Proc Natl Acad Sci USA* 96 (14): 8253-8.

Shyu JF, Inoue D, Baron R and Horne WC. 1996 The deletion of 14 amino acids in the seventh transmembrane domain of a naturally occurring calcitonin receptor isoform alters ligand binding and selectively abolishes coupling to phospholipase C. *J Biol Chem* 271 (49): 31127-34.

Shyu JF, Zhang Z, Hernandez Lagunas L, Camerino C, Chen Y, Inoue D, Baron R and Horne WC. 1999 Protein kinase C antagonizes pertussis-toxin-sensitive coupling of the calcitonin receptor to adenylyl cyclase. *Eur J Biochem* 262 (1): 95-101.

Siegel R, Frederiksen J, Zacharias D, Chan F, Johnson M, Lynch D, Tsien R and Lenardo M. 2000 Fas preassociation required for apoptosis signaling and dominant inhibition by pathogenic mutations *Science* 288: 2354-2357.

Silva O, Wisneski LA, Cyrus J, Snider RH, Moore CF and Becker KL. 1978 Calcitonin in thyroidectomized patients. *Am J Med Sci* 275 (2): 159-64.

Singer FR, Melvin KE and Mills BG. 1976 Acute effects of calcitonin on osteoclasts in man. *Clin Endocrinol (Oxf)* 5 Suppl 333S-340S.

Soltoff SP. 1998 Related adhesion focal tyrosine kinase and the epidermal growth factor receptor mediate the stimulation of mitogen-activated protein kinase by the G-protein-coupled $P_{2y2}$ receptor. *J Biol Chem* 273: 23110-7

Sowa Y, Orita T, Minamikawa S, Nakano K, Mizuno T, Nomura H and Sakai T. 1997 Histone deacetylase inhibitor activates the WAF1/Cip1 gene promoter through the Sp1 sites. *Biochem Biophys Res Commun* 241 (1): 142-50.

Spengel R and Eva C. (1994). Handbook of Receptors and Channels. Boca Raton, FL, CRC Press.

Sternweis PC. 1994 The active role of beta gamma in signal transduction. *Curr Opin Cell Biol* 6 (2): 198-203.

Stroop SD and Moore EE. 1995 Intracellular calcium increases mediated by a recombinant human calcitonin receptor. *J Bone Miner Res* 10 (4): 524-32.

Stroop SD, Thompson DL, Kuestner RE and Moore EE. 1993 A recombinant human calcitonin receptor functions as an extracellular calcium sensor. *J Biol Chem* 268 (27): 19927-30.

Su Y, Chakraborty M, Nathanson MH and Baron R. 1992 Differential effects of the 3',5'-cyclic adenosine monophosphate and protein kinase C pathways on the response of isolated rat osteoclasts to calcitonin. *Endocrinology* 131 (3): 1497-502.

Takahashi N, Akatsu T, Sasaki T, Nicholson GC, Moseley JM, Martin TJ and Suda T. 1988 Induction of calcitonin receptors by 1 alpha, 25-dihydroxyvitamin D3 in osteoclast-like multinucleated cells formed from mouse bone marrow cells. *Endocrinology* 123 (3): 1504-10.

Tam SW, Theodoras AM, Shay JW, Draetta GF and Pagano M. 1994 Differential expression and regulation of Cyclin D1 protein in normal and tumor human cells: association with Cdk4 is required for Cyclin D1 function in G1 progression. *Oncogene* 9 (9): 2663-74.

Tang H, Kerins DM, Hao Q, Inagami T and Vaughan DE. 1998 The urokinase-type plasminogen activator receptor mediates tyrosine phosphorylation of focal adhesion proteins and activation of mitogen-activated protein kinase in cultured endothelial cells. *J Biol Chem* 273 (29): 18268-72.

Tapia JA, Ferris HA, Jensen RT and García LJ. 1999 Cholecystokinin activates PYK2/CAKbeta by a phospholipase C-dependent mechanism and its association with the mitogen- activated protein kinase signaling pathway in pancreatic acinar cells. *J Biol Chem* 274 (44): 31261-71.

Taussig R, I. ñiguez Lluhi JA and Gilman AG. 1993 Inhibition of adenylyl cyclase by Gi alpha. *Science* 261 (5118): 218-21.

Teti A, Paniccia R and Goldring SR. 1995 Calcitonin increases cytosolic free calcium concentration *via* capacitative calcium influx. *J Biol Chem* 270 (28): 16666-70.

Tombes RM, Auer KL, Mikkelsen R, Valerie K, Wymann MP, Marshall CJ, McMahon M and Dent P. 1998 The mitogen-activated protein (MAP) kinase cascade can either stimulate or inhibit DNA synthesis in primary cultures of rat hepatocytes depending upon whether its activation is acute/phasic or chronic. *Biochem J* 330 (Pt 3): 1451-60.

Touhara K, Hawes BE, van Biesen T and Keftkowitz RJ. 1995 G protein beta gamma subunits stimulate phosphorylation of the Shc adaptor proteins. *Proc Natl Acad Sci USA* 92 (20): 9284-7.

Toyoshima H and Hunter T. 1994 p27, a novel inhibitor of G1 cyclin-Cdk protein kinase activity, is related to p21. *Cell* 78 (1): 67-74.

Traverse S, Seedorf K, Paterson H, Marshall CJ, Cohen P and Ullrich A. 1994 EGF triggers neuronal differentiation of PC12 cells that overexpress the EGF receptor. *Curr Biol* 4 (8): 694-701.

Udvadia AJ, Templeton DJ and Horowitz JM. 1995 Functional interactions between the retinoblastoma (Rb) protein and Sp-family members: superactivation by Rb requires amino acids necessary for growth suppression. *Proc Natl Acad Sci USA* 92 (9): 3953-7.

van Biesen T, Hawes BE, Luttrell DK, Krueger KM, Touhara K, Porfiri E, Sakaue M, Luttrell LM and Lefkowitz RJ. 1995 Receptor-tyrosine-kinase- and G beta gamma-mediated MAP kinase activation by a common signalling pathway. *Nature* 376 (6543): 781-4.

van Biesen T, Luttrell LM, Hawes BE and Lefkowitz RJ. 1996 Mitogenic signaling *via* G protein-coupled receptors. *Endocr Rev* 17 (6): 698-714.

Vertongen P, Camby I, Darro F, Kiss R and Robberecht P. 1996 VIP and pituitary adenylate cyclase activating polypeptide (PACAP) have an antiproliferative effect on the T98G human glioblastoma cell line through interaction with VIP2 receptor. *Neuropeptides* 30 (5): 491-6.

Vouret Craviari V, Van Obberghen Schilling E, Scimeca JC, Van Obberghen E and Pouysségur J. 1993 Differential activation of p44MAPK (ERK1) by alpha-thrombin and thrombin-receptor peptide agonist. *Biochem J* 289 (Pt 1): 209-14.

Wada S, Akatsu T, Tamura T, Takahashi N, Suda T and Nagata N. 1994 Glucocorticoid regulation of calcitonin receptor in mouse osteoclast-like multinucleated cells. *J Bone Miner Res* 9 (11): 1705-12.

Wada S, Martin TJ and Findlay DM. 1995 Homologous regulation of the calcitonin receptor in mouse osteoclast-like cells and human breast cancer T47D cells. *Endocrinology* 136 (6): 2611-21.

Wada S, Udagawa N, Akatsu T, Nagata N, Martin TJ and Findlay DM. 1997 Regulation by calcitonin and glucocorticoids of calcitonin receptor gene expression in mouse osteoclasts. *Endocrinology* 138 (2): 521-9.

Wada S, Udagawa N, Nagata N, Martin TJ and Findlay DM. 1996a Physiological levels of calcitonin regulate the mouse osteoclast calcitonin receptor by a protein kinase Alpha-mediated mechanism. *Endocrinology* 137 (1): 312-20.

Wada S, Udagawa N, Nagata N, Martin TJ and Findlay DM. 1996b Calcitonin receptor down-regulation relates to calcitonin resistance in mature mouse osteoclasts. *Endocrinology* 137 (3): 1042-8.

Wang J, Rout UK, Bagchi IC and Armant DR. 1998 Expression of calcitonin receptors in mouse preimplantation embryos and their function in the regulation of blastocyst differentiation by calcitonin. *Development* 125 (21): 4293-302.

Warshawsky H, Goltzman D, Rouleau MF and Bergeron JJ. 1980 Direct *in vivo* demonstration by radioautography of specific binding sites for calcitonin in skeletal and renal tissues of the rat. *J Cell Biol* 85 (3): 682-94.

Weinberg RA. 1995 The retinoblastoma protein and cell cycle control. *Cell* 81 (3): 323-30.

Weinert T. 1998 DNA damage checkpoints update: getting molecular. *Curr Opin Genet Dev* 8 (2): 185-93.

Welch SP and Olson KG. 1991 Salmon calcitonin-induced modulation of free intracellular calcium. *Pharmacol Biochem Behav* 39 (3): 641-8.

Wigler M, Silverstein S, Lee LS, Pellicer A, Cheng Y and Axel R. 1977 Transfer of purified herpes virus thymidine kinase gene to cultured mouse cells. Cell 11: 223-232.

Wind JC, Born W, Rijnsent A, Boer P and Fischer JA. 1993 Stimulation of calcitonin/CGRP-I and CGRP-II gene expression by dibutyryl cAMP in a human medullary thyroid carcinoma (TT) cell line. *Mol Cell Endocrinol* 92 (1): 25-31.

Wolfe HJ, Melvin KE, Cervi Skinner SJ, Saadi AA, Juliar JF, Jackson CE and Tashjian AH, Jr. 1973 C-cell hyperplasia preceding medullary thyroid carcinoma. *N Engl J Med* 289 (9): 437-41.

Woods D, Parry D, Cherwinski H, Bosch E, Lees E and McMahon M. 1997 Raf-induced proliferation or cell cycle arrest is determined by the level of Raf activity with arrest mediated by p21Cip1. *Mol Cell Biol* 17 (9): 5598-611.

Wu RC and Schönthal AH. 1997 Activation of p53-p21waf1 pathway in response to disruption of cell-matrix interactions. *J Biol Chem* 272 (46): 29091-8.

Xiong Y, Hannon GJ, Zhang H, Casso D, Kobayashi R and Beach D. 1993 p21 is a universal inhibitor of cyclin kinases. *Nature* 366 (6456): 701-4.

Yamamoto Y, Nakamuta H, Koida M, Seyler JK and Orlowski RC. 1982 Calcitonin-induced anorexia in rats: a structure-activity study by intraventricular injections. *Jpn J Pharmacol* 32 (6): 1013-7.

Yamin M, Gorn AH, Flannery MR, Jenkins NA, Gilbert DJ, Copeland NG, Tapp DR, Krane SM and Goldring SR. 1994 Cloning and characterization of a mouse brain calcitonin receptor complementary deoxyribonucleic acid and mapping of the calcitonin receptor gene. *Endocrinology* 135 (6): 2635-43.

Yan GZ and Ziff EB. 1997 Nerve growth factor induces transcription of the p21 WAF1/ CIP1 and cyclin D1 genes in PC12 cells by activating the Sp1 transcription factor. *J Neurosci* 17 (16): 6122-32.

Yuan ZQ, Sun M, Feldman RI, Wang G, Ma X, Jiang C, Coppola D, Nicosia SV and Cheng JQ. 2000 May Frequent activation of AKT2 and induction of apoptosis by inhibition of phosphoinositide-3-OH kinase/Akt pathway in human ovarian cancer. *Oncogene* 19 (19): 2324-30.

Zaidi M, Breimer LH and MacIntyre I. 1987 Biology of peptides from the calcitonin genes. *Q J Exp Physiol* 72 (4): 371-408.

Zaidi M, Datta HK, Moonga BS and MacIntyre I. 1990 Evidence that the action of calcitonin on rat osteoclasts is mediated by two G proteins acting *via* separate post- receptor pathways. *J Endocrinol* 126 (3): 473-81.

Zajac JD, Livesey SA and Martin TJ. 1984 Selective activation of cyclic AMP dependent protein kinase by calcitonin in a calcitonin secreting lung cancer cell line. *Biochem Biophys Res Commun* 122 (3): 1040-6.

Zhang H, Xiong Y and Beach D. 1993 Proliferating cell nuclear antigen and p21 are components of multiple cell cycle kinase complexes. *Mol Biol Cell* 4 (9): 897-906.

Zhang Z, Hernandez-Lagunas L, Horne WC and Baron R. 1999 Cytoskeleton-dependent tyrosine phosphorylation of the $p103^{cas}$ family member HEF1 downstream of the G-protein-coupled calcitonin receptor. *J Biol Chem* 274: 25093-25098.

Zhu LJ, Bagchi MK and Bagchi IC. 1998a Attenuation of calcitonin gene expression in pregnant rat uterus leads to a block in embryonic implantation. *Endocrinology* 139 (1): 330-9.

Zhu LJ, Cullinan Bove K, Polihronis M, Bagchi MK and Bagchi IC. 1998b Calcitonin is a progesterone-regulated marker that forecasts the receptive state of endometrium during implantation. *Endocrinology* 139 (9): 3923-34.

Zumpe ET, Tilakaratne N, Fraser NJ, Christopoulos G, Foord SM and Sexton PM. 2000 Multiple RAMP domains are required for generation of amylin receptor phenotype from the calcitonin receptor gene product. *Biochem* 267 (1): 368-72.

Zuo Q, Claveau D, Hilal G, Leclerc M and Brunette MG. 1997 Effect of calcitonin on calcium transport by the luminal and basolateral membranes of the rabbit nephron. *Kidney Int* 51 (6): 1991-9.

# Appendix 1

Raw sequencing data of the 5' region of the insert +ve hCTR cloned into the pRc-CMV expression plasmid.

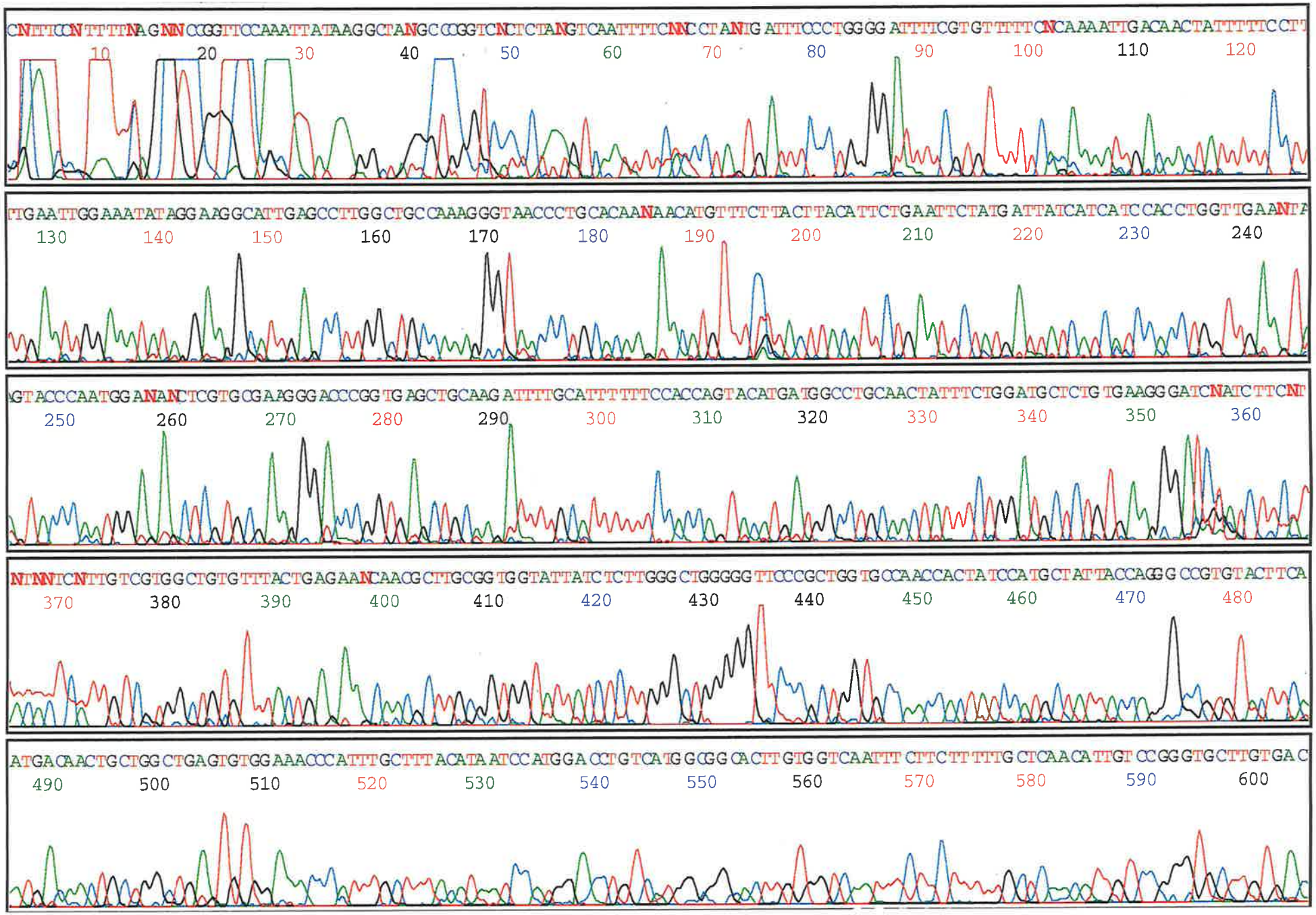

Raw sequencing data (sense direction) of the 5' region of the insert +ve hCTR sequenced using the 5pCMV primer (described in section 2.1.15)

# Appendix 2

Raw sequencing data of the 3' region of the insert +ve hCTR cloned into the pRc-CMV expression plasmid.

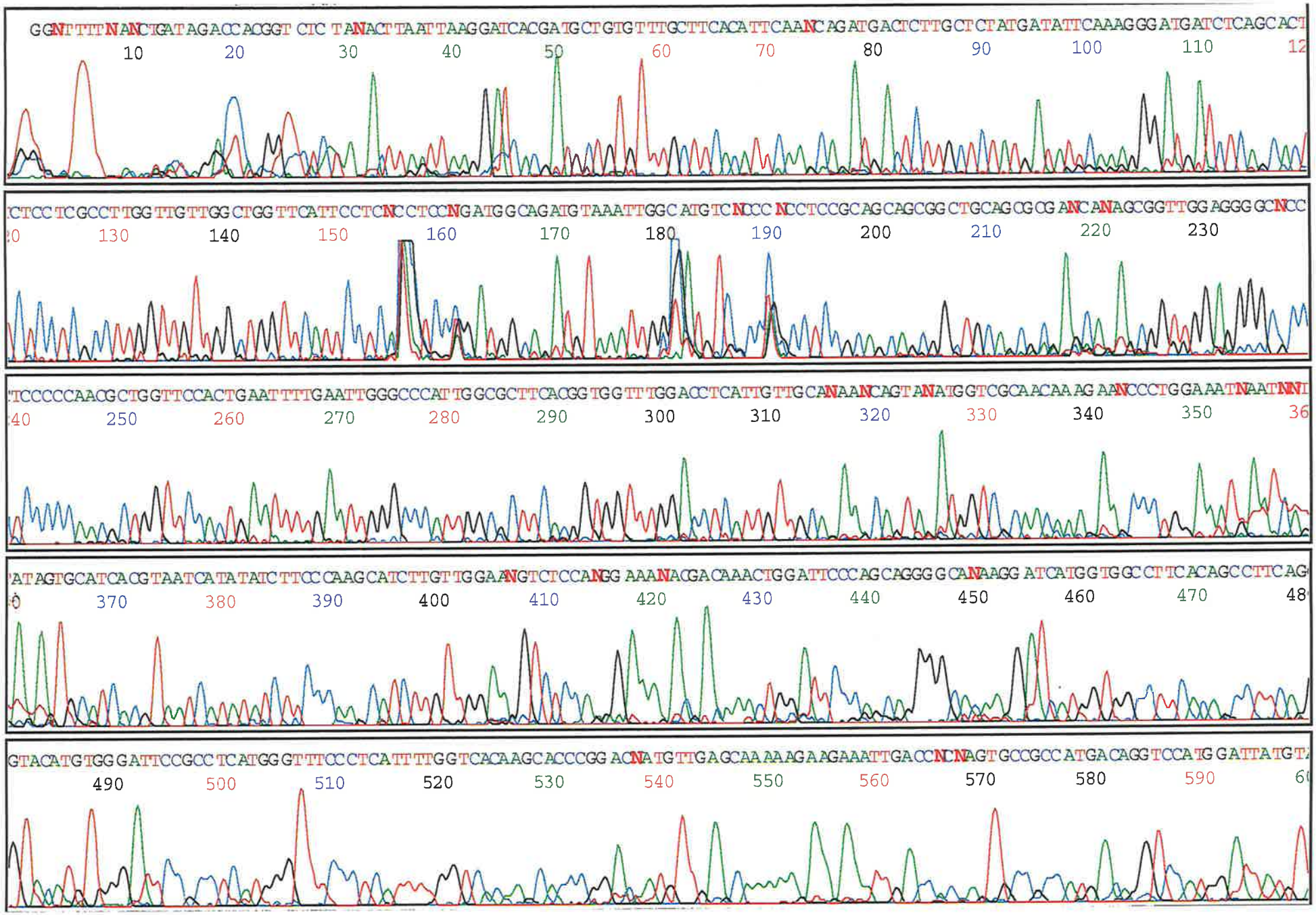

Raw sequencing data (sense direction) of the 3' region of the insert +ve hCTR sequenced using the 3pCMV primer (described in section 2.1.15)

# Appendix 3

Raw sequencing data of the 16 amino acid insert of the insert +ve hCTR cloned into the pRc-CMV expression plasmid

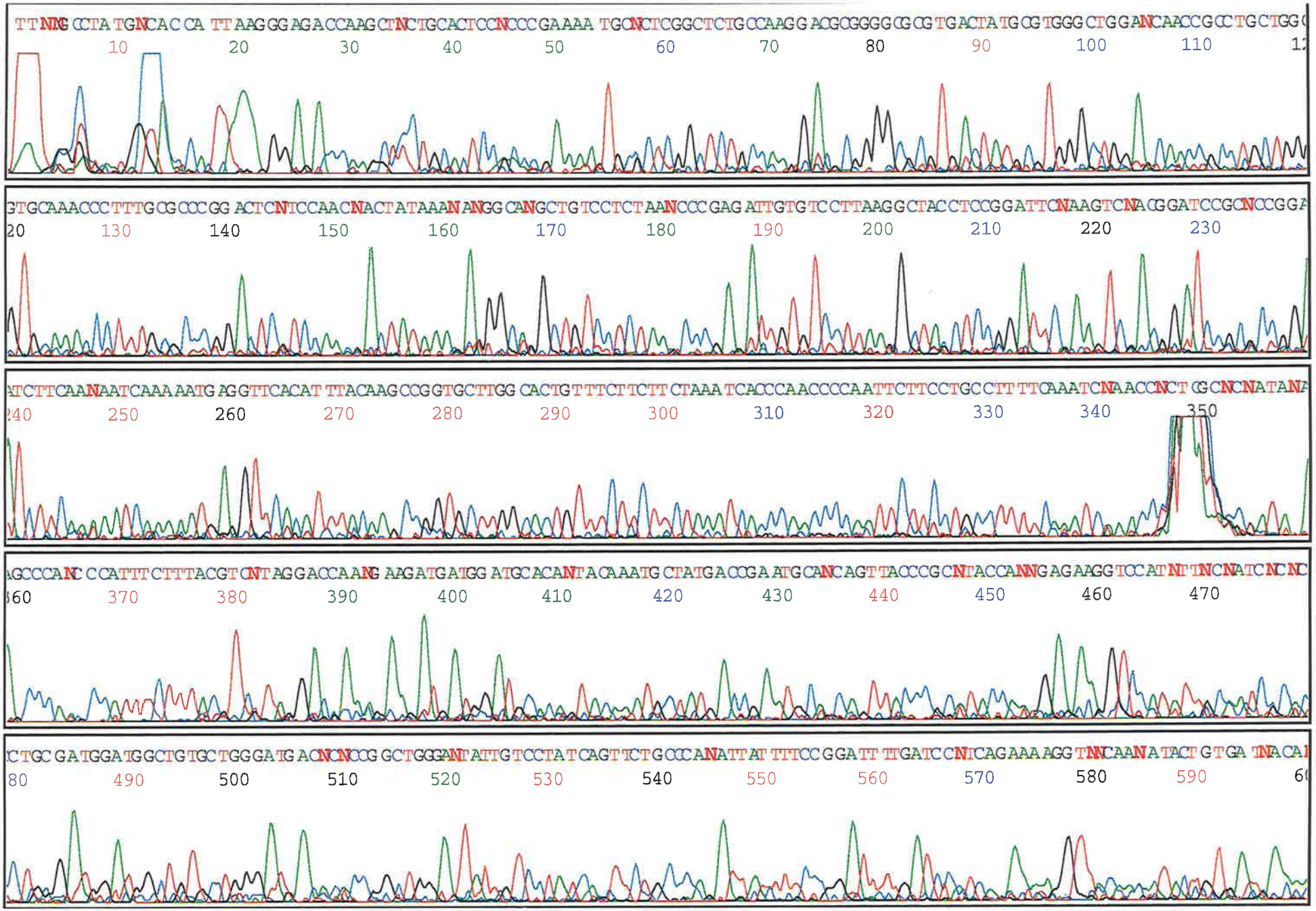

Raw sequencing data (sense direction) of the 5' region of the insert +ve hCTR sequenced using an internal 5'hCTR primer (described in section 2.1.15)